PART VI

MEASURING INSTRUMENTS AND THEIR DEVELOPMENT

This page intentionally left blank

CHAPTER

17

Measuring Temperature

OUTLINE

17.1 PART 1. HISTORICAL OVERVIEW: THE DEVELOPMENT OF EARLY THERMOMETERS AND BASIC IDEAS

17.1.1 Introduction

Modern instruments for microclimate measurements derive from early inventions mostly made for meteorological purposes. Several operating principles were tested, with different success. Knowing the various methodologies and the natural selection that has occurred over time helps to make the best choice: i.e. to choose the methodologies and the instruments that best suit any specific problem and operate with the utmost awareness.

This short historical overview includes technical comments, concerning the most relevant steps related to inventions and their development. The focus is not restricted to the past, but to help researchers in their difficult task: to devise new investigations for cultural heritage, especially when vulnerable artworks, or unplanned difficulties require new, specific solutions.

This matter is particularly useful to three categories of scholars:

- scientists active in Museums of History of Science and Technology, to better know, frame, and explain their instruments

Microclimate for Cultural Heritage
https://doi.org/10.1016/B978-0-444-64106-9.00017-1

- climatologists working to recover, homogenize and study long instrumental records, to know the weak points and correct early readings
- whoever should perform field measurements, who will expand their experience with a long list of early attempts, suggested solutions as well as their validation.

A number of science historians has studied the invention and development of weather and microclimate instruments, and have produced masterful works. This book will try to update and cast new light on this topic, taking advantage of the last historical and technical achievements and some personal experience[1] in this subject.

The thermometer was not born as a measuring instrument: it had a long evolution, and the first embryo was a fountain driven by solar radiation invented to impress people. It was then transformed into a simple device to study how a gas may behave when it is heated or cooled, and subsequently tentatively applied to better understand human physiology. After many experiments and new ideas, finally scientists were able to build a measuring instrument and to improve it. It has been, and still is, the most popular instrument in meteorology, medicine, agriculture, industry, and many other fields.

However, the thermometer is simply an instrument that measures the temperature of its bulb. The key issue is that the bulb should reach the same thermal level as the surrounding air, or the object, and that the equilibrium should not be disturbed by other factors, e.g. the solar radiation, IR sources, direct rainfall, or splashing drops. The measured value is determined by a complex interaction concerning the thermometer, the shield, the surrounding environment, and the observer. It took time for scientists to realize this key issue. Sometimes high-precision thermometers were used, but the quality of sensors and instruments was counteracted by a biased energetic balance of the shield, or other factors. This section will increase awareness and hopefully will help to take better measurements.

This chapter takes benefit of the existing literature (Boffito, 1929; Middleton, 1966, 1969; Frisinger, 1983; Landsberg, 1985; Borchi and Macii, 1997, 2009; Kington, 1997; Camuffo and Jones, 2002; Chang, 2004; Brázdil et al., 2005, 2012; Przybylak et al., 2010; Camuffo and Bertolin, 2012a,b; Camuffo et al., 2016, 2017; Camuffo, 2018) as well as a long personal experience in this field.

17.1.2 The Thermoscope

In the classical antiquity, two philosophers had genial intuitions and described some amazing devices for leisure, based on the laws of fluids. The first one was Philo of Byzantium (2nd or 3rd Century BC),[2] a Hellenistic Jewish philosopher, who described several interesting devices driven by water and air. However, only two books of the work survived in Greek[3] and the *Pneumatica* book in Arabic and partially in Latin. However, in the 16th and 17th centuries, when the thermoscope was invented, nobody knew them.[4]

The second was Heron of Alexandria (c.10–70 AD),[5] with his book *Spiritalia*. Fortunately, Heron was translated from Greek to Latin by Federigo Commandino (1575), then into Italian by Battista Aleotti (1589) and Alessandro Giorgi (1592). Commandino and Giorgi used exactly the same drawings; Aleotti has redrawn the same but with minor differences in decorations or vertical symmetry. These translations were disseminated over Europe and didn't go unnoticed because the scientific publications were extremely rare at that time. Latin was the official scientific language of that time.

Heron made several nice combinations of vessels and siphons, playing with a liquid (e.g. water, wine, oil) and air, or steam. These devices were activated by changes in the liquid level, or in air pressure. The most interesting device is the number XLVII where the solar radiation activated a fountain: the heat increased the air pressure forcing the water to move through a siphon (Fig. 17.1A). The explanation of this figure was enlightening: 'When the Sun hits the sphere EF, the air pocket pushes out some water that will go out through the tube G and will be collected in a lower vessel. However, when the sphere will return in the shade, the tube will suck back some water to fill the empty space. And this will be repeated every time the Sun will hit the sphere'. This example may have likely inspired Galileo Galilei, Sanctorius, Fludd, and Drebbel and stimulated them to build a thermoscope.

In the same period, another relevant philosopher, alchemist, playwright, and author of several books on

[1] The author has a long-term involvement in field measurements, early instruments and history of science; has recovered and corrected long instrumental series, and reads Latin (the official language of scientific works in the past centuries), Italian, French, English, Spanish and Portuguese sources in the original languages.

[2] Philo of Byzantium (c 280–c.220 BCE) who wrote '*De Ingeniis Spiritualibus*' (On Pressure Engines) that included a device that could inspire a thermoscope. Philo wrote another work but not related to the thermoscope, i.e. '*De septem orbis spectaculis*' (The Seven Wonders of the (ancient) World) that was published in Greek and Latin in 1640, translation and notes by L. Allati, printer: Mascardus, Rome.

[3] The manuscripts were stored in the *Bayerische Staatsbibliothek*, Munich.

[4] British School at Rome, 1902. Papers of the British School at Rome, vol. 67. Clay and Sons, London

[5] Heron of Alexandria (c.10–70 CE), who wrote '*Pneumatica*' (i.e. Spiritalia).

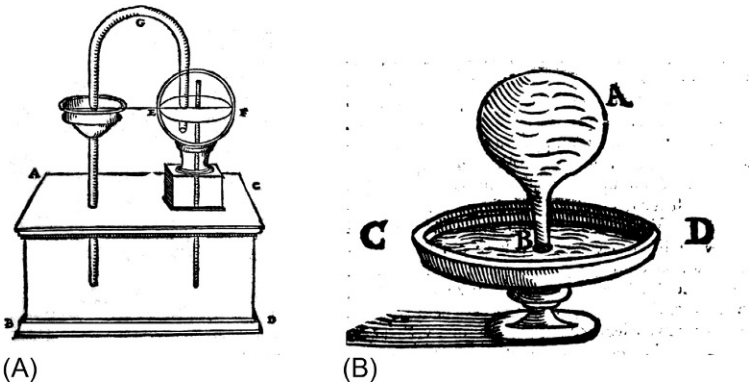

FIG. 17.1 Devices based on gas expansion and water displacement that might have inspired the thermoscope. (A) Solar fountain by Hero of Alexandria. The solar radiation increases the pressure of the air pocket in the sphere (on the right) half filled of water, triggering the siphon. This generates a flow of water until the end of the siphon is reached. A new outflow requires further heating. (B) A similar device by Della Porta. Behaviour of a flask full of water (AB), reversed on a vessel (CD) containing water. *From (A) Commandino (1575); (B) Della Porta (1607).*

scientific curiosities and instruments was Della Porta.[6] In particular, he wrote the multivolume book *Magiae Naturalis* (i.e. 'Natural Magic') in Latin, which may be considered an early encyclopaedia of science and technology with advanced ideas that drew the attention of the Inquisition. He reported most of the ancient knowledge and his own thoughts. The Book XVIII included a drawing with a stimulating discussion about vacuum and the behaviour of a reversed ampulla on a vessel from which the thermoscope could be derived (Fig. 17.1B). The work by Della Porta appeared in 1558; then it was expanded up to 20 volumes and had several reprints, two of them (i.e. Della Porta, 1584, 1607) in the period during which thermoscopes were developed.

In 1593, 1 year after the Giorgi translation, Galileo Galilei[7] was a renamed scientist at the Padua University, and Della Porta went to meet him. Nobody knows what they said, but they will certainly have discussed the scientific and philosophic novelties, e.g. new theories and the most recent books. Months later, in the same year, Galileo built a thermoscope, and used it in his lectures to demonstrate that a gas expands when heated, and that the increase in volume corresponds to the lowering of the liquid column in the glass tube (Sagredo, 1615; Viviani, 1717 posthumous).

The thermoscope consisted of an air pocket in a glass sphere sealed to a glass tube that was immersed into a vessel with a liquid (Fig. 17.2A). To make the liquid in the tube easily visible, Galileo used red wine. The sensing fluid was air, and the liquid in the vessel (either water or wine) was considered an inert medium to make visible the expansion of the air pocket. This is justified because the expansion of liquids was not yet known, and the air-to-liquid volumetric expansion coefficients are in the ratio 17.2:1.

The problem of the thermoscope, however, is that the pressure of the air pocket inside the spherical bulb on the top of the glass tube was determined by both the air temperature and the atmospheric pressure on the free surface of the liquid in the vessel. At the free surface of the liquid in the vessel, the atmospheric pressure equalled the sum of the pressure due to the air pocket in the bulb, plus the pressure of the liquid column (Fig. 17.2B). If the atmospheric pressure increased, the pressure exerted on the water surface of the vessel would have forced the water column to rise to establish a new equilibrium. In conclusion, if the thermoscope was used to highlight short-term

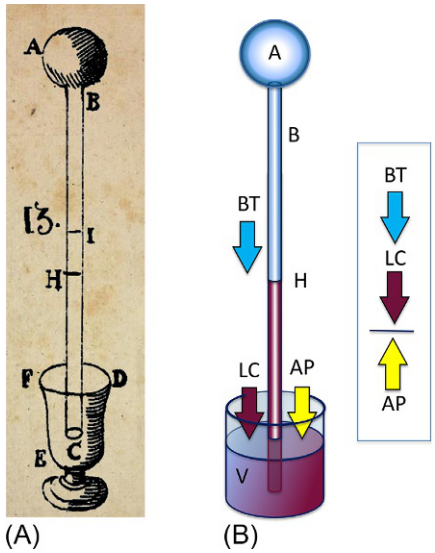

FIG. 17.2 (A) Thermoscope with an air pocket in the spherical bulb, i.e. the ampulla A on the top, B the capillary tube, H and I two levels of the liquid column and the vessel on the bottom, acting as water reservoir. (B) A coloured scheme with the bulb A, the capillary tube B with the liquid (red wine to improve visibility) reaching the height H, and the vessel reservoir V. *Arrows* indicate the pressures active at the liquid surface level, i.e. AP *(yellow)*: atmospheric pressure; BT *(cyan)* pressure for the gas temperature in the bulb; LC *(purple)*: liquid column. The box shows the combination BT + LC = − AP. *(A) From Borrelli (1670).*

[6] Giovan Battista Della Porta (1535–1615).

[7] Galileo Galilei (1564–1642).

changes, or temperature differences, e.g. the laws of gases or a fever compared to a healthy man, the atmospheric pressure had no significant changes and relative measurements were possible. However, this drawback was probably noted, but not clearly recognized because the atmospheric pressure was not yet discovered.[8] The way to counteract the pressure and transform the thermoscope into a thermometer will be discussed later.

Galileo made his experiment in 1593, did not write any paper about the thermoscope, and in 1610 moved to Florence. His experiments were soon forgotten. In 1612, again at the Padua University, Sanctorius Sanctorius[9] read Heron (as he wrote) and, like Galileo, was inspired by the Heron's drawings and explanations to build a thermoscope for medical purposes (Sanctorius, 1612). At the beginning, Sanctorius used a calliper to measure the height of the water column (Sagredo, 1612). He adjusted the calliper tips to fit the base and the top of the water column, then removed the calliper and measured with a ruler the distance between the tips. This method was possible with a linear tube, either in vertical or horizontal position. However, the length of the tube was too long, and Sanctorius thought that it was convenient to compact the instrument with a zigzag pattern by folding the glass tube (Fig. 17.3A). This complex shape made it impossible to use callipers and Sanctorius solved the problem applying the graduation of the rule directly to the tube, making measurements easier (Sanctorius, 1612). The tube graduation was made with a series of tags organized like an abacus: small tags represented ones and big tags tens. He left some drawings to explain the method and the scale (Fig. 17.3A). The patient kept in his mouth the bulb with the air pocket. The thermoscope was sized like a snake: the main part was folded and kept flat on a horizontal plane; neck and head (i.e. bulb) were kept vertical to enter the mouth; the tail too was vertical, but dipping down into a vessel to discharge the liquid leaking off. The heat of the patient's mouth expanded the air pocket and the liquid moved back in the tube; part of it was collected in a vessel located on the opposite extreme.

Thirteen years later, Sanctorius was interested to evaluate the impact of room temperature, humidity, and ventilation on the well-being of people (Sanctorius, 1625) and published a big thermoscope with graduated scale to detect indoor temperature changes (Fig. 17.3B and C). In the same book, he reported a cord hygrometer to measure ventilation[10] and a plate anemometer to measure ventilation.[11] Probably he knew the physical principles of these instruments, but he had much aptitude for quantitative assessments. He also made publications in Latin, with clear explanations and illustrations.

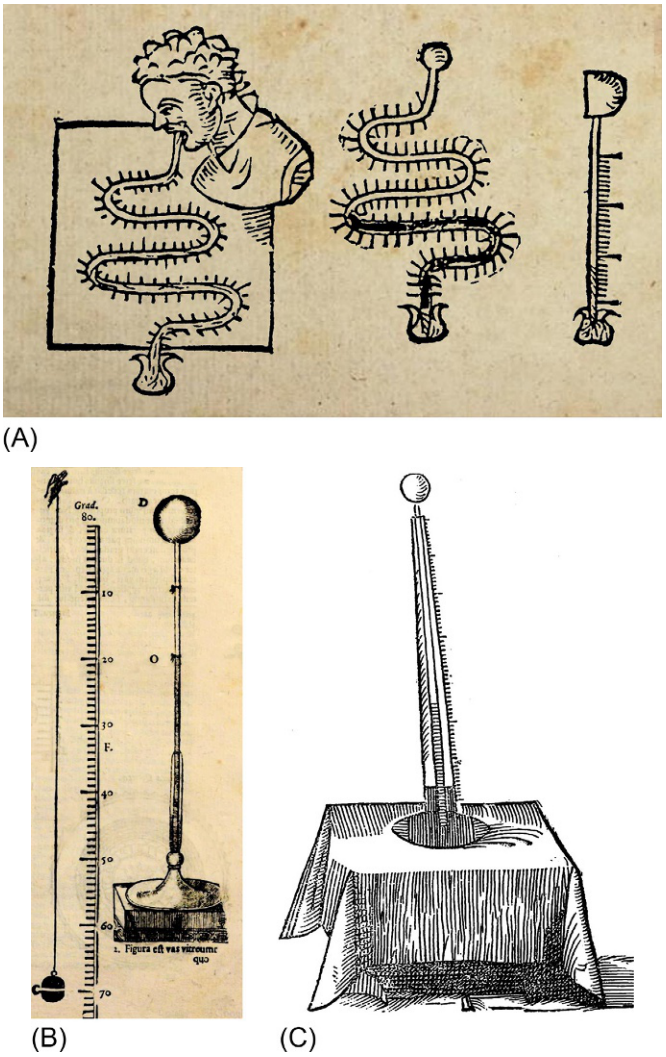

FIG. 17.3 (A) Medical thermoscope with a graduated scale by Sanctorius. Left: The patient keeps in his mouth the bulb with the air pocket, while the thermoscope lies on a flat surface. The glass tube was folded and had a scale with tags. Middle: View of the thermoscope. The liquid *(black line)* moved back in the tube and was collected in a vessel on the opposite side. Right: an equivalent, rectified view, of the thermoscope. (B) Portable thermoscope with separated graduated scale to detect room temperature changes. (C) Thermoscope with separated graduated scale, dipped into a wide water vessel. *From (A) Sanctorius (1612); (B,C) Sanctorius (1625).*

[8] In 1643, two Galileo's pupils made a revolutionary discovery. Evangelista Torricelli (1618–47), arrived to the conclusion that air had a weight, and his assistant Vincenzo Viviani (1622–1703) set up the experimental device, i.e. the barometer, to verify this theoretical thought.

[9] Sanctorius Sanctorius (1561–1636).

[10] See Chapter 18.

[11] See Chapter 20.

Cornelius Drebbel[12] was considered inventor of the thermometer (D***, 1688; van Musschenbroek, 1745; Nollet, 1749; Boehaave, 1759), for in 1598 he built an astronomical water clock powered by sunshine, very close to the Heron model. In addition, he built a graduated thermoscope probably borrowed from Della Porta (1607). The instrument was a typical thermoscope, with a spherical bulb on the top of a vertical glass tube, and the lower end of the tube immersed into a water reservoir.

Robert Fludd[13] is another controversial candidate because he built fountains driven by the solar radiation and applied a scale to the thermoscope (van Musschenbroek, 1758, 1762). Fludd (1638) wrote that, several years before, he had the opportunity of looking at an ancient manuscript that was unreadable (e.g. Philo in Arabic or Heron in Greek?) but had included some inspiring figures from which he derived his instrument. In his books, he published some interesting drawings, sometimes with a good physical explanation, sometimes with theological, magic, or occult interpretation.

Some intriguing figures by Fludd are reported. The first of them (Fig. 17.4A, Fludd, 1624) looks like the Della Porta experiment in Fig. 17.1B. The next two (Fig. 17.4B and C, Fludd, 1624, 1638) describe a solar-driven fountain that might having been inspired either by Philo or Heron, e.g. Fig. 17.1A. The next one (Fig. 17.4D, Fludd, 1726) is a thermoscope, possibly inspired by Sanctorius, e.g. Fig. 17.3B,C. The last figure (Fig. 17.4E, Fludd, 1638) is the 'glass calendar'.[14] This calendar is an attempt to follow the advancement of the seasons with a big thermoscope because the water column reaches the lowest level in summer, the highest in winter, and mid-level in the middle seasons. The theoretical ground of the air expansion with heat was clearly explained but disregarded to comment the amplitude of the daily cycle. However, he suggested other applications with a complex mystic theory

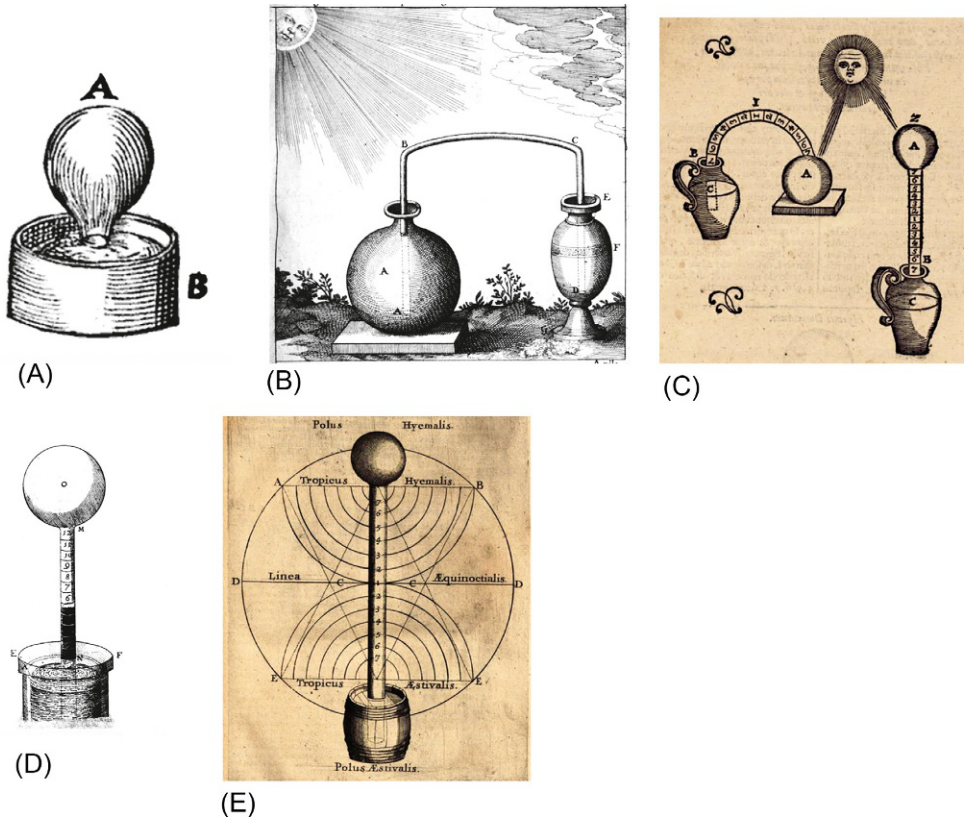

FIG. 17.4 (A) A two-vessel device, probably inspired by Della Porta. (B,C) Two solar fountains, inspired by Philo or Heron. (D) Thermoscope, probably inspired by Sanctorius. (E) Glass calendar. Latin legends from top: winter pole; winter tropic; equinoctial line; summer tropic; summer pole. *From (A) Fludd (1624); (B, C) Fludd (1624) and Fludd (1638); (D) Fludd (1626); (E) Fludd (1638).*

[12] Cornelius Jacobszoon Drebbel (1575–1633).

[13] Robert Fludd (1574–1637), also known as Robertus de Fluctibus (in Latin).

[14] '*calendarium vitreum*' in Latin.

involving the Sun, the celestial spheres, and other astrologic thoughts.

Who was the actual inventor of the thermometer has been discussed at length (Middleton, 1966) but without reaching consensus. Wrapping up, Galileo, Sanctorius, Drebbel, and Fludd were all inspired by Heron and/or Della Porta and applied the thermoscope to different aims. Galileo was the first, as confirmed by the correspondence between Galileo and Sagredo and by Vincenzo Viviani, his disciple and biographer. However, Galileo gave lectures and discussed about the physical principles of the thermoscope in private letters to pupils, but he never published his findings. Sanctorius was the first to apply a scale for quantitative evaluations and the first to publish textual and graphical descriptions.

However, none of them was the inventor of the thermometer, simply because the liquid-in-glass thermometer was not derived from the thermoscope. The thermoscope was sensitive to both the air temperature and the atmospheric pressure and could not take repetitive measurements.

17.1.3 The Air Thermometer

Around one century after the invention of the thermoscope, Amontons (1702) and Stancari (1708) found two solutions to transform the thermoscope into an instrument for quantitative and repeatable temperature readings. However, the first air thermometer was built by an anonymous scientist and was described in a book by Joachim D'Alencé,[15] but it went unnoticed and neither Amontons nor Stancari mentioned it. In 1688, D'Alencé published under the alias of 'D***' a carefully illustrated book, named 'Treatise of Barometers, Thermometers and Hygrometers' (in French) where he described the existing instruments, since their origins (D***, 1688[16]). Descriptions and drawings were scientifically sound and accurate, but the sources were not reported. Most of them are easily recognizable, but it would have been useful to know the attribution of some unknown short-lived instruments that appeared in that early period, like the air thermometer.

The instrument described by D'Alencé was a real air thermometer (Fig. 17.5A). It was a J-shaped thermoscope, with a graduated scale (like Sanctorius in 1625), but it had both ends closed to avoid any influence from the atmospheric pressure and was sensitive to temperature only. Surprisingly, this instrument has the same appearance of those by Amontons (1702) and Stancari (1708) (see later).

After Evangelista Torricelli and Vincenzo Viviani discovered the atmospheric pressure in 1644, the thermoscope was abandoned. However, Guillaume Amontons[17] considered that, in a thermoscope, the height of the mercury column was lowered when the atmospheric pressure increased (Fig. 17.5B), because the atmospheric pressure acted against the pressure of the air pocket. He also noted that the decrease in the thermoscope was equal to the increase in the barometer if the two instruments were identical.[18] At this point, it was sufficient to sum the thermometric and the barometric readings to avoid the influence of the external pressure (Amontons, 1702). The early thermoscopes (e.g. Galileo, Sanctorius, Fludd, Drebbel) had the bulb with the air pocket on the top. However, it was more convenient that the thermoscope and the barometer had similar size and shape. For this aim, he used a thermoscope with the bulb sealed to the lower arm of a J-shaped tube (Fig. 17.5C), like D'Alencé. Therefore, the Amontons thermometer[19] was a thermoscope associated with a barometer (Fig. 17.5D). Holding the glasswork tilted, Amontons introduced mercury from the open top of the tube to entrap air in the bulb, firstly to form an air pocket, and then to compress air. Compressed air was used as a powerful spring to move the heavy mercury column. Amontons might have read D'Alencé but, in any case, he was able to find an independent theoretical solution, keeping open the top of the tube, and this justifies why he did not quote him.

The Amontons thermometer was popular in the first half of the 18th century in France and Italy. However, it had some problems concerning both the instrument and the calibration (Camuffo, 2002a), as follows:

(i) Equal expansions or contractions of the air pocket in a spherical bulb caused nonlinear changes in the column height because the cross section of the bulb, where the mercury surface arrived, was continually changing. A better solution was adopted by Poleni,[20] who used a cylindrical bulb: the free

[15] The name of D***, i.e. D'Alencé, Dalancé, has been found, handwritten in pencil or ink, by some readers who noted it on the book frontpage. However, in libraries, the book is generally classified as D'Alencé, a French astronomer born in Paris, unknown date, and died in Lille in 1707.

[16] The first edition was printed in 1688 by Henry Wetstein, Amsterdam, the second in 1707 and 1708 by Paul Marret, Amsterdam; the third posthumous edition was printed in 1713, in Paris. The first edition appeared in the period of our interest.

[17] Guillaume Amontons (1663–1705).

[18] Two instruments with tubes having the same cross section avoided the capillarity problem.

[19] This chapter has rigorously followed the definitions, i.e. a thermometer is an instrument respondent to temperature only, while the thermoscope responds to both temperature and pressure. However, it is common the improper use of calling "Amontons thermometer" the "Amontons thermoscope".

[20] Giovanni Poleni (1683–1761).

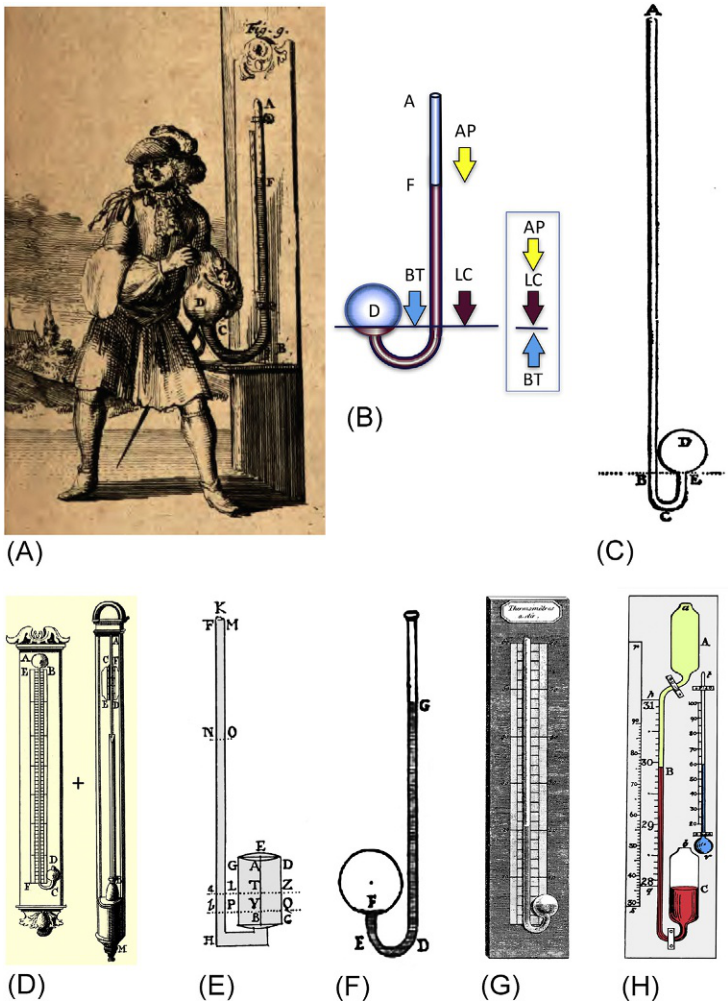

FIG. 17.5 (A) Air thermometer, composed of a J-shaped graduated air thermoscope with open top. It had very large size, i.e. 3 Paris feet (97.45 cm). (B) Scheme of the pressures *(arrows)* acting on the Amontons thermoscope: BT *(cyan)* pressure for the gas temperature in the bulb; AP *(yellow)*: atmospheric pressure; LC *(purple)*: liquid column. The box shows the combination AP + LC = − BT. The Amontons thermoscope was open in A, while D'Alencé and Stancari were closed. (C) Original drawing of the Amontons thermoscope. (D) The complete Amontons air thermometer: a thermoscope (left side) combined with a cistern barometer (right side). The thermoscope readings were summed to the pressure readings to obtain the actual temperature. (E) The Poleni thermoscope with cylindrical bulb to obtain linear response. (F) Stancari air thermometer, similar to the Amontons thermoscope, but with the top of the J tube hermetically closed. The image represents the glassware with mercury during calibration. (G) The air thermometer on a frame. Note the free mercury surface in the bulb fluctuates around the centre of the spherical volume to minimize and symmetrize the deviation from linearity. (H) Adie marine barometer called sympiesometer. Red: coloured almond oil; green: reservoir filled of hydrogen to damp oscillations. On the right, a thermometer (with blue liquid). *From (A) D*** (1688); (C) Amontons (1702); (D) Chambers (1728); (E) Poleni (1709); (F) Stancari (1708); (G) Cotte (1774); (H) Tomlinson (1861).*

surface of the mercury in contact with the air pocket always had the same cross section and the thermometer response was linear (Fig. 17.5E; Poleni, 1709).

(ii) The height of the mercury column should be measured from the mercury level in the spherical bulb that is continually variable with the temperature and the atmospheric pressure. However, the technology was poor and the instrument had a fixed scale instead of an adjustable one. The barometer had the same problem until Fortin[21] invented the adjustable cistern to tune the free mercury level.

(iii) The tube was four feet[22] in length, filled of 28 French inches of mercury, so that the air pocket in the spherical bulb was compressed up to 1 atm. Especially at low temperatures, the moisture in the compressed air pocket condensed, reducing a bit the internal pressure and depressing the mercury column. The problem was worse with thermometers built in summer, when the moisture content is higher.

(iv) A weak point of the thermometer was that it was not moveable and the high pressure in the bulb generated the risk of explosion in case of accidental hit.

(v) When this thermometer was used, the barometer readings were not corrected for capillarity, temperature, and gravity,[23] and this affected the total sum (i.e. the sum of the thermoscope reading

[21] Nicolas Fortin (1750–1831).

[22] The French foot, or Paris Foot, named '*pied du Roi*' (i.e. foot of the King) was 32.4828 cm. It was subdivided into 12 in., named 'pouces' (1 Paris inch = 27.069 mm) and a *pouce* into 12 lines 'lignes' (1 Paris line =22,557 mm).

[23] The correction to standard gravity requires to consider both latitude and height; the correction to refer the observed pressure to the mean sea level is not due to this aim.

plus the uncorrected pressure reading) that represented the actual temperature.

(vi) Air thermometers are based on the laws of perfect gases. In principle, when the equation of perfect gases is known, only one calibration point is sufficient and the ratio of the readings R_1 and R_2 at two temperatures, e.g. the fixed points, equals the ratio of the absolute temperatures, i.e. $R_1/R_2 = 373\,K/273\,K = 1.366$. However, the Amontons thermometer was filled with a nonperfect gas, in addition with moisture that could condense, and for these flaws all thermometers departed a bit from this ratio and two calibration points were necessary to reach an effective calibration curve.

(vii) The last bias was due to inappropriate calibration in combination with the barometer. To get ice, calibration was usually made in winter,[24] in an unheated room, with both the instruments, i.e. the thermoscope and the barometer, kept at freezing temperature. As opposed, the boiling point was established dipping the bulb of the thermoscope into the steam, while the barometer was at room temperature, close to the freezing point. The upper point calibration with two instruments at different temperatures (i.e. cold barometer and hot thermoscope) was different from the real-world situation when both instruments have the same temperature. This bias was largest in summer. Today this problem is known and early readings must be corrected for this bias.

Francesco Vittorio Stancari[25] was intended to improve the Amontons thermometer (Stancari, 1708). To this aim, and to follow his technique and calibration, he built an instrument identical in size and shape, but used a different strategy to avoid the influence of the atmospheric pressure: he sealed with flame[26] the top of the upper arm of the J-shaped tube (Fig. 17.5F) (Stancari, 1708; Camuffo et al., 2016, 2017). Stancari acknowledged an external input, i.e. he was discussing in Bologna how to improve the Amontons thermometer[27] and his colleague Geminiano Rondelli[28] suggested him to seal both ends, i.e. tube and bulb. Nobody can say where this idea came from. Very likely, Rondelli followed the example of the well-known Florentine thermometers (see later) that his colleague Giovan Battista Riccioli used in Bologna from 1654 to 1656 (Camuffo and Bertolin, 2012a,b). It might also be possible that Rondelli had read D'Alencé 20 years before. As a matter of fact, D'Alencé and Stancari arrived to the same instrument; the only difference was a technical detail, i.e. the sphere with the air pocket was defined 'closed' by D'Alencé and 'hermetically closed', by Stancari.[29]

The Stancari solution was good, but not perfect. When he hermetically sealed with the flame the upper part of the J tube, some air remained entrapped in it, and this air partially opposed the expansion of the air pocket in the ampulla, especially in summer when the free volume on the top of the tube was reduced, causing a small departure from linearity. The biases mentioned for the Amontons thermometer may be repeated for the Stancari thermometer, except for the need of a barometer. In the Bologna case study, one of two Stancari thermometers built in 1707 was dismissed in 1719, after 14 years of use, because it had a drift for a leakage from the junction between the sphere and the tube, favoured by the high internal pressure. The other instrument continued to be used till 1737 (Camuffo et al., 2016, 2017).

Air thermometers (Fig. 17.5G) were used in the first half of the 18th century and then were discarded because they were tall (around 1 m), delicate, and risky to move (including risk of explosion), nonlinear, difficult to build and calibrate, and readings taken with the Amontons thermometer were not comparable to those taken with the Stancari one. In conclusion, the thermoscope was the ancestor of the air thermometer that was born at the beginning of the 18th century, but the air thermometer was abandoned a few decades later.

In reality, other gas thermometers were created in the 19th century, based on the laws of gases: the constant-volume and the constant pressure gas thermometer in absolute degrees (K) operating at very high pressure (Regnault, 1847; Chappuis, 1888; Guillaume, 1889; Yavorsky and Pinsky, 1979; Doebelin, 1990). However, these are very particular instruments for advanced laboratory purposes.

[24] Following the use of Romans, snow and ice were kept in deep wells lined and covered with straw, making ice available till summer. However, this was rare and expensive. Hail was another random source of ice.

[25] Francesco Vittorio Stancari (1678–1709).

[26] It was not convenient to seal with putty because it ages and will not resist to high-pressure differences for years. This required a highly professional preparation.

[27] Stancari was studying the air thermometer and in particular he found that the water vapour present in the air pocket could condense when the volume is compressed and/or cooled, departing from the calibration curve.

[28] Geminiano Rondelli (1652–1739).

[29] The technical difference is that the simple closure, e.g. made with putty (as Honoré Flaugergues did in 1813), is less resistant and durable. As opposed, if the glass is hermetically closed, sealing it with the flame, as Stancari did, the glasswork is much more resistant (Camuffo et al., 2016).

Returning to the thermoscope, it responded to both temperature and air pressure. In a sense, it was the ancestor of the air thermometer, once the pressure dependence was controlled. It also could be considered the ancestor of the *sympiesometer* once the temperature dependence was controlled. The sympiesometer (Fig. 17.5H) was a marine barometer invented in 1818 by Adie[30] (Adie, 1819). This instrument was developed to avoid the use of vulnerable mercury thermometers in ships. It was inspired by the Amontons thermometer and the unwanted temperature contribution was removed using a traditional mercury thermometer fixed to the same frame. The barometer consisted of a J-shaped tube open at the lower end and closed at the top and used almond oil instead of mercury to increase friction and reduce free oscillations for the vessel roll and pitch. The two ends of the tube had small reservoirs. The closed reservoir on the top, and the upper part of the tube were filled with hydrogen. The use of the highly compressible hydrogen in the upper top of the tube magnified readings, as changes in pressure resulted in a larger displacement of the liquid. The coloured almond oil could move in the tube and the excess was kept in the lower reservoir that had an opening on the top to reach equilibrium with the atmosphere. However, it had several drawbacks, including short life, and was soon abandoned.

17.1.4 The Hydrometer and the Liquid-in-Glass Thermometer

The air thermometer and the liquid-in-glass thermometer had different origins and family trees (Fig. 17.6). The Greek philosopher Archimedes[31] discovered the physical principle of buoyancy. An instrument to evaluate the density of liquids, based on this principle, is the *hydrometer*, also known as *aerometer* (Fig. 17.7A). It is a graduated glass cylinder partially floating, i.e. more or less dipped into a fluid, depending on the density of the liquid. It was mentioned in a letter from Synesius of Cyrene to Hypatia of Alexandria[32] and later in the Arabic literature (11th and 12th century). In a letter dated 1612, Galileo explained how this instrument worked. In Florence, the Grand Duke of Tuscany Ferdinand II de' Medici,[33] with Galileo and pupils, members of the *Accademia del Cimento*,[34] Florence, built some hydrometers to determine the density of different liquids, either natural or man made (Magalotti, 1666; Targioni Tozzetti, 1780; Antinori, 1841, Middleton, 1971). A particular application was to recognize the percentage of spirit in alcoholic beverages, or the density of spring waters.

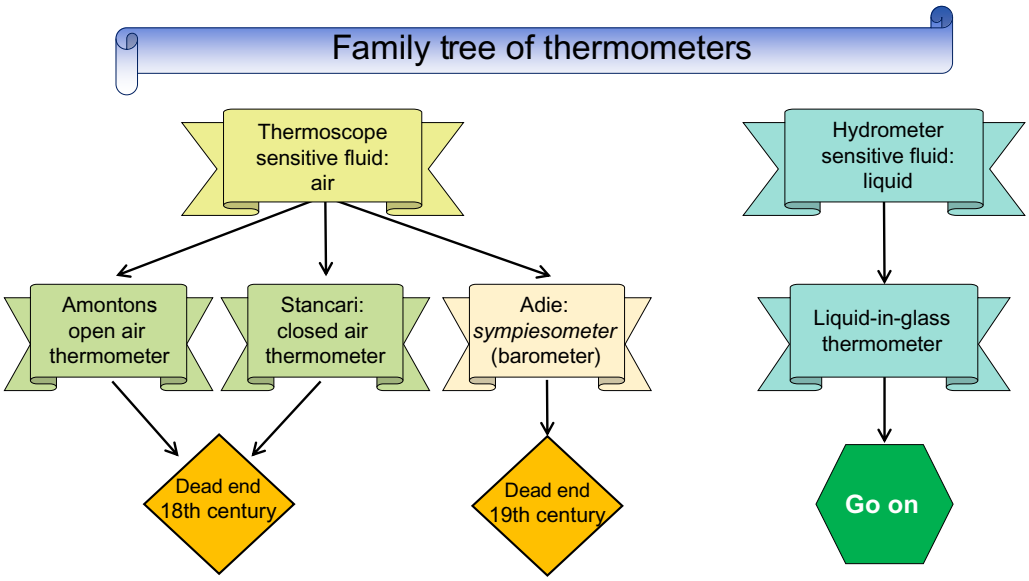

FIG. 17.6 Family tree of thermometers. The Thermoscope with air as thermometric fluid responded both to air temperature and pressure. It was the ancestor of the Amontons open-tube air thermometer and the Stancari closed-tube air thermometer. In addition, it was the ancestor of a barometer, the Adie sympiesometer. All of these instruments were short lived. The hydrometer discovered that liquids were temperature-sensitive fluids, and the liquid-in-glass thermometer was derived from it. Liquid-in-glass thermometers are still popularly used.

[30] Alexander Adie (1775–1858).

[31] Archimedes (287–215 BCE).

[32] 4th or 5th century CE.

[33] Ferdinand II de' Medici (1610–70).

[34] I.e. 'Experiment Academy', active from 1657 to 1667.

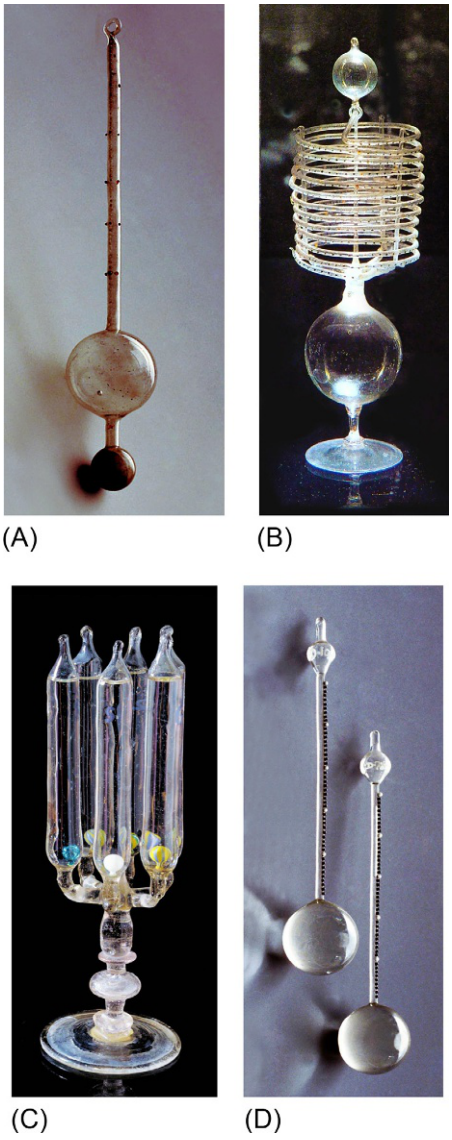

FIG. 17.7 (A) A Florentine *hydrometer* to measure the density of liquids. The lower sphere includes mercury as a ballast; the upper sphere includes air. Their combination determines the vertical position and the density range, readable on the graduations of the upper tube. (B) Florentine Spiral Thermometer, i.e. a thermometer with very long tube, twisted in spiral shape. (C) The Galileo 'sluggish thermometer' based on changes of spirit density. This thermometer is composed of six sealed tubes, containing spirit and a glass sphere, each of them with different density. The spheres heavier than the spirit lie at the bottom of the tube, the lighter spheres float on the surface, and the sphere with the same density is in neutral equilibrium. (D) Two Little Florentine Thermometers. In Florentine Thermometers, black enamel beads were tags for ones, white enamel beads for tens. *Courtesy of A. Lenzi and S. Bernacchini, © Museo Galileo—Institute and Museum of the History of Science, Florence, used with permission.*

The Academicians recognized that liquids changed density with temperature and thought that it was possible to build thermometers with liquids. They tested various liquids, including water, ethyl alcohol, oil, and mercury. The volumetric expansion coefficient of ethyl alcohol is about 1/3 of that of the air, but is 6.2 greater than that for mercury, and 1.6 greater than that for oil. Water has a coefficient similar to mercury, but departs very much from linearity. However, this was still unknown and it was impossible to establish which of the two was preferable. Water was rejected for the risk of damage in case of frost. The preferred liquid was pure ethyl alcohol because it had the largest expansion coefficient and the instrument resolution is strictly related to it. The main drawback was that it was poorly visible, but the addition of dies resulted in the staining of the glass tube, thus worsening the situation.

Several types of liquid-in-glass thermometers were devised, for instance, a thermometer with a very long graduated tube twisted in spiral shape (Fig. 17.7B). Galileo invented a curious thermometer, based on liquid density, the so-called sluggish thermometer, for its long response time (Fig. 17.7C). This thermometer was composed of some glass spheres, each with different density, that were immersed in spirit, and depending on the temperature and the liquid density changes, the lighter spheres were buoyant and the heavier ones were lying on the bottom. Only the sphere with the same density had neutral floating position. Each sphere had the value in degrees marked to recognize the actual temperature.

Among the various thermometers, the most accurate and reliable one was the Little Florentine Thermometer (Camuffo and Bertolin, 2012a,b) with scale divided into 50 Galileo degrees (1°G = 1.44°C) (Fig. 17.7D). The main contributors to this invention were Evangelista Torricelli[35] and the Grand Duke Ferdinand II[36] (Viviani, 1717 posthumous). The exact date on which the liquid-in-glass thermometer was invented is unknown. However, Alessandro Segni, Secretary of the Academy wrote in a log, called *Diario Grande* (i.e. Main Diary), daily reports concerning the scientific activities. In 1641, i.e. the last year of Galileo's life, this diary reports that a Little Florentine Thermometer was built (Targioni Tozzetti, 1780; Antinori, 1841). Several identical instruments were produced, exactly with the same size and calibration to provide comparable results. The Grand Duke of Tuscany organized the first international meteorological network, the *Medici Network*, active from 1654 to 1670, with 11 stations over Europe, all with the same instruments and the same observation protocol, and the same outdoor exposure to make comparable readings. Readings were taken

[35] Evangelista Torricelli (1608–47) the inventor of the barometer.

[36] Ferdinand II de' Medici (1610–70), Grand Duke of Florence.

every 3–4 h both by day and night and the daily logs were sent to the Grand Duke. These constituted the earliest records and were of excellent quality. Robert Boyle[37] was in Florence in the last year of life of Galileo, and years later studied the laws of gases using a replica of the Little Florentine Thermometer.

17.1.5 Calibration of Early Liquid-in-Glass Thermometers

Before the invention of the thermometer, nobody knew whether ice forms and melts at the same temperature, if the changes of state (e.g. freezing, boiling) always occur at the same temperature, or changed with height or latitude, or with other circumstances (e.g. the atmospheric pressure). Briefly, the Cimento Academicians had in mind to observe, investigate, and discover the laws of Nature. The choice of the thermometric liquid was crucial. The liquid should have a high expansion coefficient; it should not freeze in the real operation range and should not adhere to the glass tube, but the problem of nonlinearity had as yet not occurred to them.

The earliest calibration points were arbitrary and the comparison of readings was essentially based on the exact replica of the same reference thermometer, e.g. tube and bulb size, and quantity of alcohol inside. The scale of the Florentine thermometers was composed of enamel beads sealed to the tube and representative of the same calibration range. To obtain comparable readings required that the manufacturer be extremely precise in his work. The measuring unit (°G after Galileo) was determined by the distance between tags.

In air thermometers, i.e. Amontons, Stancari, the temperature was defined as the height of the liquid column in the capillary tube, like a barometer reading, and the 'degrees of heat' were measured in length units, i.e. inches and lines. Air thermometers needed one calibration point, but two calibration points were generally provided because they departed from the theoretical model.

Several calibration scales were proposed, each with pros and cons (Middleton, 1966; Camuffo, 2002a). Liquids with (almost) linear expansion (e.g. mercury, oil (Camuffo and della Valle, 2017)) needed two calibration points; nonlinear liquids (e.g. alcohol (Camuffo and della Valle, 2016)) needed more calibration points. However, this was discovered later. When two reference calibration points were established, the 'degree of heat' became a fraction of the range. In general, the scale started from the bottom, i.e. from lower temperatures (e.g. the centigrade scale in use after the Celsius's death, Fahrenheit, Réaumur, Kelvin); some scales started from the top, i.e. from higher temperatures, and were named 'reversed scale' (e.g. Delisle, original Celsius scale). The Florentine Thermometers had graduations but not numbering, and could be read either from the bottom or the top, adding or subtracting the number of degrees left until the lower, or the upper end of the scale.

In 1665, Christian Huygens[38] suggested that either the melting point of ice or the boiling point of water could be used for reference point; his suggestion concerned only one point because air thermometers needed only one calibration point. These reference points were selected for their 'almost' precise determination: in fact, the influence of atmospheric pressure on phase transitions was not yet known. In 1694, Renaldini[39] suggested that both the melting point of ice and the boiling points of water should be used as standard lower and upper limits. In 1701, Isaac Newton[40] proposed a scale with the extremes being melting snow and human body temperature. Around 1702, Roemer,[41] who used a spirit thermometer, added two fixed points to the Huygens scale, i.e. the body temperature (the blood temperature of a healthy adult male), and a mixture of sea salt and crushed ice. In 1717, Fahrenheit[42] adopted Roemer's idea but using the body temperature as upper limit and the mixture of ice and ammonium chloride as lower limit. The improvement was that the calibration points were strictly related to the temperature range in central and northern Europe. Fahrenheit used mercury in his thermometers and this was an excellent choice because the expansion of mercury is linear. In 1742, Celsius[43] proposed the centigrade scale, still in use to date, but inverted, with 100°C for the freezing point and 0°C for the boiling point. When Celsius died, Linnaeus[44] reversed the Celsius scale that became the popular 'centigrade' scale. Many other scales were proposed. For instance, Cotte (1774) published a table that compared 15 of the most popular scales, and Landsberg (1985) a table including 36 scales. Some confusion was generated because the scales could only be comparable if the thermometric liquid was the same. Today, only a few of

[37] Robert Boyle (1627–91).

[38] Christian Huygens (1629–95).

[39] Carlo Renaldini (1616–98).

[40] Isaac Newton (1643–1727).

[41] Olaf Christiansen Roemer (1644–1710).

[42] Daniel Gabriel Fahrenheit (1686–1738).

[43] Anders Celsius (1701–44).

[44] Carl Linnaeus (1707–78).

the historical scales survive, and the most popularly used are Kelvin, Celsius, Fahrenheit, and Réaumur.

In most early thermometers, the scale was fixed to the frame, separated from the tube. The tube was not rigidly fixed, with the risk of losing the matching with the calibration. In addition, some thermometers had the frame foldable to make free the bulb (Fig. 17.8A) and measure the temperature in liquids, chemical reactions, steam, and to make easier calibration (Negretti and Zambra, 1864).

The calibration procedure was as follows. First, the bulb was dipped in hot steam and in melting ice. The two levels reached by the thermometric liquid were marked on the tube tying a black silk thread in each position. The distance between the two silk threads was measured and divided into a number of equal parts, and the result was impressed on a strip, i.e. the thermometer's scale. Finally, the strip with the scale was fixed to the frame on the side of the tube taking care of the zero offset, or in correspondence with another calibrated thermometer.

A consequence of this poor technology was that the glassware was tied to the wooden frame with an iron wire passing through small holes (Fig. 17.8B). When the humidity changed, the dimensional changes of wood caused problems. In dry environments, or when the wooden frame was hit by solar radiation, the frame shrank, the wire ligature became slack, and the glassware slipped down, creating a drift with the scale. As opposed, in damp environments, or when the tablet was reached by rain, the frame was swollen, the ligature was tightened, and the glassware risked to break. For this reason, it was not possible to keep normal thermometers outdoors until the second half of the 18th century, when metal, glass, or ceramic frames were adopted.

When different thermometric liquids were used, or the alcohol had different ABV (alcohol by volume) concentrations, readings became hardly comparable and scientists complained about the impossibility of a correct interpretation of data and started to cross compare the response of different thermometers dipped in the same bath (Derham, 1709; du Crest, 1765; De Luc, 1772).

In the early instrumental period, the choice of the thermometric liquid in combination with the calibration procedure was crucial. By definition at the calibration points all readings were homogeneous, but the discrepancy increased with the distance from the calibration points, reaching the maximum differences in the middle. In the absence of an absolute reference, when a departure was found, it was not clear which reading, which instrument or which method was better or which worse. Baths at known intermediate temperature were obtained by mixing selected amounts of boiling and freezing water. At the end, it was discovered that mercury is the most linear thermometric liquid, followed by linseed oil as in the thermometer proposed by Newton (Camuffo and della Valle, 2017). Although oil had a good performance, it was soon abandoned because it adhered to the tube making readings difficult. The largest departures from linearity were found with spirit-in-glass thermometers. The typical thermometer produced following the instructions by Réaumur,[45] filled with 'water-of-life' or 'evaporated spirit' 95% ABV, calibrated at melting ice and boiling water, made underestimations that followed the parabolic departure:

$$\Delta t = a_1 t^2 + a_2 t \tag{17.1}$$

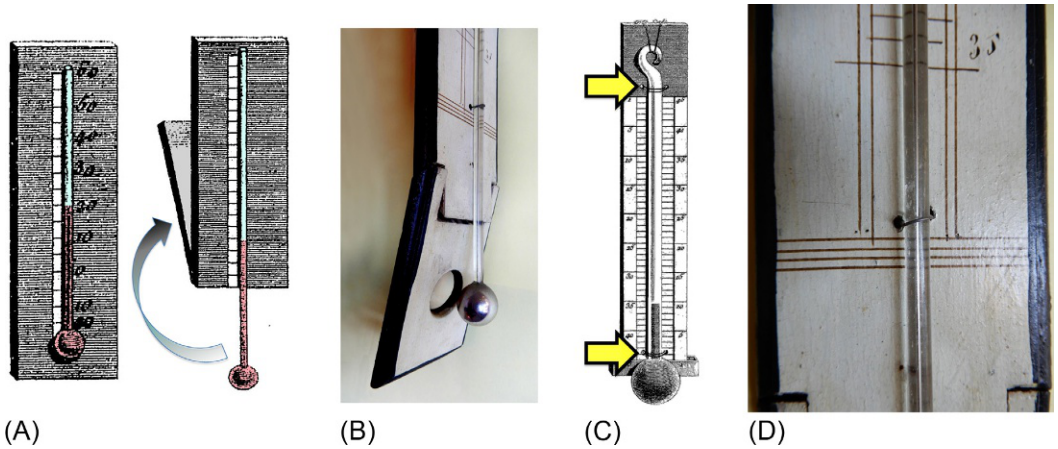

FIG. 17.8 (A) In early thermometers, wooden frames were foldable for calibration, i.e. to dip the bulb into melting ice, and expose it to the steam of boiling water. (B) A foldable Réaumur thermometer. The hole is to hold the spherical bulb. (C) Thermometer with glassware tied to the wooden frame with an iron wire (see *arrows*). (D) Detail of the iron wire that ties the capillary tube. *(A,C) From Cotte (1774); (B,D) Courtesy of Sofia Talas, Museum of History of Physics, Padua University, © used with permission.*

[45] René-Antoine Ferchault de Réaumur (1683–1757).

with $a_1 = 0.0025°C^{-1}$ and $a_2 = -0.2481$, and reached the maximum value −6°C when the ambient temperature was 50°C (Fig. 17.9). The situation was worse with less refined alcohol and the bias increased very much when the alcoholic concentration was below 60% ABV (Camuffo and della Valle, 2016).

Inside the glassware, a certain quantity of thermometric liquid is present, and the empty space is filled with vapour evaporated from the liquid until it reaches the saturation pressure (Chapter 3). When the temperature (and the empty space) changes, some liquid will evaporate, or some vapour will condense, to reach the novel saturation pressure. Inside the free space of the glass tube, the total pressure is the saturation pressure of the liquid, and in such conditions, the liquid is always at its boiling point (Chapter 4). However, boiling is not visible because it is stopped by the vapour pressure reached inside the limited volume. For this reason, an alcohol thermometer has no physical discontinuities when crossing the 80°C that correspond to the boiling point of alcohol at 1000 hPa atmospheric pressure. Simply, when the alcohol thermometer reaches 80°C, its pressure inside the capillary tube equals the external one; when the T<80°C, its pressure is lower (and the glassware resists the external pressure for the capillary curvature), and when T>80°C, it is higher. In the early period, it was easier to produce thermometers leaving some air inside the capillary when sealing the top, and this air altered the internal pressure balance and the thermometer response.

The linearity departure of linseed oil used by Newton (Fig. 17.9) was much smaller. It also followed a parabolic law, but with coefficients $a_1 = 0.0004°C^{-1}$ and $a_2 = -0.0429$, and reached the maximum value −1°C at 50°C (Camuffo and della Valle, 2017).

However, if the calibration was made with calibration points at shorter distance between them, e.g. the Little Florentine thermometer was calibrated with the water of the Arno River in winter as lower reference and the hot summer in Florence as upper reference, the distortion dropped to 0.5°C (Camuffo and della Valle, 2016). Newton, and then Fahrenheit, had the brilliant idea of limiting the upper temperature calibration point to a reference close to the actual range of interest. For this reason, they made reference to the blood temperature (Fahrenheit, 1724) that was a reasonable upper limit for the summer temperature in northern Europe, and was acceptable for medical purposes too.

Another calibration bias in early thermometers resulted from immersing only the bulb in the hot steam or in melting ice, while the tube was at ambient temperature (Nollet, 1749; Cotte, 1774). This and other problems related with the calibration of thermometers are discussed elsewhere (Camuffo and Jones, 2002; Camuffo et al., 2016, 2017).

17.1.6 Self-Registering Thermometers for the Maximum and Minimum Temperatures

In meteorological observations, it was crucial to ascertain the range extremes reached over a given period of time, while the observer was absent. A number of instruments have been proposed, and the two most popular solutions are here described.

A maximum–minimum registering thermometer (Fig. 17.10A,B) was invented in 1780 by Six[46] and later

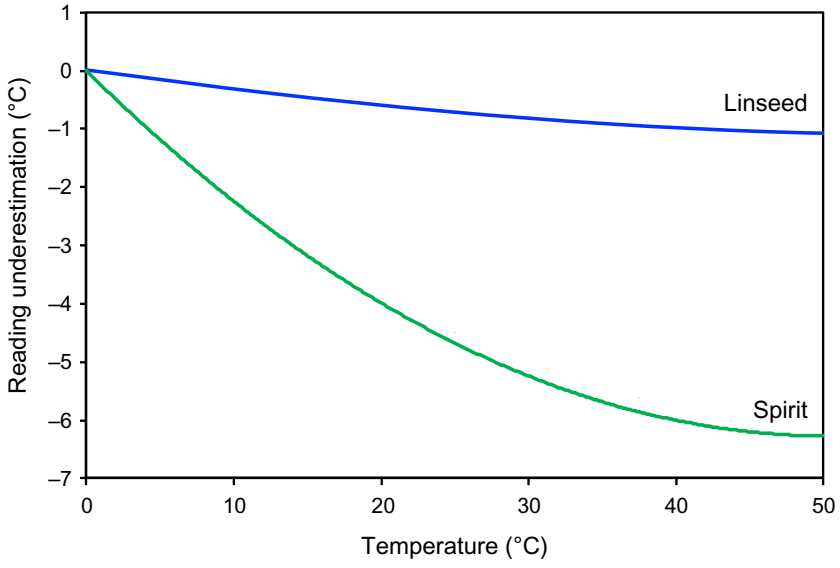

FIG. 17.9 Temperature underestimation when a spirit-in-glass thermometer, or a linseed thermometer, calibrated at 0°C and 100°C, is used.

[46] James Six (1731–93).

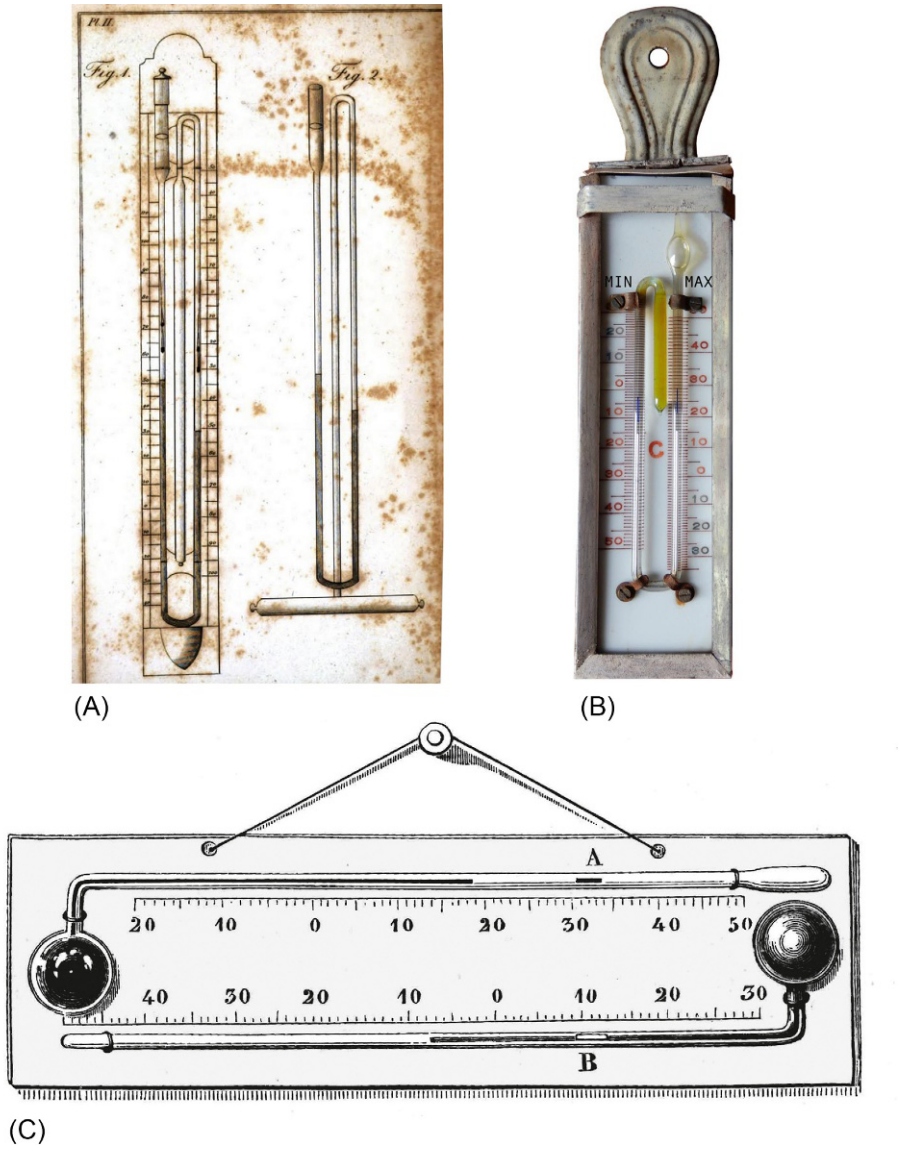

FIG. 17.10 (A) Original drawing of Six's thermometer: mounted on a frame (*Fig.1*) and schematic view of the glasswork with the thermometric liquids (*Fig.2*). (B) Six and Bellani self-registering thermometer. (C) Rutherford maximum and minimum self-registering thermometers. The maximum thermometer (mercury) is higher, with index A; the minimum (spirit) is lower, index B. *From (A) Six (1794); (C) Ganot (1960).*

improved by Bellani[47] (Six, 1794; Brewster, 1832; Austin and McCollen, 1980). It consists of a U-shaped glass tube with two separate temperature scales set along each arm of the U, one for the maximum and one reversed for the minimum temperature. The tube is filled of alcohol, and mercury in the lower part. Both arms terminate with a sealed bulb, with different shape. The bulb at the top of the minimum scale is a long cylinder, full of alcohol; the other bulb is smaller and contains a bubble of alcohol vapour. The mercury in the lower part of the U tube is to give motion to two small rod-indices, one for the maximum and one for the minimum temperature, which move for the push of the mercury column. The indices are made by enamel but contain a steel core, and they are shaped to freely move within the tube and allow the spirit to pass, but not mercury. When the mercury advances, it pushes the indices, but when it recedes, they remain in the highest point where the mercury stood, i.e. the most extreme temperature, until they are reset with a magnet.

A pair of maximum and minimum self-registering thermometers (Fig. 17.10C) was invented in 1794 by John Rutherford.[48] The instrument (Rutherford, 1795, 1796; Brewster, 1832; Leslie, 1838) is composed of a spirit

[47] Angelo Bellani (1776–1852).

[48] Some confusion is made about the name because the instrument description was communicated by the famous Daniel Rutherford (1749–1819), MD, FRS (Medicine Doctor, Fellow of the Royal Society), Professor of botany at the University of Edinburgh and joint founder of the Royal Society of Edinburgh. Daniel Rutherford made the communication on behalf of John Rutherford, MD (Medicine Doctor), of Middle Balilish who was not member of the Royal Society and could not make presentations at the Royal Society.

thermometer for the minimum temperature and a mercury thermometer for the maximum. Both are fixed on the same frame, but have independent scales. In the most popular mounting, both thermometers are horizontal, the index of the maximum thermometer is of steel, and the index of minimum is of glass with a small knob at each end. In the maximum thermometer, the index is pushed by mercury when the temperature rises, and is left in the position of the highest temperature. The original paper (Rutherford, 1795) had the explanation with indices made with a conical piece of ivory but the friction with the interior of the tube advised to change with steel and use a magnet to reset it, as in Six's thermometer. In the minimum thermometer, the index lies in the spirit, which freely passes around when the temperature rises; however, when the temperature falls the index is carried back, so that it remains in the position of the lowest temperature, until it is reset. This instrument was used in most weather stations.

17.1.7 Metallic and Bourdon-Tube Thermometers

Metallic thermometers have been conceived as small portable instruments (i.e. pocket instruments) and are known since the second half of the 18th century, although the inventor remains unknown (Middleton, 1966). The most popular metal sensors were the bimetallic strips and the Bourdon tube.

The bimetallic strip is composed of two strips of different metals joined together throughout their length. The metals are selected with different expansion coefficients. One end of the strip is fixed to a supporting frame; the other end is free to move, but is connected with a detection mechanism. When heated, the different expansions cause the strip to bend in a certain direction; when cooled, in the opposite one. The displacement of the tip is amplified with mechanical systems, and transmitted to a recording pen or other devices. In 1862, Hipp[49] patented[50] a self-registering instrument (Fig. 17.11A), based on a bimetallic spiral connected to a telegraph transmitter in Morse code (Imray, 1862) that was soon adopted by weather stations and ships. The English instrument maker Short and Meson Ltd. produced self-recording thermometers with bimetallic spiral (Shaw, 1932).

Breguet[51] invented a three-metal thermometer (Fig. 17.11B) based on the unequal expansion three metal strips, made of platinum (upper, less sensitive), gold (middle, with intermediate expansibility), and silver (lower, more sensitive), passed through a rolling mill to form a very thin and long metal ribbon (Ganot, 1860). Three metals with gradual expansibility were used to avoid too strong internal mechanical stress and fracture of the ribbon. The ribbon was coiled in spiral form, with one end fixed to a frame, and the other end free to rotate with a needle that indicated the temperature over a circular scale. When the temperature rises, the differential expansion forces the spiral to unwind itself moving the nail. The circular scale was graduated in Celsius by comparison with a standard mercury thermometer.

In 1849, Bourdon[52] patented the Bourdon tube (Fig. 17.11C) in France and in United Kingdom as a liquid-in-metal sensor. It is composed of a flat tube, with a large radius of curvature, made of very thin brass or other metals, and filled with alcohol. One end of the flat tube is fixed and the other is free. When heated, the alcohol expands more than the metal, exerts higher pressure inside the tube, and the radius of curvature increases. As opposed, when cooled, the alcohol pressure is lower and the radius of curvature decreases. The temperature is measured by the travel of the tip of the tube. The Bourdon tube has also been used as pressure gauge, and is more famous to detect pressure than temperature. The French instrument-maker Richard Frères, Paris, active since 1880s, produced Bourdon-tube thermographs (Gerosa, 1898; Crestani, 1931; Shaw, 1932).

Metallic thermometers had some key advantages, i.e. they were robust, and could be connected to a pointer with an ink pen. Combined with a clock-driven drum, they became a popular recording instrument: the mechanical strip-chart recording thermograph (Fig. 17.11D). A thermograph in association with a hair hygrometer became a thermo-hygrograph, and registered both the temperature and the *RH* on the same strip chart.

The mechanical thermo-hygrograph became the most popular recording instrument in museums and galleries. Its quality, however, is rather poor, for a number of reasons connected to the instrument and the recording apparatus. Mechanical instruments driven by clockwork and recording with an ink pen became outdated in the second half of the past century, when the electromechanical generation appeared, and became even more outdated with the advent of electronic instruments and dataloggers. However, the early sensors (the sensors, not the mechanical recorder!) are still valid. This instrument is mentioned here among the early technology and will be discussed later in this Chapter to highlight that although it was developed early, it still is used even today for temperature recording in museums.

[49] Matthaeus Hipp (1813–93).

[50] Great Britain, Patent Office, Patent No. 2574 19 Sept. 1862 entitled 'improvements in apparatus for telegraphing and signalling by means of electricity'.

[51] Louis François Clément Breguet (1804–83).

[52] Eugène Bourdon (1808–84).

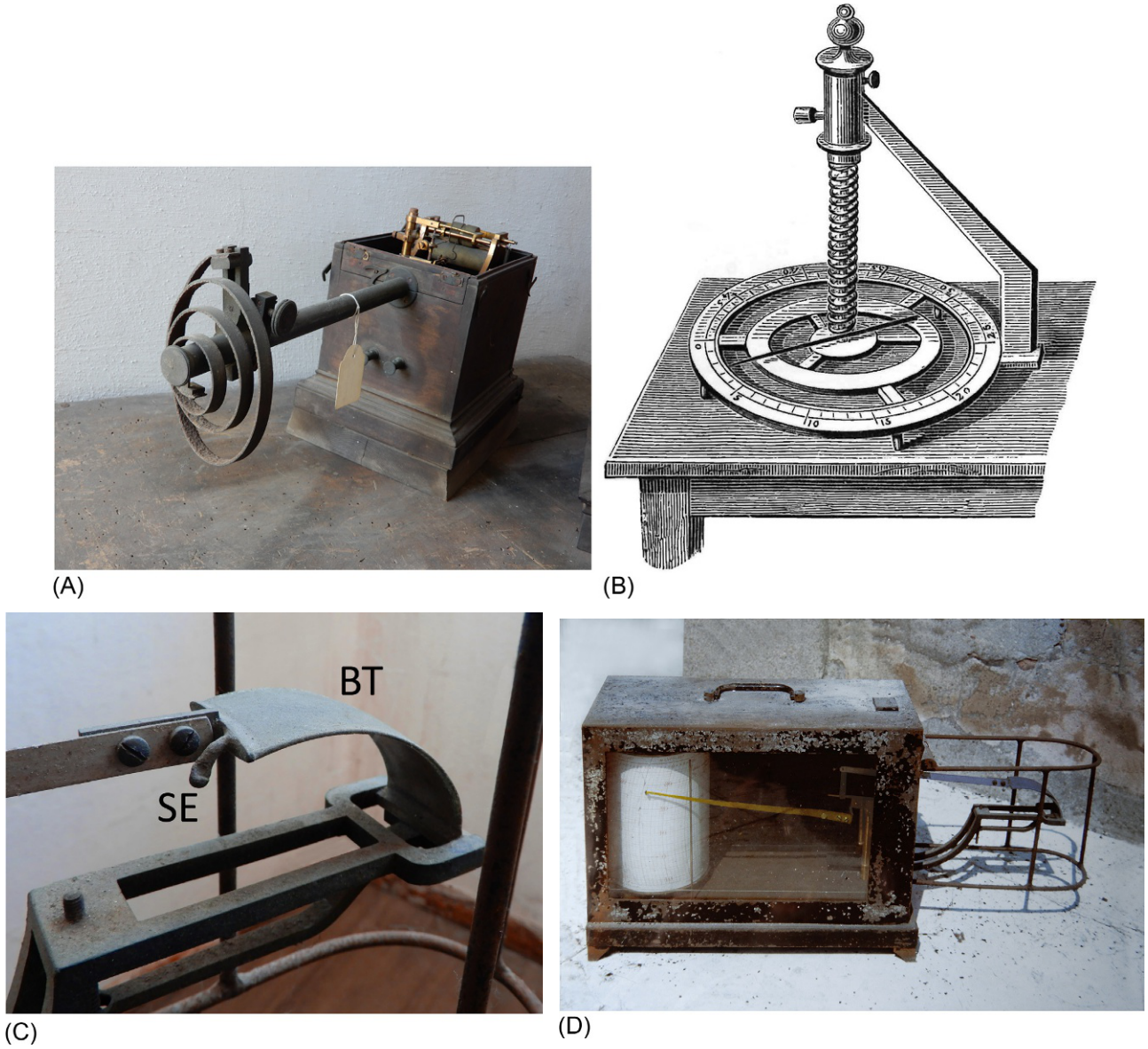

FIG. 17.11 (A) Hipp bimetallic sensor with telegraph transmitter. (B) Breguet three-metal spiral thermometer. (C) Bourdon-tube (BT) is a flat curved tube used as temperature sensor in Richard Frères mechanical thermographs. The sealed end (SE) of the thin duct to insert alcohol is visible. (D) Richard Frères mechanical thermograph, Paris, with the rotating drum and the pen protected inside the box, while the Bourdon-tube sensor it external to it to reach equilibrium with the room temperature. *(A,C,D) Courtesy of Valeria Zanini, INAF—Astronomical Observatory, Padua, © used with permission); (B) From Ganot (1860).*

17.1.8 Differential Thermometers and Actinometers

Leslie[53] studied the diffusion of heat (Leslie, 1804, 1838) and invented the differential thermometer (Fig. 17.12A). The instrument consists of a tube, bent twice at right angles, upon each end is a bulb with an air pocket inside. The U shaped tube includes a coloured liquid. When both bulbs are at the same temperature level, the two vertical liquid columns will reach the same height. When one bulb is heated, the liquid will be displaced and the two columns will have uneven levels.

The differential thermometer, known as Rumford's[54] thermoscope (Fig. 17.12B), is very similar to Leslie's[55] but with longer horizontal connection tube, and the

[53] John Leslie (1766–1832).

[54] Benjamin Thomson, Count of Rumford, alias Benjamin Graf von Rumford (1753–1814).

[55] In reality, Leslie's and Rumford's instruments are very similar, but the two Authors published the same year, so that it is impossible to establish who first had the idea.

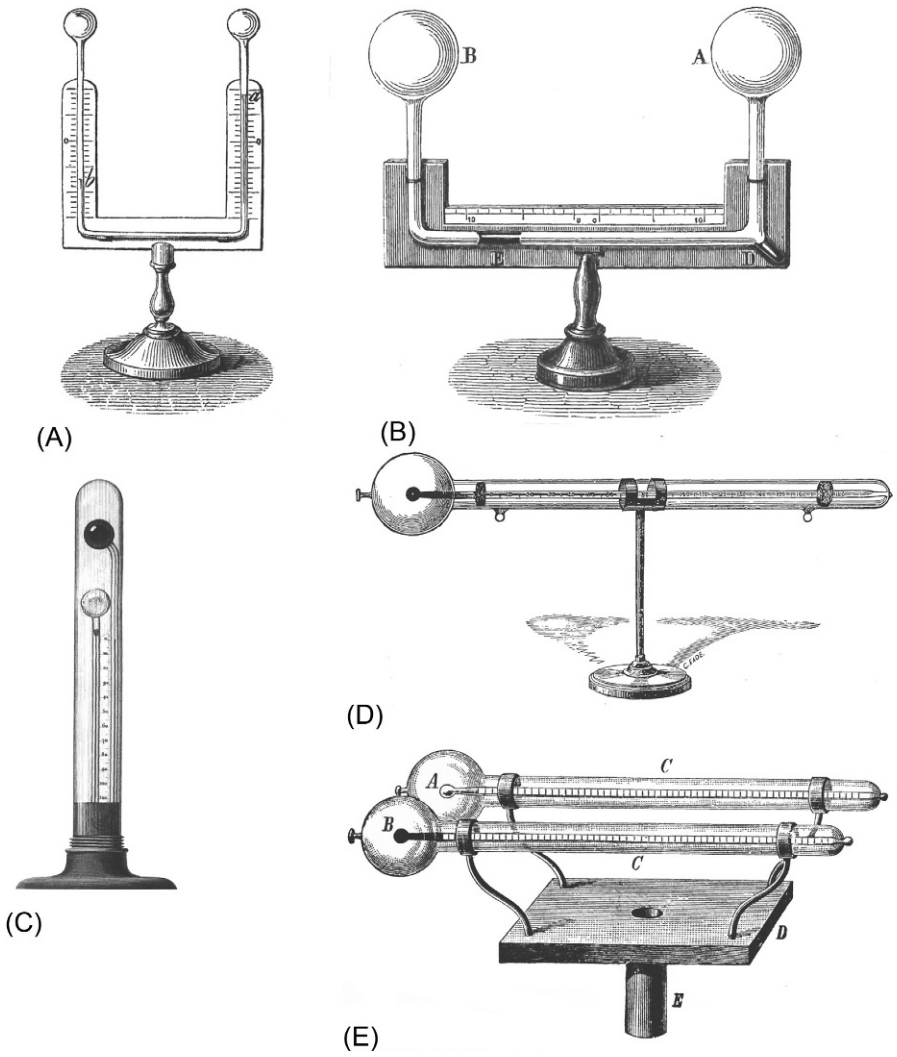

FIG. 17.12 (A) Leslie differential thermometer. (B) Rumford's thermoscope. (C) Leslie photometer with two thermometers: one with transparent, and one with black bulb. (D) Hick's improved black bulb thermometer kept in a vacuum environment. (E) Arago-Davy actinometer composed of two Hick's thermometers but one with transparent, and one with black bulb. *From (A,B) Ganot (1860); (C) Leslie (1804); (D) Hicks (1875); (E) Gerosa (1898).*

temperature difference is read after the displacement of an index located in the middle of the horizontal tube (Rumford, 1804).

The solar radiation was detected by comparison of the different heating on a *Leslie thermometric photometer* (Fig. 17.12C), derived from a differential thermometer: it had two identical air thermometers, but one with transparent bulb, and one with blackened bulb (Leslie, 1804; Comstock, 1853; Chen, 2005). Blackening was made holding the bulb in the smoke of burning pitch (Foote, 1856). In the upper part, the bulbs included air pockets, and the liquid in the lower U-shaped manometer was alcohol. The differential thermometer was enclosed within a glass case to avoid wind disturbances. To be compact and portable, it had one bulb above the other. The weak points of this instrument were the low sensitivity and the long time needed to reach equilibrium, i.e. 40 min (Buchwald and Franklin, 2005).

In order to overcome the problem of the low sensitivity and reduce the external disturbances, the thermometer was kept in the vacuum, as stressed by James Hicks (1875) (Fig. 17.12D). The most popular solution with two separate thermometers is the *actinometer* (Fig. 17.12E) proposed by Arago and Marié-Davy.[56] It is composed of two identical thermometers, one with blackened and one with bright bulb, either exposed or in vacuum, following the Hicks style (Gerosa, 1898; Abbe, 1905; Pulling, 1919). However, even in the vacuum, the instrument had low sensitivity.

17.1.9 Thermometer Screen

A thermometer furnishes the temperature of the sensor, which is not exactly the same as that of the air, as each sensor responds in a different way to the *IR* radiation as well as with regards to conductivity and convection. For

[56] Dominique François Jean Arago (1786–1853); Edme Hippolyte Marié-Davy (1820–93).

this reason, every thermometer will provide a (slightly) different reading, and if different kinds of thermometric transducers are used it is difficult to establish which reading is better respondent to the actual value of the air temperature. This problem is not solved with calibration. When different kinds of well-calibrated sensors are immersed in a water or oil bath for comparison, they give the same output because their temperature is controlled only by the bath temperature. In fact, the external *IR* radiation is shielded by the bath vessel or is completely absorbed after the radiation has penetrated a few micrometres into the liquid. The specific heat of water is three orders of magnitude greater than that of air. Sensors responding in the same way to the air temperature, but not to the radiometric forcing, may provide different readings and generate confusion. Screens may attenuate this problem, but will not solve it.

The thermal equilibrium of the sensor includes not only the conductive heat exchange with the air that comes into contact with the sensor but also the energy obtained from visible or *IR* radiation from remote bodies. In fact, the air is transparent to visible light and to the main part of the *IR* spectrum. The incoming radiation is an important source of error and may cause departures from some tenths to several degrees. A number of screens have been invented to reduce the bias (Burnt, 2012), although it is never possible to reflect completely the energy income or avoid the nocturnal radiative loss.

The shield against weather injuries (e.g. rain, hail, sunshine) changed over time, e.g. a metal sheet, a curtain, a louvered wooden or metal box, or the multiplate assembly made of PVC or metal. It is useful to review the situation since the origins of instrumental records because the adoption of a screen is crucial for the quality of temperature and relative humidity records.

The early Medici Network (1654–70) started with a virtuous comparison of two identical thermometers, hung on the same wall, built outdoors aligned with the east–west direction. One thermometer was in the shadow, facing north, and one exposed to sunshine, facing south. This was the earliest protocol of regular measurements and provided excellent records (Camuffo and Bertolin, 2012a,b).

The earliest screen was in Padua, a cardboard applied by Giuseppe Toaldo in 1785 to shield the thermometer that was exposed to north, but in certain periods was reached by solar radiation (Camuffo, 2002a).

The *Societas Meteorologica Palatina*, Mannheim, flourished in 1780–95, recommended thermometers suspended outside in the shade, away from buildings (Hemmer, 1783). This was not a screen in the modern design, but was effective against direct solar radiation, like the Medici Network protocol.

Middleton (1966) suggested that screens started to be used after 1835. In the early period, thermometers were sheltered from rain that would have damaged the instrument, especially swelling the wooden tablet.

The most common situation after the second half of the 18th century was to take outdoor temperatures with thermometers exposed out of windows facing north. To resist to weather, the window thermometers were enclosed in a glass cylinder with a top, and had the scale made of porcelain, glass or ivory. The support was made of metal (Fig. 17.13A).

In terraces of gardens, the most popular outdoor shelter was very simple: essentially, it consisted of a wooden frame, where thermometers could be hung, and a roof to shield them from rain. Although the nomenclature was uncertain, this type of shelter was called 'stand' (Fig. 17.13B and C).

Later, more attention was paid to solar radiation, both direct and indirect, which was sheltered in different ways, in all directions. The most popular solution was to adopt louvered wooden boxes of various shapes, with or without bottom, with forced or natural ventilation. A shelter that considered the solar radiation was called 'screen' (Middleton, 1966). In several cases, a bias for temperature maxima prior to 1860 may be due to unshielded thermometers (Böhm et al. 2010) or inadequate exposure of them.

When in 1860s the National Meteorological Services started to operate, and opened the discussions in view of coordination, various types of screens were used. For instance, in Italy, Denza[57] recommended a big wooden cage (Fig. 17.13D) to be installed externally to a north-facing window (Denza, 1882, Camuffo, 2002b), and this solution became popular also elsewhere (Parker, 1994) because most weather observations were taken in astronomical observatories and were conceived integrated with the scientific activity performed inside the building: the astronomer observed the near and the far sky from the same place. Metal shields were used in France, Saxony (Germany), Canada (Kingston, 1874), and Italy (IMAIT, 1872). In the Paris Observatory, a metal thermometer shield was attached externally to the terrace, on the northern side (Fig. 17.13E). It is composed of a cylindrical shield and is topped with three cones, all in metal. The cover, composed of three spaced metal cones to favour ventilation and reduce radiant heat emission, can be considered a precursor to the multiplate screen. In the same Observatory, thermometers were also kept in the free air, but protected by a canvas awning (Fig. 17.14A,B), and the readings were compared between them. In Italy, the metal sheet had a regular array of small holes to favour ventilation (Fig. 17.13F). The shield was fixed to a mobile

[57] Francesco Denza (1834–94).

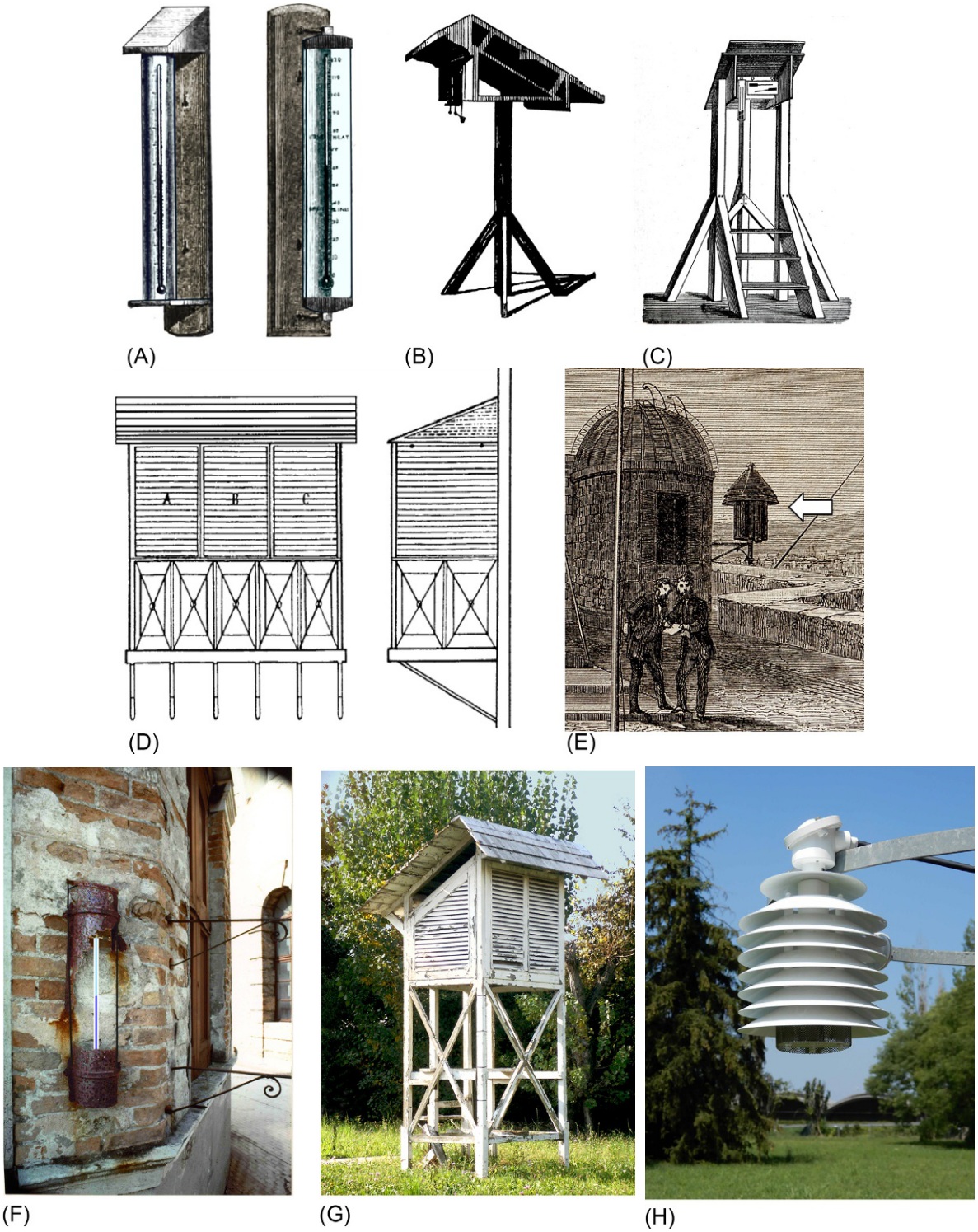

FIG. 17.13 (A) Two window thermometers resistant to weather. (B) Side view of a stand to protect from rainfall (and partially from direct solar radiation) used in the 19th century. (C) Front view of a stand. On the frame, an August psychrometer and Rutherford's minimum and maximum thermometers are visible. (D) Front and side view of the Denza's big wooden cage attached to the wall used in Italy to protect from rainfall, direct and diffuse solar radiation. (E) Metal cylindrical shield with cover composed of three metal cones on the terrace of the Observatory, Paris. (F) Metal thermometer screen in the Astronomical Observatory, Padua, with a regular array of small holes to favour ventilation. Rust has completely eroded the central part of the screen. The thermometer was in the illustrated position. (G) The traditional Stevenson screen with louvered wood walls. It includes a bottom layer to protect from soil thermal emission. It needs maintenance to avoid paint from peeling off. (H) Multiplate aluminium screen. *From (A, B) Negretti and Zambra (1864); (C) Gerosa (1898); (D) Denza (1882); (E) Flammarion, 1872.*

arm to be easily read; however, often it was directly fixed to a wall. In some way, it was derived from the tradition of the window-thermometers.

In the same period, Stevenson[58] proposed a new wooden screen, with double row of louvered boards and no bottom (Stevenson, 1864). After some improvements, and the addition of the bottom, it became the standard screen for weather stations (Fig. 17.13G), i.e. a box made of a low conductivity material (generally wood), painted white inside and outside to reflect visible radiation, that enables good ventilation while minimizing the effects of radiant heat. The roof is made of two layers of wood with free air spacing between them, and the floor is slatted to permit free air circulation. In the northern hemisphere, the door is on the north facing side and enables the personnel to observe or maintain the instruments. The Stevenson screen should be placed between 1.25 and 2 m above the ground. Meteorological shelters need to be cleaned frequently and repainted every year, but this recommendation is often neglected. In days of strong sunshine and calm wind, they may overheat by +2.5°C, and in clear night the thermal loss may reach −0.5°C (WMO, 2008). During precipitation, the wet surface of the louvered wood generates the wet-bulb temperature. Recently, Stevenson screens were produced with plastic and fibreglass, to improve the quality and reduce maintenance costs. In United Kingdom, plastic and wooden types have been compared between them, and very small departures were observed, e.g. average 0.1°C and 0.25°C for extremes. Also, *RH* departures were in the order of 1% (Perry et al., 2007). At least in mild climate regions, plastic louvered screens may be a good alternative to the traditional ones made of wood, especially in view of the problem of the deterioration of painted wood. Further research is due to verify the behaviour in different climate conditions.

Wild[59] studied the performances of wooden and metal screens. When in 1860 he was director of the Bern Observatory, he adopted a cylindrical double screen, composed of two thin metal sheets, using zinc as good reflector, with conical top and open bottom, like the model at the Observatory in Paris. When in 1868 he became director of the meteorological observatory in St Petersburg, he adopted a louvered box screen, similar to the Stevenson screen, but made of zinc. Then, in 1874, he returned to the metal cylindrical screen, placed outside, facing north, similar to the metal screen in Paris, but was kept inside a wooden box for further protection (Wild, 1874; Middleton, 1966). However, his solutions needed improvement and did not convince most colleagues from other nations. Criticisms were that in the daytime the temperature inside the screen was higher than the air outside, and better results were obtained by taking away the Wild screen and hanging the thermometer in the outside wooden shelter.

In 1892, Assmann[60] returned to the idea of a metal screen, composed of two concentric cylinders with the thermometer in the axial position, and used this method in his aspirated psychrometer.[61] Similarly, WMO (2008) suggests two concentric cylindrical shields with the thermometer placed on the axis of them, possibly with fan ventilation, following the style of the aspirated psychrometers.

Aitken[62] was not satisfied of the performances of the Stevenson screen, especially the 'thermal inertia' of wood. He returned to metal, and suggested a louvered cylinder with a protecting cone on the top (Aitken, 1921). To avoid air stagnation inside the shield employed for the maximum temperature thermometer, he suggested a chimney on the top to extract warm air. Similarly, he suggested a chimney on the bottom of the shield for the minimum temperature. However, this solution was complex and required a shield for each thermometer, and was disregarded.

The Aitken idea was very reasonable, except the drainage, and his circular, louvered screen became the so-called *multiplate radiation shield* for temperature and *RH* sensors (Fig. 17.13H). Compact size and light weight made possible new applications, e.g. to detect temperature and moisture profiles in meteorological masts or for air pollution studies. The earliest models were made of aluminium (Wood, 1946). In addition to aluminium, nowadays they are produced with plastic, with an acrylic white coating. The metal and the plastic types have been compared between them and with wooden boxes. Either metal or plastic plates, they shown excellent results, with overall mean daytime difference −0.023°C and night-time −0.018°C. The overall aluminium-plastic difference was 0.021°C and had standard deviation of 0.13°C (Hadlock et al., 1972). The multiplate screen is better resistant to outdoor environments and over time it has substituted, or is substituting, the traditional Stevenson screen.

[58] Thomas Stevenson (1818–87).

[59] Heinrich Wild (1877–1951).

[60] Adolf Richard Assmann (1845–1918).

[61] See Chapter 18.

[62] John Aitken (1839–1919).

Other more sophisticated screens have been designed to house electrical-type temperature sensors. They are characterized by a single or double, highly reflective shield (mirror or white paint) with natural or forced ventilation. The shield may consist of one or two concentric cylindrical tubes and a single or double dome or multiple plates, made of metal, plastic, or mirrored glass. In windy, rainy regions, the radiation error is negligible, ventilation is not necessary, and the shield must protect the sensor against rainfall arriving from any angle. In sunny, low-wind regions, a motor blower to force ventilation (e.g. 3 m s^{-1}) around the sensor should be applied to reduce stagnant air and overheating. For nonventilated shields, the overheating bias varies with the wind speed and insolation.

Good results were obtained with a double-walled glass tube, silvered on the interior surface, then evacuated and sealed, like heavy-duty vacuum bottle, but with an open bottom. The cylinder is kept vertical, with the open bottom facing downwards and a blower located at the upper top that continually forces ventilation inside. In this case, the error is within ±0.05°C.

Indoor measurements also need a screen, but if no direct solar beams or incandescent lamp light reach the sensor, the screen may be less sophisticated. Good results are obtained with two methods commonly used for radiosondes: (1) a tube made of white polystyrene foam that is reflective in the visible window, is a bad conductor, and has a very low thermal capacity; and (2) a tube built with a very thin foil of aluminium, reflecting on the outer side and blackened on the internal one. In the case of a metal shield, disturbance is reduced with a double concentric shield and this caution can be used in the absence of forced ventilation. A common size is a cylinder of 10 cm diameter and 20 cm height and the sensor placed in the middle of the tube. Only if the sensor is located in sites with homogeneous temperature and without relevant sources of radiant energy (e.g. windows, incandescence lamps), no shields are needed.

17.1.10 International Agreements and Weather Stations in 1870s

Reasonably accurate instruments and protocols to measure meteorological variables were available around mid 19th century with the occurrence of a series of fundamental events, as follows. National weather services were created in Europe. In 1860, Airy[63] of the Greenwich Observatory and Urbain Jean-Joseph Le Verrier[64] of the Paris Observatory signed the first international agreement to collect British and French observations and to forecast marine storms. After the preparatory conferences in Leipzig (1872) and Vienna (1873), the *International Meteorological Committee* was established in 1873, followed by a conclusive conference in Rome (1879) for the items left uncertain that needed further experimentation. In 1950, this Committee was transformed into the *World Meteorological Organization*.

A visual example of a Meteorological Observatory in this period is given by Flammarion (1872), who described the Paris Observatory. The situation is particularly interesting because it shows the state of the art in this crucial period when modern meteorology was developing. On the roof, the Observatory had the dome for astronomical observations and a terrace for meteorological instruments (Fig. 17.14). Additional measurements were taken in the garden to study how the variables changed with the level above ground, or to test various instruments. The same effort was made by the national weather services in all countries.

Thermometers were exposed in three different ways. An electrical thermometer was held with a mast 5 m above the terrace. A metal shield composed of a cylinder and conical top was attached externally to the terrace, on the northern side. In the free air, but sheltered under a canvas awning, the picture shows a number of instruments. On the left, a cistern barometer. A vertical frame contains an array of thermometers kept horizontally. Most probably, the thermometers include a mercury, or an alcohol-in-glass thermometer for the hourly temperature readings, and in addition the two Rutherford self-registering thermometers, one for the maximum and one for the minimum temperatures. On the right, an August psychrometer[65] with a long wick entering a water reservoir. Finally, a Leslie differential thermometer with one blackened bulb to measure the solar radiation.

The sensor for the wind speed was a four-cup Robinson anemometer that constituted a very relevant improvement compared to the uncertain pressure exerted on a tablet.

The sensor for the wind direction was a flat metal vane, shaped like a comet, built with the old technology and likely had poor dynamic performances. The direction was read on the site from a pointer fixed to the vane. The pointer rotated over a metal circle fixed to the terrace with a letter for the four compass directions (i.e. North, East, South, and West) and several intermediate tags. The observer had to count the tags from/to the nearest main compass direction and report the reading on his log.

[63] George Biddel Airy (1801–92)

[64] Urbain Jean-Joseph Le Verrier (1811–77).

[65] See Chapter 18.

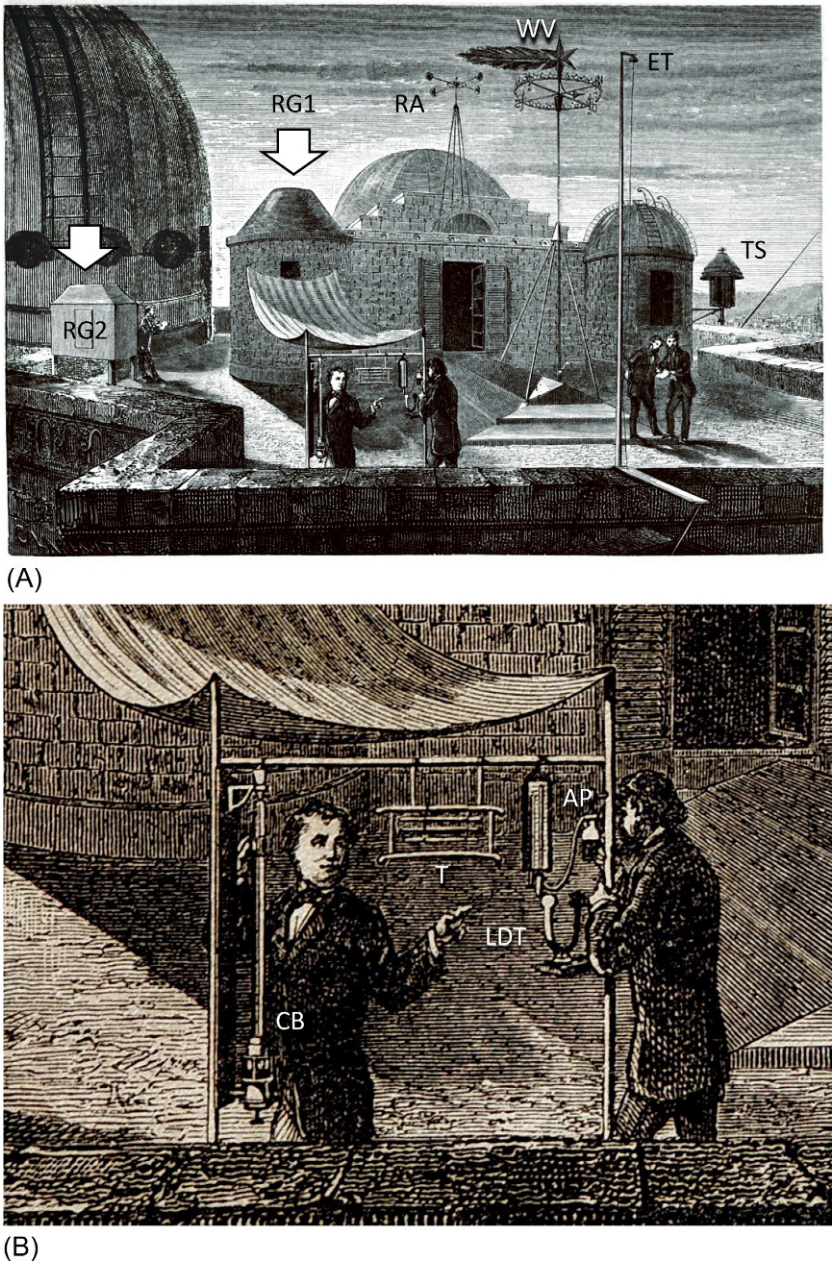

FIG. 17.14 (A) Meteorological instruments on the roof of the Paris Observatory. A four-cup Robinson anemometer (RA). A comet-shaped wind vane (WV) that rotated above a metal circle with the four compass directions and intermediate tags for on-site readings. Two meteorologists on the right side seem to be reporting the readings on a paper log. Inside the truncated cone roof of the turret *(white arrow)*: a raingauge (RG1). Another raingauge (RG2) is on the left, also with *white arrow*. On the mast, 5m above the terrace, an electrical thermometer (ET). On the right side, the metal thermometer screen (TS) composed of a cylinder topped with three cones. (B) Detailed view under the canvas awning: cistern barometer (CB); array of three Réaumur thermometers (T): one of them was normal, and the other two Rutherford's maximum and minimum thermometers; August psychrometer (AP) with wick and water reservoir; Leslie differential thermometer (LDT) with U shape and one bulb white and one black, used as a photometer *From Flammarion (1872).*

Two raingauges were on this terrace. One was installed on the turret with truncated cone roof that hosted the catchment funnel.[66] Another raingauge has the appearance of a big box with a funnel on the top. Other raingauges were located in the garden to monitor the difference between the amount of rain collected at different elevations.

In this period, in United Kingdom, Airy (1874) presented a precise list of instruments existing at the Greenwich Astronomical, Magnetical and Meteorological Observatory. Several thermometers were in use: dry-bulb thermometers by Newman and Glaisher; wet bulb by Negretti and Zambra; maximum self-registering thermometers, both wet and dry; the same for minimum, also Negretti and Zambra. They were kept outside, some of them on a mobile vertical board that was continually moved to avoid solar disturbance. A self-registering radiation thermometer with blackened bulb also from Negretti and Zambra. The humidity was in addition compared with a Daniell hygrometer.[67] For wind, since 1866,

[66] Details about the funnel, reservoir, and instrument are shown in Chapter 21.

[67] See Chapter 18.

the Observatory used a self-registering Osler anemometer produced by Newman and modified by their technician. A pencil pushed by the wind force made a mark upon a paper affixed to a board, which was moved uniformly. In 1866, a Robinson cup anemometer was also mounted. A pencil automatically recorded the wind speed. Eight rain gauges were used, placed in different locations. Since 1840, the Observatory had a standard barometer built by John Frederick Newman, with glass cistern. This barometer was daily compared with the Royal Society's flint-glass standard barometer. A Negretti and Zambra barometer was added later. The barometer had included a photographic self-registering apparatus. Other instruments existed, for astronomy, magnetism, and other purposes.

When Italy was unified between 1861 and 1870, the first Meteorological Service was founded in 1865 for the navy and in 1876 a second one for general civil purposes. In 1872, the Italian Ministry for Agriculture, Industry, and Trade published the protocol for weather observations, specifying observations, sampling methodology, and instruments (IMAIT, 1872). Temperature was observed with a thermometer, a mercury thermograph for the daily maximum and minimum, and in addition an alcohol thermometer to record the daily minimum and a mercury thermometer for the maximum. Thermometers were placed outside of the window, shielded by a metal screen, fixed to a mobile arm to be easily read. Humidity was detected with a blade psychrometer with centrifugal ventilation. Evaporation was assessed with a screw evaporimeter.[68] Wind was recorded with the anemograph Parnisetti-Brusotti with Robinson cups and flat vane.[69] The upper wind was observed from the cloud movement. Precipitation had precise indication about funnel size, exposure, and so on, but no reference was made about the instrument type. In a next directive, the siphon rain gauge recorder, Palazzo model,[70] was recommended. However, in Italy, a number of weather services existed for specific purposes, and each of them adopted a different type of rain gauge, considered more convenient for their particular aims. Pressure was read on a Fortin barometer. The atmospheric electricity was also measured, as well as other weather phenomena.

Wrapping up, in Paris, Greenwich, and Rome, and in other stations as well, the instruments for temperature, pressure, and wind were similar. Shields were different: Paris shielded thermometers with a metal shield and canvas awning; Greenwich used a mobile vertical board; Rome a metal shield, but also a louvered wooden cage. Raingauges were different and their location was uncertain. Harmonization began with the funnel and exposure. Briefly, some coordination was starting between the meteorological observatories, but further time was needed to reach homogeneity.

17.1.11 Further Developments

Various types of thermometers were developed for temperature measurement for weather records, based on electrical or electronic principles, e.g. the very precise platinum resistors, thermocouples, thermistors, diode junctions. The advancement of technology and the method to gather and transmit readings had a fundamental impact. The main milestones have been in 1842 the use of the telegraph for the transmission of readings, in real time or with daily frequency, to build weather tables and maps for early forecast (at that time named 'prognosis'). Around the mid 20th century, electrical instruments and recorders substituted the mechanical ones. Around the 1970s, the advent of electronic records on dataloggers provided better and less distorted storage of readings, allowed easy data handling, the application of real-time environmental control, and other preventive measures. The recent development of data acquisition and transmission systems changed significantly both the indoor and outdoor microclimate control systems.

The same can be said for weather measurements and climate series. The conclusion is that any long temperature record has a high cultural value, but also contains uncertainties and bias that preserves the memory of the instrument maker as well as of the observer, and the period in which they lived. Long climate series need correction and homogenization to detect the true climate signal and distinguish it from the bias due to instrument changes, observation protocol, sampling time, relocations, screens, and many other factors. This is possible only after a critical analysis of all instruments, calibration, exposure, operational protocol, etc.

17.2 PART 2. MODERN TECHNOLOGY TO MEASURE AIR TEMPERATURE

17.2.1 Introduction: The Choice of the Sensor

Several kinds of reliable sensors are commercially available, not all equally applicable for microclimate study. The principal types are liquid-in-glass thermometers (i.e. mercury or spirit thermometers), bimetallic thermometers; electrical resistance thermometers (metal

[68] See Chapter 18.

[69] See Chapter 20.

[70] See Chapter 21.

resistance sensors and thermistors) and thermocouples. The choice is determined by several factors, i.e. compatibility with the ambient conditions, measuring range, resolution, accuracy, response time, drift, compatibility with the recording instrument, and cost.

Outdoor measurements generally require a much greater temperature range than indoor ones. If the sensor has a sufficiently elevated resolution, by limiting the range and expressing data as a percentage of the range, more accurate measurements can be obtained. In this sense, indoor measurements can be more precise than outdoor ones.

A short description is presented here of the most commonly used instruments, discussing their advantages and limits, especially in view of their application in the field of microclimate analysis and diagnostics.

17.2.2 Mercury-in-Glass Thermometers

Mercury-in-glass thermometers are, or at least were, the most popularly used instrument for routine measurements and a secondary laboratory standard to compare with sensors that undergo rapid ageing or drift. Meteorological station mercury thermometers are some 40 cm long and cover the range −30°C to +60°C with scale division 0.2°C. The advantages of mercury as thermometric liquid are small thermal capacity, high thermal conductivity, small deviation from linearity, high boiling point, and freezing point at −38°C. This is a problem only for mountain sites or polar regions, but with the addition of thallium the freezing point is lowered to −58°C. The change of output, expressed as change of the mercury column height Δh due to the temperature change ΔT, is given by the equation

$$\Delta h = \Delta T \frac{V_0(\beta_1 - \beta_2)}{A} \tag{17.2}$$

where V_0 is the volume of mercury inside the bulb at standard temperature, β_1 and β_2 are the coefficients of volumetric thermal expansion of mercury and thermometric glass, i.e. $\beta_1 = 1.81 \times 10^{-4}{}^{\circ}\mathrm{C}^{-1}$, $\beta_2 = 2.53 \times 10^{-5}{}^{\circ}\mathrm{C}^{-1}$, respectively, and A is the cross-section area of the capillary. The sensitivity of the mercury thermometer is given by the ratio $\Delta h/\Delta T$ and the larger the reservoir V_0 and the smaller the section A of the capillary, the higher is the sensitivity. This can be represented by the equation

$$\frac{\Delta h}{\Delta T} = \frac{\Delta V}{\pi r^2 \Delta T} = \frac{V_0(\beta_1 - \beta_2)\Delta T}{\pi r^2 \Delta T} = \frac{V_0(\beta_1 - \beta_2)}{\pi r^2} \tag{17.3}$$

where r is the capillary radius. This equation shows that sensitivity increases proportional to the bulb volume and with the inverse of the capillary radius squared. However, the larger the volume V_0, the greater the heat capacity and the longer the time constant of the thermometer, so that sensitivity and time of response have opposite requirements.

The main errors of this kind of thermometer are

1. *Thermometer heating:* when the observer goes close to the thermometer for reading the scale, and remains close for too long, the temperature is influenced; also, if the thermometer is not adequately shielded against infrared (*IR*) radiation.
2. *Parallax*: when the reading is made with the eye placed not at the same height as the top of the mercury column.
3. *Emergent stem*: when the temperature of the bulb is not the same as that of the surrounding medium, i.e. when the thermometer is not completely surrounded by one medium having the same temperature. This error may be important for measurements of solid bodies.
4. *Drift*: when the characteristics of the thermometer change slowly with time, e.g. the bulb of the thermometer tends to contract slowly over a period of years, thus increasing the temperatures.
5. *Departure from linearity* from the inequality in the expansion of the liquid and glass.
6. *Capillarity:* this may influence the height of the mercury in the capillary tube.
7. *Elastic errors:* occurs due to exposure to a large range of temperature in a short time or to large changes in external pressure.
8. *Scale division and calibration.*

Spirit or other thermometric liquids are also used for their greater sensibility, resulting from a far larger expansion coefficient, but they have some problems: adhesion to the glass, stronger deviation from linearity, drift due to polymerization and slow changes of the liquid properties as well as breaking of the liquid column. Therefore, their use is possible, but not recommended.

17.2.3 Liquid-in-Metal Thermometers

Liquid-in-metal or pressure thermometers consist of a sensitive bulb, an interconnected capillary tube, and a pressure-measuring device such as a Bourdon tube. They follow an equation similar to the Eq. (17.2), which was discussed for liquid-in-glass thermometers, i.e.

$$\Delta V = V_o\,(\beta_1 - 3\alpha)\Delta T \tag{17.4}$$

but with the appropriate coefficients and β_2 substituted with 3α, where α is the coefficient of linear thermal expansion of the bulb material. In meteorology, this sensor is used to drive the arm of the recording pen of thermographs and, in the United States, this is accomplished according to the Weather Bureau specification No. 450.1201. The time constant is some minutes, so that the short-period temperature fluctuations are smoothed

out. This kind of transducer is used in industry and sometimes in meteorology but is not relevant for microclimate studies.

17.2.4 Bimetallic Thermographs

The bimetallic thermograph is commonly used both in standard meteorological stations and in museums; they are produced under a new guise but with old technology. It is mainly associated with a hair hygrometer and the resulting instrument is the well-known thermohygrograph. The bimetallic sensor is composed of two thin metal strips having different coefficients of thermal expansion roll welded together along one of its flat sides. It provides a mechanical output, i.e. the displacement of the free end of the strip. This end is usually connected with a pen, whose movement is amplified and used to trace the temperature records in clock thermographs. It is useful to remark the main characteristics of this instrument:

1. The thermograph is a *linear* transducer, as the displacement of the free end of the strip is a linear function of the temperature change.
2. The *sensitivity* of the sensor is directly proportional to the square of the length of the strip and proportional to the difference in the coefficients of thermal expansion of the two metals, but is inversely proportional to the thickness of the strip.
3. The *time constant* is a few minutes, so that this instrument smooths out the short-period temperature fluctuations.
4. The *resolution* in the strip chart recorder is generally from 1 to 1.5 mm per °C and the time scale division is 15 min for daily clocks and 2 h for weekly clocks. The resolution in reading the strip chart is some 1°C.
5. The *accuracy* is no better than ±1% of the range, which generally varies between 45°C and 90°C.
6. The *friction* between pen and chart is excessive compared with the force supplied by the bimetallic strip, so that the graph is smoothed out, with underestimation of growing temperatures and maxima and overestimation of decreasing temperatures and minima.

Bimetallic thermographs do not comply with the accuracy required by the EN 15758.[71] standard and are not included in the list of recommended instruments. The most common sources of error are

1. Lack of maintenance and periodic calibration.
2. Exposure in a location, e.g. near room corners where air is stagnant and on the floor, at a height different from that of the exhibits, therefore not representative of the areas where artwork is located.
3. Dirt, dust, and pollution, which increase the friction of the instrument.
4. Excessive friction between pen and strip chart.
5. Corrosion or mechanical damage to the bimetallic strip.

To avoid these causes of error, the instrument requires frequent cleaning. In particular, the bimetallic strip and the pen should be carefully cleaned with alcohol. After cleaning, the instrument calibration should be controlled as well as the fine regulation of the three adjusting screws (i.e. bimetallic element, magnification, and pen pressure). Although monthly control and maintenance is recommended, in the real world, this fundamental operation is neglected.

17.2.5 Platinum Resistance Sensors

Although iron, copper, nickel, and other metals have a temperature coefficient of electrical resistance greater than platinum, platinum resistance sensors are preferred for being noncorrodible and their stability over time, which are important characteristics, especially in humid or polluted environments. The platinum resistance sensor is an electrical resistance made of very pure platinum wire, 0.1 mm in diameter or less, used sometimes as a wire and, in general, wound on a glass or ceramic rod. However, thin deposited platinum films are also common, as well as several types of probes with special windings for different purposes.

For a metal, the electrical resistance $R(T)$ is described by the MacLaurin expansion of the successive powers of the increase of temperature

$$R(T) = R(T_o)\left(1 + a\,\Delta T + b\,\Delta T^2 + c\,\Delta T^3 + \cdots\right) \qquad (17.5)$$

where $R(T_o)$ is the resistance of the sensor at the reference temperature $T_o = 0°C$; ΔT is the temperature change; and a, b, c, … are constants characteristic of the metal used. The platinum resistance is characterized by the following values: $a = 3.968 \times 10^{-3}°C^{-1}$, $b = -5.847 \times 10^{-7}°C^{-2}$, $c = -4.22 \times 10^{-12}°C^{-3}$, but within the interval of meteorological observations, the first two linear terms of the series suffice and provide a very good approximation that is linear within ±0.3% of the whole range. As it presents an excellent stability, the measurements are reproducible within 0.01°C. Another advantage of these sensors is that they are cheap. Metal resistance thermometers should be compared with a standard every year.

17.2.6 Thermistors

Thermistors are essentially semiconductors that behave as resistors with a high-temperature coefficient

[71] See Chapter 15.

of resistance. The electrical resistance varies with the temperature and is usually negative, i.e. decreases with increasing temperature, unlike metals. The response function is an exponential

$$R(T) = R_o \exp\left(\frac{A}{T}\right) \tag{17.6}$$

where the coefficients are constant, and depend on the material used. By differentiating the equation, the temperature coefficient B is obtained

$$B = \frac{\mathrm{d}\ \ln R}{\mathrm{d}T} = -\frac{A}{T^2} \tag{17.7}$$

which has a negative parabolic dependence on temperature. The sensitivity of thermistors varies with temperature but at ordinary values, it is one order of magnitude higher than that of platinum resistance sensors.

It is important to note that thermistors are heated by the current load and that the supply should be very well calibrated in view of the limited natural heat dissipation. Thermistor thermometers should be compared with a standard thermometer every year if they are of good quality or every month if they are of low quality, and recalibrated because the characteristics of the sensors are not very stable and suffer ageing.

The main disadvantage of thermistors is the functional dependence characterized by a nonlinear resistance versus temperature. Linearization is mainly obtained using analogue circuit techniques, but sensor linearization is also possible and has been accomplished producing linear output thermistor assemblies. These consist of two or three thermistors assembled as a single thermistor and of an additional resistor. With an appropriate choice of the elements, these packages are interchangeable within a stated tolerance. Linear response transducers have the advantage of a simpler electronic circuit or data processing and have a homogeneous accuracy on the whole range. Linear thermistors in a selected range of temperatures are obtained with a suitable combination of two subcomponents: a thermistor composite and a resistor set composed of a compensating network of two or three precision metal film resistors. Further details on basic of these and other temperature transducers can be found elsewhere (Schooley, 1986; Doebelin, 1990; Michalski et al., 1991; Nicholas and White, 1994; Lipták, 2003).

A common method to obtain linearization of standard thermistors is to use a Wheatstone bridge circuit (Fig. 17.15) with the resistance sensor $R_T(T)$ that constitutes one arm of the bridge and measuring the output voltage in the deflection mode (i.e. with the bridge out of balance). This is, in general, a linear function of the bridge excitation E (i.e. the bridge battery voltage after stabilization), but a nonlinear function of the resistance of the elements R_1, R_2, R_3, and $R_T(T)$ of the four arms. When the sensor calibration curve $R_T(T)$ is known, and

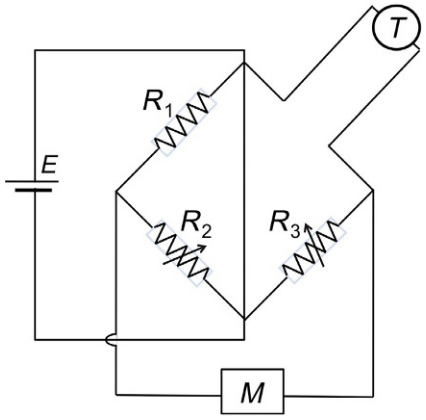

FIG. 17.15 The basic Wheatstone bridge in deflection mode for the case of a thermistor T. The two resistors R_2 and R_3 are adjustable to set up the bridge to make linear the response of T, as seen by the metre M. E is the stabilized excitation voltage.

expressed with a polynomial regression, the appropriate resistance of R_1, R_2, and R_3 of the other three arms can be properly calculated and adjusted, so that the exponential curvature of the sensor is compensated by the nonlinearity of the bridge circuit, which has been appropriately unbalanced.

The metre M, which measures the output voltage across terminals, instantly follows the variations of the sensor, and with an appropriate choice of R_1, R_2, and R_3, the output voltage directly equals the value of the thermistor temperature. Output accuracy and departure from linearity can be better than 0.1°C. Main sources of errors are instability of the bridge excitation; condensation or rainfall, which results in a shunt of liquid water between the thermistor leads if these are not well insulated; and drift of the thermistor or other resistors of the bridge.

For psychrometric measurements, the assembly of two basic Wheatstone bridges for two thermometric sensors T_1 and T_2 is necessary. It is possible to change from the reading of T_1 to T_2, or vice versa, operating on a commutator to control any imbalance between the two sensors. Two adjustable resistors are used to set up the bridge for the thermistor, during the calibration of the device. If the metre has elevated impedance (as most of the electronic meters have), the current across it vanishes and the metre measures the output voltage $e(T)$:

$$e(T) = \left(\frac{R_1}{R_1 + R_2} - \frac{R(T_1)}{R(T_1) + R_3}\right) E \tag{17.8}$$

Both platinum resistance sensors and linear thermistor transducers are very small (Fig. 17.16), accurate (better than 0.1°C), repeatable, reliable, linear or transformable into linear, interchangeable within 0.1°C, and fast response, e.g. time constants <1 s can be found. However, it is advisable to buy one or some dozen(s) of sensors and calibrate all together in a calorimetric bath.

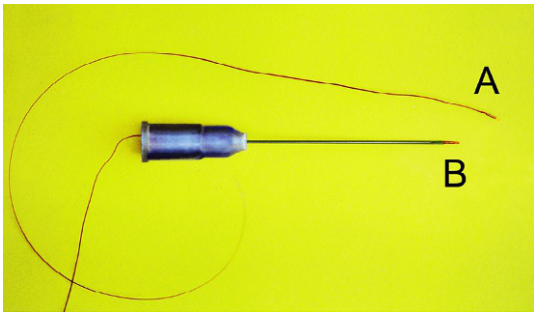

FIG. 17.16 Small thermistors used for fast response in psychrometers: one is free (label A) and one is inserted into a hypodermic needle (label B), forming a fast response probe.

It is then possible to identify those that provide the closest responses, so that they can be substituted for each other or match two or more of them with a very similar response. In practice, the precision of 0.1°C is satisfactory in most cases and matching of the order of ±0.01°C can be done without difficulty. Thermistors are more sensitive than platinum resistance transducers.

17.2.7 Thermocouples

Thermocouples are based on the *Seebeck effect*, i.e. a small thermoelectric current is generated when two different metal wires are put into contact at both ends with their junctions having a different temperature. If one junction is open, a contact electromotive force is generated. The current, or the electromotive force, is to a first approximation proportional to the temperature difference ΔT between the two junctions. A better approximation is obtained with a MacLaurin expansion with the second power of ΔT. The electromotive force for some of the most common junctions is reported in Table 17.1.

The strongest electromotive forces are obtained with the less-expensive junctions, not with metals that are generally used to resist high temperatures. Metals used for thermocouples should be carefully aged by electrical annealing because the electromotive force is sensitive to mechanical deformations.

The main advantages they offer are that they have very low sensitivity to *IR* radiation and short time constant, of the order of 1 s. If more than one set of thermocouple junctions is used in series, the electromotive force is increased proportionally to the number of junctions.

TABLE 17.1 Electromotive Force of Some of the Most Common Junctions

Junction	EM force (μV/°C)	Junction	EM force (μV/°C)
Iron–constantan	52	Copper–constantan	43
Copper–manganin	41	Manganin–constantan	41
Chromel–alumel	41	Platinum–constantan	34
Platinum–rhodium	6.4		

As thermocouples respond directly to differences in temperature, they are convenient to measure temperature gradients. However, the wire is thermally conductive and in the case of gradients, or different thermal levels between a surface and the air, it may transport heat and form a thermal bridge, attenuating the temperature difference. Thermal bridges can be avoided if they are long enough to minimize the heat transport from one joint to another. With this precaution, they are convenient to measure the wet bulb depression in psychrometers, as this instrument requires better accuracy in detecting the temperature difference between two sensors than in knowing the exact value of the dry bulb thermometer. However, the electromotive force generated by the wet bulb depression is very weak. The sensitivity of a thermocouple to temperature changes is much lower than that of a platinum resistance sensor and particularly to that of a thermistor.

For absolute temperature readings, thermocouples need a cold reference junction that was realized dipping the cold joint in a bath of melting ice. This fact limits the practical use of these sensors. Another alternative is to compensate the cold junction temperature by using a resistance bridge compensation circuit (WMO, 1986, No. 622) or other electronic methodologies. The change of resistance of the thermocouple with changing ambient temperature creates an out-of-balance bridge potential, compensating for the missing cold junction. A further possibility is to measure with an independent thermometer the reference temperature at one junction of the thermocouple and then measure the difference in temperature at the other junction.

17.2.8 Quartz Thermometer

In this instrument, the sensor is a quartz piezoelectric resonator that is connected to an electronic solid-state oscillator. The latter supplies a small amount of power to the resonator that acts as a highly selective filter that holds the oscillation frequency very close to the natural frequency of the resonator. The resonant frequency of the quartz crystal sensor undergoes a change that depends on the change in temperature, following a third-order polynomial equation of T. By a proper choice of the cutting planes of the crystal, the coefficients of the second- and third-order powers of T can be nullified and, in this case, the resonant frequency becomes a linear function of the temperature (Michalski et al., 1991).

Once the probe has reached equilibrium with the surrounding fluid, the quartz thermometer readings are very accurate and may constitute a good reference standard

for calibrating other thermometers or may be used in precision calorimeters. The response time of a probe is a few seconds in stirred water but is quite long in still air. However, by counting all the oscillation pulses, it is possible to integrate with great precision over a time interval: the longer the integration time, the higher the resolution. For this reason, commercially available instruments have options for different sampling intervals and corresponding resolutions, e.g. increasing by 10 the sampling period, the last digit represents a resolution 10 times greater, so that incredibly high resolutions, as far as 10^{-5}°C or 10^{-6}°C, are attained. It should be remembered, however, that these readings are accurate only in the case the probe has really reached equilibrium with the fluid and the temperature is stationary; otherwise the precision is merely illusory and misleading, being only a precise average of the sensor temperature during the sampling time interval.

17.2.9 Blackbody Globe Thermometer

A blackbody[72] globe thermometer has the opposite function of the screen: it absorbs instead of reflecting the electromagnetic radiation. The rise of temperature of a thermometer exposed to intense light or environmental *IR* radiation is the principle on which the *blackbody globe thermometer* (also called *black globe thermometer* or, simply, *globe thermometer*) is based (Bedford and Warner, 1934). It consists of a temperature sensor placed at the centre of a hollow 'black' sphere (Fig. 17.17) that absorbs, and emits, *IR* from surrounding surfaces and is regulated by the international standards ISO 7243, ISO 7727, and EN 27726. The equilibrium is reached after the contributions of conductivity (determined by ambient air temperature), *IR* balance (radiation exchanges with the ambient and hot sources), and convection (ventilation and convective motions). Frequently, these globes are made of metal (e.g. copper, aluminium) and the sphere is painted with black varnish. There is no doubt that the sphere absorbs the visible radiation and appears black to the eye but the metal below the coating may reflect *IR* radiation, as it often occurs if the coating is not properly made. Emissivity of thick oil paints generally ranges from 0.90 to 0.97 with the mode around 0.94. For this reason, the coating should be made of pigments absorbing in the *IR* region, which do not necessarily appear black to the eye. After the sphere has reached equilibrium with air temperature, air movements, and *IR* radiation, the temperature measured at the centre of the sphere gives an approximate measure of the effective temperature experienced by people or objects in that room. The overheating, i.e. the globe thermometer temperature minus the air temperature, gives a crude indication of the contribution of the radiant heat. This method is used in health physics to study the heat stress in workshops.

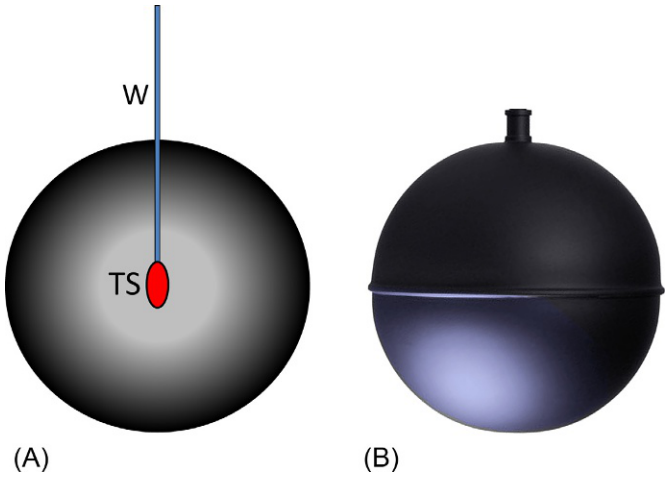

FIG. 17.17 The blackbody globe thermometer is a hollow sphere, generally made of metal, but coated with a paint absorbing UV, visible light, and IR. (A) Schematic cross section: in the centre of the sphere, a temperature sensor (TS) connected to the external recording instrument with a wire (W). (B) External view. On the top, the opening for the thermometer or the connection wire.

It should be noted that *IR* radiation affects any thermometric measurement and is negligible only for very thin metallic sensors that reflect *IR* radiation, e.g. thermocouples and uncoated platinum resistance transducers.

Abundant literature exists on this subject and special reference has to be made to UK Meteorological Office (1981), Benedict (1984); Schooley (1986), WMO (1986, 2008), Michalski et al. (1991), Wylie and Lalas (1992), Nicholas and White (1994), Bentley (1998), Michalski (2000), Lipták (2003), Camuffo and Fernicola (2010), Kantor and Unger (2011).

17.2.10 Instrument Location

The site of a standard weather station should be meteorologically representative of the area in which it is located and free from local perturbations generated by trees, buildings, water bodies, and air pollution. A lawn of level ground, in size 6 by 9 m and covered with short grass, is generally used for the installation of meteorological instruments.

Meteorological phenomena take place in time and space scales completely different from those of monuments, which are governed by local microclimate. In

[72] A *black body* is an idealized physical body with absorbance $\varepsilon = 1$, i.e. absorbing all incident electromagnetic radiation, regardless of frequency or angle of incidence.

contrast to standard meteorological or airport observations, it is not possible to develop similar guidelines for conservation. In the case of microclimate measurements for cultural heritage, observations must be made when and where necessary, according to the aim of the survey.

However, it might be useful to remember that the air temperature is not the same at all heights and that the choice of the height is very important. Outdoor, the air temperature is essentially governed by the soil temperature: during night-time, the soil is colder, and the temperature increases with height; during daytime, the soil is warmer and the temperature decreases with the height. In summertime, in the central part of the day, bare sand may reach 70°C and the air temperature rapidly decreases by 30°C to 40°C over the first 2 m of atmosphere. This shows how the 'air temperature' will change depending on whether the sensor is placed a bit higher or lower. The essential point is that there does not exist a generic 'air temperature' T, but T is a punctual and instantaneous value of a function that is variable in space and time coordinates. Also, in closed rooms, the temperature is not the same at all heights but tends to stratify in horizontal layers, the warmer air being trapped below the ceiling and the colder and denser air being closer to the floor, with a difference that is of the order of 1°C or 2°C in usual conditions but that may reach 20°C or more. Measurements made to test the horizontal homogeneity of the temperature in a room or a floor must all be exactly made at the same horizontal level. For instance, in churches with warm air heating, vertical gradients of 7°C m^{-1} were found and a vertical displacement of 10 cm of the sensor will introduce an apparent change of temperature of 0.7°C.

When ambient monitoring can be performed using only one instrument (e.g. a thermo-hygrograph), it is extremely important to know the representativeness of the instrument location, with reference to the whole room or the site. In fact, temperature and humidity vary either temporally or with space, e.g. responding to the solar radiation through glass panes, the opening of doors and windows or turning light on or off as well as other heating, ventilating, and air conditioning (HVAC) systems. Measurements made at points particularly shielded or exposed to air currents, in proximity to HVAC, or perturbed by the presence of hot or cold water pipes are not representative of the real situation and their interpretation may induce wrong management of the ambient conditions. To determine the temperature distribution inside a room, a micromapping survey should be made in order to choose the most representative point for the location of the instrument and especially of the sensors for the control of the temperature and humidity in the room.

17.2.11 Measuring Vertical Profiles of Air Temperature

Vertical profiles of air temperature are important because they constitute a measurement of the atmospheric stability that is responsible for the dispersion of airborne pollutants and their deposition. Weather balloons are used to carry radiosondes or as a free-rising tracer, transported by wind and useful to reconstruct the vertical wind profile.

In the case of heavy radiosondes or if there is a moderately to strong wind, the preferred carriers are tethered balloons, e.g. *kytoons* (Fig. 17.18), which substantially are moored balloons, sized 40 or 80 m^3. The primary advantage of a kytoon is that it remains up and at a reasonably stable position above the tether point, irrespective of the wind, except for very strong winds. Stability is provided by some soft wings on the back. The soft wings are normally floppy and have some inflation openings at the front. In the case of wind, air blows through the openings, inflates wings and stabilizes the kytoon by damping the oscillations caused by wind gusts and turbulence.

FIG. 17.18 A tethered kytoon used as radiosonde carrier. The kytoon is shaped like a traditional aerostat but with floppy wings at the back. In the case of wind, air blows into the wings through some inflation holes; wings are self-blown up and the kytoon becomes stabilized. Launching from the CNR campus, Padua, in the late 1970s.

The gas generally used to inflate balloons is hydrogen, but this gas should be handled only by well-trained personnel because it is highly explosive and the risks of explosion and burning are particularly enhanced in the proximity of electrically charged bodies, e.g. the operator when the air is dry. Helium is safe but much more expensive and provides slightly less buoyancy (the mass of helium is twice the hydrogen molecule; at STP the density of hydrogen is 90 g m^{-3}; helium 179 g m^{-3}, and the buoyancy of hydrogen is 8% greater than helium). The suggested practice is to fill balloons with a mixture of hydrogen and helium (generally H_2: 5% and He: 95%), popularly used to inflate children's balloons because it is less expensive than pure helium and nonexplosive. In urban areas, with the onset of wind, the balloon may reach the ground far from the operator, thus introducing an extra risk.

Small weather balloons are also used, made of latex of natural rubber or neoprene. They have various sizes and weight, e.g. 1000 g for medium radiosondes, 300 g for mini radiosondes, and 100 g for the so-called *pilot balloons* to reconstruct the vertical wind profiles. Balloons are used deflated and pear shaped when they should reach high levels and low pressures, or are swollen-to-spherical size if they should not rise too much. When a weather balloon is blown too much, or too rapidly, or in a cold environment, or the lattice is not homogeneously distributed, or has some porosity, it may burst and fall.

Carrier balloons should be carefully inflated to a size that will provide the appropriate lift. In urban environments, miniaturized systems are preferred, but small balloons risk exploding from the tension when they are recovered. In urban areas, it is not advisable to use a single balloon with adequate buoyancy, but it preferable to use a small cluster of smaller balloons (Fig. 17.19) with parachute for safety reasons. This solution is excellent when the radiosonde is launched and is in free ascent. The problem occurs when the balloon is tethered, during the recovery.

Meteorological radiosondes and low troposphere radiosondes (resolution 0.1°C, 1% *RH* and 0.5 hPa atmospheric pressure) with latex or neoprene balloons are used only once and then they are left to fly away. However, if the study is limited to the lower part of the planetary boundary layer (PBL), e.g. the nocturnal inversion layer and first kilometre of the diurnal mixed layer, the same radiosonde may be used several times. The method consists in tethering the balloon, which can be launched and recovered with a nylon fishing line 0.7–1.2 mm diameter (Camuffo, 1980, 1982). During the ascent, the buoyancy force of the balloon allows it to freely turn and roll with the fishing line.

The descent is more problematic, adding a force generated by winding the fishing line on the roll by means of an electric motor. This operation is possible only if there is no wind, or if the wind has low or moderate speed. When there is calm, the forces are only two, opposed along the vertical: F_B, the upward buoyancy and F_T, the downward traction of the wire. The operation is easily made by controlling the downward force. In the presence of wind, the balloon is subjected to three forces (Fig. 17.20): F_W horizontal, moderate to strong, due to the wind drag; F_T along the wire due to the tension that becomes dominant during the recovering operation and forms an obtuse angle with F_W; and finally, the vertical force due to the buoyancy F_B. The resultant of these three forces will make the balloon descend slantwise and the wire curvature risks to approach, or even touch ground.

FIG. 17.19 A mini radiosonde *(white box)* carried by a cluster of three small weather balloons, launched from the Papadopoli Palace garden, in Venice. The *white line* connecting the radiosonde to the balloons is the transmitting antenna.

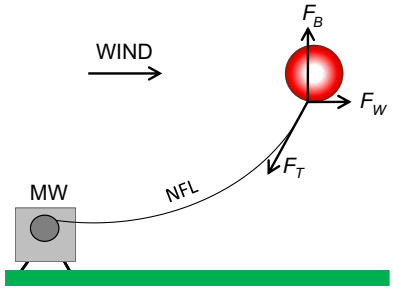

FIG. 17.20 Forces acting on a tethered balloon *(red sphere)*: F_B vertical, due to balloon buoyancy, F_W horizontal, moderate to very strong, due to the wind drag and F_T along the nylon fishing line due to the tension during recovery. Legend: *MW*, motor winch; *NFL*, nylon fishing line.

In the case of balloon clusters, the turbulence generated by the cluster forces violent vibrations and increases the risk of bursting. An effective remedy to reduce latex tension and turbulence has been found by enveloping the balloon, or the cluster, with a soft hunting or fishing net and attaching the tethered fishing line to the net envelope. The surface stress of the balloons is better distributed and breakdown risk is reduced, but not completely.

Minisondes carried by a balloon (size: 1 m^3) or a balloon cluster make possible vertical runs also in city centres, operating in very small gardens or small roof terraces. Using tethered balloons means using the same radiosonde several times, thus reducing costs. In addition, the data of each run are taken with the same instrument and are homogeneous without the problem of intercalibration errors. Regarding the carrier for ascent, the use of minisondes borne by small balloon clusters is much cheaper than the use of 80 m^3 tethered balloons (e.g. kytoons) with heavy envelope. By the way, the latter need a much larger operating space and can only be used in rural environments. By reporting the results of each run in a diagram and drawing isolines, vertical time cross-sections of the thermodynamic properties of the PBL are obtained.

Fixed towers or portable masts may be used for profiles on a smaller vertical extent. Some 10-m folding masts with a tripod basement are commercially available. Extensible masts, with the antenna composed of an assemblage of five concentric sections with clamp collars from which the instrument can be hung, are also easy to use. Masts are extended by pumping air with a hand pump. On opening the valve and loosening the clamp collars, the mast retracts.

Inside buildings, under unperturbed conditions, the air is often stratified in horizontal layers, whose density decreases with height. The layers are not horizontal, or the stratification may even disappear, when there are sources of momentum (air currents) or heat (formation of convective cells). In addition, in museums, vertical profiles show the difference of temperature of the air masses that come into contact with the lower part and the top of a painting or a statue. In museums, small portable masts with sensors placed at the floor level and at 1, 2, and 3 m are in general sufficient, as this height is representative of the air layer where most exhibits are exposed.

When rooms or churches with large domes are too tall to be controlled with a portable mast, should they have small openings on the ceiling, e.g. for raising/lowering chandeliers, it is possible to let down a rope with sensors and record the temperature and humidity profile on that vertical. This method was used several times, e.g. for the Giotto's Chapel, Padua (Camuffo and Schenal, 1982), with thermistors or high-resolution radiosondes for the lower troposphere. An easier system, not conditioned by the presence of openings, is to fill with a hydrogen and helium mixture a black tethered meteorological balloon and control its vertical ascent. The balloon envelope made of thin latex reaches thermal equilibrium quickly with the surrounding air. With a laser pointer radiometer, we can read the latex temperature that equals the air temperature at selected heights, determined from the length of the tethering wire. The balloon should not be overinflated in order to preserve elasticity and reduce vulnerability in the case it accidentally comes into contact with a rough surface; dark colour is preferable to avoid reflection of visible radiation. In order to be easily visible in high-ceilinged rooms, the balloon may be 2 m in diameter, and 300-g latex balloons are needed to reach this size. For rooms that are not so high, 100-g latex balloons may be enough. To be considered is that the tethered balloon methodology is more attractive than easy to implement.

A common sampling time for indoor temperature and humidity is 10 min or less, in order to monitor transient phenomena such as room cleaning, windows and doors opening for room ventilation, and indoor air exchange. Longer intervals (e.g. one acquisition per hour) might not monitor important perturbations, e.g. room cleaning with open windows.

A number of criteria exist for the measurement of atmospheric stability.[73] Most of them consider that the atmospheric turbulence is determined by two main factors:

1. vertical temperature gradients generated by the contrast of temperature between air and soil, which in the case of warm soil causes convective mixing and instability; in the opposite case of colder soil, thermal layering and stability
2. eddies generated by the wind and expressed in terms of wind gustiness, shear, and speed

It is evident that wind plays an important role outdoors, but inside a building it is practically absent or substituted by weak ventilation and/or local convective motions. For this reason, inside the thermal factor becomes largely dominant and, in general, it is sufficient to measure the vertical profile of the air temperature with a chain of sensors or to measure the floor and ceiling temperatures with two radiometers, as previously discussed.

However, dealing with a closed environment, several causes of stability and instability should be considered in addition to the floor and ceiling temperatures. Stable conditions are generated when HVAC systems introduce in the room new air with density different from the ambient air. In the case of warm air, it rises due to its buoyancy till

[73] See Chapter 10.

it reaches the ceiling and diverges and part of it mixes with the ambient air. The warm air cushion aloft, the cold ambient air at the bottom, and the mixed air at the intermediate levels determine some thermal layering and a stable atmosphere. Similarly, when cold air is introduced, it sinks generating again a thermal layering. In the absence of HVAC, thermal stability is generated only when the floor is colder, the ceiling is warmer, and the walls have intermediate temperatures. A cold ceiling generates instability like a warm floor for the symmetric reason; warm walls induce uprising air currents and cold walls induce descending ones; in general, this perturbation is appreciable only close to the walls, but these are often painted or have paintings or tapestries. As floor, ceiling, and wall temperature anomalies cannot be excluded, the indoor stability is better monitored by an integrated system composed of a vertical chain of air temperature sensors and some fixed radiometers pointing at the floor, the ceiling, and the walls.

If some ventilation (either natural or forced) exists, a measurement of the air speed should be included. If only one air speed sensor is used, e.g. a hot wire anemometer, the stability can be expressed in terms of the Högström ratio, which considers the ratio between the vertical gradient of temperature and the destabilization effect of the wind kinetic energy, measured at only one point, intermediate between the two points at which the temperature sensors are placed.

Vertical temperature gradients could be measured with thermocouples. This kind of sensor simplifies the problem of the perfect intercalibration of sensors and is theoretically convenient when differential measurements are needed, because the electromotive force that is generated is a function of the temperature difference between the two junctions. However, in order to overcome the problem of a weak signal generated by a small temperature difference, well-calibrated and matched platinum resistance sensors or thermistors are generally preferred.

17.3 PART 3. MODERN TECHNOLOGY TO MEASURE ARTWORK SURFACE TEMPERATURE

17.3.1 Introduction to Measurements of Cultural Assets

Measuring the temperature of cultural heritage objects is a particular task, because the surface is precious, vulnerable, and always exposed to risk when handled or studied. Although it is possible to use sensors commonly employed in other fields (e.g. meteorology, industry, and agriculture), their handling and limitations are different. A number of standards exist on temperature measurements, but the European standard EN 15758 (2010)[74] is the only one specifically tailored for cultural heritage. It considers three methodologies:

- contact sensors placed in physical contact with the sensed object
- quasicontact sensors placed in close proximity to the surface but without any physical contact with it
- remote sensing, with the instrument located at safe distance from the surface

In theory, it would be preferable to avoid, or to limit, direct contact with cultural heritage objects, but this is not always possible. The first methodology is based on the exchange of heat between two bodies (i.e. the sensor and the sensed object) entering into physical contact. The other two are based on the thermal *IR* emission of bodies and are conditioned by the surface emissivity of the material under investigation.

For ethical reasons, contact sensors cannot be used when the physical contact is potentially damaging to the object. For practical reasons, they cannot be used when the physical contact is difficult, the object is remote or very thin, is in motion, or has extremely low thermal capacity (e.g. lace, tapestry, a paper sheet). Contact sensors may be used with stone, glass, metals, or wood. On the other hand, they constitute the only possible method to measure the temperature of polished metals or other surfaces with low *IR* emissivity.

Quasicontact sensors constitute an excellent alternative to contact sensors, except in the case of polished metals. Although quasicontact sensors collect the total radiation (i.e. both direct and diffuse radiation) emitted by a surface and are therefore independent of the actual value of the specific emissivity ε of the surface, the surface should have a reasonably high emissivity (e.g. $\varepsilon > 0.7$); otherwise, readings are generally uncertain and contact sensors are preferable. There is no problem in using quasicontact sensors for thin objects or low-thermal-capacity materials.

Remote sensing is the most difficult technique because it requires high precision and very expensive instruments; furthermore, the readings are determined by the *IR* emitted by the target body in proportion to its emissivity, and the complement is the radiation emitted by third bodies and reflected by the target surface, i.e.

$$\mathrm{RR} = \mathrm{EM} + \mathrm{ER} \tag{17.9}$$

where RR is the radiation received, EM is the radiation emitted by the target surface, and ER is the external radiation reflected by the target surface; RE and RR follow the proportions ε and $(1-\varepsilon)$.

[74] See Chapter 15.

It has the great advantage of measuring remote surfaces (e.g. a ceiling without needing scaffolding) or mobile objects. The surface should have reasonable emissivity (therefore it is not appropriate for polished metals) and should be opaque to the specific wavelengths of the thermal radiation monitored by the instrument (e.g. glass may be misleading because it is mostly opaque, but also partly reflecting, in proportions variable with the wavelength).

EN 15758 recommends that the measurements in air should be of good quality and be representative of the process that is being investigated. In addition, measurements of surface temperature require a special care if these surfaces are vulnerable and should consider the special characteristics of some materials. For instance, polished metals are resistant and have low *IR* emission. For them, *IR* monitoring is impossible and contact sensors are needed. Stones and masonry are in general resistant to gentle use of contact sensors, but their surface emissivity is high enough and *IR* measurements are possible and often preferable. In the case of tapestry, paintings on canvas or panels, books, mummies, wooden objects, murals, heavily oxidized metals, or other vulnerable surfaces with medium-to-high emissivity, it is preferable to avoid any risk of contact with sensors. For this reason, quasicontact devices based on total *IR* emission are preferable.

Quasicontact sensors constitute the only technically possible method for surfaces like paper sheets, paintings on canvas or tapestry, if remote sensing is excluded. Remote observations of high emission bodies made with *IR*-based instruments (e.g. pyrometer, thermal imaging camera) are possible and sometimes particularly useful, especially in the absence of scaffolding, but it should be taken into account that their accuracy is generally low, except for high-quality, very expensive instruments (Camuffo and Fernicola, 2010; Camuffo, 2010). The following discussion re-addresses the characteristics, advantages, and problems of the various methodologies and instrument types according to EN 15758.

17.3.2 Contact Sensors

Contact sensors have a flat surface that is put into contact with the object under investigation (Fig. 17.21). The equilibrium is reached when the exchange of heat at the interface between the sensor and the target surface (i.e. the measurand[75]) has been concluded. However, a bad contact may also lead to the same result, leaving the sensor and surface at different temperatures. This particularly happens when the surface is rough so that only a few points of the artefact are in contact with the sensor, because the small air pocket between the artefact surface and the sensor acts as a good insulator. In order to improve the thermal contact, grease or gelatine can be smeared on the flat side of the sensor. A commonly used material in industry is silicone grease with some metal powder included to improve heat transmission. This medium, however, cannot be applied on cultural heritage objects, as it stains the surface, and other noninvasive, clean methodologies should be used.

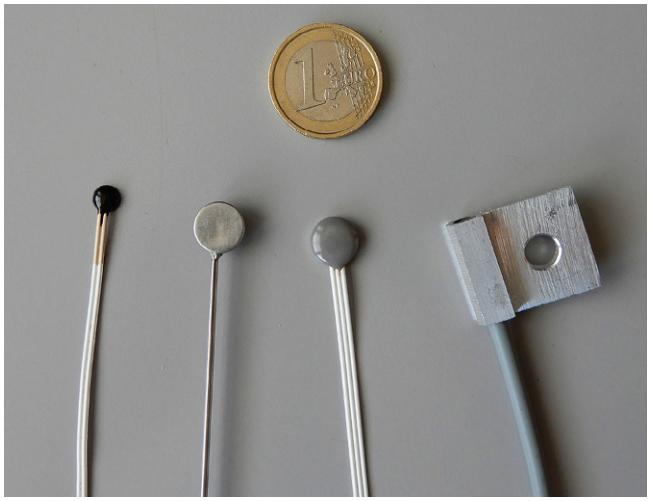

FIG. 17.21 Contact sensors and 1 Euro coin for size reference. The first and the third are viewed from the epoxy insulation on the top; the second from the stainless steel contact surface; the fourth has a hole to be fixed with a screw. Screws may be convenient for common use, hardly for cultural heritage.

Another problem is that the outer side of a contact sensor is exposed to atmospheric agents, e.g. different air temperature and solar radiation. To minimize these perturbing factors, this side is insulated but if it is exposed to direct solar radiation, it needs an extra shield.

A further problem is that the presence of the sensor perturbs the surface temperature, especially in the case of a surface that is warmed by solar radiation. In fact, the skin of the surface that is hit by solar beams is warmed, but the small area to which the sensor is attached remains shielded and colder. The sensor exchanges heat with the deeper layers below it, in the colder area, and mainly comes in equilibrium with them, although it receives some heat that converges laterally from the warm lighted surface. Consequently, the surface sensor instead of measuring the skin temperature measures the temperature of a colder, subsurface layer. This problem results from the measuring approach used; it is not an instrumental error.

[75] The *measurand* is the quantity intended to be measured. JCGM, 2012. VIM (International Vocabulary of Metrology) 3rd edition, Joint Committee for Guides in Metrology (JCGM), JCGM 200:2012 (E/F).

The opposite occurs during night-time, when the monument loses heat by *IR* radiation, except the small area that is in contact with the sensor. Similarly, when the monument is wet and its surface temperature drops to the wet bulb temperature, the area in contact with the sensor is not affected by forced evaporation and a different temperature is measured. As always, the variable that is monitored is the sensor temperature and the actual surface temperature remains unknown, except for the contact sensor approximation.

In steady-state conditions, it is assumed that a body is in equilibrium with its surrounding atmosphere. When a sensor comes in contact with a surface, it alters the radiative balance and the conductive and convective exchanges, so that the thermal distribution of the body surface is locally altered. The sensor generates a new heat flow from (or to) the surface, and where the thermal contact is not ideal, a thermal contact resistance is introduced. Therefore, it can be concluded that a sensor will always interact with the surface under investigation, and that the measurements will be perturbed in any case.

When passing from a steady-state to dynamic conditions, the difference between the actual temperature and the measured value will increase. This is apparently expected when the thermal response of the sensor is slower than the response of the body surface but, in practice, this always happens because the presence of the sensor perturbs the surface-environment heat exchange.

Only when the radiative balance does not affect too much the surface temperature, and the ambient conditions remain stationary for a sufficiently long time, does the measurement become representative of the surface temperature. When the radiative gain or loss makes the skin temperature of the body different from the subsurface layer, a possible way to monitor the real temperature is to leave free the surface and then touch it with the sensor for a very short time. However, the heat capacity of the sensor affects the temperature of the few protruding points of the surface in contact with the sensor. For this reason, it is necessary to proceed with further steps. The method consists in repeatedly touching the monument surface with the sensor at different points from that under observation in order to bring the sensor to a closer and closer temperature so that the observed point will not be affected by the presence of the sensor. When the sensor touches a surface, in a short time it reaches a new equilibrium and its temperature gets closer to the unknown value under examination. Repeating a number of times this operation, a better approximation is obtained with the sensor approaching more and more the undisturbed skin temperature. After some of these measurements, when the output readings remain unchanged, the asymptotic value is reached and it is possible to read the temperature of the point under observation minimizing the influence of the sensor. This method has been successfully applied several times, e.g. the Aurelian and Trajan columns, Rome (Camuffo and Bernardi, 1993), or Pisa Tower; but it requires an operator. This was a necessary practice before the advent of quasicontact sensors that constituted a milestone improvement.

17.3.3 Quasicontact Sensors

Quasicontact sensors are placed at small distance from the surface but not in physical contact with it. They are also called *total radiation sensors* because they receive both the *direct* and the *diffuse IR* radiation emitted by the surface. The sensor is located on the focus of a parabolic, mirroring cavity made of stainless steel, which has a low emissivity $\varepsilon = 0.07$ (Fig. 17.22). In addition to the direct *IR* emitted by the surface towards the sensor, the internal

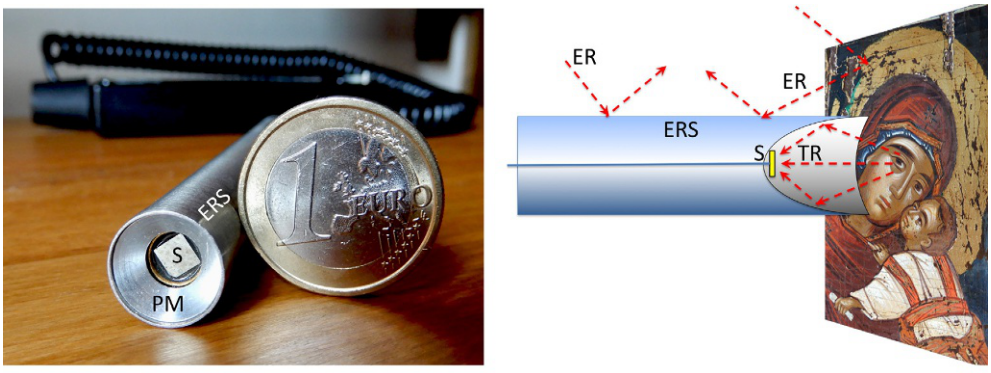

FIG. 17.22 Quasicontact sensor. (A) A view of the sensor. *ERS*, external reflecting shield; *PM*, internal parabolic mirror; *S*, the IR sensor. One Euro coin for size reference. (B) Operation principle of a quasicontact sensor, while measuring the temperature of the icon eye. The sensor S is positioned on the focus of a mirroring parabolic cavity and receives the total radiation TR (i.e. direct and diffuse) emitted by the surface. The external metal case ERS shields from environmental radiation (ER) emitted by third bodies. In practice, the sensor receives only the radiation TR emitted by the surface under investigation.

mirroring parabolic cavity conveys on the sensor the diffuse *IR* emitted by the surface. In practice, the sensor is virtually enveloped by the mirror image of the surface and, in this way, it is only hit by the radiation emitted by the object surface, if the small contribution (i.e. 7‰) of the mirror is disregarded. The external mirroring surface shields the sensor from the external *IR* emitted from third bodies. In practice, the sensor is shielded and encased in the mirroring probe and only (or almost only) receives the *IR* emitted by the object surface. This apparatus increases the efficiency of the emitting body surface, as it has an emissivity $\varepsilon = 1$ or, more exactly, $\varepsilon = 0.993$ if we consider the influence of the stainless-steel mirror. In conclusion, quasicontact sensors can be used with any type of material with high or average emissivity. The external shield removes external reflections and the parabolic mirror multiplies the radiation emitted from the target. The mirrored image behaves as the original target surface. The instrument virtually transforms a high or average emissivity into an almost perfect blackbody. This instrument cannot be used with materials having very low emissivity, e.g. polished metals, because the low *IR* emission is insufficient and falls into the range of background noise. A polished metal target is indistinguishable from the metal mirroring cavity.

17.3.4 Radiometers and Remote Sensing

Radiometers provide indirect measurements of small- or large-area temperatures, based on measuring the *IR* emission of bodies. In order to reduce the effects of atmospheric absorption of some *IR* bands due to the presence of water vapour (which is the most important greenhouse contributor), CO_2, O_3, and other greenhouse gases, the most used spectral windows are: 1.5 to 5.0 μm, 3.5 to 5.0 μm, and 8 to 14 μm. Radiometers are essentially of two types: those that reproduce the thermal image of objects and the nonimaging transducers that measure the total power of the *IR* radiation that reaches the sensor. These measurements have the advantage that they do not physically perturb the surface under investigation and do not cause damage to the works of art where contact sensors cannot be used. They constitute a noncontact and nondestructive method that is particularly appreciated in the field of works of art.

Another important aspect is that they are remote-sensing devices and make possible measurements on ceiling or other surfaces that are reached with difficulty, or for moving surfaces. Finally, their output is representative of a more or less large area, being less conditioned by local departures or fluctuations. On the other hand, measurements are affected by: (1) the presence of extraneous reflected *IR* radiation that constitutes a serious problem for outside measurements during the daytime, (2) the emissivity of the surface and its Lambertian[76] nature, and (3) suspended aerosols or moisture that absorb *IR* signals. For further details, see Wolfe and Zissis (1989), Kondratyev et al. (1992).

Imaging instruments are thermal imaging cameras, similar to a normal camera but reproducing images in false colours and sensitive to some wavelengths in the near *IR* band, and thermovision, based on television-sensing systems using electron beam scanning. Such instruments are expensive but a thermal image is of immediate understanding for specific problems, showing gradients, warm or cold spots, energy loss and leakages, and cold zones that might possibly be generated by water percolation or other unknown reasons. They are useful in building diagnostics, especially when rapid temperature changes and uneven heat transmission pinpoint surface temperature anomalies due to subsurface inhomogeneity. The methodology can be used either in active or in passive mode. The active mode is when the surface under investigation is deliberately heated to monitor temperature pattern emerging during the quick heating or cooling phase. Subsurface discontinuities may appear when there are different heat transmissions. In the passive mode, the surface is observed during its natural conditions, either stationary or variable. It is also possible to recognize internal discontinuities especially when the object is naturally affected by temperature changes, either for the daily cycle or for the alternation of sunshine and shade.

The false-colour images, called thermograms, are constituted of pixels that in practice indicate temperature levels distributed over a bi-dimensional matrix x–y, i.e. the geometric coordinates of each pixel on the surface. This map is useful in calculating the distribution of *RH* in the viscous layer at the interface between the surface and the air in rooms. If the mixing ratio (*MR*) inside the room is measured, and it is homogeneously distributed, one can calculate the *RH* at the interface from the *MR* in air and the surface temperature, repeating the operation pixel by pixel in order to obtain a visual image of *RH* in false colours. This practice is very useful in environmental diagnostics, e.g. to see whether some heating caused by exhibition lamps or by sunbeams passing through windows may be noxious to paintings, furniture or other objects, as discussed in Chapter 12.

Nonimaging instruments (*IR* thermometers) are commonly employed in field surveys for measuring the temperature of inaccessible surfaces. They measure the heating of a sensor placed at the point of convergence of the cone of the flux of *IR* radiation, whose optical angle is controlled by a diaphragm. The diaphragm is fixed or

[76] For Lambertian definition, see Chapter 12.

adjustable; adjustable diaphragms allow the use of the instrument for close or remote monitoring or for averaging the temperature over a small or wide area. Close position and/or small angles give high resolution and point measurements; long range and/or wide angles give the temperature averaged over a wide area. A cause of error is the diffraction of the collecting radiation at the limiting aperture, which depends on the *IR* wavelength and therefore on the object temperature.

A real surface both *emits* and *reflects* radiation with a relative intensity that varies from one material to another; the measurement is based on the emitted component but the radiometer does not differentiate it from the reflected one. The mechanism is also complicated because the reflected radiation from liquid or solid bodies consists of two components: the well-known *surface reflection* and the *bulk reflection*, i.e. the portion of the radiation transmitted into the material and reflected by internal backscatter; the latter is independent of the surface condition. The problem of taking reliable measurements arises when there are other important sources of *IR* radiation or the surface under investigation has low emissivity and high reflectivity. In this case, the measurement is not representative of the body temperature. When a metal or another reflecting surface is investigated, special care should be taken in order to avoid the *IR* radiation emitted by the operator, or other bodies, in particular sun and clouds. If the surface is Lambertian (this approximation is particularly good for a rough surface), the operator influence can be avoided by observing the surface at slanted angles. However, for most surfaces, the emissivity depends on the viewing angle and drops near grazing incidence. In this case, a nearly normal incidence is preferred.

Radiometric measurements are based on the knowledge of the surface emissivity ε and the spectral radiance in the band used by the instrument. The simplest case (blackbody) is $\varepsilon = 1$ and corresponds to a known, continuous spectrum; however, in general, the uncertainty of these two characteristics is a source of error. Bodies with the same temperature but different emissivity generate different radiometer outputs. An adjustable emissivity control on the instrument permits to correct the output, adapting the transducer to the characteristics of each surface, in order to obtain accurate temperature measurements. However, the emissivity of the object is unknown. One method used is to cover the target surface with a coating (e.g. soot) or a film with known emissivity in the *IR* band used for the radiometric measurement. However, this may alter the body–atmosphere interactions and the surface temperature. The actual value of ε can be found empirically, adjusting ε on the radiometer setting until the true surface temperature (known by means of a surface thermometer) is indicated.

It is necessary to consider that the emissivity of a surface may change with time from a value typical of the dry material to a value close to 1 (i.e. surface wet by rainfall or covered with a film of water when the surface temperature is below the dew point), and this happens frequently with outdoor monuments. The emissivity changes during the day with the water content of the surface layer, in the presence of drying–wetting cycles, and with the surface temperature or wind speed. However, surface soiling, particle deposits, efflorescence, hydrophilic salts, biopatinas, and other factors may substantially alter the surface emissivity. The same occurs for the surface reflectivity and this also changes with the angle of incidence. For instance, the reflectance R from a water surface varies from 2.5% at normal incidence (i.e. at 0 degrees angle incidence from the normal) and becomes $R = 8\%$ at 60 degrees, 35% at 80 degrees, and 97.5% at 90 degrees, i.e. at grazing incidence.[77] As the emissivity is $\varepsilon = 1 - R$, this factor is very important, as a wet surface observed at small incidence (grazing) angles becomes a pure reflector and the emissivity of the water film that envelops the body vanishes. In such a condition, the only *IR* radiation that reaches the instrument is generated by third bodies.

Another important factor is that the emissivity is a function of the spectral wavelength λ, i.e. $\varepsilon = \varepsilon(\lambda)$ and materials may have a more or less low value in the spectral emissivity, which can fall in the instrument bandwidth, thus changing the apparent radiometric temperature. Most organic materials, e.g. wood and parchment, have a low emissivity in the visible part of the spectrum, and high emissivity in the *IR* region. On the other hand, metals covered with a thin layer of oxide seem very dark but the oxide becomes transparent at longer wavelengths, so that in the *IR* range the surface becomes reflecting and with low emissivity, typical of a pure metal (Nicholas and White, 1994).

Of course, it is convenient to compare radiometric observations with other homogeneous (i.e. radiometric) measurements, and for this reason, a complete set of measurements (e.g. ceiling, floor, walls and murals) should be made with the same type of transducer. The instrument calibration should be verified before and after use, by pointing the radiometer at a reference surface, which behaves as a perfect blackbody. A used reference is the free surface of water in a bucket as in the normal direction $\varepsilon = 0.96$, i.e. close to 1. However, care must be taken since the water tends to stratify in layers with different density and the surface layer is affected by evaporation so that its temperature tends to drop to the wet bulb temperature. As the *IR* radiation is absorbed in a few micrometres of water,

[77] The colour of the water of a great lake, or the sea, is determined by the sky reflection. A small mountain lake assumes the colour of the trees on the opposite slope.

the radiation emitted originates from the very surface layer whose temperature is different from the bulk water, where the bulb of the true thermometer is immersed.

The best reference is obtained by pointing the radiometer at a blackbody cavity, which has an emissivity that approaches unity. This can be obtained with a can blackened inside having a very large internal size and a very small aperture, so that the internal reflections are so many that an equilibrium is established and any external radiation that penetrates is practically extinguished. However, if the internal surface of the cavity has temperature gradients, the blackbody emission is a combination of spectra and introduces an error in the calibration. In order to be isothermal, the can should be immersed in a mixed liquid with known temperature. Mixing should be made by generating turbulence with up and down movements, not with rotation that does not destroy density layering.

When the reflectivity of an external radiation is zero, the emissivity also equals unity. A practical formula that determines the effective value of the emissivity ε_{eff} of a cylindrical cavity with a small opening is

$$\varepsilon_{\text{eff}} = 1 - (1 - \varepsilon_c)\frac{r_a^2}{r_c^2} \tag{17.10}$$

where ε_c is the emissivity of the internal surface of the cavity, and r_a and r_c are the radii of the aperture and the cavity, respectively (Nicholas and White, 1994).

Real materials emit radiant energy at a fraction of the perfect blackbody reference. It is useful to know the emissivity of some materials. Table 17.2 lists the emissivity of some selected materials used for cultural heritage or taken as an example. The table suggests that stones or heavily oxidized metals can be measured with a radiometer, but this method is not recommended for polished or slightly oxidized metals or other *IR*-reflecting surfaces.

As an example of the characteristics of commercially available instruments, the main technical specification of the *IR* transducers mostly used for microclimate measurements is: spectral band pass ranging from 8 to 14 μm, field of view from 4° to 20°, scale range from −30°C to 100°C, accuracy of ±0.5°C, repeatability of ±0.1°C, resolution of ±0.1°C, noise effective temperature <0.05°C, response time <1 s, operating environment ranging from −10°C to 50°C and $RH \leq 90\%$. More sophisticated instruments are also available, with accuracy, repeatability, and resolution improved at least by an order of magnitude, but they are far more expensive. They are particularly useful in detecting anomalous areas during transient conditions. However, the better the instrument characteristics, the more elevated the cost and the thinner the surface layer that takes advantage of the finer investigation, as very small and short period temperature changes (i.e. $\Delta T \approx \pm 0.01$°C) are smoothed out in a very short depth so that only disturbances on the skin, or just below it, can be detected.

TABLE 17.2 Emissivity ε of Selected Materials

Material	Emissivity	Material	Emissivity
Water	0.96	Plastics	0.91
Grass	0.90–0.98	Asphalt	0.96
Snow (old-fresh)	0.82–0.99	Basalt	0.90–0.92
Clay (dry-wet)	0.95–0.97	Dolomite	0.96
Sand (dry-wet)	0.84–0.96	Limestone	0.90–0.96
Soil (dry-wet)	0.90–0.98	Dunite	0.89
Lacquer (white-dark)	0.92–0.97	Feldspar	0.87
Oil paint	0.87–0.98	Gypsum	0.85–0.93
Paper (white)	0.93	Granite	0.81–0.93
Wood (oak)	0.90	Quartz (agate)	0.71
Hardwood across grain	0.82	Silicon sandstone	0.91
Hardwood along grain	0.68–0.73	Brass (polished-oxidized)	0.03–0.61
Glass	0.91–0.94	Bronze (polished)	0.1
Porcelain, glazed	0.92	Copper (polished-oxidized)	0.05–0.78
Brick (glazed-red)	0.75–0.93	Iron (polished-oxidized)	0.21–0.78
Mortar	0.87–0.94	Iron rust	0.75
Plaster (rough coat)	0.91	Iron heavily rusted	0.91–096
Concrete	0.92–0.95	Lead (polished-oxidized)	0.05–0.63
Soot on a solid surface	0.91–0.94	Steel (polished-oxidized)	0.07–0.79

Data from Platridge and Platt (1976); Oke (1978); Green and Maloney (1984); Wolfe and Zissis (1989); Lide (1990).

Comparing a radiometer having accuracy ±0.5°C with a contact thermometer with the same accuracy, one should expect observations with ±1°C maximum departure. However, this is not always true, even if we exclude errors due to *IR* reflection from third bodies. The reason is that a radiometer and a thermometer are based on different physical principles, thus measuring temperature at different depths below the surface. The radiometer measures the *effective radiation temperature,* which is representative of a temperature below the surface at a depth of $1/A(\lambda)$, where $A(\lambda)$ is the spectral absorption coefficient of the material. In absorbing materials, this layer is the skin. On the other hand, to reach equilibrium, a contact thermometer exchanges heat with a deeper layer, whose extent depends on the heat capacity of the sensor and the initial difference of temperature, so that the measurement is more properly representative of a deeper layer. This problem arises when there are subsurface gradients,

which occur in dynamic conditions, or when the body is irradiated by direct or diffuse solar radiation, or is cooling via *IR* emission or is utilizing latent heats of evaporation or condensation. Historic buildings or stone monuments may sustain very large temperature gradients, as their heat transfer to the atmosphere is very low. This makes comparisons between radiometry and thermometric observations difficult.

17.3.5 Blackbody Strip

The effective temperature resulting from a thermal balance between air temperature, *IR* radiation, and air convection is determined with a fast responding method, i.e. the blackbody strip.

The blackbody strip was first used in some field surveys to solve some problems concerning fast response and high space resolution. It was introduced to assess the level of the thermal comfort in churches among the pews during the continually variable temperature when a warm air heating system was turned on or off or when *IR* heaters were used. This was critical because heating should be reduced to a minimum acceptable level and/or to restricted areas. At the same time, it was useful to detect the areas hit by *IR* and to evaluate the impact that the *IR* radiation might have on paintings, tapestry, furniture, etc. or to determine what could happen if some *IR* heaters were to be installed or displaced from one position to another (Camuffo et al., 2007, 2010a,b).

In principle, it is similar to the globe thermometer but is fast responding and better tailored for cultural heritage purposes. The blackbody strip is constituted of a low thermal inertia, blackbody target, like a strip of black textile having high emissivity (Fig. 17.23). It soon reaches equilibrium with the incoming radiation, ambient air temperature, and ventilation. The equilibrium temperature of the blackbody strip should be accurately measured using the procedures for the measurement of surface temperature described for a quasicontact thermometer, using a radiometer, or using a thermal imaging camera.

In general, a blackbody strip is useful to measure spot temperature levels at selected positions and space gradients and to determine vertical or horizontal profiles, with high spatial resolution. After these tests, it was included in the EN 15758 standard.

17.3.6 Good Practices and Misleading Interpretations

Generally speaking, environmental diagnostics based on the results of only one methodology may be misleading and a good norm is to cross-compare findings derived from independent methodologies. The problem is that a number of different mechanisms may produce the same thermal image and a thermogram may be useful, but if it is considered alone, it is neither necessary nor sufficient to identify which of the various mechanisms is going on. While thermograms constitute a useful investigation tool, they are not per se sufficient to draw conclusions without the support of other specific investigations that are always necessary for confirmation. In the following discussion, some useful examples will be reported in order to explain this methodology.

Critical factors are cold spots, capillary rise, and water percolation. Most handbooks suggest that dampness in masonry, e.g. capillary rise and water percolation are

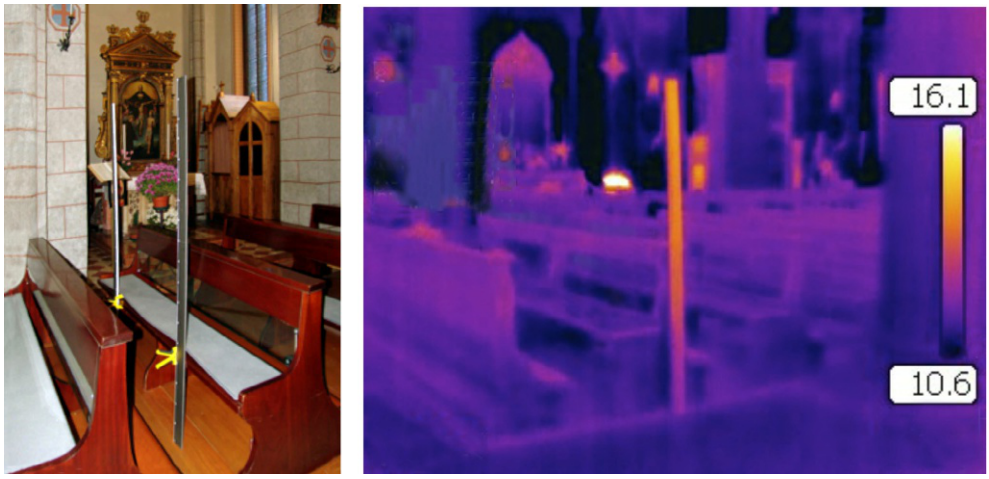

FIG. 17.23 Blackbody strip to monitor the efficiency of heating systems, either based on *IR* emission or warm air, or both. The blackbody strip temperature is sampled with a radiometer at regular height levels (e.g. every 10 cm) to obtain a vertical profile or is recorded with a thermal imaging camera. In this example, blackbody strips are used to evaluate the thermal comfort for standing persons inside the pew area. One can observe that the head is warmer and feet remain cold, which is not the best for comfort. *From Camuffo (2010), by kind permission of Nardini Editore, see credits.*

easily recognized from the cold spot generated by evaporation from the damp surface. The reason is that the latent heat of evaporation is supplied partly by the air and partly by the surface that is consequently cooled. This is generally true, as shown in Fig. 17.24.

However, several examples have been found where the coldest part of the thermogram is not damp, or even where dampness is found in the warmest part of it, as shown in Fig. 17.25. In Grimani palace, Venice, unsealed windowsills allowed rainwater to percolate into the wall on both sides forming damp spots (Camuffo et al., 2011). The spots were cold in the morning as generally expected but warm in the afternoon. The reason is that dampness in the wall constitutes a thermal bridge, connecting the inside with the outside surface. In the early morning (Fig. 17.25A), the damp spots were the coldest areas not only because of reduced evaporation but also because the inside heat was transported by conductivity to the outside. In the afternoon (Fig. 17.25B), the heat flow was reversed: the external surface, facing east, was overheated during the whole morning and the external heat entering the room formed the hot spots. Dampness increases the thermal conductivity and the thermal capacity. When the conductivity increases, it forms a thermal bridge and the heat flow too increases, and this effect may largely dominate over a weak evaporation cooling. Also, the window posts facing the solar beams and the glass panes were overheated and formed secondary warm bands inside.

In the next thermogram (Fig. 17.26), windows of a historic palace are contoured by cold bands in winter. Possible

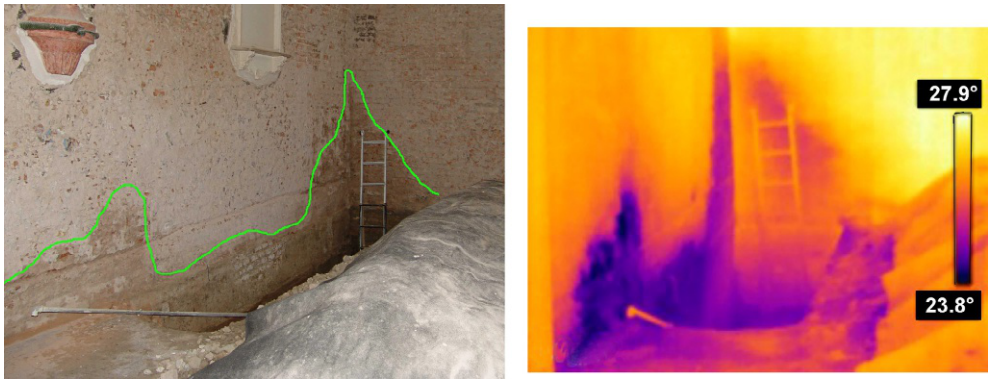

FIG. 17.24 Visible and *IR* image of dampness for capillary rise and gutter percolation on the corner. The damp area is contoured with the *green line* in visible picture and appears as the colder part in the thermogram.

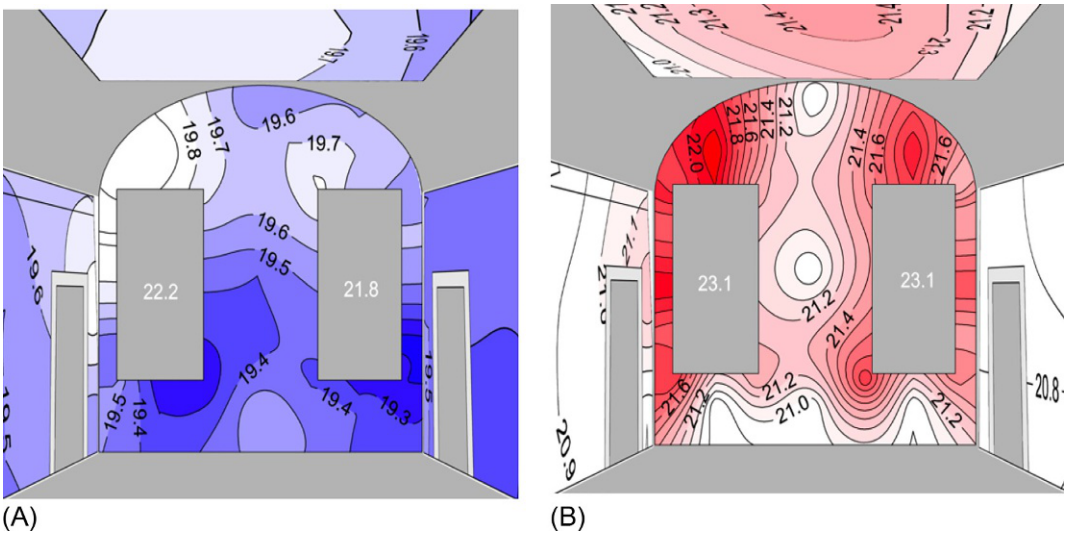

FIG. 17.25 Water infiltration: sometimes a colder spot, sometimes a warmer one. Temperature (°C) mapping of a room with damp spots on a wall. Damp spots of percolated water lie on both sides of the windowsills, on 14 May 2008. At 9:00 (A), the damp spots constitute the coldest areas; at 15:00 (B), they are warm for the thermal bridge established with the exterior. Other warm spots correspond to heating from window posts and glass panes. Thermogram executed sampling with a nonimaging radiometer and plotting with computer mapping. *From Camuffo et al. (2011) by kind permission of Nardini Editore, see credits.*

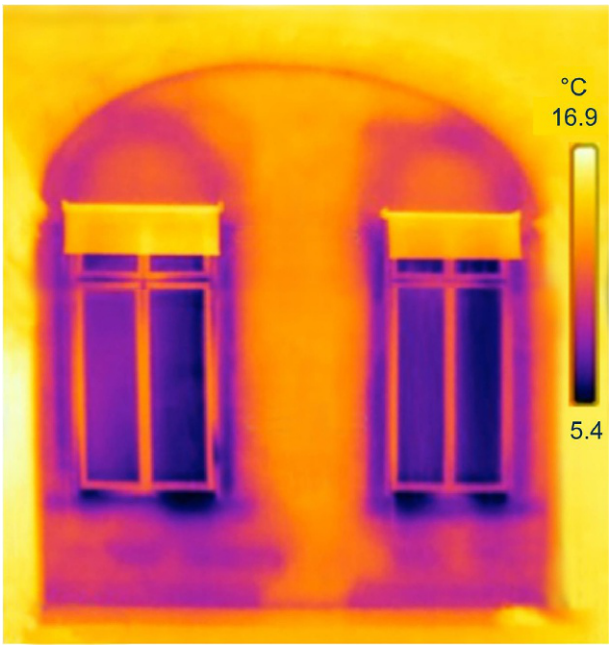

FIG. 17.26 These windows are surrounded by cold bands. Cold bands may be caused by air leakage through the frame, water infiltration, and shorter path for heat transfer. See text for explanation. *From Camuffo et al. (2011) by kind permission of Nardini Editore, see credits.*

hypotheses are: (1) the wooden frame is affected by leakage and cold air blows in, cooling the nearby masonry; (2) some water percolated into the wall from the window and the evaporation causes the cooling in the damp area; and (3) the outdoor temperature is lower, and heat naturally passes from higher to lower temperature levels crossing the wall and the window pane, which is colder. However, some heat crosses diagonally the wall via a shorter path going out through the windowsill and the two lateral posts, forming a cold band all around the window. In this case, the vertical cold bands on both sides were due to heat transferred across the shorter diagonal path; the cold area under the window, where individual bricks are distinguishable, is due to water percolation that locally increases the heat conductivity across the masonry, forming a thermal bridge with different efficiency corresponding to bricks or mortar. The problem with thermograms is that different mechanisms may have the same appearance.

Other two examples of warmer evaporating surfaces: in winter, the water flowing in the Venice canals is mild being continually exchanged with the sea that acts as a huge thermal buffer. In contrast, the temperature of the air in this region is cold or very cold. Palaces built on the side of the border of canals have their basement immersed in water and continually receive heat by conductivity. In the first example (Fig. 17.27), the basement is damp and characterized by a green–brown belt of algal infestation. Although this band is damp and evaporates, it is warmer than the upper part of the building, which is dry, but is in contact with the cold air without benefitting from the heat supplied from seawater.

In the second example, a funeral monument in a Venice church has a basement in contact with the soil, which is mostly damp due to a variable water table fed by the tide level (Fig. 17.28). The underground water migrates transporting heat. The damp funeral basement has modest indoor evaporation, but especially benefits from the heat supply. Once again, this evaporating surface is warmer than the rest of the church.

In these examples, evaporation was occurring in the warmest part of the image. The next thermogram will show another potentially misleading example: a cold area, but not related to dampness. In the warm season,

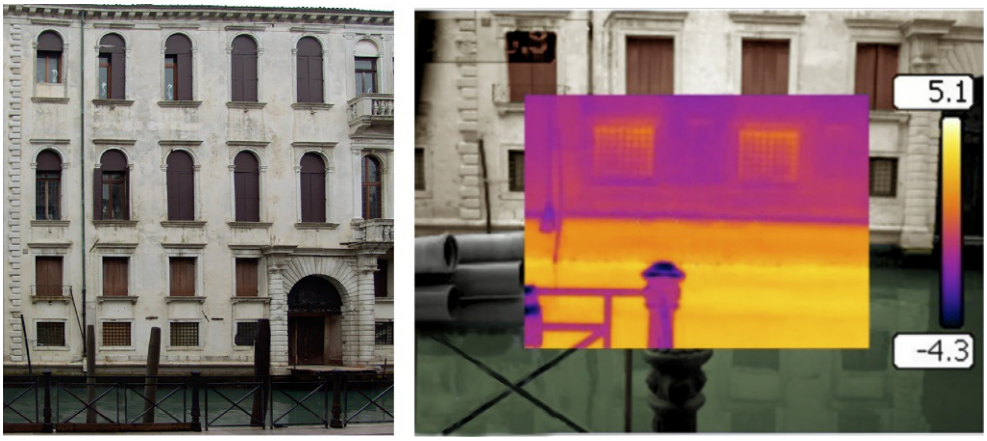

FIG. 17.27 Sometimes rising damp is warmer. Grimani palace, Venice, visible and *IR* mixed picture. In winter, the water temperature in the canal is at 4°C *(yellow–orange)* and the damp band infested by algae on the building *(orange)* has almost the same level. The upper part of the wall, dry, is colder *(magenta)*. The heat supplied by the canal is dominant over the heat lost due to (modest) evaporation. The evaporating band in the basement is warmer.

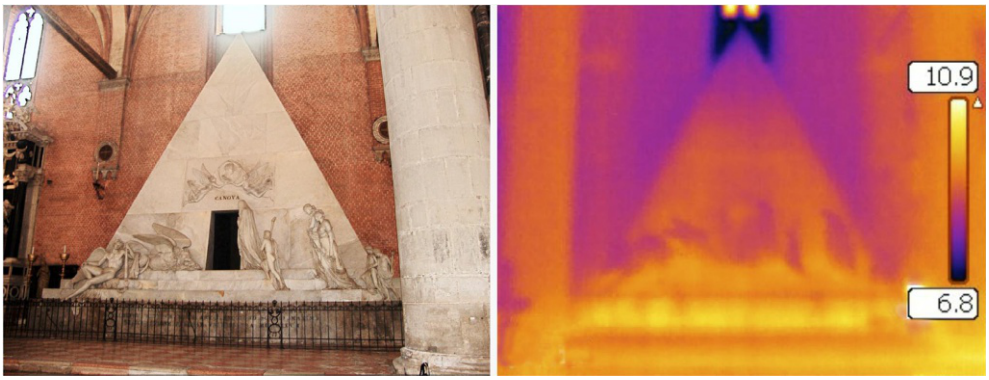

FIG. 17.28 Sometimes rising damp is warmer. The funeral monument of Canova, inside the Basilica dei Frari, Venice, is affected by capillary rise of water originating from the canal. However, the indoor evaporation occurs at a very slow rate and the heat transported by the mild canal water is dominant over the loss of latent heat due to evaporation. *Courtesy of Curia Patriarcale of Venice ©, used with permission.*

in this crypt (Fig. 17.29), warm air is penetrating from outside, heating pillars, ceiling, and walls. However, corners and the edge between floor and walls are hardly reached by the warm air entering the crypt.

The result is that all corners and edges are colder and sometimes this cold may cause elevated moisture levels and a favourable habitat for mould colonization. In this case, the cold areas are not due to capillary rise and evaporation but only due to reduced ventilation; for this reason, they might be affected by condensation, i.e. the opposite of evaporation.

Glass is mainly transparent, partially reflecting and slightly absorbing the visible light, while it is mainly absorbing, partially reflecting, partially transparent in the near infrared (NIR) (i.e. partially transparent for wavelengths from 750 nm to 3 μm), and almost opaque to the *IR* radiation above 3 μm. For this reason, radiometric readings monitor the radiant heat from the glass but are also affected by the reflection from bodies in front of the glass, e.g. the operator (Fig. 17.30A and B). An example of *IR* absorption is given in Fig. 17.30C where a glass pane, 2 mm thick, is put in front of a cup of tea, covering the right-hand side, which becomes invisible to the thermal camera that operates in the 8-to-14-μm window. If a thermal camera operating in the 1.5-to-5.0-μm range had been used, a faint image of the half-cup would have appeared by glass transparency.

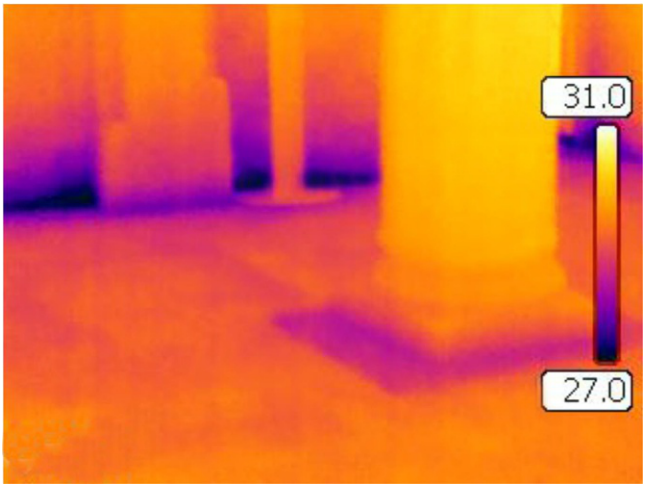

FIG. 17.29 Do colder area always represent rising damp? A ventilated crypt in the warm season. The external air warms pillars and walls but hardly reaches corners and edges, which remain colder. The floor (in brick) and the column (in squared stone blocks), with higher conductivity. For this reason, the floor at the base of the column is colder. This is not capillary rise but higher conductivity compared with bricks (by the way, bricks are more porous and favour capillary suction).

Metals are good *IR* reflectors and behave as mirroring surfaces. For this reason, radiometers are not suitable to measure metal (or glass) temperature. A trick solution is to stick on the metal (or the glass) surface a black vinyl electrical tape characterized by high emissivity (see later). In a few minutes, the tape will assume the temperature of the metal, allowing to measure the temperature of this black surface, avoiding reflected or transmitted radiation.

A good use of paper (emissivity $\varepsilon = 93\%$) is to allow measuring the air temperature. Air is transparent to *IR*, but a sheet of paper reaches equilibrium with the air temperature and a radiometer, or a thermal imaging camera, may measure it. Unrolling a jumbo roll of thick Kraft wrapping paper, or a roll of thick paper towels, a long strip is obtained that may be raised in vertical from the floor to the ceiling to measure the thermal layering of the air in the room. This method has the advantage of taking readings of both the surface and the air temperature using the same instrument, i.e. a thermal camera, thus avoiding errors due to the particular response (or calibration) of different methodologies.

A very advantageous practice (Camufo, 2010; Camuffo et al., 2010b) is to use a roll of paper to obtain vertical temperature profiles, as in Fig. 17.31, during a field survey in a church to control efficiency and risks of a warm-air heating system. Once the paper roll is raised vertically, it is sufficient to take repeated

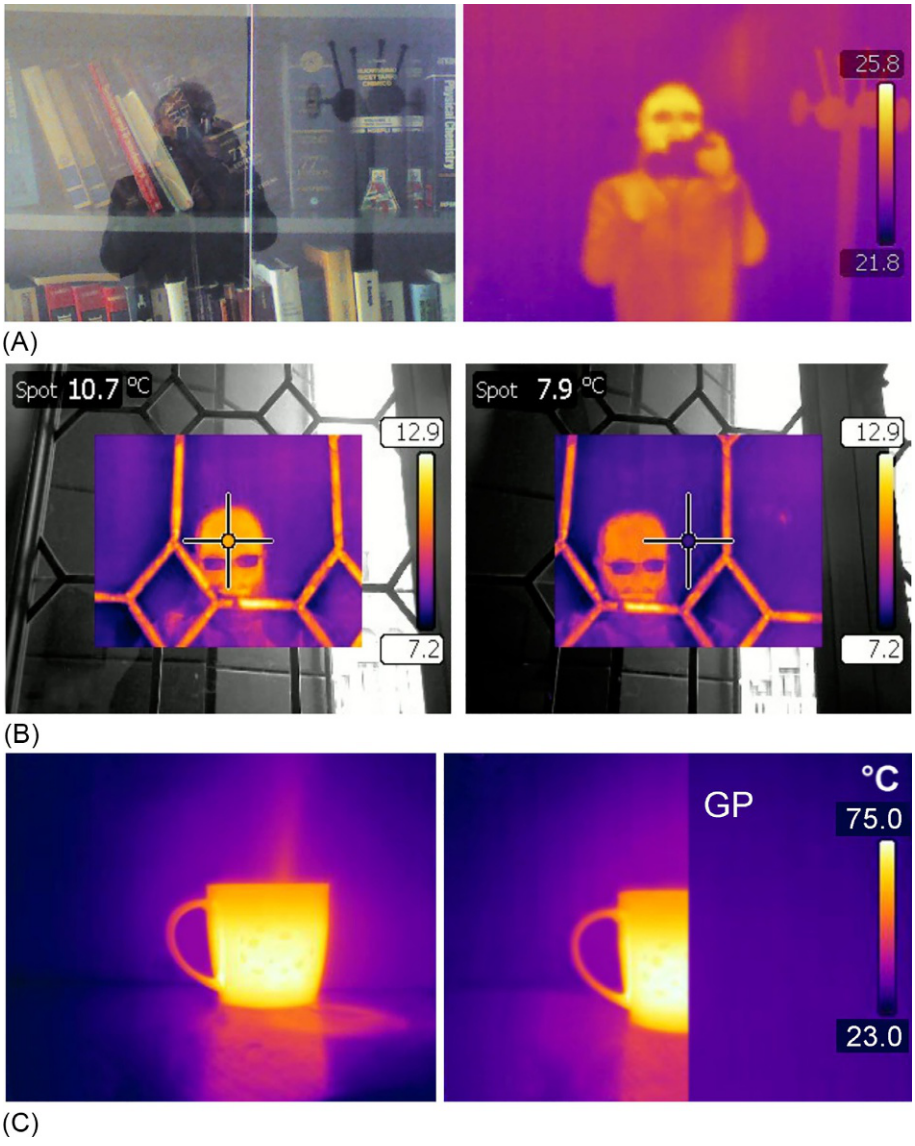

FIG. 17.30 Problem of reflection and transmission met with glass. (A) Visible light and *IR* reflection on the glass panes of a glass door bookcase. The reflected image of the operator apparently increases by some 4°C the glass temperature. (B) *IR* reflection on stained glass panes. The temperature difference pointing just at the forehead or outside it is 2.8°C. The metal frames appear warm because they reflect the *IR* emitted by the operator. (C) A cup of tea, and the same with a thin glass pane (GP) placed in front of it, on the right-hand side. The *IR* absorption of the glass pane makes it invisible to the thermal camera operating in the 8-to-14-μm window. *(A,B) From Camuffo (2010), by kind permission of Nardini Editore, see credits.*

thermograms at regular time intervals to monitor how heat is distributed and the resulting thermal layering.

The same thermograms show, in addition to the thermal profile in air, the direct impact of heating on objects, decorations, and structures that will respond in a different way, depending on their heat conductivity. This method is particularly useful because the image provides at the same time forcing factor (i.e. warm air) and effect (i.e. response of all objects). The thermogram is accurate because paper and the materials most commonly found inside historic buildings, i.e. mortar, bricks, plaster, frescoes, tapestry, and wood, all have almost the same emissivity, i.e. $0.90 < \varepsilon < 0.94$. This methodology is useful for environmental diagnostics and preventive conservation purposes, as well as for tuning the heating system, e.g. lowering the warm air temperature or increasing the air blowing rate to reduce internal layering and overheating in the upper part of the building.

In general, radiometers and thermal radiation cameras are equipped with a knob to adjust the emissivity value. Let us suppose an extreme case where the target is an object made of stainless steel with $\varepsilon = 7\%$. This means that only 7% of the radiation emitted by the target will contribute to determine the reading, while 93% of the radiation is originated from other bodies and reflected by the target. In this example, the target behaves as a mirror. The temperature of the object is irrelevant and the instrumental reading will be high or low, depending on the reflected radiation, i.e. if the surrounding environment is warm or cold. To correct the instrument, one should adjust both the knob of the surface emissivity and supply the surrounding temperature; nonetheless, the signal-to-noise

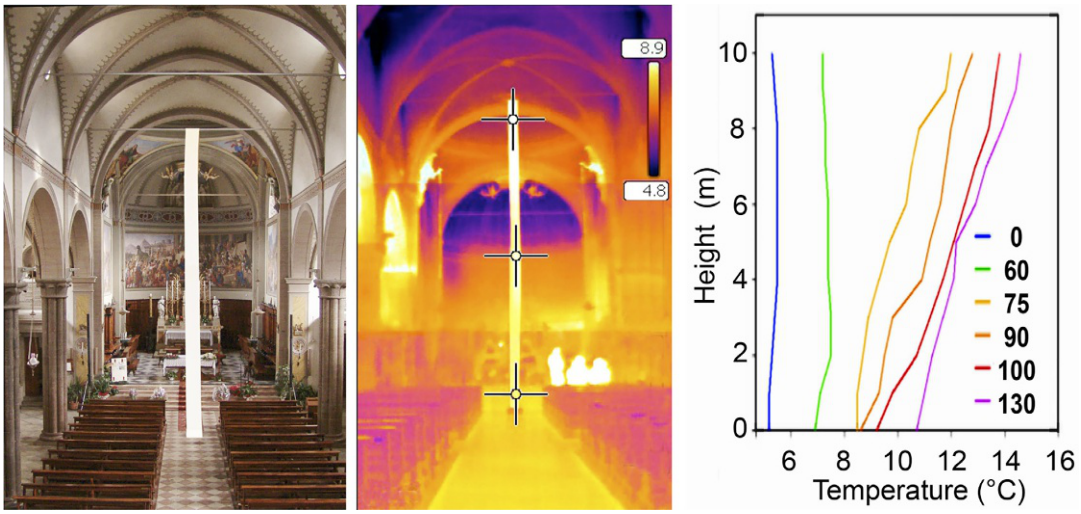

FIG. 17.31 Air and surface temperature simultaneously detected with a thermal imaging camera. Plaster, wood, and paper have almost the same emissivity. With a vertical strip of paper, it is possible to monitor both the surface and the air temperature in the same thermogram. The vertical temperature profile is obtained from the pixels sampled on the paper strip. On the right, the vertical temperature profiles made with repeated thermograms starting when the warm air heating was turned on, i.e. at time 0 min *(blue line)*, and after 60, 75, 90, 100, and 130 min (colour codes in the legend). After 2 h, the top level was heated by 10°C, churchgoer level by 5°C. *Source Church in Agordo, Italian Dolomites; From Camuffo (2010), see credits.*

ratio is so small that the reading is exceedingly uncertain. A metal temperature cannot be measured with a radiometer or a thermal camera. As opposed, if the object is a book with $\varepsilon = 93\%$, only the 7% of the radiation constituting the signal is reflected, then it makes sense to correct the reading. This means to adjust the emissivity knob, but also to specify the temperature of the environment from which the perturbing radiation is emitted.

A popular solution to avoid the reflection from third bodies is to simulate a black body with the help of a black vinyl electrical tape (ASTM E1933-14, 2014). The method consists in applying a piece of black tape ($95 < \varepsilon < 97\%$) on the target surface, waiting a few minutes so that the tape reaches thermal equilibrium, and then pointing and taking a shot of the tape.

This black tape method is also used to determine the unknown emissivity of surfaces. The unknown emissivity may be recognized in various ways, e.g. traditionally by comparison with a reference and with the help of some formulae and measurements based on: (i) a known reference emitter; (ii) a reference temperature measured directly (e.g. with a thermocouple); (iii) two different, known temperatures to which the target is raised; (iv) reflectivity of an object at different temperature (Madding, 1999), or with an image processing software (Pitarma et al., 2016). The instruction manual of the thermal camera may provide further details about these or other possibilities.

If the surrounding environment includes emitting surfaces at different temperatures, e.g. hot or cold spots, incandescent lamps, windows, persons, and the white-body temperature differs from the target temperature, it is necessary to perform a correction based on the target emissivity and the effective ambient temperature.

Opposed to the black tape method that avoids the background radiation diffused in the environment, the background radiation may be determined with the help of a diffusive mirror, i.e. a 'white body'.[78] This can be obtained with a finely crumpled foil of reflective polished aluminium ($\varepsilon = 5\%$); where the crumpling transforms directional reflectivity into diffuse reflectivity. Pointing and shooting this white body surface positioned near the target, one obtains a reading that is 95% representative of the environment temperature and only 5% of the aluminium.

After these determinations, it is possible to adjust the emissivity knob of the IR thermal camera to the appropriate emissivity value, and add the input of the effective temperature that characterizes the background radiation. This operation will allow performing more precise temperature determinations of the target object. However, it may be useful to clarify that a precise determination does not imply that the thermogram will provide a nice image. An example is shown of a thermogram of some objects taken in winter in a heated room and then repeated in summer. In winter (Fig. 17.32A), the wall temperature is around 20°C, but the air is a few degrees warmer for the convector radiators and the most exposed parts of the objects gain some heat and become

[78] A *white body* is an idealized physical body with absorbance $\varepsilon = 0$, which reflects all incident electromagnetic radiation.

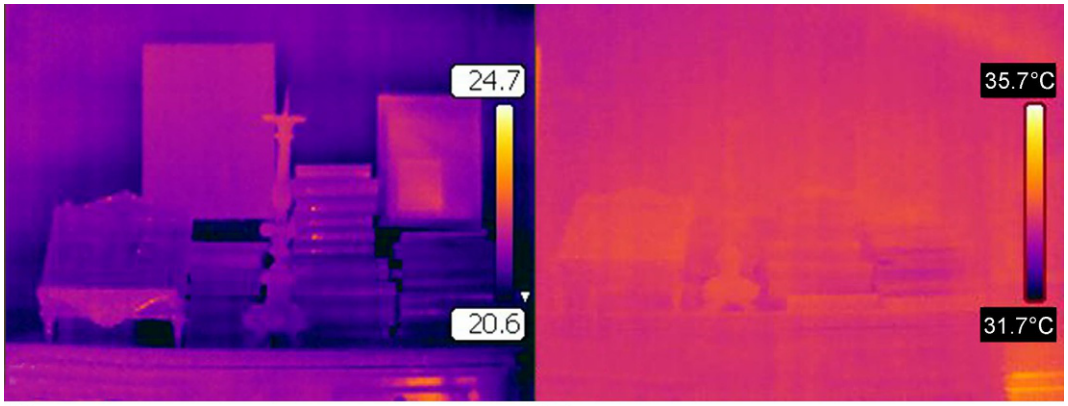

FIG. 17.32 (A) Thermogram of some objects in winter, in a heated room, when air and objects are a bit warmer than the wall and become distinguishable (left). (B) The same in summer, but in a room without air conditioning, where the temperature is homogeneous and objects are indistinguishable from the wall (right).

distinguishable from the wall behind them. Books with golden titles on the spine are visible because they reflect the *IR* emitted by the operator. In summer (Fig. 17.32B), the room is not conditioned, and walls and objects are at the same temperature level, or with very small differences. This uniformity makes the objects undistinguishable from the background. In winter, the image is aesthetically nice for the contrast of temperatures; the temperature determination may require emissivity correction. In summer, the image is obscured because everything is homogeneous, there is no need for correction and the temperature determination is very precise. This follows a principle that pleasant images having nice colour contrasts do not necessarily reflect precise temperature determinations and may need corrections, and vice versa.

References

Abbe, C., 1905. A First Report on the Relations Between Climates and Crops. Government Printing Office, Washington.

Adie, A., 1819. Specification of the patent granted to Alexander Adie, of Edinburgh, optician; for an improvement of the air barometer, which improved instrument is to be called sympiesometer. In: The Repertory of Arts, Manufactures and Agriculture, No CCIX, Vol. 35, Second Series, pp. 257–265.

Aitken, J., 1921. Screens. Proc. Roy. Soc. Edinb. 11, 172–181.

Aleotti, G.B., 1589. Artifitiosi et Curiosi Moti Spiritali di Herrone. Vittorio Baldini, Ferrara (Tradotti da Gio. Batista Aleotti d'Argent).

Amontons, G., 1702. Discours sur quelques propriétés de l'air, et le moyen d'en connaître la température dans tous les climats de la Terre. Mémoires de l'Académie Royale des Sciences, Paris, pp. 155–174.

Antinori, V., 1841. Notizie istoriche relative all'Accademia del Cimento. Tipografia Galileiana, Florence.

Airy, G.B., 1874. Astronomical and magnetical and meteorological observations made at the Greenwich observatory, Greenwich, in the year 1872. Eyre and Spottiswoode, London.

ASTM E1933-14, 2014. Standard Practice for Measuring and Compensating for Emissivity Using Infrared Imaging Radiometers. ASTM International, West Conshohocken, PA.

Austin, J.F., McCollen, A., 1980. James six FRS. Two hundred years of the six's self-registering thermometer. Notes Rec. R. Soc. Lond. 35 (1), 49–65.

Bedford, T., Warner, C.G., 1934. The globe thermometer in studies of heating and ventilation. J. Hyg. 34 (4), 458–473.

Benedict, R., 1984. Fundamentals of Temperature, Pressure, and Flow Measurements. Wiley, New York.

Bentley, R.E., 1998. Handbook of Temperature Measurement: Temperature and Humidity Measurement. Springer Verlag, Berlin.

Boehaave, H., 1759. Elementa Chemie. Coleti, Venice.

Boffito, G., 1929. Gli strumenti della scienza e la scienza degli strumenti. Seeber, Florence.

Böhm, R., Jones, P.D., Hiebl, J., Brunetti, M., Frank, D., Maugeri, M., 2010. The early instrumental warm-bias: a solution for long Central European temperatures series 1760–2007. Clim. Chang. 101 (1–2), 41–67.

Borchi, E., Macii, R., 1997. Termometri e termoscopi. Tipografia Coppini, Florence.

Borchi, E., Macii, R., 2009. Meteorologia a Firenze. Nascita ed evoluzione. Pagnini Ed., Florence.

Borrelli, A., 1670. De motionibus naturalibus a gravitate pendentibus. Ferri, Pisa.

Brázdil, R., Pfister, C., Wanner, H., von Storch, H., Luterbacher, J., 2005. Historical climatology in Europe—the state-of-the-art. Clim. Chang. 70, 363–430.

Brázdil, R., Bělínová, M., Dobrovolný, P., Mikšovský, J., Pišoft, P., Řezníčková, L., Štěpánek, P., Valášek, H., Zahradníček, P., 2012. History of Weather and Climate in the Czech Lands, Vol. IX. Temperature and Precipitation Fluctuations in the Czech Lands During the Instrumental Period. Masarykova Univerzita, Brno.

Brewster, C., 1832. The Edinburgh Encyclopedia. First American ed vol. 2. Parker, Philadelphia.

Buchwald, J.Z., Franklin, A., 2005. Wrong for the Right Reasons. Springer, Dordrecht.

Burnt, S., 2012. The Weather Observer's Handbook. Cambridge University Press, Cambridge.

Camuffo, D., 1980. Fog and related diffusion potential at Venice: two case studies. Bound.-Layer Meteorol. 18, 453–471.

Camuffo, D., 1982. The nocturnal IBL over a hilly island with reference to the diffusion of radioactive nuclei. Bound.-Layer Meteorol. 22, 233–240.
Camuffo, D., 2002a. Calibration and instrumental errors in early measurements of air temperature. Clim. Chang. 53 (1–3), 297–330.
Camuffo, D., 2002b. History of the long series of the air temperature in Padova (1725-today). Clim. Chang. 53 (1–3), 7–76.
Camuffo, D., 2010. The role of temperature and moisture. In: Camuffo, D., Fassina, V., Havermans, J. (Eds.), Basic Environmental Mechanisms Affecting Cultural Heritage—Understanding Deterioration Mechanisms for Conservation Purposes. Nardini, Florence. COST Action D42 "Enviart".
Camuffo, D., 2018. Evidence from the archives of societies: early instrumental observations. In: White, S., Pfister, C., Mauelshagen, F. (Eds.), The Palgrave Handbook of Climate History. Palgrave McMillan, London, pp. 83–92.
Camuffo, D., Bernardi, A., 1993. Microclimatic factors affecting the Trajan Column. Sci. Total Environ. 128, 227–255.
Camuffo, D., Bertolin, C., 2012a. The earliest temperature observations in the world: the Medici Network (1654–1670). Clim. Chang. 111, 335–363.
Camuffo, D., Bertolin, C., 2012b. The earliest spirit-in-glass thermometer and a comparison between the earliest period of the Central England temperature series and the instrumental observations of two Italian stations of the medici network, active 1654–1670. Weather 67 (8), 206–209.
Camuffo, D., della Valle, A., 2016. A summer temperature bias in early alcohol thermometers. Clim. Chang. 138, 633–640.
Camuffo, D., della Valle, A., 2017. The Newton linseed oil thermometer: an evaluation of its departure from linearity. Weather 72 (3), 84–85.
Camuffo, D., Fernicola, V., 2010. How to measure temperature and relative humidity. Instruments and instrumental problems. In: Camuffo, D., Fassina, V., Havermans, J. (Eds.), Basic Environmental Mechanisms Affecting Cultural Heritage—Understanding Deterioration Mechanisms for Conservation Purposes. Nardini, Florence, pp. 31–41 COST Action D42, "Enviart".
Camuffo, D., Jones, P. (Eds.), 2002. Improved Understanding of Past Climatic Variability from Early Daily European Instrumental Sources. Kluwer Academic Publishers, Dordrecht, Boston, London.
Camuffo, D., Schenal, P., 1982. Microclima all'interno della Cappella degli Scrovegni: scambi termodinamici tra gli affreschi e l'ambiente. Ministero dei Beni Culturali ed Ambientali: Giotto a Padova, special issue of Bollettino d'Arte, Poligrafico dello Stato, Rome, pp. 107–209.
Camuffo, D., Pagan, E., Schellen, H., Limpens-Neilen, D., Kozlowski, R., Bratasz, L., Rissanen, S., Van Grieken, R., Spolnik, Z., Bencs, L., Zajaczkowska-Kloda, J., Kloda, P., Kozarzewski, M., Mons Santi, G., Chmielewski, K., Jütte, T., Haugen, A., Olstad, T., Mohanu, D., Skingley, B., Sáiz-Jiménez, C., Bergsten, C.J., Della Valle, A., Don Russo, S., Bon Valsassina, C., Accardo, G., Cacace, C., Giani, E., Giovagnoli, A., Nugari, M.P., Pandolci, A.M., Rinaldi, R., Acidini, C., Danti, C., Aldrovandi, A., Boddi, R., Fassina, V., Dal Prà, L., Raffaelli, F., Bertoncello, R., Romagnoni, P., Camuffo, M., Troi, A., 2007. Church Heating and Preservation of the Cultural Heritage: A Practical Guide to the Pros and Cons of Various Heating Systems. Electa Mondadori, Milano.
Camuffo, D., Bertolin, C., Fassina, V., 2010a. Microclimate monitoring in a church. In: Camuffo, D., Fassina, V., Havermans, J. (Eds.), Basic Environmental Mechanisms Affecting Cultural Heritage—Understanding Deterioration Mechanisms for Conservation Purposes. Nardini, Florence. COST Action D42 "Enviart".
Camuffo, D., Pagan, E., Rissanen, S., Bratasz, Ł., Kozłowski, R., Camuffo, M., della Valle, A., 2010b. An advanced church heating system favourable to artworks: a contribution to European standardisation. J. Cult. Herit. 11, 205–219.
Camuffo, D., Della Valle, A., Bertolin, C., Leorato, C., Bristot, A., 2011. Humidity and environmental diagnostics in Palazzo Grimani, Venice. In: Del Curto, D. (Ed.), Indoor Environment and Preservation—Climate Control in Museums and Historic Buildings. Kermes Quaderni, Nardini, Florence, pp. 9–14, 195–196.
Camuffo, D., della Valle, A., Bertolin, C., Santorelli, E., 2016. The Stancari air thermometer and the 1715–1737 record in Bologna, Italy. Clim. Chang. 139, 623–636.
Camuffo, D., della Valle, A., Bertolin, C., Santorelli, E., 2017. Temperature observations in Bologna, Italy, from 1715 to 1815; a comparison with other contemporary series and an overview of three centuries of changing climate. Clim. Chang. 142 (1–2), 7–22.
Chambers, E., 1728. Cyclopædia: Or a Universal Dictionary of Arts and Sciences. Table of Pneumaticks, vol. 2. Knagton et al., London
Chang, H., 2004. Inventing Temperature. Measurement and Scientific Progress. Oxford University Press, Oxford.
Chappuis, M.P., 1888. Études sur le thermomètre à gaz et comparison des thermomètres à mercure avec le thermomètre à gaz. Gauthier-Villars et fils, Paris.
Chen, X., 2005. Visual photometry in the early 19th century: a "good" science with "wrong" measurements. In: Buchwald, J.Z., Franklin, A. (Eds.), Wrong for the Right Reasons. Archimedes (New Studies in the History of Philosophy of Science and Technology). In: vol. 11, Springer, New York, pp. 161–183.
Commandino, F., 1575. Heronis Alexandrini Spiritualium liber. A Federigo Commandino Urbinate ex Greco, nuper in Latinum Conversus. Frisolino, Urbino.
Comstock, J.L., 1853. Elements of Chemistry in Which the Recent Discoveries in the Science Are Included. Pratt, Woodford, New York.
Cotte, L., 1774. Traité de Météorologie: contenant 1. l'histoire des observations météorologiques, 2. un traité des météores, 3. l'histoire & la description du baromètre, du thermomètre & des autres instruments météorologiques, 4. les tables des observations météorologiques & botanicométéorologiques, 5. les résultats des tables & des observations, 6. la méthode pour faire les observations météorologiques. Imprimerie Royale, Paris.
Crestani, G., 1931. Climatologia. UTET, Torino.
D*** (alias D'Alencé, J.), 1688. Traittéz des Barométres, Thermométres et Notiométres ou Hygrométres. Westein, Amsterdam.
De Luc, J.A., 1772. Récherches sur les modifications de l'atmosphère: contenant l'histoire critique du baromètre et du thermomètre. Tome I. Printed by the Author, Geneva.
Della Porta, G.B., 1584. Magiae Naturalis sive de Miraculis Rerum Naturalum Libri Viginti. Horatium Salvianum, Neaples.
Della Porta, G.B., 1607. Magiae Naturalis sive de Miraculis Rerum Naturalium Libri Viginti. Hempelius, Frankfurt.
Denza, F., 1882. Istruzioni per le osservazioni meteorologiche e il barometro altimetrico. Associazione Meteorologica Italiana, Torino.
Derham, W., 1709. Tables of barometrical altitudes at Zurich in Switzerland in the year 1708 observed by Dr. J. J. Scheuchzer... in those different parts of Europe. Philos. Trans. 26, 342–366.
Doebelin, E.O., 1990. Measurement Systems—Application and Design. McGraw-Hill, New York.
du Crest, M., 1765. Kleine Schriften von den Thermometern und Barometern. Klett, Augsburg.
EN 15758, 2010. Conservation of Cultural Property—Indoor Climate—Procedures and instruments for measuring temperatures of the air and of the surfaces of objects. European Committee for Standardization (CEN), Brussels.
Fahrenheit, D.G., 1724. Experimenta circa gradum caloris liquorum nonnullorum ebullentium instituta. Philos. Trans. 381 (23), 1–3.
Flammarion, C., 1872. L'Atmosphère. Description des grands phénomènes de la Nature. Hachette, Paris.

Fludd, R., (alias De Fluctibus, R.), 1624. Tractatus secundus, de naturae simia seu technica macrocosmi historia. Roetelii, Frankfurt.
Fludd, R., (alias De Fluctibus, R.), 1626. Philosophia sacra & vere Christiana seu Meteorologia Cosmica, Bryan, Frankfurt.
Fludd, R., (alias De Fluctibus, R.), 1638. Philosophia Moysaica in qua sapientia et scientia creationis explicantur. Ramazzeni, Gouda.
Foote, E., 1856. In: Silliman, B., Silliman Jr., B., Dana, J.D. (Eds.), On the Heat in the Sun's Rays. In: vol. 22. American Journal of Sciences and Arts. Putnam & Co, New York, pp. 377–381.
Frisinger, H.H., 1983. The History of Meteorology: To 1800. American Meteorological Society, Boston.
Ganot, A., 1860. Traité de physique expérimentale et appliquée, et de meteorology. Chez l'auteur-éditeur, Paris.
Gerosa, G., 1898. Meteorologia. UTET, Torino.
Giorgi, A., 1592. Spiritali di Herone Alessandrino ridotti in lingua volgare da Alessandro Giorgi da Urbino. Ragusi, Urbino.
Green, W., Maloney, G.O. (Eds.), 1984. Perry's Chemical, Engineers Handbook, sixth ed. McGraw-Hill, Singapore.
Guillaume, C.E., 1889. Traité pratique de la thermométrie de précision. Gauthier-Villars et fils, Paris.
Hadlock, R., Seguin, W.R., Garstang, M., 1972. A radiation shield for thermistor development in the atmospheric boundary layer. J. Appl. Meteorol. 11, 393–399.
Hemmer, J.J., 1783. Descriptio instrumentorum meteorologicorum, tam eorum, quam Societas distribuit, quam quibus praeter haec Manheimii utitur. Tomus 1, Ephemerides Societatis Meteorologicae Palatinae, pp. 57–90.
Heron of Alexandria, c.10–70 AD. Spiritalia. Harleian Collection No 5605. British Museum, London.
Hicks, J.J., 1875. An improved vacuum solar radiation thermometer. Q. J. R. Meteorol. Soc. 2, 98–101.
IMAIT, 1872. Norme per le osservazioni meteoriche. Supplemento alla Meteorologia Italiana. Italian Ministry for Agriculture, Industry and Trade, Rome, pp. 28–33.
Imray, J., 1862–1874. A Communication From Mattheus Hipp. Patents for Inventions: Abridgments of Specifications Relating to Electricity and Magnetism. Part II. A.D. 1858–1866, Great Britain Patent Office, Eyre, London, pp. 503–504.
Kantor, N., Unger, J., 2011. The most problematic variable in the course of human-biometeorological comfort assessment—the mean radiant temperature. Cent. Eur. J. Geosci. 3 (1), 90–100.
Kingston, G.T., 1874. Exposure of thermometers. In: Authority of the Meteorological Committee, Report of the Proceedings of the Meteorological Congress at Vienna. Protocols and Appendices. Eyre and Spottwood, London, pp. 84–86.
Kington, J., 1997. Observing and measuring the weather. In: Hulme, M., Barrow, E. (Eds.), Climates of British Isles: Present Past and Future. Routledge, London, pp. 137–152.
Kondratyev, K.Y., Kozoderov, V.V., Smokty, O.I., 1992. Remote Sensing of the Earth From Space: Atmospheric Correction. Springer-Verlag, Berlin.
Landsberg, H.E., 1985. Historic weather data and early meteorological observations. In: Hecht, A.D. (Ed.), Paleoclimate Analysis and Modeling. Wiley, New York, pp. 27–70.
Leslie, J., 1804. An Experimental Inquiry Into the Nature and Propagation of Heat. J. Mawman, London.
Leslie, J., 1838. Treatises on Various Subjects of Natural and Chemical Philosophy. Black, Edinburgh.
Lide, D.R. (Ed.), 1990. CRC Handbook of Chemistry and Physics, 67th ed. CRC Press, Boca Raton, FL.
Lipták, B.G., 2003. Instrument Engineers' Handbook: Process Measurement and Analysis. The Instrumentation System and Analysis (ISA). vol. 1. CRC Press, Boca Raton, FL.
Madding, R.P., 1999. Emissivity measurement and temperature correction accuracy considerations. In: SPIE Vol. 3700, 0277-786X199. Conference on Thermosense XXI, Orlando, FL.
Magalotti, L., 1666. Saggi di naturali esperienze fatte nell'Accademia del Cimento. Cocchini, Florence.
Michalski, S., 2000. Guidelines for Humidity and Temperature in Canadian Archives. Canadian Conservation Institute, Ottawa.
Michalski, L., Eckersdorf, K., McGee, J., 1991. Temperature Measurement. Wiley, New York.
Middleton, K.W.E., 1966. A History of the Thermometer and Its Use in Meteorology. J. Hopkins University Press, Baltimore, MD.
Middleton, W.E.K., 1969. Invention of the Meteorological Instruments. The Johns Hopkins University Press, Baltimore, MD.
Middleton, W.E.K., 1971. The Experimenters: A Study of the Accademia del Cimento. The Johns Hopkins University Press, Baltimore, MD.
Negretti, E., Zambra, J.W., 1864. Meteorological Instruments: Explanatory of Their Scientific Principles, Method of Construction, and Practical Utility. William and Strahams, London.
Nicholas, J.V., White, D.R., 1994. Traceable Temperatures—An Introduction to Temperature Measurement and Calibration. Wiley, New York.
Nollet, J.A., 1749. Nozioni di Fisica Sperimentale. vol. 4 Pasquali, Venice.
Oke, T.R., 1978. Boundary Layer Climates. Methuen, London.
Parker, D.E., 1994. Effects of changing exposure of thermometers at land stations. Int. J. Climatol. 14, 1–31.
Perry, M., Prior, M.J., Parker, D., 2007. An assessment of the suitability of a plastic thermometer screen for climatic data collection. Int. J. Climatol. 27 (2), 267–276.
Philo of Byzantium, 2nd or 3rd Century BC. De Ingeniis Spiritualibus. Codex Latinus Monacensis 534 (codex of the XIVth century) Bayerische Staatsbibliothek. München, Munich.
Pitarma, R., Crisóstomo, J., Jorge, L., 2016. Analysis of materials emissivity based on image software. In: Rocha, Á. et al., (Ed.), New Advances in Information Systems and Technologies, Advances in Intelligent Systems and Computing 444. Springer, New York, pp. 749–757.
Platridge, G.W., Platt, C.M.R., 1976. Radiative Processes in Meteorology and Climatology. Elsevier, Amsterdam.
Poleni, G., 1709. Johannis Poleni Miscellanea hoc est: I Dissertatio de Barometris et Termometris. Aloysium Pavinum, Venice.
Przybylak, R., Majorowicz, J., Brázdil, R., Kejan, M. (Eds.), 2010. Climate of Poland and Central/Eastern Europe During the Past Millennium Combining Instrumental, Documentary and Other Proxy Data. Springer Verlag, Berlin.
Pulling, H.E., 1919. Sunlight and its measurement. Plant World 22 (7), 187–209.
Regnault, H.V., 1847. Relation des expériences entreprises par ordre de Monsieur le Ministre de travaux publics et sur la proposition de la Commission centrale des machines à vapeur pour déterminer les principales lois et les données numériques qui entrent dans le calcul des machines à vapeur. vol. 21 Typ. de Firmin Didot frères, Paris, pp. 1–748. Also: Mémoires de l'Académie Royale des Sciences.
Rumford (alias Thomson, B., Count of Rumford), 1804. An inquiry concerning the nature of heat and the mode of its communication. Philos. Trans. R. Soc., 175–181 (summarized); full length, with the same title in: The Complete Works of Count Rumford, vol. 3, pp. 23–130, Macmillan, London (1876).
Rutherford, D., 1795. A description of an improved thermometer. In: The Edinburgh Magazine, or Literary Miscellany, Vol. IV New Series. Symington, London, pp. 282–283.
Rutherford, D., 1796. A description of an improved thermometer. Trans. R. Soc. Edinb. 8, 430.

Sagredo, G.F., 1612. Letter to Galileo, dated 30 June 1612. Manoscritti Galileiani, Carteggio Galileiano. Mss. Gal., P. VI, T. VIII, car. 18-20, Biblioteca Centrale Nazionale di Firenze, Florence.
Sagredo, G.F., 1615. Letter to Galileo, dated 11 April 1615. Manoscritti Galileiani, Carteggio Galileiano. Mss. Gal., P. VI, T. IX, car. 251-253, Biblioteca Centrale Nazionale di Firenze, Florence.
Sanctorius, S., 1612. Commentaria in Artem Medicam, pars 3. Coll. 229, Giac, Antonio Somasco, Venice.
Sanctorius, S., 1625. Commentaria in primam fen primi libri Canonis Avicennae. Iacobus Sarcina, Venice.
Schooley, J.F., 1986. Thermometry. CRC Press, Boca Raton, FL.
Shaw, N., 1932. Manual of meteorology. In: Meteorology in History. vol. 1. Cambridge University press, Cambridge.
Six, J., 1794. The Construction and Use of a Thermometer for Showing the Extremes of Temperature in the Atmosphere, During the Observer's Absence, Together With Experiments and Variations of Local Heat; and Other Meteorological Observations. Blake and Wilkie, London. posthumous.
Stancari, V.F., 1708. De Thermometro ab Amontonio recens inventis. Ex epistula ad Maraldum. Printed posthumous in: Schedae Mathematicae, Barbiroli Archigymnasium, Bologna, pp. 53–55. 1713.
Stevenson, T., 1864. New description of box for holding thermometers. J. Scott. Meteorol. Soc. 1, 122.
Targioni Tozzetti, G., 1780. Notizie degli aggrandimenti delle Scienze Fisiche accaduti in Toscana nel corso di anni LX del secolo XVII. Tomo I Bouchard, Florence.
Tomlimson, C., 1861. The Tempest: an Account of the Origin and Phenomena of Wind in Various Parts of the World. Society for Promoting Christian Knowledge, London.
UK Meteorological Office, 1981. Handbook of Meteorological Instruments. Measurement of Temperature. vol. 2. Her Majesty's Stationary Office, London.
van Musschenbroek, P., 1745. Elementa Physicae conscripta in usus Academicos. Recurti, Venice.
van Musschenbroek, P., 1762. Introductio ad Philosophiam Naturalem, vol. 2. Luchtmans, Leiden.
van Musschenbroek, P., 1758. Ephemerides meteorologicae et magneticae conscriptae primo Ultrajecti, deinde continuatae Leydae ab anno 1729 ad finem anni 1758. Handschrift, University of Leiden, Leiden.
Viviani, V., 1717. Racconto istorico della vita di Galileo. Manuscripts in Biblioteca Centrale Nazionale di Firenze. posthumous. Reprinted in Favaro, A. (Ed.), 1907. Opere di Galileo, vol. XIX, pp. 597–632, Barbera, Florence.
Wild, H., 1874. On the exposure of thermometers for the calculation of air temperature. Suppl. V In: Authority of the Meteorological Committee, Report of the Proceedings of the Meteorological Congress at Vienna. Protocols and Appendices. Eyre and Spottwood, London, pp. 77–80.
WMO, 1986. Compendium of lecture notes on meteorological instruments for training class III and class IV meteorological personnel. WMO Technical Publication No. 622, World Meteorological Organization, Geneva.
WMO, 2008. Guide to meteorological instruments and methods of observation. WMO Technical Publication No. 8, World Meteorological Organization, Geneva. updated 2010.
Wolfe, W.L., Zissis, G.J., 1989. The Infrared Handbook. Environmental Research Institute of Michigan, Ann Arbor, MI.
Wood, L.E., 1946. Automatic weather stations. J. Meteorol. 3, 115–121.
Wylie, R.G., Lalas, T., 1992. Measurement of Temperature and Humidity. WMO 759 Secretariat of the World Meteorological Organization, Geneva.
Yavorsky, B.M., Pinsky, A.A., 1979. Fundamentals of Physics. vol. 1 Mir, Moscow.

Further Reading

Privat-Deschanel, A., 1870. Elementary Treatise on Natural Philosophy. Blackie and Son, London.

This page intentionally left blank

CHAPTER

18

Measuring Air Humidity

OUTLINE

18.1 PART 1. HISTORICAL OVERVIEW: THE DEVELOPMENT OF EARLY HYGROMETERS AND BASIC IDEAS

18.1.1 Introduction

Several instruments, based on various physical principles, have been devised to measure the humidity in air (Wolf, 1961; Middleton, 1969; Frisinger, 1983; Turner, 1983; Bud and Warner, 1998; Borchi and Macii, 2007; Kämpfer, 2012; Camuffo et al. 2014; Korotcenkov, 2018, 2019). A short historical overview of the most interesting types is made to explain the present-day technological development and make the best use of it. The aim is to inform users about technical and normative issues, to appreciate the genial solutions found in the past, and to stimulate the most traditionalist users to update their instruments to obtain reliable records.

18.1.2 Hygrometers Based on Moisture Absorption and Weight Increase

The earliest hygrometers appeared in the 15th century, and were based on the change of weight of some hygroscopic materials (e.g. seeds, cotton, wood, or sponges) for the absorption or loss of moisture to reach equilibrium with the ambient air. The weight was determined with a precision balance (Fig. 18.1). Key persons that studied this method were Nicolaus Cusanus (1565), Leon Battista Alberti (1485), and Leonardo da Vinci (1487).[1] The method required the accurate conservation of the test specimens to repeat the measurement and detect the change. It was a clever idea, but not a practical method. The figure reports three representations of the method, the first one drawn in the second half of the 15th century (Leonardo, 1487); the second was published in the second half of the 17th century (D***, 1688), the third

[1] Nicolaus Cusanus (1401–64); Leon Battista Alberti (1404–72); Leonardo da Vinci (1452–1519).

https://doi.org/10.1016/B978-0-444-64106-9.00018-3

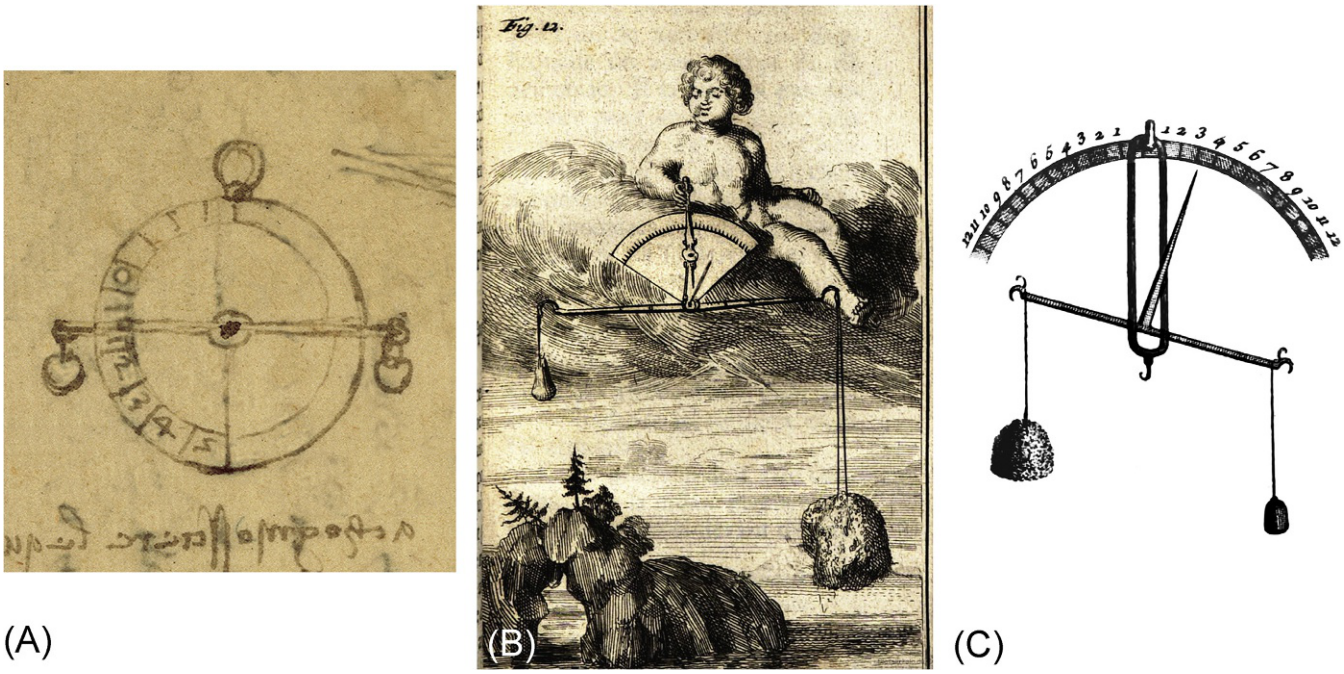

FIG. 18.1 The weight of a hygroscopic specimen is controlled with a precision balance to detect changes in moisture content as an index of drier or moister air. *From (A) Leonardo (1487) Codex Atlanticus sheet 675 recto, ©Veneranda Biblioteca Ambrosiana/Metis e MidaInformatica/Mondadori Portfolio, Milano, Used with permission; (B) D*** (1688); (C) Cotte, 1774.*

almost three centuries later (Cotte, 1774). Method and instrument have remained the same. They disappeared a few years later, in 1783, when De Sussure invented the hair hygrometer. However, several other inventions were needed to reach this finding.

18.1.3 Hygrometers Based on Dimensional Changes or Torsion

A more practical method was based on linear dimensional changes or torsion of leather, wood, paper, etc. Hygroscopic materials shrink when humidity drops and swell when humidity increases. Similarly, cordage and catgut are shortened and untwisted by moisture.

Sanctorius[2] invented a hygrometer where a cord was stretched horizontally and had a ballast ball suspended in the middle (Fig. 18.2A, Sanctorius, 1625). When the relative humidity increased, the cord was tightened lifting the ball.

In Florence, Folli and Viviani,[3] two scholars of the Accademia del Cimento, developed around 1664 other similar instruments[4] 'to measure the air dryness or dampness' based on the elongation of cords, strings, or paper (Targioni Tozzetti, 1780), but closely inspired to Sanctorius. The Folli instrument,[5] based on a horizontal strip of paper, holding a ballast in the middle, moving up (dry) and down (wet) on a graduated scale, is shown in Fig. 18.2B. The Folli and Viviani hygrometer was realized with parchment that was more sensitive, more resistant, and supported heavier ballasts. The parchment was wound around a pulley system and connected with a wire to a pointer (Fig. 18.2B). A problem was that when parchment was dried too much, it was impossible to return to the original conditions, even moistening it (D***, 1688). In other experiments, a long cord was used, fixed at one extreme and ballasted at the other one. The ballasted rope was connected to a mobile pointer (Fig. 18.2D; Macfarquhar and Gleig, 1797). In order to reduce the exceedingly long space required by the cord, this was folded over a number of times with pulleys (Fig. 18.2E; D***, 1688). In the case of cord torsion, the cord was fixed to a rotating pointer or graduated wheel (D***, 1688; Macfarquhar and Gleig, 1797; Fig. 18.2F).

[2] Sanctorius Sanctorius (1561–1636).

[3] Giovanni Francesco Folli (1624–85); Vincenzo Viviani (1622–1703).

[4] See Chapter 6.

[5] See also Chapter 6, Fig. 6.15.

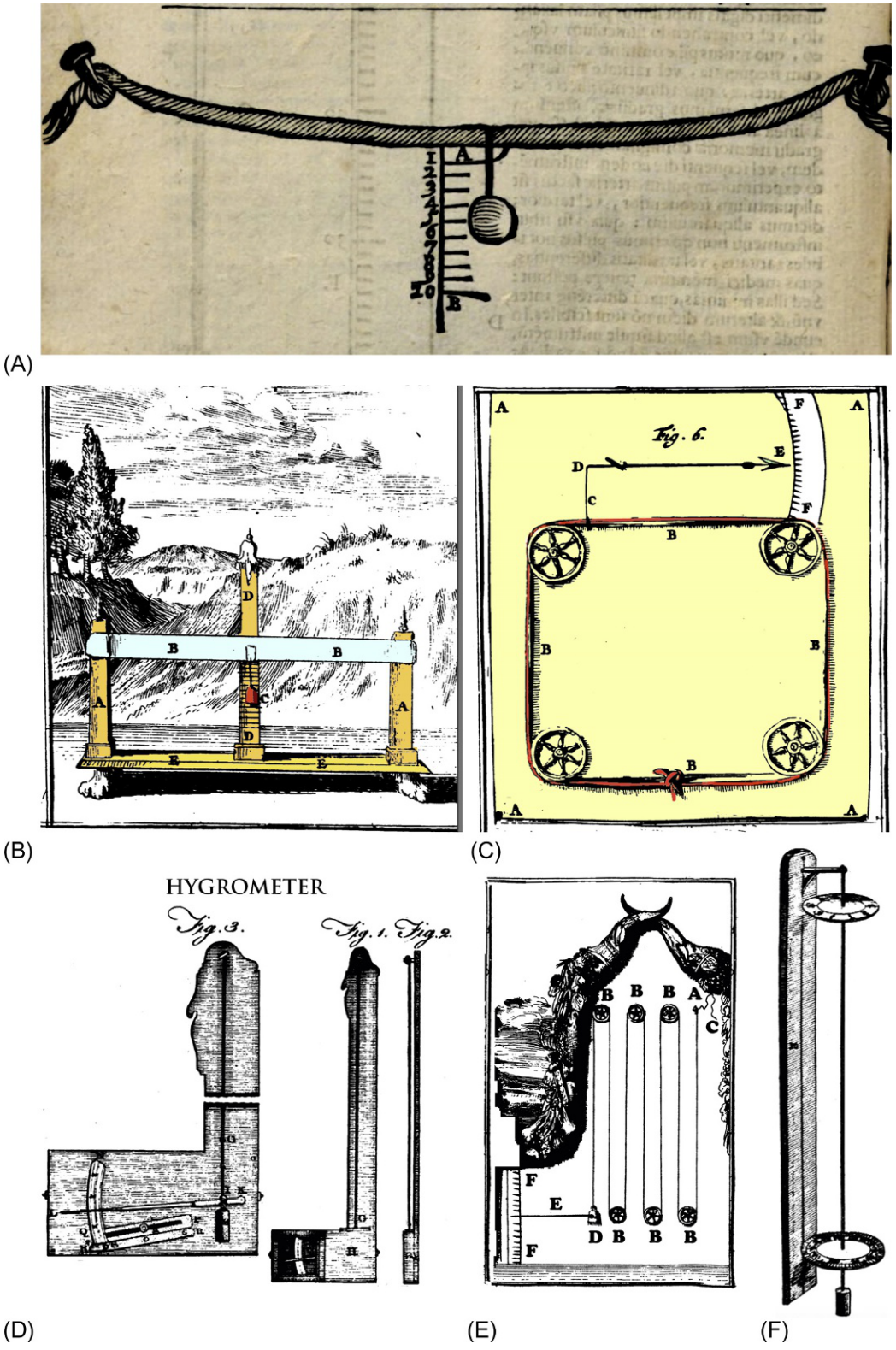

FIG. 18.2 (A) Hygrometer by Sanctorius where a cord was stretched horizontally, fixed to the wall with two nails. It had a ballast ball suspended in the middle, moving from A to B that was divided into 10 tags. (B) Folli hygrometer composed of a horizontal strip of paper (BB, *cyan*), holding a ballast (C, *red*) in the middle, moving on a vertical graduated scale (DD). The frame structure *(orange)* was made of copper. (C) Folli and Viviani hygrometer composed of strip of parchment (BBBB, *red*) wound around four pulleys fixed on a frame (AAAA, *yellow*) and connected with a wire (C) to a pointer (DE), moving on a graduated scale (FF). (D) Details to build a cord elongation hygrometer with pointer [indicated *Fig. 1*: the instrument assembled, *Fig. 2*: detail of the cord with ballast; *Fig. 3*: detail with expanded view of the pointer and scale]. (F) Early cord elongation hygrometer, with the cord (C) fixed in A, folded over a number of times with pulleys (B), with a load (D) to which a pointer (E) was fixed, and moved across the scale FF. (F) A cord torsion hygrometer. *From (A) Sanctorius (1625); (B, C, E) D*** (1688); (D, F) Macfarquhar and Gleig (1797).*

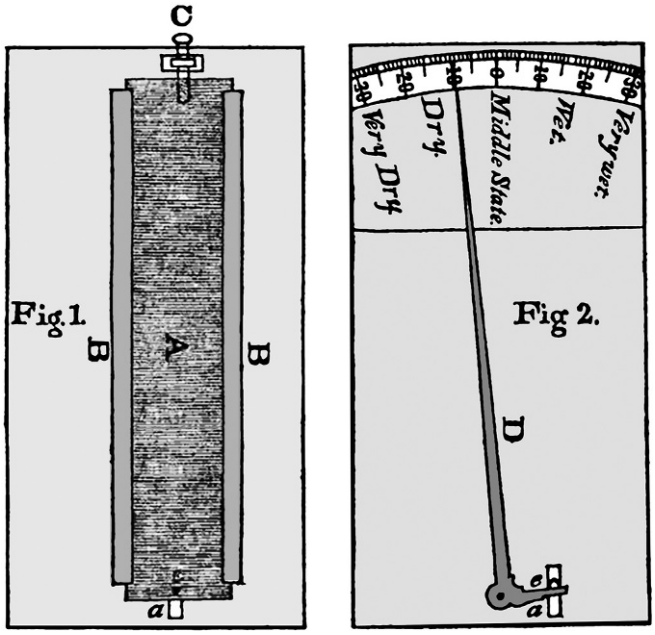

FIG. 18.3 Nairne's Wood shrinkage/swelling hygrometer: (Fig. 1) *Hatched area A*, the wooden sensor; *BB*, sensor guides; *C*, regulation screw; *a*, pin to transmit the deformation to the pointer. (Fig. 2) detail of the pointer and scale with graduations: *Very Dry – Dry – Middle State – Wet – Very wet*. *From Nairne (1783).*

In 1663, Hooke[6] used catgut made from the beard of a wild oat[7] (Birch, 1756) and Johann Heinrich Lambert built an improved catgut hygrometer (Lambert, 1769, 1772, 1774).

The instrument maker Nairne[8] wrote to Benjamin Franklin proposing an interesting hygrometer based on shrinkage swelling of wood (Fig. 18.3; Nairne (1783). The sensor was a piece of wood (A) cut crosswise the grain and slid freely between two pieces of wood (BB) having grooves for it. There was a screw (C) for adjusting the piece of wood and the pointer on the scale. A pin was fixed to the sensor and moved the pointer on the scale from very dry to very wet. In hindsight, this sensor is not convenient for precise measurements of *RH*, but may be considered an interesting proxy to highlight in real time the response of wooden assets to *RH* and temperature changes, i.e. a detection and early warning sensor for preventive conservation purposes.

18.1.4 The Hair Hygrometer

The hair hygrometer belongs to the family of sensors based on dimensional changes, but merits a special consideration because for almost two centuries it has been the most popular instrument in galleries and museums (Macleod, 1983; Thomson, 1986; Michalski, 2000), where curators, custodians and visitors may check on their diagrams whether everything is normal. As a matter of fact, it had constituted the most practical, or even the only possible methodology, up to the 1970s, when electronic sensors were produced. It apparently has easy use, if one disregards periodic maintenance and calibration.

De Saussure[9] proposed the hair hygrometer (Fig. 18.4A; De Saussure, 1783) and presented it to the tender of the *Theodoro-Palatina Academy of Sciences*, Mannheim, for the most reliable instrument to be used in the novel climate network (Hemmer, 1783). However, this instrument was rejected with severe criticisms: 'a complicated instrument; the variable nature of the hair and the uncertainty in preparation; the uncertainty of dryness and dampness extremes; the weight that opposes the contraction of the hair; the danger of its being injured by dust and cobwebs; the limited extent of the scale; the rules for determining the absolute quantity of vapours in the atmosphere, while the attention should be directed only to the moisture and dryness which the air exhibits' (Smollett, 1788).

Despite these problems, this was the best hygrometer developed in the eighteenth century, able to provide reasonably correct, direct reading on an analogue scale. Not only in weather stations but also in other application fields, the thermo-hygrograph, i.e. a combination of a thermometer and a hair hygrometer, became very popular in museums, galleries, archives, and libraries. Combined with a spring clock motor and a rotating drum, continuous records on a strip chart were possible (Fig. 18.4B and C). Records were made by means of an ink pen fixed to a mobile arm connected to the hair whose elongation was proportional to the equilibrium relative humidity (*RH*). Air temperature and *RH* were plotted with two ink pens on weekly or monthly charts fixed to a rotating drum.

At first sight, the routine use of such instrument is very simple, as it is sufficient to replace the strip chart at fixed intervals and fill the ink pen when necessary. However, this instrument requires periodic maintenance and calibration. If such care is omitted, readings may depart very much from the truth and misleading readings might cause dangerous consequences when controlling the *RH* in archives, museums, or galleries.

[6] Robert Hooke (1635–1703).

[7] Wild oat is a cereal, *Avena sativa*.

[8] Edward Nairne (1726–1806).

[9] Horace Bénédict De Saussure (1740–1799).

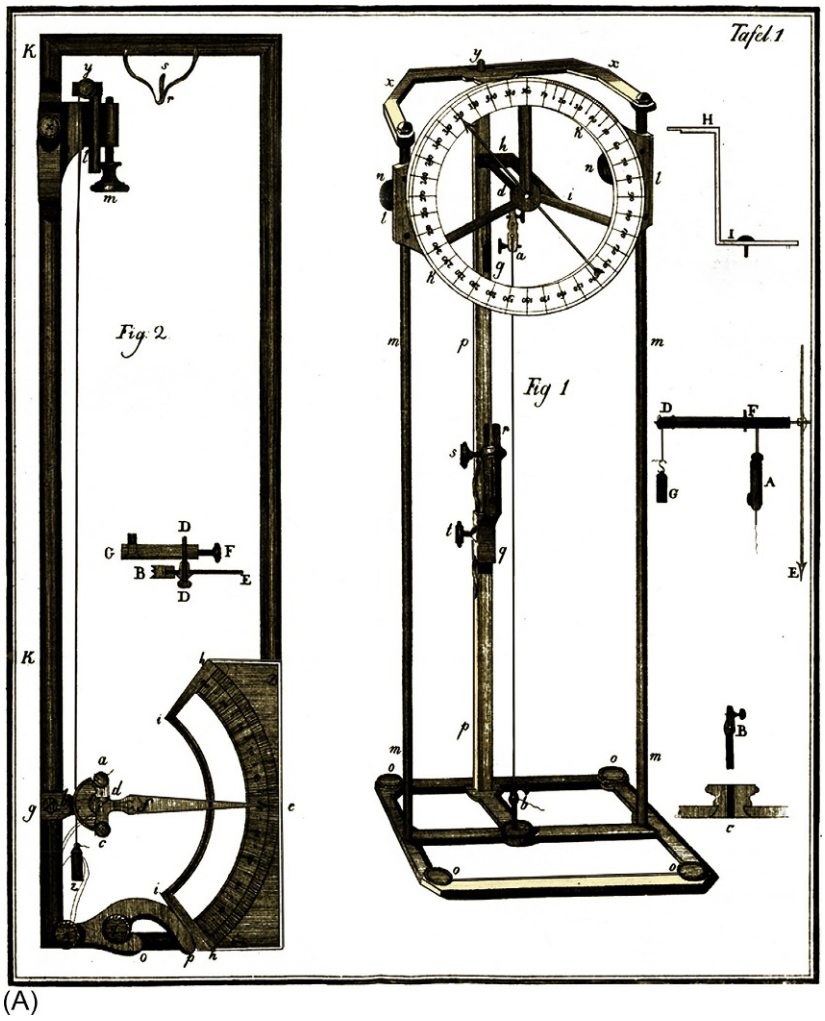

FIG. 18.4 (A) Two prototypes of hair hygrometer proposed by De Saussure. (B) View of a mechanical hair hygrograph, with ink pen recording on a rotating drum. The mechanism is very similar to the De Saussure prototype in (A), left side.

(*Continued*)

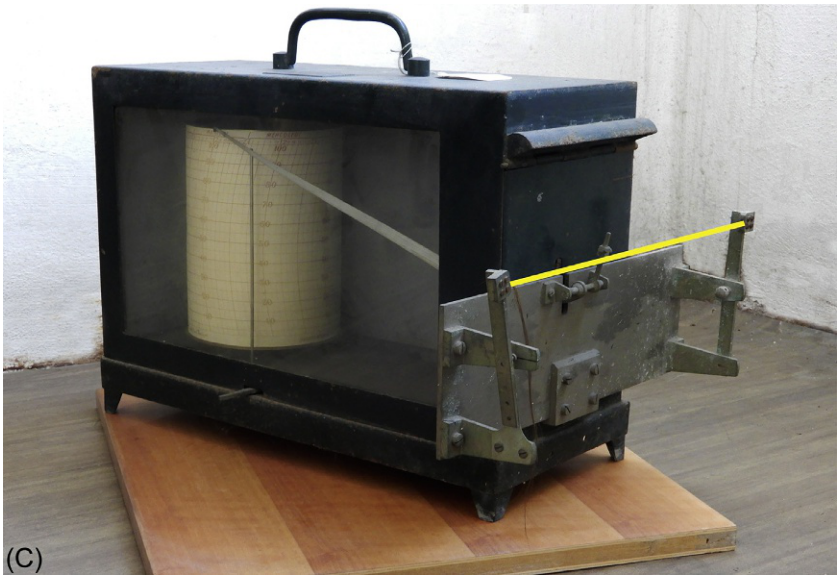

FIG. 18.4—cont'd (C) Mechanical hair hygrograph produced by Richard Frères, Paris. The bundle of hair is broken and the *yellow line* shows its normal position. *From (A) De Saussure (1783); (B) Vercelli (1933); (C) Courtesy of Valeria Zanini, INAF,* Astronomical Observatory, *Padua, © Used with permission.*

The user needs to be informed about errors (typically between ±5% and ±30%), advantages and limitations of this dated methodology (Davey, 1965). The response of the hair sensor is only slightly affected by temperature but is changeable with hair hydration (i.e. memory of the past humidity levels), hair tension (i.e. mechanical load), contamination, and ageing.

The length of human hairs, when the natural grease has been thoroughly removed, increases by a value ranging from 1.7% to 2.5% when the *RH* rises from 0% to 100%, and the elongation $\triangle L/L_o$, where L_o is the dry air length, is approximately proportional to the logarithm of *RH*, at least for not too dry environments, i.e. for $RH > 20\%$, and is usually calculated by means of the equation:

$$\frac{\Delta L}{L_o} \approx k \ \ln(RH) \tag{18.1}$$

where k is a coefficient of proportionality. However, better approximations on the whole range $0 \leq RH \leq 100\%$ for increasing values of *RH* and hydrated hair are given by the functions:

$$\frac{\Delta L}{L_o} \approx k_1 \sqrt{RH} \tag{18.2}$$

$$\frac{\Delta L}{L_o} \approx k_2 \ln^2(1+RH) \tag{18.3}$$

$$\frac{\Delta L}{L_o} \approx k_3 \ln^2\left(1+\sqrt{RH}\right) \tag{18.4}$$

$$\frac{\Delta L}{L_o} \approx k_4 \ln(1+RH) \ln\left(1+\sqrt{RH}\right) \tag{18.5}$$

$$\frac{\Delta L}{L_o} \approx k_5 \, \mathrm{RH}^2 + k_6 \, RH + k_7 \tag{18.6}$$

which give similar results, and the constants depend upon the final elongation at saturation; in general, $17\times10^{-4} \leq k_1 \leq 25\times10^{-4}$; $8\times10^{-4} \leq k_2 \leq 12\times10^{-4}$; $30\times10^{-4} \leq k_3 \leq 44\times10^{-4}$; $15\times10^{-4} \leq k_4 \leq 22\times10^{-4}$; $k_5 \approx -2\times10^{-6}$; $k_6 \approx 4\times10^{-4}$; $k_7 \approx 1\times10^{-3}$. The 'dry', i.e. the lower transfer function, due either to hysteresis for decreasing values of *RH*, or dehydration of the hair, is not so well defined, and a crude calculation can be done with the equation:

$$\frac{\Delta L}{L_o} \approx k_8 \sqrt{RH} \ln(1+RH) \tag{18.7}$$

where $37 \times 10^{-5} \leq k_8 \leq 54 \times 10^{-5}$. All these formulae are plotted in Fig. 18.5.

From the graphs, it is evident that approaching saturation, the hair loses sensitivity: it has the same elongation at $RH = 100\%$ and when it is immersed into water. For this reason, immersion in distilled water is an easy method to calibrate the transducer at the upper limit of its range.

The response time of the hair is not constant: it depends on temperature, stress on the hair, *RH* value, and direction of *RH* change. It increases when the air temperature decreases. At room temperature, the time constant varies from 0.5 to 3 min. Measurements below freezing temperature need far more minutes to reach equilibrium, and at −40°C the hair becomes insensitive.

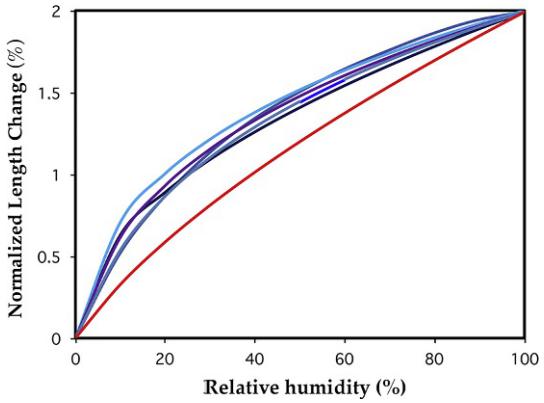

FIG. 18.5 Elongation of a hydrated hair *(thick black line)* for increasing *RH* and elongation computed with the formulae in Eqs (18.1), (18.6) *(thin violet lines)*. The best approximation, i.e. $(\triangle L/L_o) = 9.3\times10^{-4}$ $\ln^2(1+RH)$, is shown with a *thick line*. Tensile load: 1 g. The *red line* shows Eq. (18.7) for poorly hydrated hair or hysteresis for decreasing *RH*.

The response is faster for high humidity levels as well as with increasing humidity levels, following the natural hair hygroscopicity. It is also faster for hair under stress when charged with external load (e.g. the tension due to the series of linkage to the recording pen arm); however, tension generates long-term drift.

The sensor is affected by hysteresis, so that the same output can be observed for different values of *RH* depending on the past environmental values to which the sensor has (temporarily) adapted. The largest errors occur in dry conditions and the permanence in dry environments decreases the hair sensitivity. The hair is composed of different layers that respond in different ways. When the sensor is well hydrated, it presents the so-called *wet* calibration curve to which all instruments refer; however, after some days in dry condition, it reduces the hydration level of the outer layers and follows another 'dry' curve. To minimize the uncertainty due to hysteresis, both the calibration curves (i.e. for the 'wet' and 'dry' hair) are always measured at increasing humidity. The transition from 'wet' to 'dry' occurs only after continual permanence at low *RH* as is the case of most heated rooms and museums in winter. For this reason, hairs should be regenerated very frequently, keeping them into distilled water. The frequency of this operation is determined by the ambient *RH* and the span of daily cycles; the dryer the ambience, more frequently should the regeneration be repeated. For instance, in an ordinary room, the regeneration should be made at least every week by keeping the hairs immersed in water for a whole night. In very dry environments, this operation should be made more frequently. This imposes an unacceptable limitation.

Hairs are affected by chemical contaminants and it is necessary to clean them with ether every time hairs have been exposed to air pollution, contaminated with soot deposits or natural grease, or touched with bare fingers. Ideally, the transducer calibration should be made weekly, when the chart strip is changed. If the reading is not precise, the calibration should be made to evaluate the drift and correct the most recent readings and tune the instrument before the use, after having cleaned and regenerated the hairs. Without all these operations, it is not clear which ambient *RH* corresponds to the instrument output.

A clear indication that the instrument being used is out of calibration is given when the sensor reaches saturation and the pen remains for several hours very stable at the same level, different from 100%. Such maxima may be found at any value between 75% and 120% and show how much the upper limit of the span has changed.

The response time can be reduced by flattening the hair. Hair-rolled flat is much faster than ordinary hair: at room temperature, it is 3–5 times faster; below zero, one order of magnitude or even more. The speed may also be further increased by applying a greater rolling pressure. The faster response also involves negative aspects: for rolled hairs, the 'wet' to 'dry' transition occurs after a few hours of dry environment. Another drawback is that rolled hairs have their strength decreased and, consequently, their drift increased.

In conclusion, the hair hygrometer has been the best methodology up to the 1970s, but nowadays it ranks lowest in quality. It has been considered unsuitable as a standard instrument for measuring humidity (UK Meteorological Office, 1981). The European Standard EN 16242 (2012) points out that this instrument has low accuracy level and considers its use acceptable in exceptional circumstances for visual inspection only but not for spot or routine measurements, for controlling indoor climate, or for data collection to be used in statistical analyses for conservation purposes.

Even today some of these instruments are still visible in galleries and museums. However, their role should be changed from measuring instruments to historic exhibits.

18.1.5 Bulb Hygrometers

Other hygrometers were inspired by the structure of a thermometer. The basic idea was to have fixed on the same wooden frame three basic weather instruments, with strict analogies between them: thermometer, cistern barometer, and hygrometer (Fig. 18.6). These are composed of a tube of glass kept vertical, quicksilver as instrumental liquid, and a bulb or a cistern where the quicksilver had the input from weather. This was an early weather station with the key atmospheric variables. Thermometer and hygrometer had the same length to be comparable between them and correct the humidity readings for the mercury expansion. The length of the frame was 115 cm.

Amontons[10] applied at the bottom of the glass tube a leather bag filled of mercury. When air was moist, the leather bag expanded and mercury descended in the tube (Amontons, 1685, 1695). In order to reach a more resistant and compact bulb structure, Amontons substituted a horn filled of mercury, but increased the time of response (Berryat, 1754). The main problem was that the mercury in the bulb and the tube responded to temperature as a thermometer. Only one century later was the temperature correction carried out by Chiminello (1785).

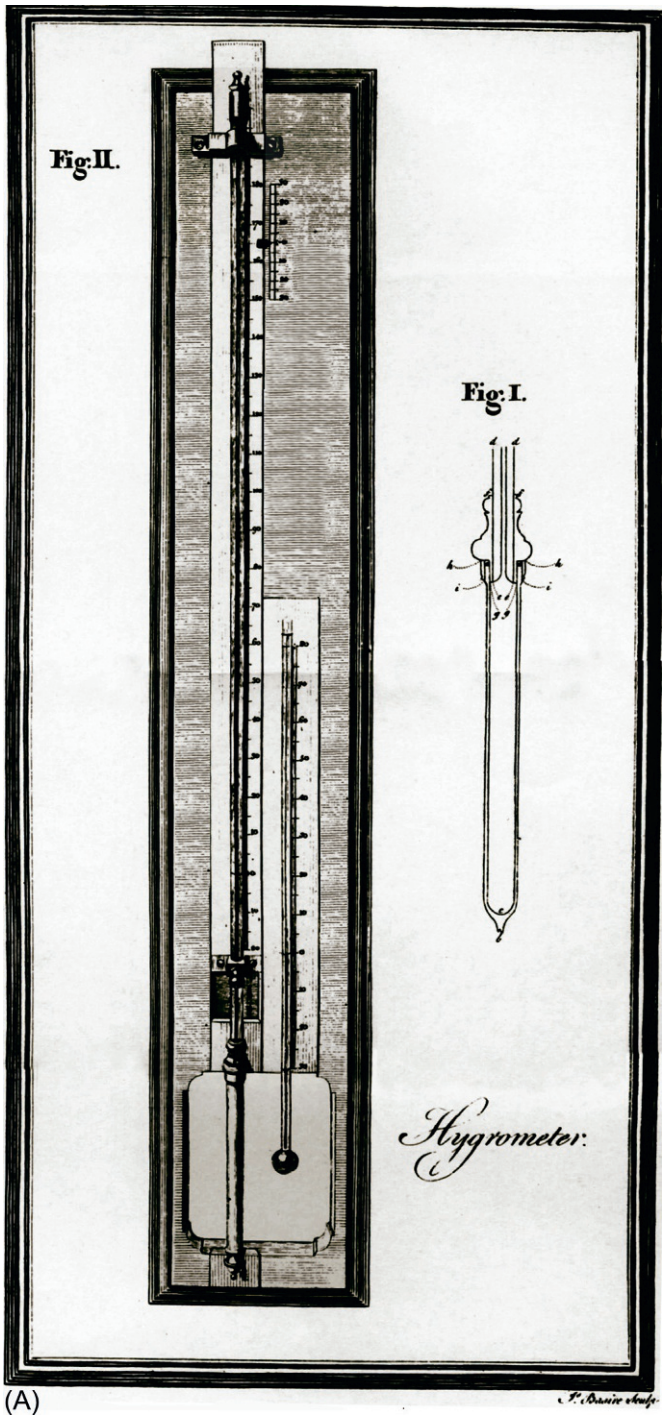

FIG. 18.6 (A) De Luc hygrometer (on the left) mounted on a wooden frame with a small thermometer and detail (indicated 'Fig. I') of the ivory bulb.

(*Continued*)

[10] Guillaume Amontons (1663–1705).

FIG. 18.6—cont'd (B) General view and details of the upper and lower ends of an early 'weather station' composed by Réaumur thermometer, Torricelli barometer, and Chiminello goose quill hygrometer. *(A) From De Luc (1773–74); (B) Courtesy of the* Library of the Botanical Garden, *University of Padua, © Used with permission.*

De Luc[11] improved the horn hygrometer using an ivory cylinder (De Luc, 1773–74) (Fig. 18.6A). Ivory was homogeneous and could be thinned to reduce the time response. In 1774, De Luc won the prize of the Academy of Amiens, France, although it had problems in correcting the temperature dependence (Cotte, 1788). De Luc later developed another type based on a whalebone sensor (De Luc, 1791). The whalebone was resistant to weather, needed less maintenance, and was appreciated for its reliability. The problem, however, was that its response

[11] Jean André De Luc (1727–1817).

was different from the response of other instruments, in particular from the De Saussure hair hygrometer. This caused a serious problem for the definition of the humidity scale, the extremes, and the average that was generally considered the medium between the two extremes, i.e. the median. This idea was derived from Aristotle[12] and was applied to all disciplines, including mathematics and meteorology. For instance, the early temperature series were based on two samplings, one near sunrise, i.e. the minimum, and one after noon, i.e. the maximum. The average of these two extremes, however, was very close to the real daily average (Camuffo, 2002).

Retz[13] substituted the complex and expensive ivory bulb with a quill (Retz 1779; Retz and Held 1786). The quill was cheap, required little preparation, had small drift and quick response. However, the problem was to interpret readings and relate them to some dry or moist references.

Chiminello[14] studied how to reach absolutely objective humidity readings (Chiminello, 1785). He scratched and annealed the goose quill, considered the correction for temperature by comparison with a thermometer with the same size, established a calibration protocol with four reference situations considering both humidity and temperature, i.e. for saturation dipping the quill in boiling water (hot dampness) and in water with melting ice (cold dampness), and for dryness exposing the quill in front of a light fire (hot dryness) and a mixture of hygroscopic salts (cold dryness). He applied two scales: one 'relative' for actual readings related to the specific instrument, and one 'absolute' after correction that could be compared with corrected readings from other instruments. In 1783, Chiminello won the prize of the Theodoro-Palatina Academy of Sciences, Mannheim, for his hygrometer (Fig. 18.6B) that became the official hygrometer of the Palatina Network. The Padua record has been recovered and compared with the parallel record made with De Saussure hygrometer. The data homogenization and correction for the Chiminello hygrometer was heavier than for De Saussure's (Camuffo et al., 2014). This explains why these instruments have not been further used. It should be noted that horn, hair, and quill feathers have a protein in common, i.e. keratin.

18.1.6 Hygrometers Based on Changes of Phase: Condensation Hygrometers and Psychrometers

Condensation inspired two instruments; the first one was developed in Florence, the Grand Duke of Tuscany, Ferdinand II,[15] founder of the *Accademia del Cimento*, with Torricelli,[16] the inventor of the barometer, used a brass vessel in the shape of cone, filled it with ice, and the moisture that condensed on the cold surface dipped into a graduated glass vessel (Fig. 18.7; Magalotti, 1667).

The second one was invented by Daniell[17] in 1823. This was the precursor of the dew-point meter with a condensation hygrometer cooled by evaporation of ether (Fig. 18.8; Daniell, 1823, 1845). Daniell built a closed glass system terminating in two communicating spherical bulbs. One was covered with muslin and soaked of ether to cool the whole system. The other was a black glass sphere with a thermometer to read the dew-point temperature when dewing started. The sphere was of black glass to make small droplets more distinguishable.

The psychrometer had various improvements, starting from the basic idea attributed to Leslie.[18] It was constituted of two identical thermometers, but one of which with the bulb covered with a muslin wick and kept continually moist by being connected with a reservoir of water (Leslie, 1813). The evaporation from the muslin lowered the temperature of the wet bulb. By comparing the temperatures of the dry- and the wet-bulb thermometers, it was possible to calculate the relative humidity and other variables with the help of diagrams, tables, or formulae (Baer, 1859; Tomlinson, 1861; Lardner, 1877; Sprung, 1888; Middleton, 1966, 1969).

August[19] proposed a basic psychrometer (August, 1825, 1830). It was simply composed of two thermometers fixed on a frame, i.e. dry and the wet bulb exposed to the natural ventilation, and a water reservoir (Fig. 18.9A). It had neither ventilation nor shield against the radiation. The evaporation cooling was not uniquely defined because it varied with the level of the environmental ventilation and its changes. Indoor and outdoor readings were not comparable being strongly affected by different ambient conditions.

[12] Aristotle, Nicomachean Ethics, book 2, Chapter 5.

[13] Noel Retz (1758–1810).

[14] Vincenzo Chiminello (1741–1815).

[15] Ferdinand II de' Medici (1610–70).

[16] Evangelista Torricelli (1608–47).

[17] John Frederic Daniell (1790–1845).

[18] John Leslie (1766–1832).

[19] Ernst Ferdinand August (1795–1870).

FIG. 18.7 Condensation hygrometer by the Grand Duke of Tuscany, Ferdinand II, and Evangelista Torricelli. The brass cone was filled of ice and the condensed water was collected on the graduated vessel under the cone. The cone has an exhaust pipe to drain melted water. *From Magalotti (1667).*

In the sling psychrometer, the two thermometers were fixed on a revolving frame that had to be whirled at a certain (subjective) speed by the observer for some twenty seconds (Fig. 18.9B). Then the observer quickly read the two temperatures, starting from the wet bulb, before it returned in equilibrium with the still air. The operation had to be repeated until a number of similar readings were obtained. This method improved the ventilation, but left a wide margin to subjective biases.

The ventilated psychrometer was an improvement made adding a mechanical ventilation in proximity of the wet bulb. A spring-driven motor was employed to rotate vertical blades like a fan and produce a ventilation driven by the centrifugal force (Fig. 18.9C). This reduced the uncertainties that in the August or sling psychrometers were due to uneven ventilation. However, the problem was not completely removed, because every air current affected readings. This instrument was intended for indoor use, or to be used inside a radiation shield for outdoor observations.

Assmann[20] developed the aspirated psychrometer: an advanced instrument for accurate measurement of atmospheric humidity and temperature (Fig. 18.9D) (Assmann, 1892). The two main innovations consisted in the spring-driven aspiration fan on the top, and in addition the bulbs were surrounded by a double metal sheath to shield them from radiation. The bulbs were inside a cylindrical duct that shielded not only from radiation, but also from external ventilation. The instrument was compact, portable, and reduced various uncertainties. It reached 1°C accuracy, or even better. The aspirated psychrometer was soon produced by Rudolf Fuess' factory in Germany, followed by other producers. It became very popular till the advent of electronic instruments.

Psychrometers constituted a qualitative improvement in comparison with other hygrometers. However, they had a number of limitations, e.g., it was not possible to use them in cold environments to avoid the risk of frost on the muslin; any reading of the dry- and wet-bulb temperatures required the help of tables or diagrams to be interpreted. Continuous *RH* monitoring was not possible except for mechanical records made with metal sensors kept at natural ventilation as in the August psychrometer (Fig. 18.9E)

Today electronic psychrometers may perform automatic sampling with the electric ventilation fan switched on and off in connection with readings, and may calculate the required hygrometric variables. However, they still have the frost limit.

18.2 PART 2. MODERN TECHNOLOGY TO MEASURE AIR HUMIDITY

18.2.1 Introduction to the Various Methods

In the 1970s, with the advent of electronics and the progress in material science, new sensors were developed

[20] Adolf Richard Assmann (1845–1918).

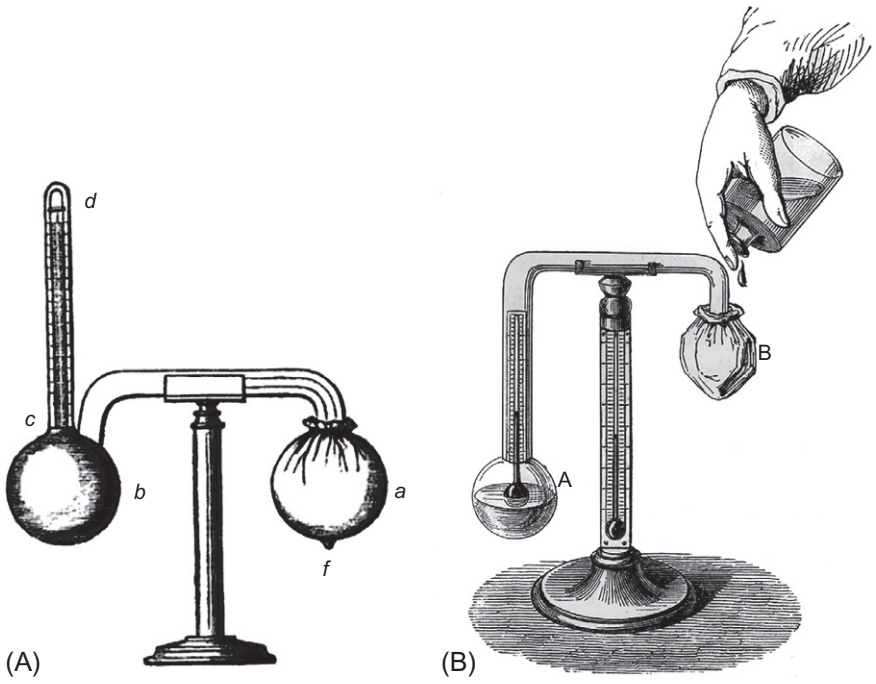

FIG. 18.8 (A) The original Daniell dew-point meter, composed of two communicating spheres: one (label 'a') covered with muslin wet of ether; the other (label 'b') was a black sphere with a thermometer (label 'cd'). (B) Development of the Daniell dew-point meter with better thermometer organization. *From (A) Daniell (1845); (B) Ganot (1860).*

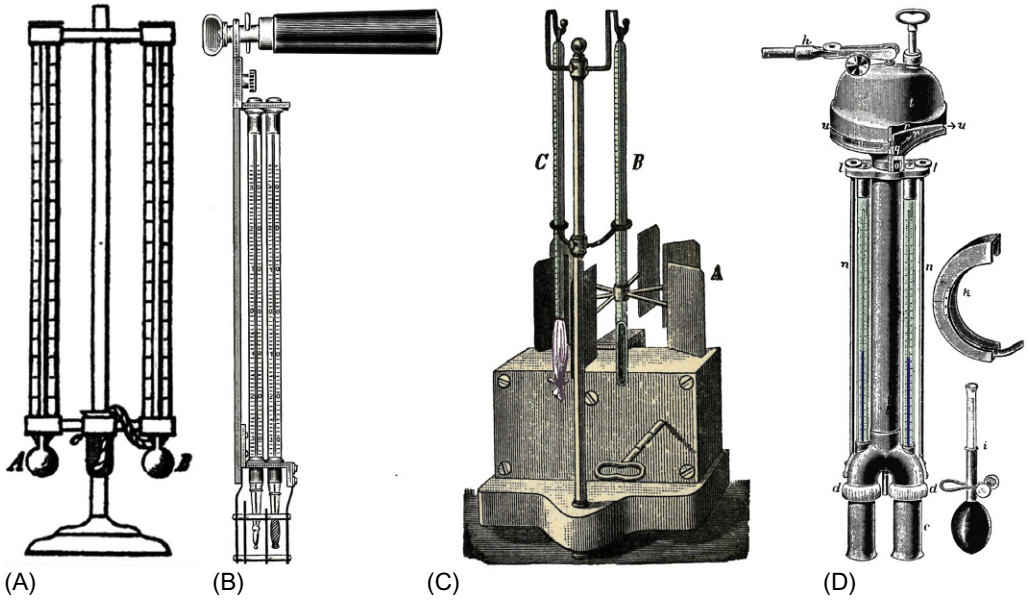

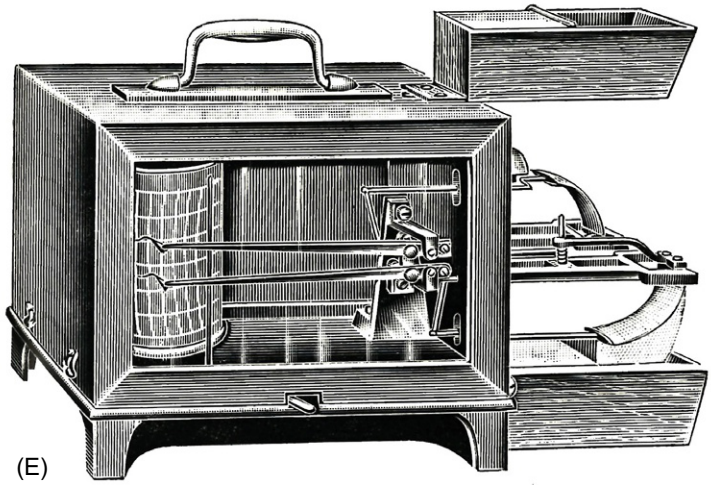

FIG. 18.9 (A) The August psychrometer with natural ventilation. (B) Sling psychrometer with man–made ventilation, early 1900s. (C) Ventilated psychrometer with spring-driven fan. (D) The aspirated psychrometer by Assmann. (E) A mechanical recording psychrometer with two Bourdon-tube sensors and a water reservoir. The sensors are exposed to natural ventilation. *From (A) Baer (1859); (B, E) Vercelli (1933); (C) Gerosa (1898); (D) Eredia (1936).*

and the measurement of relative humidity was radically changed (except for the unjustified tradition of hair hygrometers and thermo-hygrographs).

From the user point of view, hygrometers can be grouped as follows:

1. Dew-point meter, an optical device based on accurate temperature measurements, useful for calibration purposes. It is a high-quality, primary instrument serving to calibrate secondary instruments.
2. Electronic fan psychrometers, also based on accurate temperature measurements, are useful for field measurements (when possible). It is a high-quality instrument; if pressure too is considered in the formula used by the producer to calculate the output, it is useful to make spot checks to control whether secondary instruments need to be substituted or calibrated.
3. Thin-film capacitive or resistive hygrometers useful for field measurements. These are secondary instruments, of average quality, but able to provide reasonably accurate readings if periodically checked and calibrated. Only the extremes remain uncertain.
4. A variety of instruments based on different principles, e.g. electrolyte hygrometer thermal conductivity hygrometer, with variable reliability, not recommendable for standardization purposes.

The European standard EN 16242 (2012) 'Conservation of cultural property—Procedures and instruments for measuring humidity in the air and moisture exchanges between air and cultural property' recommends instruments of types 1 to 3. The use of the hair hygrometer is not recommended and is only accepted in exceptional circumstances for visual inspection, in the absence of vulnerable objects that need a precise microclimate control. More details and comments on the use of this standard can be found in Chapter 15 and Camuffo and Fernicola (2010).

Looking at the physical operational principle, the following classification is possible:

1. Hygrometers based on *condensation*, e.g. dew-point (*DP*) or frost-point hygrometers and water equilibrium hygrometers for particular saturated salt solutions.
2. Hygrometers depending on the *addition or removal of water vapour*, e.g. psychrometer and diffusion hygrometer and gravimetric, volumetric, and pressure methods. The psychrometer should be kept in consideration; other methods are of less relevance.
3. Hygrometers based on *sorption methods*, e.g. mechanical hygrometers with human hair or parchment sensors; electric hygrometers with thin-film capacitive sensor; resistance polymer; aluminium oxide, polyelectrolyte, carbon; and piezoelectric sensors. The measuring principle may be a mechanical displacement; a change of the electric resistance, capacity, or inductance; or a change of vibration frequency. These sensors, and in particular, thin-film capacitors or resistors are largely used in commercial instruments because of their low cost, high resolution, and fast response. The negative aspect is drift, especially after contamination.

None of them is fully reliable at extremes, i.e. very low and very high, *RH* levels. All of them present important drifts or departures after contamination and/or ageing. For this reason, careful periodic maintenance and frequent calibration are needed.

An analysis of all these transducers is too long and of limited interest, as only few types can be recommended for this field. In the following discussion, only the most important types will be discussed; further details are given by Wexler (1965), UK Meteorological Office (1981), WMO (1986, 2008), Carr-Brion (1986), Doebelin (1990), Harriman (1990), Bentley (1998), Wylie and Lalas (1992), and Lipták (2003).

18.2.2 Dew-Point Meter

This instrument is based on detecting the temperature of a cooled mirror at the point where condensation forms, i.e. the *DP*. Since only the accurate temperature measurement of the chilled mirror is required, it provides accurate readings and EN 16242 (2012) recommends the dew-point meter as a primary instrument for calibration. The mirror is electrically cooled with a Peltier plate and the temperature level is controlled by an electronic feedback to keep dynamic equilibrium between evaporation and condensation, thus closely following the dew-point temperature changes. An infrared (*IR*) beam impinges on the chilled mirror and the intensity of the reflected beam is continually monitored. When the mirror starts to mist over by initial condensation, the reflection drops. The instrument provides a reading of the critical temperature at which evanescent microdroplets start to form or cease to leave. For this reason, it is known as *chilled mirror dew-point meter*. If the chilled mirror can reach low temperatures, it might be used to detect the frost point too.

The chilled mirror dew-point meter provides the most accurate humidity measurements and is recommended as a reference instrument for calibration of other hygrometers. It operates in the full *RH* range, from about 0% to 100%. To guarantee high precision, the instrument requires periodic control and cleaning of the optical components.

In the market, there are instruments that are improperly classified as 'dew-point meter': they are normal hygrometers but with a chip able to calculate the *DP*. They are based on a combination of temperature and *RH* sensors (generally capacitive or resistive *RH* sensors)

and from their outputs they calculate the dew-point value. The output of hygrometric sensors is not as accurate as temperature readings, which lowers the instrument quality. EN 16242 (2012) warns against using such instruments as primary instruments.

18.2.3 Psychrometer

Today, the historic Assmann psychrometer has been abandoned and substituted with automatically operated electric fans and more advanced temperature sensors, e.g. platinum resistance, thermocouples, and thermistors. Electronic psychrometers are recommended by EN 16242 (2012) to periodically control if other humidity sensors (e.g. thin-film capacitive or resistive sensors) provide accurate readings or need calibration. It can be connected to a data logger and with a water reservoir that allows medium-term autonomy, to provide routine monitoring at selected sampling intervals.

The psychrometer is an instrument based on the readings of a matched pair of sensitive thermometers (i.e. they must read alike at any given temperature), joined side by side: one being normal, called the 'dry bulb' to be distinguished from the other that has its bulb covered with a wet cotton cloth wick, called 'wet bulb'. At equilibrium, i.e. when the heat Q_v lost by evaporation from the wet bulb equals the sensible heat Q_s transferred from the ambient air to the colder wet bulb, the psychrometric formula is obtained,[21] i.e.

$$e = e_w - A\,p\,(T - T_w) \tag{18.8}$$

where A is the psychrometric coefficient, which is independent of the evaporating surface area, i.e. the size of the wet-bulb wick covering, but is slightly dependent on ventilation rate and, to an even minor degree, on psychrometer design, size and dimension of the dry and wet bulb, ambient temperature, and RH. However, when ventilation is in excess of 2.5 m s^{-1} (and particularly in the range between 3 and 5 m s^{-1}), A is nearly constant and suggested values for the classical Assmann psychrometer with mercury-in-glass thermometers are $A = 6.2 \times 10^{-4}$ K^{-1} (WMO No. 8, 1986, 2008) and $A = 6.667 \times 10^{-4}$ K^{-1} (UK Meteorological Office, 1981). Some values of A versus ventilation rate v are in Table 18.1

In order to get an idea of the error derived by an incorrect value of A, at $t = 20$°C, when A changes by 10%, the error that is generated in RH, i.e. ΔRH, varies with the actual RH level as reported in Table 18.2.

At temperature and humidity levels usually found in museums and galleries, the error is of the order of ±2%; it decreases at higher temperature and increases at lower temperature. This is an acceptable uncertainty.

TABLE 18.1 The Psychrometric Coefficient A at Selected Ventilation Speeds

v (m s^{-1})	0.12	0.50	1.0	2.0	4.0
A (K^{-1})	13.0×10^{-4}	9.0×10^{-4}	7.8×10^{-4}	7.1×10^{-4}	6.7×10^{-4}

Data from WMO (1986).

TABLE 18.2 Error Derived by an Incorrect Value of A, at $t = 20$°C, When A Changes by 10%, at Selected RH Levels

RH (%)	0	20	40	60	80	100
ΔRH (%)	4.0	3.0	2.2	1.4	0.7	0

Data from UK Meteorological Office (1981).

Both dry- and wet-bulb thermometers are ventilated with a forced air flow with speed generally ranging from 3 to 5 m s^{-1}, where the given proportionality coefficients are more constant and less dependent on the ventilation rate. WMO No. 8 (1986, 2008) suggests a wider interval from 2.5 to 10 m s^{-1}, but 2.5 m s^{-1} is close to the limit of error (2 m s^{-1}) and every slow down of the fan, e.g. for a not well-charged battery, may cause a super evaluation of the wet-bulb temperature and, consequently, of the measured RH. On the other hand, a faster ventilation rate causes unnecessary power consumption. For elevated RH values, slower ventilation rates are sufficient but when RH drops, fast ventilation is necessary to cool the wet bulb to its full depression. The fan speed is a limiting factor in dry environments.

Accurate measurements taken with a psychrometer can be considered as a home standard, i.e. a useful reference to compare and check calibration of other instruments. In particular, when RH is very high or approaches saturation, the psychrometer is superior to all other sensor types (Wiederhold, 1975, 1997). However, it has three important limits. First, it cannot be conveniently used when the wet bulb drops below the freezing point. This means that readings may be impossible in dry air at temperature below 10°C. Although reference may be made to the latent heat and saturation pressure for ice, instead of water, the measurement becomes less accurate; the water supply is interrupted and the water reservoir may be damaged. Secondly, when RH drops below 20%, it becomes difficult to cool the wet bulb to the equilibrium depression, even when the sensors are aspirated at airstream rate of 10 m s^{-1}. The reason for this is that the water of the wet bulb evaporates before the wet bulb reaches its maximum depression temperature (Fisher et al., 1981). For this reason, the use of this instrument is suggested in the RH range from 20% to 100%, which fortunately covers the main parts of the practical cases. No other sensors provide a wider range of reliability. Finally,

[21] See Chapter 3.

it is slightly sensitive to atmospheric pressure and readings taken on mountain sites should be corrected.

The most common causes of error are as follows:

1. Breathing in proximity of the sensor or keeping the instrument close to the observer's body will cause an exceedingly high value of moisture. Another frequent misuse is to handle a psychrometer with raised arm, as the air heated by the body follows the upward chimney path along the arm and is then aspirated by the psychrometer fan. The correct position is to handle the instrument with a lowered arm or to hang the instrument from an extension pole.
2. Reading the thermometers (in particular the wet-bulb one) before it has reached equilibrium: it might be useful to remember that the fan does not affect the temperature of the dry bulb but lowers the wet bulb. Although covering the bulb with a thin tubular cotton wick reduces the thermometer time constant, when the fan is switched on, the dry sensor remains in the previous condition of equilibrium but the wet sensor begins to lower its temperature and needs time to reach equilibrium. This error is frequent with sensors having a slow response time.
3. Errors in thermometer reading: this error may be important with mercury-in-glass thermometers, when the operator stays with his face close to the thermometers for too much time to read the small-scale divisions of both of them and the *IR* emission from the face and the breath may warm the sensors. This problem has been eliminated in electronic psychrometers where the display is well visible and placed far from sensors. Some of them have an automatic recording and there is no need to read the display, except for controlling that the equilibrium has been reached.
4. Insufficient ventilation of the wet bulb: this error is frequent and becomes important for ventilation below $2\ \mathrm{m\,s^{-1}}$. Controlling the airspeed of ordinary psychrometers because it is common to find insufficient ventilation speed. Often a solution can be found by reducing the cross-section of the suction tube to increase the airstream speed. In clockwork-aspirated psychrometers, observations made too early (i.e. with reference to the instrument time response) are affected by error, as well as those made too late, when the spring is losing its energy and the fan is slowing down. Electrical fans should be preferred to spring-driven mechanical fans that might have uneven ventilation speed.
5. Tubular cotton wick covering the wet bulb is not completely wet.
6. Contaminated wick covering, or use of regular water rather than pure distilled water: after some time, the forced ventilation will cause contamination of the covering. Monitoring in coastal area (i.e. marine aerosols) or polluted environments requires frequent changes of the wick covering. When a new cotton wick is used, it must be previously boiled in distilled water to remove extraneous substances that may alter the surface tension of absorbed water.
7. Too thick a wick covering of the wet bulb (or even frost) may increase the time constant.
8. Temperature below 0°C freezes the wick, stopping the water supply, and the equilibrium is reached with ice instead of water.

All the hygrometric variables can be obtained after the dry-bulb temperature and wet-bulb depression with the help of tables, diagrams, or formulae,[22] but the same can also be obtained from the air temperature and *RH*.

The psychrometer gives very accurate measurements only when it is correctly operated. The effect of an error in wet-bulb reading varies with the temperature and humidity level. An example of the propagation of errors is shown in Fig. 18.10 by supposing that $RH = 50\%$ and that T_w is read with an error of -0.1°C. In the most frequent range of indoor climate, i.e. $10 \leq T \leq 30$°C, the error is relatively small, i.e. less than 1% for *RH*, between one to a few tenths of the related units for specific humidity (*SH*), absolute humidity (*AH*), *DP* and *e* (vapour pressure). In the meteorological range of variability, the error of *RH* increases exponentially with decreasing temperature below 0°C but in this span, psychrometric measurements are impossible due to the formation of ice. For elevated temperatures, the error of *AH* becomes important. However, it should be noted that this propagation of errors affects the accuracy of all the measurements, but systematic errors affect very little the differences from point to point or from time to time. It is very important to check before use if the two sensors, both dry, provide exactly the same temperature readings. Even in the case that they measure the actual temperature with a small error (although identical for both sensors), the error is systematic, affects in the same way all readings, and is therefore negligible in the calculation of the variability of the hygrometric variables in terms of gradients over space or trends over time. This is especially true when plotting the distributions of these variables in horizontal maps, as differential values are involved, and the departures from the average of the local minima and maxima remain practically unchanged.

In order to monitor and map the distribution of temperature and humidity over a horizontal cross-section of a room, a number of samplings with dry- and wet-bulb readings should be made in a short time. This means that the instrument should have quick response and reading repeatability. Precision electronic psychrometers have

[22] See Chapter 3.

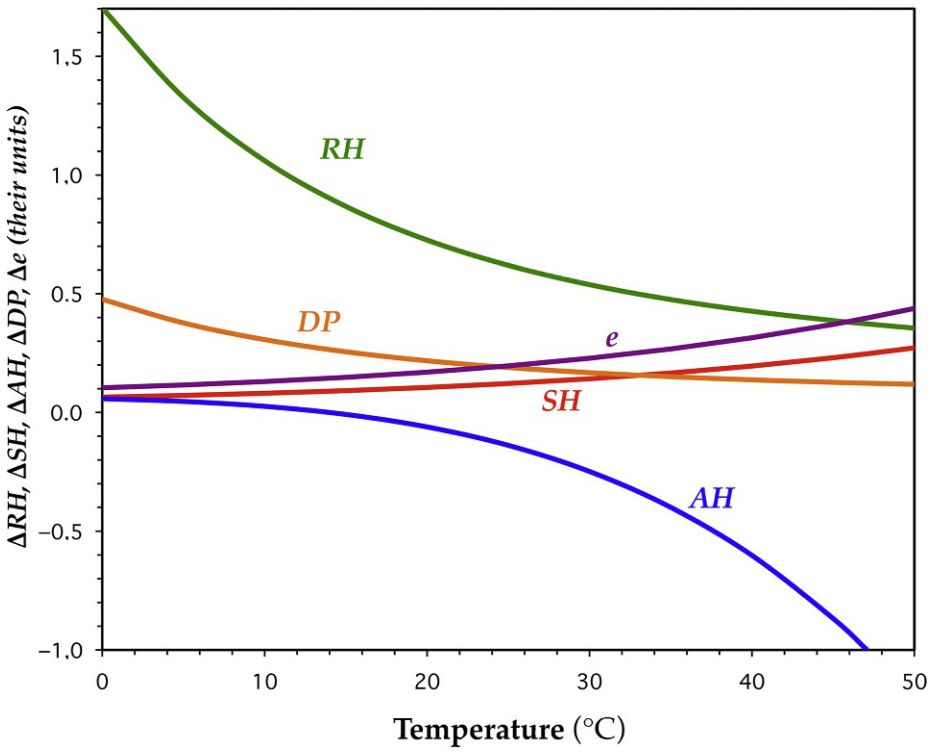

FIG. 18.10 Error generated in computing relative humidity (*RH*, %), specific humidity (*SH*, g/kg), absolute humidity (*AH*, g/m^3), dew point (*DP*, °C), and vapour pressure (*e*, hPa), when the wet-bulb temperature T_w is affected by −0.1°C error, at ambient $RH = 50\%$.

been designed and built in laboratory, with a better accuracy than 0.1°C and fast response. Although sensors with a time constant better than 1 s were used, the overall time constant was 5 s, which includes the thermal inertia of the screen, mechanical parts, and electronics. The combination of different time constants reflects in the fact that on plotting the normalized temperature change for the step ambient variation versus time in a logarithmic paper, the plot departs from a straight line. The resulting time constant limits the number of observations per run. The critical factor is that the total time needed to perform a whole run should not exceed a certain duration where the ambient conditions may be considered stationary. For instance, in the case that the acceptable total duration is 10 min and that the time needed to move from one point to another and to take readings is 30 s, only 20 sampling points are possible, i.e. $30\text{ s} \times 20 = 600\text{ s}$. Runs should be made with the fan uninterruptedly operating even when moving from one sampling point to the next one, in order to reduce the time to reach equilibrium. In fact, during the move, as the operator approaches the next position, the sensor too is passing to levels closer to that of the final equilibrium point.

All components (i.e. sensors, screen, and electronic circuits) of psychrometers should be tested separately and then in conjunction to optimize the overall time constant and accuracy. Either linear or nonlinear thermistors, or platinum resistance sensors, are fast sensors. Linear outputs avoid unnecessary electronic transformations of the signal, but miniaturized thermistors can equally be linearized and have a shorter time constant, which is a very important feature, especially when several measurements are made in each run. Two types of screen give the best results, i.e.: (1) a white polystyrene foam that is reflective, has a very low thermal capacity and is a good thermal insulator; its response time, measured with a radiometer, is less than 2 s; and, (2) a thin aluminium foil reflecting outside and blackened inside.

Low-power-consumption fans are used in order to reduce weight, volume, and cost of rechargeable batteries. The velocity of blown air at the matched sensors is regulated by narrowing the internal cross-section of the tube corresponding to the sensors or changing the fan speed. The dry- and wet-bulb sensors are placed side by side or the wet bulb is midway between the dry one and the aspirating fan.

The output should be clearly visible in a display; it may be printed on paper or saved to a computer.

18.2.4 Thin-Film Capacitive Hygrometer

Physical Principle and Characteristics of the Sensor

This sensor is composed of a thin film of hydrophilic material (e.g. acetal polymer,[23] cellulose acetate butyrate, metal oxides) surrounded by at least two electrodes. The substrate is typically glass, ceramic, or silicon. Thin-film

[23] Acetal polymer is also known as polyoxymethylene (POM).

capacitive sensors may include monolithic signal conditioning circuitry integrated onto the substrate. The water adhesion to the thin film is characterized by physical hydrogen bonds with the hydrophilic groups of the polymer molecules, but its behaviour is dynamic, and the moisture content (*MC*) of the film is in thermodynamic equilibrium with the vapour phase, responding to changes of *RH* and temperature (Eren and Kong, 1999; Smit et al., 2013). The thin film with its *MC* is used to vary the capacity in an electronic circuit and any change of *MC* is measured with a capacitance bridge. The output is linear and almost independent of the actual value of the air temperature. At high humidity, linearity and stability of the capacitive sensor are better than the resistive sensor (Griesel et al., 2012). The resolution is high, e.g. it may vary from 0.1% to 1%. Hysteresis is low, e.g. ±1% (or less) for measurements between 5% and 95% *RH*. The response time of thin film sensors is dependent on the polymer ability to reach equilibrium with air, which in general is very fast, ranging from 1 or a few seconds to a few minutes. However, in operation, the response time increased for the protective filter against dust that slows down the free exchange with the atmosphere and increases the actual response time. Similarly, thermal inertia of the surrounding probe may severely affect readings in case of fluctuations or sharp changes. This may not be a problem when monitoring unmanned heavy buildings with thick walls and stable indoor climate, but becomes an important limit in the real world when fast response measurements are needed.

In the long term, the main problem is drift, especially in polluted environments (Bell et al., 2017). For this reason, the probe is often inserted into a filter that protects the sensor against air pollution, dirt, or splashing droplets; also, oil and grease vapours may form a film that alters or prevents the adsorption of water molecules.

They need to be calibrated every few months, or every year in the most optimistic case. In order to avoid the problem of drift, the best instruments run calibration automatically after setup, activating two calibration points, at low and high *RH*, obtained by means of reference saturated salt solutions.

Thin-film capacitive hygrometers are recommended by EN 16242 (2012) for indoor/outdoor measurements because they constitute a reliable method when the temperature drops below the freezing point or when measurements should continue unattended for relatively long periods, e.g. months.

Thin-film sensors have accuracy that may vary with temperature and *RH*, as in the indicative example given for guidance with intervals drawn just to clarify ideas, not to assess thresholds.

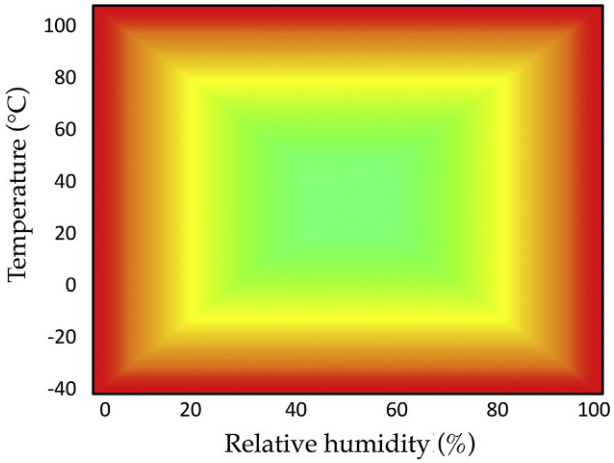

FIG. 18.11 Uncertainty of thin-film capacitive sensors. *Green*: the best performance interval in the middle of the *T*, *RH* range (e.g. 1%–2%). Yellow: uncertainty increasing with the departure from the central interval. *Red*: large-to-very-large uncertainty in proximity of the range limits (e.g. 6% but may reach 30% in dampness). The indicated values are only illustrative to explain the context, and may vary depending on the sensor and producer.

The best performances of this sensor are provided in the middle of the relative humidity and temperature range (Fig. 18.11). In this interval, the sensor accuracy may reach ±1 to ±3% *RH*, depending on product type and manufacturer, and the measurement uncertainty increases when the environmental conditions approach the extremes of the range (Eren and Kong, 1999; Griesel et al., 2012; Smit et al., 2013; Bell et al., 2017; Camuffo et al., 2018; Camuffo, 2019). At very low or very high *RH* levels and/or temperatures, the uncertainty increases with the departure from the best interval and the *RH* tolerance may reach ±6% or even more (Bell et al., 2017). The temperature dependence is also strong, because at usual calibration temperature, i.e. 20°C, the relative permittivity[24] ε of water is $\varepsilon = 80.1$ at 20°, but changes with temperature. However, not all the sensors available on the market have been accurately calibrated over the whole range, and if reference is made to two *RH* calibration points at 20°C, and the sensor is not compensated for temperature variations, any change in relative permittivity will reflect in *RH* departures with the same proportion, as exemplified in Table 18.3 calculated after the values of ε (Malmberg and Maryott, 1956).

Use Under Extreme Conditions

In the case of fog, rain, overnight condensation, humid indoor environments, or whenever the probe approaches the dew point, condensation may occur on the thin film. The consequence is that the sensor does not respond

[24] Also called *specific inductive capacity* or *dielectric constant*. For the temperature dependence see Chapter 8, Fig. 8.9A.

TABLE 18.3 Percentage Departure of the Relative Permittivity ε of Water at Selected Temperatures From the Reference Value at 20°C

T (°C)	% Departure	T (°C)	% Departure	T (°C)	% Departure
0	+9.54	40	−8.67	80	−23.81
10	+4.66	50	−12.72	90	−27.19
20	0	60	−16.59	100	−30.46
30	−4.43	70	−20.28		

The same applies to *RH* readings, for sensors without temperature compensation or not calibrated over the whole temperature range.

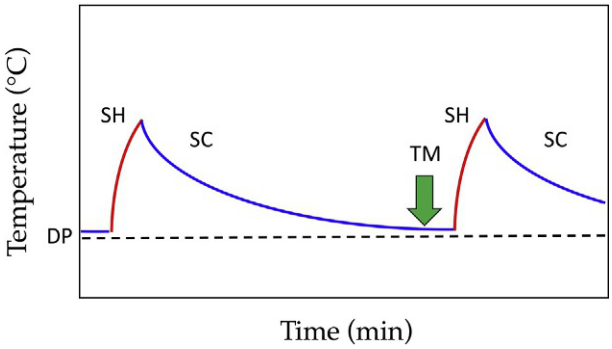

FIG. 18.12 Cycles of heated (demisted) capacitive sensors. When the sensor approaches the dew point (DP), the internal heater generates a sharp heating (SH). Then the heater is switched off and the sensor follows a slow cooling (SC) until it returns to the starting level. At this point the system takes the measurement (*arrow* TM). Afterwards, another heating cycle is repeated. *From Camuffo (2019), by courtesy of Elsevier.*

when *RH* begins to decrease, and may require several hours before drying, being unable to detect (rapid) drops in *RH* thus providing false readings. The worst scenario corresponds to when the *DP* is below freezing temperature and the sensor is covered with frost.

Continuous high humidity conditions represent a challenge for capacitive humidity sensors causing increased errors and calibration drift. After some time in saturation condition, capacitive sensors behave as follows: most sensors cannot detect condensation at all because manufacturers limit their output to 100% *RH*; some sensors show readings beyond tolerance, e.g. values up to 130% *RH*; other sensors cannot withstand continuous high humidity condition at all and cut off data acquisition. This is particularly dangerous because high humidity levels are very common in cultural heritage buildings, or outdoors, and lead to several deterioration mechanisms. Internally, the capacitive sensor is in a critical state, which can lead to calibration drift or damage. Problems with polymer humidity sensors under condensing conditions were observed leading to unacceptable time response of half a day or more. The reason for this is condensation or sublimation on the sensor or the sensing element. (Griesel et al., 2012).

To solve this problem, some manufacturers have produced heated sensors, to avoid accumulation of water on the sensor. The commercial name is 'heated capacitive sensor', but it might be more properly named 'demisted sensor' because the sensor does not operate when heated, but after having been demisted. *Demisted capacitive sensors* are thin-film capacitive sensors that may operate close to saturation. These sensors are controlled with a chip, equipped with an internal heater that is cyclically operated at fixed intervals to demist the thin film (Fig. 18.12). When the sensor approaches the dew point, the internal heater is automatically operated for a short time and generates a sharp heating. Then the heater is switched off and the sensor will relax with slow cooling until its temperature T will return to the starting level, i.e. $T = DP$. Before condensed water forms again, the system takes the measurement. After that, a new heating cycle is repeated to prevent condensation.

Demisted sensors operate at very high humidity levels, close to saturation, at the borders of their performances, and readings are characterized by the highest uncertainty. In addition, T returns close to the unperturbed starting level, but it is not guaranteed that it will exactly reach it, and this is a further source of uncertainty. Demisted sensors have very long time response but shorter than when the thin film is soaked. They may produce false outputs, but far less than unheated sensors. Briefly, they show better performances than traditional, unheated ones (Griesel et al., 2012) and can be employed in very humid environments, e.g. unmanned buildings, caves, and hypogea (Frasca et al., 2018), but they do not provide a solution to all monitoring problems in damp environments.

The best condition would be to operate with sensors in the T, *RH* interval of best performance and highest accuracy, avoiding the intervals with increasing uncertainty, and especially those near the limits of the range. This situation can be obtained even in conditions of saturation, with a simple expedient dictated by theory, using normal sensors (Camuffo, 2019). The system requires a pair of sensors, i.e. a temperature sensor (T_{IN}) and a thin-film capacitive sensor RH_{IN} that may be integrated in the same sensing element. A simple home solution is to locate both sensors in the middle of a heated cavity, e.g. a segment of a sphere or a tube, gently heated by Joule or Peltier effect (Fig. 18.13). A third sensor T_E is left external and measures the undisturbed air temperature.

It is not necessary to finely tune the open cavity temperature as in the demisting case, but it is sufficient to lower the *RH* to reach the best performance interval where the accuracy of the *RH* sensor is highest. For instance, the heating element may be controlled by RH_{IN}, e.g. with 60% set point, and this may require around 10°C heating above the ambient temperature.

From the matched T_{IN} and RH_{IN} readings, it is possible to calculate the *DP* of the air inside the cavity that is

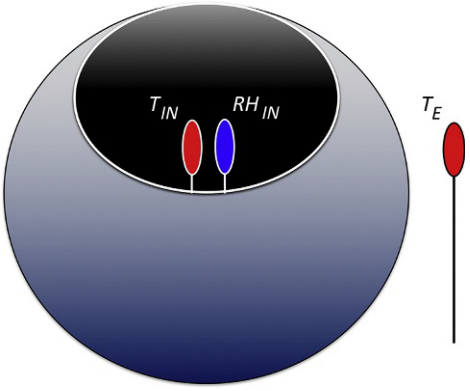

FIG. 18.13 Schematic diagram representing the heated cavity, with inside the pair of temperature (T_{IN}) and relative humidity (RH_{IN}) sensors, and the external temperature sensor T_E.

the same as for the external air, because the *DP* is invariant to temperature changes. The *DP* may be calculated with the empirical formula by Magnus (1844) and Tetens (1930),[25] i.e.

$$DP = \frac{243.12\, ln\left(\frac{RH_{in}}{100} \times 10^{\frac{7.65 t_{in}}{243.12 + t_{in}}}\right)}{17.62 - ln\left(\frac{RH_{in}}{100} \times 10^{\frac{7.65 t_{in}}{243.12 + t_{in}}}\right)} \tag{18.9}$$

where t_{in} is the T_{IN} reading in °C. This formula is satisfactory for calculations of measurements inside buildings, or normal weather, and is recommended by EN 16242 (2012) but may reach departures of 2% under extreme conditions (e.g. below −20°C).

Combining the external reading T_E with *DP* as additional input in the inverse formula, it is possible to compute the *RH* external to the heated cavity (RH_E), i.e.

$$RH_E = 100 \times 10^{\left(\frac{7.65 t_d}{243.12 + t_d} - \frac{7.65 t_E}{243.12 + t_E}\right)} \tag{18.10}$$

where t_d is the dew point in °C and t_E is the temperature external to the cavity, in °C. The same can be done with *MR* instead of *DP*, because this variable too is invariant to temperature changes.

The temperature readings may be accurate to 0.1°C or better, up to the lowest uncertainty threshold of temperature calibration reached by metrological institutes, i.e. 0.05°C. If the *RH* sensor is operated in the most reliable *T* and *RH* interval, the calculated humidity too gains in accuracy, e.g. up to 1%–2%, not being affected by the large uncertainties that concern readings in proximity of the extreme borders of the allowable range, e.g. 6% or worse. Of course, this applies to commercial sensors distributed without individual calibration certificate.

This method was applied to take records in foggy or very humid environments with instruments not resistant to internal condensation kept outdoors. It was observed that in clear nights the infrared thermal loss lowered the temperature of the top of instruments by some 3°C below the air temperature (Camuffo and Giorio, 2003). When the free air was at saturation level, oversaturation was reached inside the instruments, and a remedy became necessary. The vulnerable instruments, including a *T* and *RH* sensor, were placed into a naturally ventilated box, e.g. a Stevenson screen, and a gentle radiant heating (e.g. a 24-V car light bulb, but fed at 12 V to generate radiant heat without light) was applied inside. A temperature sensor was placed outside the box to correct the *RH* record taken inside, removing the bias caused by the anticondensation heating.

So far, the open cavity has been useful to illustrate the concept, and to warm-up normal sensors. However, this technology of the heated (demisted) sensors can be applied, with matched *T*, *RH* sensors, but continually heated to reach the best performance interval typical of thin-film sensors. It is possible to use the cyclic heating-cooling system, but operated at different proportions, e.g. long heating and short cooling phases, to warm-up the sensor and the air in contact with it. The heater (e.g. platinum resistance Pt 100, Pt 1000) may be controlled by the *RH* sensor as discussed before. Measurement can be taken at every instant, regardless of the reached equilibrium and temperature, or whether the sensor is in a heating or a cooling phase.

In this section, the physical principle and a homemade solution have been presented. A more advanced device can be obtained by combining together a *T* and *RH* sensor, forming a unique, integrated micro-package. Both sensors will have two roles: the *RH* sensor acting as a sensor and driver to control the feeding power of the *T* sensor (or a separate heater), and the *T* sensor acting as a sensor and gentle heater. This integrated device will reach the most accurate interval for the *RH* sensor and will measure the dew point. Another external *T* sensor will record the undisturbed ambient temperature.

The method to take measurements with capacitive sensors warmed up to reach their best performance interval allows readings with the highest accuracy and the shortest time response. The use of this method is not necessarily limited to take more accurate *RH* readings under extreme dampness, but may be normally applied to improve the quality of readings with sensors that will operate in their best performance area.

Again, if the *RH* sensor is heated, either capacitive or resistive sensors may be used, because the conditions of extreme dampness that are deleterious for resistive sensors are avoided.

[25] See Chapter 3.

Finally, this strategy might be used even in very dry environments by cooling the controlled cavity in order to raise *RH* and bring the sensor into the best performance area.

18.2.5 Thin-Film Resistive Hygrometer

Resistive sensors usually consist of noble metal electrodes either deposited by thick-film printing techniques on a glass or ceramic substrate, or wire-wound electrodes on a plastic or glass cylinder. The sensor is made of hydrophilic materials and its *MC* quickly reaches equilibrium with the ambient *RH*. The electrical resistance changes with the *MC*, which makes possible to calibrate the resistance versus *RH* at equilibrium. The response is not purely resistive because of some capacitive effects, so that it properly consists in an impedance measurement. The impedance range of typical resistive elements varies from 1 kΩ to 100 MΩ and the response is typically an inverse exponential, so that it is usually converted and rectified to a linear signal, proportional to *RH*.

The resistive sensor has response time from 10 to 30 s for a 63% step change, is generally stable and accurate, usually interchangeable within ±2% *RH*, so that it is replaceable in case of need. It may provide long-term monitoring on-site either indoors or outdoors, except in the case of extreme environmental conditions, especially dampness. In case the sensitive element is an electrolyte, it may be damaged after a long period at very high humidity, in wetting conditions or in the presence of contaminants.

Its performance is similar to that of thin-film capacitive sensor, although the latter has smaller sensitivity and is more affected by temperature fluctuations. It is recommended by EN 16242 (2012) for cultural heritage field monitoring.

18.2.6 Electrolyte Hygrometer

This sensor measures the impedance of a hygroscopic substance, an electrolyte, which absorbs water molecules to produce a solution. The hygroscopic electrolyte tends to establish equilibrium with the surrounding atmosphere, without drift, and has fast response. Commercially available sensors proclaim having a time constant less than 10 s, a repeatability of 0.1% *RH*, and a range unusually extended towards dryness, i.e. from 0% to 95%. However, although this sensor has a good performance, it is fast only after it has reached thermal equilibrium with ambient air and this stabilization requires 2–3 min. This stabilization time is the limiting factor and should be considered as a more realistic time constant in the field, when both temperature and humidity are variable. Manufacturers suggest calibration with adjustment every 6–12 months and more care is needed when used in polluted environments.

18.2.7 Thermal Conductivity Hygrometer

The thermal conductivity of a gas mixture varies with its composition. For a binary mixture composed of dry air and water vapour, thermal conductivity is an indicator of the relative proportions of the two constituents. A thermal conductivity bridge may detect the mixing ratio by quantifying the difference between the thermal conductivity of dry air and that of air containing water vapour (Tewles and Giraytys, 2016). The sensor is composed of two matched negative temperature coefficient thermistor elements in a bridge circuit. One sensor is encapsulated in dry nitrogen, while the other is exposed to the environment. As current passes through the thermistors, resistive heating increases their temperatures. The sealed sensor dissipates more heat than the exposed sensor. This difference in heat dissipation results in the two thermistors having a difference in resistance. This difference is directly proportional to the mixing ratio, which can then be calculated. The method is not convenient for field measurements.

18.2.8 Calibrating Hygrometers

All hygrometers need periodic calibration, made by an accredited laboratory in compliance with EN ISO/IEC 17025 'General requirements for the competence of testing and calibration laboratories'. However, some basic maintenance and preliminary checks should be made first using a reference instrument. Such an instrument is to be used for checking the calibration of other secondary instruments by comparison to obtain an early detection of calibration departures.

Metrological Institutes can calibrate humidity sensors in the temperature range from −40°C to 100°C with uncertainty from 0.5% to 1.5% *RH* (Fernicola, et al., 2008). A qualified laboratory can perform satisfactory calibrations with a chilled mirror dew-point meter. Calibrations should be made in a closed box calibration chamber, in equilibrium, under controlled temperature and humidity levels. Laboratories usually perform calibrations in one of the two following methodologies. For both of them, it is necessary to operate in a controlled calibration chamber.

The first calibration methodology is based on the comparison between a primary, well-calibrated instrument and one or more secondary instruments. Both the primary and the secondary instruments should be kept in a calibration chamber until equilibrium has been reached at a number of selected *RH* levels and at a given temperature. It is not necessary that the selected levels be exactly reproduced but that the equilibrium is reached. At this moment, one exactly knows the actual *RH* and temperature level inside the chamber (i.e. the dew-point meter readings) and the individual readings of the secondary instruments that need calibration. Repeating this

operation, it is possible to plot the readings of each instrument versus the reference readings and obtain the individual calibration plots. This is the most accurate method, but it requires a calibration chamber and, particularly, a good reference instrument.

The second calibration methodology is based on the possibility of producing a number of (more or less) accurate *RH* levels inside the calibration box and on the assumption that the instrument can be tuned to them. The method is less expensive because no primary instruments are needed, and the chamber requires a less rigorous control. The reference *RH* levels are usually obtained with salt solutions in saturation equilibrium. This has the further advantage that there is no need for temperature regulation and this simplifies procedures, reducing time and costs. However, the supersaturated salt solution method is only an approximation (i.e. within a few percent of *RH*) and is not accepted as a calibration method by EN ISO/IEC 17025.

The method is based on the fact that a supersaturated salt solution is spread in an area as large as possible and air mixing provides homogeneity inside the calibration box. An excess of the solid salt is suggested, in order to ensure saturation even when a large amount of water vapour is absorbed by the solution with two possible negative consequences: (1) the excess of solid salt disappears and the solution is not longer saturated; and (2) a density stratification forms, with the upper layer enriched with absorbed water, not saturated and in equilibrium with a higher *RH*.

A list of substances that might be used to this aim is given in Table 18.4. Please note that vacuum is the easiest way to reach $RH = 0\%$, but it might damage some sensors. In general, calibration is made with two or three points from the 30% to 70% *RH* interval.

A popular home check is to compare hygrometers with a psychrometer, whose readings are based on thermometers that are more accurate than hygrometers. This should be considered as a controlling test (not a calibration!) to be repeated frequently to verify if some macroscopic breakdown or drift has occurred to the hygrometers, if they should be replaced or sent for recalibration.

It is recommended to avoid the erroneous practice of cross-comparing two instruments of the same type, e.g. two capacitive sensors, because both may be affected by the same drift and uncertainties. Finding that both exactly provide the same readings generally means that both of them are affected by the same types of errors; only exceptionally that both are accurate.

TABLE 18.4 Obtaining Constant Relative Humidity Levels Within a Calibration Chamber

Saturated solution or vacuum	*RH*	Saturated solution	*RH*	Saturated solution	*RH*
Air pump vacuum	0%	LiCl	15%	$MgCl_2{\cdot}6H_2O$[a]	32%
$CaCl_2{\cdot}6H_2O$	32%	$Zn(NO_3)_2{\cdot}6H_2O$	42%	$K_2CO_3{\cdot}2H_2O$	44%
$Mg(NO_3)_2{\cdot}6H_2O$[a]	56%	$NaBr{\cdot}2H_2O$	58%	NaCl[a]	76%
KBr	84%	$ZnS0_4{\cdot}7H_2O$	90%	$Na_2CO_3{\cdot}10H_2O$	92%
$Na_2SO_4{\cdot}10H_2O$	93%	KNO_3[a]	95%	H_2O	100%

[a] *Substances suggested by the Smithsonian Institute.*
When the supersaturated solution method is used, an excess of the listed substances should remain in excess in the solid phase inside the saturated aqueous solution at 20°C.
Data from List (1971); Weast (1977/78); Perry et al. (1984).

18.2.9 Measuring Heat and Moisture Exchanges between Air and Monuments

A fast psychrometer or a combination of a fast thermometer with a fast hygrometer is used to monitor exchanges of heat and vapour between air and surfaces, e.g. between air and frescoed walls. In analogy with molecular diffusion, fluxes are proportional to the negative gradient of the diffused property. The same theory has been applied for the diffusivity of heat,[26] i.e. the flux of heat $\mathcal{H}$ is

$$\mathcal{H} = -K_H \frac{\partial T}{\partial n} \tag{18.11}$$

where n is the normal to the surface and K_H is the coefficient of heat exchange in the direction of n (i.e. the normal to the surface) and depends on the physical mechanism responsible for the heat transport.

In the case of still air in a closed environment, K_H is determined by the thermal conductivity of air, i.e. $K_H = k_T$; when an internal dynamic boundary layer develops along the surface, the turbulent transport becomes dominant over the conductivity and when turbulence is well developed, as in outdoor environments, K_H is given by the eddy diffusivity K_E. Of course, K_E is a function of the Richardson number, increasing when *Ri* decreases (for experimental values see Plate, 1982). The eddy diffusion coefficient applies when the eddy motions are rapid enough and are the dominant factor in heat transfer. However, if the wall is directly hit by solar radiation, or the temperature gradient is measured outside, in the convective boundary layer that forms over the ground when the solar radiation overheats it, the mechanism of transfer changes, being characterized by the buoyancy and not by the momentum transfer. For this reason, the subscript H is a reminder that the eddy diffusion coefficient for heat exchanges may differ from the eddy diffusion coefficient for momentum exchanges.

When mechanical transfer dominates, eddies preserve their properties over an average displacement l, called

[26] See Chapter 10.

mixing length, and then mix with the surrounding environment. From the definition of *eddy flux*, i.e. the capability of transporting along the vertical (or the normal) mechanical mixing, the coefficient of eddy diffusivity K_E is given by

$$K_E \approx < w' l > \tag{18.12}$$

For a neutral shear flow, the physical factors governing the mean flow are the surface stress, the distance from the surface, and the fluid density. Dimensional considerations lead to find the following equation in terms of the shearing stress τ, which is linked with the dynamic viscosity and the wind shear:

$$K_E = C_E \sqrt{\frac{\tau}{\rho}} \tag{18.13}$$

where C_E is a constant (Goody, 1995).

In conclusion, when an observation of the temperature gradient near a surface is made, a quantitative evaluation of the heat exchange needs a careful examination of the dynamic state of the air motion, as the exchange coefficient varies with it. Hence, it might be better to limit the analysis to pinpoint the presence, the sign, the time of appearance, and the place where temperature gradients appear and avoid the risk of macroscopic errors. The only reliable quantitative case is found in closed rooms, with calm, stable stratified air. Under these circumstances, the quantitative value of the molecular heat exchange is obtained by substituting in Eq. (18.11) the actual value of the thermal conductivity $k_T = 6.26 \times 10^{-5}$ cal cm^{-1} s^{-1} K^{-1} (or 26.2 mW m^{-1} K^{-1}) at $T = 300$ K, i.e.

$$\mathcal{H} = -6.26 \times 10^{-5} \frac{\partial T}{\partial n} \left(\text{cal cm}^{-2}\ \text{s}^{-1}\right) \tag{18.14}$$

where the coefficient -6.26×10^{-5} gives the flux per unit gradient of T. Similarly, the flux of moisture M_v is given by

$$M_v = -\rho K_w \frac{\partial MR}{\partial n} \tag{18.15}$$

where ρ is the air density and K_w is the diffusivity for water vapour. As in the previous case, K_w is not constant but varies between $D_{aw} \leq K_w \leq K_E$, where the extremes are the molecular diffusivity D_{aw} of vapour in still air in closed indoor environments and the eddy diffusivity K_E outdoors, where turbulence and mixing dominate.

In order to get an idea of the numerical value of the moisture flux in a closed room with stable air, it is possible to substitute in the above equation the actual values of $\rho = 1.16 \times 10^{-3}$ g cm^{-3} and $D_{aw} = 0.24$ cm^2 s^{-1}, i.e.

$$M_v = -2.77 \times 10^{-4} \frac{\partial MR}{\partial n} \left(\text{g cm}^{-2}\ \text{s}^{-1}\right) \tag{18.16}$$

where the coefficient -2.77×10^{-4} gives the flux per unit gradient of MR.

Exchanges of heat or moisture are always associated with gradients of T or MR but in many cases, exchanges are small and the gradients are difficult to measure as they are weak, close to the surface, easily dissipated by air motions and turbulence, and are easily perturbed by the experimental apparatus. For this reason, it is not only very difficult to arrive at a precise quantitative evaluation of $\mathcal{H}$ and M_v, but also difficult to identify the occurrence of these fluxes. Therefore, it is practically convenient to measure in finite terms ΔT and ΔMR close to the surface and far from it; although this measurement does not give the value of the actual gradient at the interface, it in any case offers an objective observation in finite terms.

However, when positioning the aspirated psychrometer near the surface, the local air is perturbed and the excess (or defect) of heat and/or moisture is immediately aspirated by the fan. Keeping in the same position the instrument for the time necessary for the measurement, the fan suction brings new air that quickly passes near to the surface without having time to reach equilibrium with the moisture exchanges between the air and the surface. This problem can be partially overcome by inserting on the psychrometer intake a thin insulating disk, with three soft spacers, some 3 mm thick, glued to the disk. Once the spacers are put into contact with the surface, e.g. a fresco, the air is obliged to flow between the target surface and the topping disk until it arrives at the centre of the disk where the sensors and the fan are located (Fig. 18.14). The air remains longer in contact with the wall surface exchanging heat and moisture and reaching a better (even if partial) equilibrium before reaching the sensors. In order to avoid, or to minimize, heat exchanges between the disk and the air, the disk should be made of a material both insulating and with low density, e.g. polystyrene foam. We have used polystyrene foam disks with 30 cm diameter, to which three small spacers were attached (e.g. 3 to 4 mm) made of felt or soft

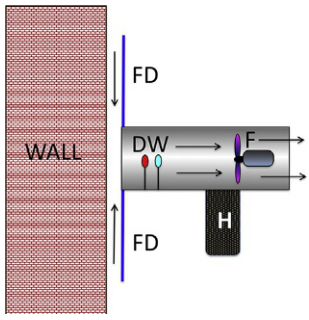

FIG. 18.14 Vertical cross section of a wall and a psychrometer with a front disc (FD) to highlight air–wall interactions. A disc with low thermal capacity is inserted at the inlet of the psychrometer tube to force the intake air to increase the interaction with the wall surface while passing between the disk and the wall. *Red and cyan dots*, dry- and wet (DW)-bulb sensors; *F*, fan; *H*, handle with electronic circuits and wick water reservoir. *Arrows*, direction of inlet air.

silicone for two reasons: (1) to ensure a regular distance between the disk and the wall and (2) to avoid damage when the disk touches the wall.

18.2.10 Evaporimeter and Atmometer

Open-Pan Evaporimeter

The open-pan *evaporimeter* (e.g. Wright, Summerland evaporimeter) consists of a pan filled of water where the quantity of liquid that has been lost by evaporation over a period of time is measured. Of course, the reading should be rejected in the case of precipitation; alternatively, the precipitation should be measured and subtracted. This suggests that evaporimeters cannot be left unattended over long periods. Evaporimeters are traditionally applied for irrigation or other agricultural purposes. Generally, they have small water tanks sunk into the ground (in order to reach similar temperatures), or the pan is floating on lakes, depending on the environmental situation that needs to be monitored. Small models exist to evaluate the evaporation in small environments, e.g. courtyards or indoors, e.g. the Wild weighing evaporimeter in Fig. 18.15A, or the screw evaporimeter with upper umbrella to shield it from radiation and precipitation (Fig. 18.15B).

The evaporation rate is governed by the vapour pressure difference in the free air and over the pan surface as well as by the local wind intensity, solar radiation, air and soil temperature. An accelerated evaporation near sunset may be due to birds drinking in the pan, if the pan is not adequately protected and surrounded by a net to keep out animals from drinking water, and leaves. Wire cages against big animals were available (Fig. 18.16).

Consider the following situation for an evaporimeter in summertime, after a rainfall followed by some clear days. In the first day, when the ground is wet, the evaporation rate is small from both the pan and the ground, and similar between them, because both of them have water availability and the air is close to saturation. In the next days, the situation tends to differentiate because the air is dry, and the ground has lost most of the moisture in the surface layer, and the evaporation is reduced progressively, until it ends because the ground is dry. In opposition, the evaporimeter has water availability, is located in a very dry environment, and will have an increased evaporation rate.

Briefly, evaporimeters have limitations that exceed their advantages and are unable to provide measurements representative of the true evaporation over a terrain or a water reservoir (Houghton, 1985). For this reason, the parameter derived from them is called 'potential evaporation' that is a purely hypothetical quantity. In agriculture, evaporimeters may indicate when the air is becoming too

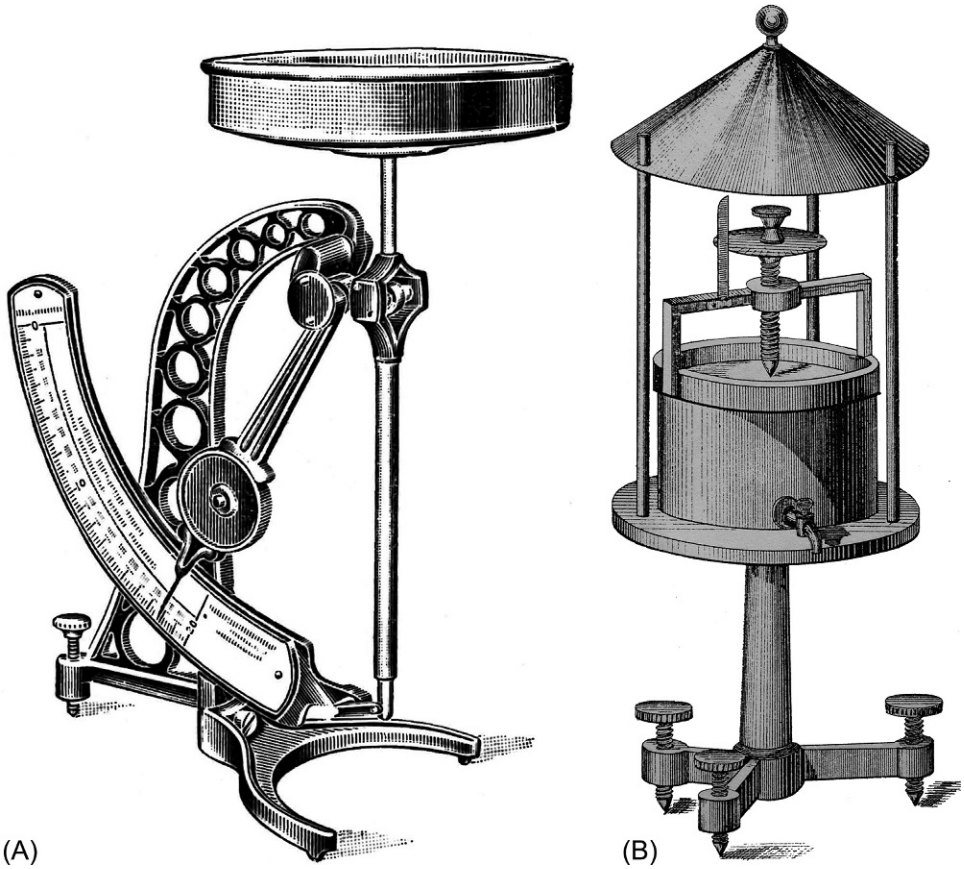

FIG. 18.15 Evaporimeters: (A) Wild weighing evaporimeter and (B) screw evaporimeter with upper umbrella to shield it from radiation and precipitation. *From (A) Vercelli (1933); IMAIT (1872).*

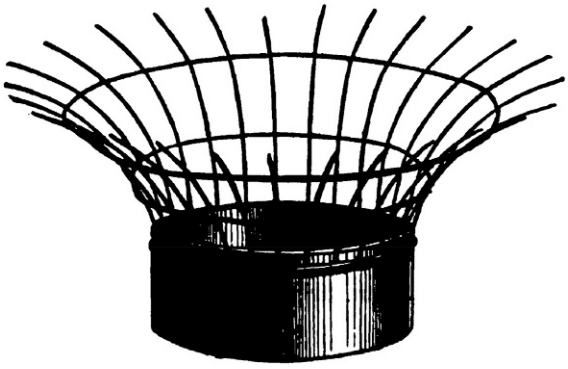

FIG. 18.16 Wire cage round the evaporation gauge to prevent big animals from drinking water. *From Negretti and Zambra (1864).*

dry and crops may require irrigation. If the evaporation rate becomes higher than normal, the climate of that area tends to suffer from drought and water resource shortages. *Budyko's aridity*, or *dryness index* φ (Budyko, 1974), is defined as the ratio of annual potential evaporation to precipitation, i.e. in an arid region, all water provided by precipitation evaporates ($\varphi = 1$), and if there are large water bodies, the total evaporation may exceed the local precipitation ($\varphi > 1$). As opposed, if the region is humid and rainy, not all rainwater can evaporate, and it will feed rivers or the water table ($\varphi < 1$) (Arora, 2002).

In the field of cultural heritage, evaporimeters may give a crude indication whether wooden monuments (e.g. the mediaeval *Stave Churches*[27] in northern and eastern Europe) are exposed to risky conditions related to mould infestation or mechanical issues of the wood (shrinking or swelling). However, direct measurements of relative humidity in air, or moisture content in the wooden structure, are preferable.

Atmometer

Other smaller evaporimeters exist that are often named with their original name 'atmometers'[28] to distinguish them from the bigger pan evaporimeters. However, in the real world, the choice of their name atmometer/evaporimeter is subjective and depends on the user's

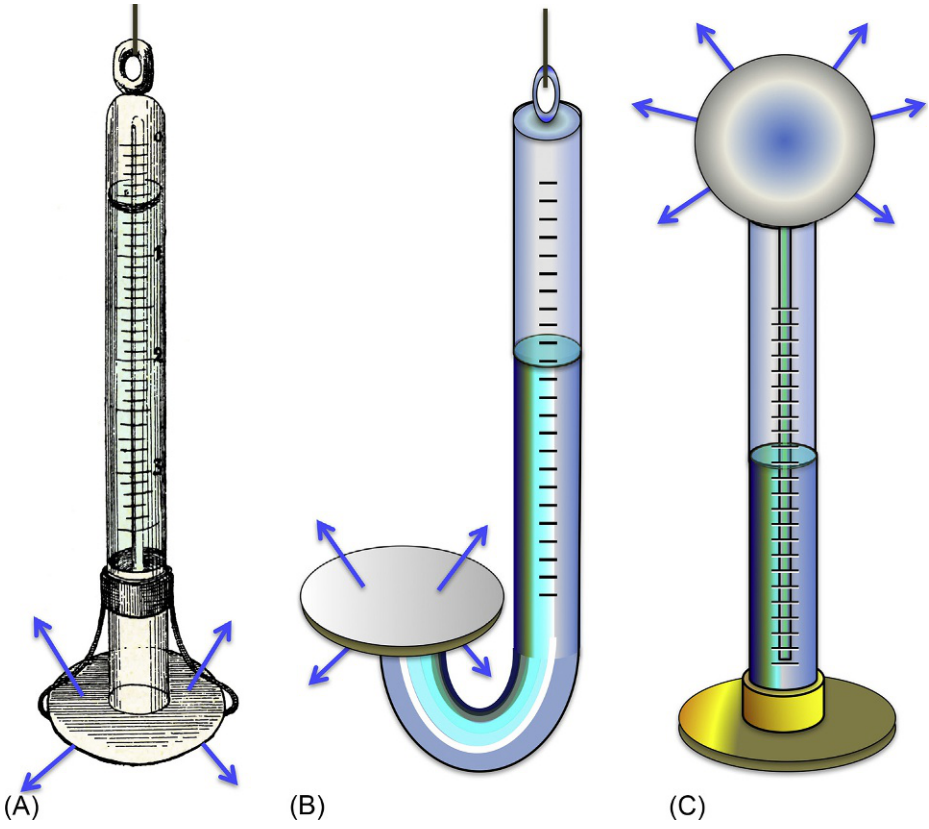

FIG. 18.17 Atmometers. (A) Bellani atmometer composed of an upside-down graduated tube, hung with a string. Evaporation *(arrows)* occurs from the porous disc at the bottom. (B) Piche atmometer composed of a J-shaped graduated tube and an evaporating disc on the lower arm. (C) Livingston atmometer composed of a standing graduated tube. Evaporation occurs from the porous sphere on the top. *From (A) Eredia (1936).*

[27] See Chapter 14.

[28] 'Atmometer' derives from the Greek *ατμος* (*atmos*) that means breath, puff, vapour, steam, and μετρον (*metron*) that means measure or something used to measure. Hence the names 'atmosphere' for the air enveloping our planet, and 'atmometer' for an instrument to measure something like a breath that releases moisture.

background. Atmometric measurements may be considered an index of the (potential) evaporation that might occur if a spot of dampness is accidentally made on a wall.

The Bellani atmometer (Bellani, 1816, Fig. 18.17A) may be used for conservation purposes, either outdoors or indoors. It consists of a graduated glass tube (e.g. 1.5 cm diameter and 30 cm long) open at one end and closed at the other. The tube is filled of distilled water and a flat ceramic disk or a filter paper is placed in position and held to the tube with a small spring. Then the tube is placed upside down, hung with a string. Evaporation takes place from the wet disc at the base, and lowers the water level in the tube, so that evaporation can be read directly from the gradations, i.e. scale. Readings are taken at regular time intervals, e.g. one or more hours, or one day. The evaporation rate is obtained by dividing the loss of water by the time elapsed between two readings. The potential evaporation rate was measured in the Sistine Chapel having *RH* around 50%, and the readings were consistent with formula (18.16) (Camuffo and Bernardi, 1986).

The Piche atmometer (Fig. 18.17B) is very similar to Bellani's, but the tube is J shaped. The upper arm is topped and graduated, and the evaporating disc is placed on the lower arm.

The Livingston atmometer (Fig. 18.17C) is also similar, but the graduated tube is standing, and on the top is open and has a porous sphere above it, connected with the water reservoir with a thin capillary on glass or brass to feed the sphere. The evaporation is read on the graduated tube.

The Bellani, Piche, Livingston, and other atmometers are not recommended for environmental studies and resource surveys, unless no weather stations are available in that region (WMO, 2008). However, they may be useful in small-scale surveys to characterize indoor climates. Their advantage is that they may provide essential, basic information about dryness (i.e. high evaporation rate), or dampness (i.e. low evaporation rate) in a room, with a very simple and low-cost instrumentation. However, direct measurements of air dryness taken with relative humidity sensors are preferable.

References

Alberti, L.B., 1485. De re aedificatoria Libri decem. Book 10 (Chapter 3), Torrentino, Florence.

Amontons, G., 1685. Observations sur un nouvel hygrometre. In: Memoires de l'Académie Royale des Sciences, Tome 2. Paris, p. 22.

Amontons, G., 1695. Remarques & Expériences Physiques sur la construction d'une nouvelle Clepsidre, sur les Barometres, Termometres & Hygrometres. Jombert, Paris.

Arora, V.K., 2002. The use of the aridity index to assess climate change effect on annual runoff. J. Hydrol. 265, 164–177.

Assmann, A.R., 1892. Das Aspirations-Psychrometer. Ein Apparat zur Bestimmung der wahren Temperatur und Feuchtigkeit der Luft. Abhandlungen des Koniglich Preussischen Meteorologischen Instituts. vol. 1. Asher, Berlin, pp. 115–270. No. 5.

August, E.F., 1825. Ueber das Psychrometer. Ann. Phys. Chem. 5, 69–88. 335–344.

August, E.F., 1830. Ueber die Fortschritte der Hygrometrie in der neuesten Zeit. Trautwein, Berlin.

Baer, W., 1859. Die Chemie des praktischen Lebens. vol. 1. Bigand, Leipzig.

Bell, S.A., Carroll, P.A., Beardmore, S.L., England, C., Mande, N., 2017. A methodology for study of in-service drift of meteorological humidity sensors. Metrologia 54, S63–S73.

Bellani, A., 1816. Delle riflessioni critiche intorno all'evaporazione. Dell'aria e dei vapori. In: Brugnatelli, G. (Ed.), Giornale di Fisica, Chimica, Storia Naturale Medicina ed Arti. In: Tome IX, Galeazzi, Pavia, pp. 188–197.

Bentley, R.E., 1998. Handbook of Temperature Measurement: Temperature and Humidity Measurement. Springer Verlag, Berlin.

Berryat, 1754. Anneé MDCLXXXVII. Physique Générale. In: Histoire de l'Académie des Sciences de Paris, Tome II, p. 22. In Recueil de mémoires ou Collection de pièces Académiques, Tome I p. 131. Fournier, Auxerre et Desventes, Dijon. .

Birch, T., 1756. The History of the Royal Society of London for improving of natural knowledge. In: Meeting of July 6th 1663. Millar in the Strand, London.

Borchi, E., Macii, R., 2007. Igroscopi & Igrometri. Pagnini, Florence.

Bud, R., Warner, D.J., 1998. Instruments of Science. An Hystorical Encyclopedia. Garland Publishing Inc., Taylor and Francis Group, New York, London.

Budyko, M.I., 1974. Climate and Life. Academic Press, Orlando, FL.

Camuffo, D., 2002. Errors in early temperature series arising from changes in style of measuring time, sampling schedule and number of observations. Clim. Chang. 53 (1–3), 331–354.

Camuffo, D., 2019. A method to obtain precise determinations of relative humidity using thin-film capacitive sensors under normal or extreme humidity conditions. J. Cult. Herit. 37, 166–169.

Camuffo, D., Bernardi, A., 1986. Dinamica del microclima e scambi termoigrometrici tra pareti e atmosfera interna nella Cappella Sistina. Boll. Mon. Mus. Gall. Pont. 6, 211–257.

Camuffo, D., Fernicola, V., 2010. How to measure temperature and relative humidity. Instruments and instrumental problems. In: Camuffo, D., Fassina, V., Havermans, J. (Eds.), Basic Environmental Mechanisms Affecting Cultural Property—Understanding Deterioration Mechanisms for Preventive Conservation Purposes, COST Action D42 "Enviart". Nardini, Florence.

Camuffo, D., Giorio, R., 2003. Quantitative evaluation of water deposited by dew on monuments. Bound.-Layer Meteorol. 107, 665–672.

Camuffo, D., Bertolin, C., Bergonzini, A., Amore, C., Cocheo, C., 2014. Early hygrometric observations in Padua, Italy, from 1794 to 1826: the Chiminello goose quill hygrometer versus the de Saussure hair hygrometer. Clim. Chang. 122 (1–2), 217–227.

Camuffo, D., della Valle, A., Becherini, F., 2018. A critical analysis of one standard and five methods to monitor surface wetness and time-of-wetness. Theor. Appl. Climatol. 132 (3–4), 1143–1151.

Carr-Brion, K., 1986. Moisture Sensors in Process Control. Elsevier Applied Science, Amsterdam.

Chiminello, V., 1785. Ricerche sulla comparabilità dell'igrometro: memoria del signor abate Chiminello. Turra, Vicenza.

Cotte, L., 1774. Traité de Météorologie: contenant 1. l'histoire des observations météorologiques, 2. un traité des météores, 3. l'histoire & la description du baromètre, du thermomètre & des autres instruments météorologiques, 4. les tables des observations météorologiques & botanicométéorologiques, 5. les résultats des tables & des observations, 6. la méthode pour faire les observations météorologiques. Imprimerie Royale, Paris.

Cotte, L., 1788. Memoires sur la Météorologie. Imprimerie Royale, Paris.

D*** (alias D'Alencé J.), 1688. Traittéz des Barométres, Thermométres et Notiométres ou Hygrométres. Wetstein, Amsterdam.
Daniell, J.F., 1823. Meteorological Essays and Observations. vol. 1. Underwood, London.
Daniell, J.F., 1845. An Essay Upon Hygrometry and the Construction and Uses of a New Hygrometer. vol. 2. Parker, London.
Davey, F.K., 1965. Hair humidity elements. In: Wexler, A. (Ed.), Humidity and Moisture, Principles and Methods of Measuring Humidity in Gases. In: vol. 1. Rehinold, New York, pp. 571–573. 647 pp.
De Luc, M.J.A., 1773–74. Account of a new hygrometer. Philos. Trans. 63, 404–460.
De Luc, M.J.A., 1791. A second paper on hygrometry. Philos. Trans. 81, 111–117.
De Saussure, H.B., 1783. Essais sur l'Hygrometrie. Fauche, Neuchatel.
Doebelin, E.O., 1990. Measurement Systems-Application and Design. McGraw Hill, New York.
EN 16242, 2012. Conservation of Cultural Property—Procedures and Instruments for Measuring Humidity in the Air and Moisture Exchanges Between Air and Cultural Property. European Committee for Standardization (CEN), Brussels.
Eredia, F., 1936. Gli strumenti di meteorologia ed aerologia. Bardi, Rome.
Eren, H., Kong, W.L., 1999. Capacitive sensors—displacement. In: Webster, J.G. (Ed.), The Measurement, Instrumentation, and Sensors Handbook. CRC Press, Boca Raton.
Fernicola, V., Banfo, M., Rosso, L., Smorgon, D., 2008. Investigations on capacitive-based relative humidity sensors and their stability at high temperature. Int. J. Thermophys. 29, 1668–1677.
Fisher, P.D., Lillevik, S.L., Jones, A.L., 1981. Microprocessors simplify humidity measurements. Trans. Instr. Meas. IM-30 (1), 57–63.
Frasca, F., Caratelli, A., Siani, A.M., 2018. The capability of capacitive sensors in the monitoring relative humidity in hypogeum environments. IOP Conf. Ser.: Mater. Sci. Eng. 364, 012093.
Frisinger, H.H., 1983. The History of Meteorology: To 1800, second ed. American Meteorological Society, Boston.
Ganot, A., 1860. Traité de physique expérimentale et appliquée, et de meteorologie. Chez l'auteur-éditeur, Paris.
Gerosa, G., 1898. Meteorologia. UTET, Torino.
Goody, R., 1995. Principles of Atmospheric Physics and Chemistry. Oxford University, New York.
Griesel, S., Theel, M., Niemand, H., Lanzinger, E., 2012. Acceptance test procedure for capacitive humidity sensors in saturated conditions. WMO, CIMO TECO-2012, Brussels.
Harriman, L.G., 1990. The Dehumidification Handbook. Munters, Cargocaire.
Hemmer, J.J., 1783. Descriptio instrumentorum meteorologicorum, tam eorum, quam Societas distribuit, quam quibus praeter haec Manheimii utitur. Ephemerides Societatis Meteorologicae Palatinae 1, 57–90.
Houghton, D.D., 1985. Handbook of Applied Meteorology. Wiley, New York.
IMAIT, 1872. Norme per le osservazioni meteoriche. Supplemento alla Meteorologia Italiana. Italian Ministry for Agriculture, Industry and Trade, Rome, pp. 28–33.
Kämpfer, N., 2012. Monitoring Atmospheric Water Vapour: Ground-Based Remote Sensing and In-Situ Methods. vol. 10. Springer, New York.
Korotcenkov, G., 2018. Handbook of Humidity Measurement, Spectroscopic Methods of Humidity Measurement. Vol. 1. CRC Press—Taylor & Francis, London.
Korotcenkov, G., 2019. Handbook of Humidity Measurement, Electronic and Electrical Humidity Sensors. Vol. 2. CRC Press—Taylor & Francis, London.
Lambert, J.H., 1769. Experiments on hygrometry. Memoir de l'Acad. Roy. des Sciences de Berlin, 68.
Lambert, J.H., 1772. On hygrometry: continued. Memoir de l'Acad. Roy. des Sciences de Berlin, p. 65.
Lambert, H.J., 1774. Hygrometrie oder Ubhandlung von den Hygrometern. Aletts, Augsburg.
Lardner, D., 1877. Hand-Books of Natural Philosophy and Astronomy: Heat. Lockwood, London.
Leonardo da Vinci, 1487. Codex Atlanticus. Biblioteca Ambrosiana, Milano (Also published in the book: Il Codice Atlantico di Leonardo da Vinci nella biblioteca Ambrosiana di Milano, Hoepli, Milan, 1894-1904).
Leslie, J., 1813. Short Account of Experiments and Instruments Depending on the Relations of Air to Heat and Moisture. Blackwood and Ballantyne, Edinburg.
Lipták, B.G., 2003. Instrument Engineers' Handbook: Process Measurement and Analysis. The Instrumentation System and Analysis (ISA). vol. 1. CRC Press, Boca Raton, FL.
List, R.J., 1971. Smithsonian Meteorological Tables. Smithsonian Institution, Washington, DC.
Macfarquhar, C., Gleig, G., 1797. Encyclopædia Britannica: Or, A Dictionary of Arts, Sciences, and Miscellaneous Literature. vol. IX. Bell and Macfarquhar, Edinburgh.
Macleod, K.J., 1983. Relative Humidity: Its Importance, Measurement and Control in Museums. Canadian Conservation Institute, Ottawa.
Magalotti, L., 1667. Saggi di naturali esperienze fatte nell'Accademia del Cimento. Giuseppe Cocchini, Florence.
Magnus, G., 1844. Über die Ausdehnung der Gase durch die Warme (On the expansive force of steam). Poggendorff Annalen der Physik und Chemie LXI, 225–247 (translated from German by W. Francis. In: Taylor, R. (Ed.), 1846. Scientific Memoirs Selected From the Transactions of Foreign Academies of Science and Learned Societies and From Foreign Journals, vol. IVR. J. Taylor, London).
Malmberg, C.G., Maryott, A.A., 1956. Dielectric constant of water. Research Paper 2641. J. Res. Natl. Bur. Stand. 56 (1), 1–8.
Michalski, S., 2000. Guidelines for Humidity and Temperature in Canadian Archives. Canadian Conservation Institute, Ottawa.
Middleton, K.W.E., 1966. A History of the Thermometer and Its Use in Meteorology. J. Hopkins Press, Baltimore.
Middleton, W., 1969. Invention of the Meteorological Instruments. John Hopkins Press, Baltimore.
Nairne, E., 1783. Hygrometers. From Edward Nairne to Benjamin Franklin. A Hygrometer on a new construction—M. De Luc' Hygrometer, posthumous in B. Franklin and J. Sparks: The Works of Benjamin Franklin: Containing Several Political and Historical Tracts. vol. 6. Wittmore Niles et Hall, Boston, pp. 449–450 (1856).
Negretti, E., Zambra, J.W., 1864. Meteorological Instruments: Explanatory of their Scientific Principles, Method of Construction, and Practical Utility. William and Strahams, London.
Nicolaus Cusanus, 1565. posthomous. D. Nicolai de Cusa cardinalis vtriusque iuris doctoris in omnique philosophia incomparabilis viri, Opera. In: Officina Henricpetrina, Sebastian, Basel, p. 176.
Plate, E.J., 1982. Engineering Meteorology. Elsevier, Amsterdam.
Perry, R.H., Green, D.W., Maloney, J.O., 1984. Chemical Engineers' Handbook. vol. 6. McGraw-Hill, New York.
Retz, N., 1779. Traité d'un nouvel Hygrometer, comparable de celui de M. de Luc. Méquignon l'ainé, Paris.
Retz, N., Held, C.F., 1786. Abhandlung von Eiflusse der Witterung auf die Urznenwissenschaft und den Uderbau, nebst der Beschreibung eines vergleichbaren Hygrometers. Henning, Greiz.
Sanctorius, S., 1625. Commentaria in primam fen primi libri Canonis Avicennae. Iacobus Sarcina, Venice.

Smit, H., Kivi, R., Vömel, H., Paukkunen, A., 2013. Thin film capacitive sensors in monitoring atmospheric water vapour. In: Kämpfer, N. (Ed.), Monitoring Atmospheric Water Vapour: Ground-Based Remote Sensing and In-Situ Methods. In: vol. 10. Springer Science & Business Media, New York, pp. 11–38.

Smollett, T.G., 1788. Foreign literary intelligence. In: Appendix to the Critical Review or Annals of Literature. vol. 65. Hamilton, London.

Sprung, A., 1888. Über die Bestimmung der Luftfeuchtigkeit mit Hilfe des Assmannschen Aspirationspsychrometers. Z. Angew. Meteorol. Das Wetter 5, 105–108.

Targioni Tozzetti, G., 1780. Notizie degli aggrandimenti delle Scienze Fisiche accaduti in Toscana nel corso di anni LX del secolo XVII, Tomo I. Bouchard, Florence.

Tetens, O., 1930. Uber einige meteorologische Begriffe. Z. Geophys. 6, 297–309.

Tewles, S., Giraytys, J., 2016. Meteorological Observations and Instrumentation. American Meteorlogical Society. Lancaster Press, Lancaster, PA.

Thomson, G., 1986. The Museum Environment, second ed. Butterworth - Heinemann Series in Conservation and Museology, London.

Tomlinson, C., 1861. The Dew-Drop and the Mist: An Account of the Phenomena and Properties of Atmospheric Vapour. Society for Promoting the Christian Knowledge, London.

Turner, G.L.E., 1983. Nineteenth-Century Scientific Instruments. Sotheby Publications, University of California Press, Berkeley.

UK Meteorological Office, 1981. Handbook of Meteorological Instruments. Measurement of Humidity. vol. 3. Her Majesty's Stationary Office, London.

Vercelli, F., 1933. L'aria, nella natura e nella vita. UTET, Torino.

Weast, R.C., 1977/78. CRC Handbook of Chemistry and Physics. CRC Press, West Palm Beach, FL.

Wexler, A., 1965. Humidity and Moisture. Principles and Methods of Measuring Humidity in Gases. vol. 1. Reinhold, New York.

Wiederhold, P., 1975. Humidity measurements part I: psychrometers and percent RH sensors. Instrum. Sci. Technol. 22, 31–37.

Wiederhold, P., 1997. Water Vapour Measurement: Methods and Instrumentation. Marcel Dekker, New York.

WMO, 1986. Compendium of lecture notes on meteorological instruments for training class III and class IV. Meteorological personnel. WMO Technical Publication No. 622, World Meteorological Organisation, Geneva.

WMO, 2008. Guide to meteorological instruments and methods of observation. WMO Technical Publication No. 8, World Meteorological Organization, Geneva (updated 2010).

Wolf, A., 1961. A History of Science, Technology, and Philosophy in the Eighteenth Century. vol. 1. Harper Torchbook, New York.

Wylie, R.G., Lalas, T., 1992. Measurement of temperature and humidity. WMO 759 Secretariat of the World Meteorological Organization, Geneva.

This page intentionally left blank

CHAPTER

19

Measuring Time of Wetness and Moisture in Materials

OUTLINE

19.1 MEASURING THE TIME OF WETNESS

19.1.1 Introduction to the Time of Wetness

The time of wetness (ToW) is an important variable in conservation science, as several physical, chemical, and biological deterioration mechanisms are possible only in the presence of liquid water. ToW is considered 'heritage climatology', that is a specific branch of science that employs particular parameters useful for predicting the effect of climate alone, or in synergism with pollution, on cultural heritage. ToW is defined as the amount of time a material surface remains wet during atmospheric exposure, and represents the cumulative duration of all individual time intervals, expressed in number of hours per year, in which a surface is wet, i.e. covered with a film of liquid water or droplets, depending on whether the surface is hydrophilic or water repellent. Although the basic concept and importance of ToW in governing atmospheric corrosion is generally agreed upon, what is meant by 'wet' has generally remained ambiguous and its practical determination has been widely varied throughout its history (Schindelholz and Kelly, 2012).

It might be assumed that ToW takes into account when the moisture in the local air is at saturation, or close to saturation, i.e. $RH = 100\%$. However, by considering that the temperature of objects may differ from air, that the *RH* sensors increase uncertainty at high humidity, and in the absence of specific devices, the definition is usually extended to the period in which the ambient *RH* exceeds a selected lower threshold, e.g. 90%, 80%, in which corrosion or microbiological life may occur. For instance, the atmospheric corrosion of a metal is an electrochemical process proceeding under a thin electrolyte film, the

https://doi.org/10.1016/B978-0-444-64106-9.00019-5

thickness of which is mainly determined by the relative humidity of the atmosphere (Xia et al., 2017). ToW should reproduce the total time in which the electrolyte film is active.

It may be useful to keep in mind that ToW is a composite atmospheric variable, determined by the mixing ratio (*MR*) of the water vapour in air, the object surface temperature T_s, and the surface contamination. Only when T_s drops below the dew point (*DP*), the surface becomes wet and it is possible to start measuring ToW, which is related to the ambient *RH*, but not exactly coincident with any specific *RH* level. In reality, ToW should coincide with the total time during which the surface temperature remains below the *DP* but, in reality, it is slightly longer for two reasons: the surface may be contaminated by hydrophilic substances that increase ToW by earlier wetting and later drying; even in the case of perfectly clean surfaces, when T_s rises above *DP*, some time is needed to evaporate the water drops lying on the surface, e.g. dew.

A number of methods and devices have been considered to measure ToW, as an index of potential corrosivity or mould attack, as follows.

19.1.2 The International Standard ISO 9223 on Corrosion of Metals and Alloys

The international standard ISO 9223 (2012) 'Corrosion of metals and alloys. Corrosivity of atmospheres. Classification' establishes a classification system for the corrosivity of atmospheric environments. The guiding corrosion values are based on experience obtained with a large number of exposure sites and service performances. Corrosion occurs in synergism with wetness, and ISO 9223 establishes that ToW can be obtained from two conditions: $RH > 80\%$ and temperature $T > 0°C$. This is an empirical assumption, and may be supported with theoretical arguments. At $RH > 80\%$, a metal or glass surface is likely covered with a number of molecular layers of water (Leygraf and Graedel, 2000; Camuffo, 2010), the most external of them in the liquid state, and able to develop corrosion or feed microbiological life. In addition, the condition that the ambient temperature is above freezing point is justified to deal with real water and not with frost. From the practical point of view, ISO 9223 provides a very simple and reasonable definition.

The ISO 9223 definition has, however, some flaws, as follows (Camuffo et al., 2018): it is oriented to air variables and avoids considering the complexity deriving from of uneven temperature distributions. A comparison between ISO 9223 and indoor/outdoor field surveys has found relevant discrepancies between calculations and observations caused by uneven surface temperature and other factors (Veleva and Alpuches-Aviles, 2002; Corvo et al., 2008). Hydrophilic contaminants may change the vapour/liquid transition threshold, e.g. SO_2, NO_x, NaCl, biological layers. Rain is not considered, although short summer showers typically occur in relatively dry air, and surfaces remain wet until all water has evaporated. All *RH* sensors are supposed to respond to the manufacturer's assertions and to provide accurate results even at high *RH* levels, which in reality are most uncertain having departures of ±10% or more.[1] It is essential that *RH* sensors be calibrated including even the upper border of the range (not only in two internal points of the range, e.g. 45% and 60%, as generally occurs) and comply with the European standard EN 16242 (2012).

19.1.3 Dew Point From *T* and *RH* Sensors

The dew point method is also oriented to air variables, i.e. *T* and *RH* measurements, but it may be integrated with the temperature of objects. The method considers that liquid water is formed when the air (or a surface) temperature reaches the *DP*. Taken literally, this method is more restrictive than ISO 9223 because at $T = DP$, $RH = 100\%$. However, the set points of possible control system may be regulated one or two °C above the *DP*, to leave a reasonable uncertainty band at the border line as discussed for ISO 9223. For instance, in the temperature range from 0°C to 40°C, when the *RH* sensor departs by 10%, the error in *DP* ranges from 1.4°C to 1.9°C. This method is popularly used for sites or collections in thermal equilibrium with the air, or supposed to be in equilibrium with it. However, it may be improved considering the difference between the DP and the surface temperature of the reference object and establishing a threshold on it.

19.1.4 Capacitive Wetness Sensor

The basic module consists of a silicon integrated stray capacitor, a temperature sensor, and an integrated capacity-frequency converter. The water condensing on the sensor surface increases the sensor capacity, which, in turn, changes the output frequency. Finally, the frequency is converted into voltage and expressed in an arbitrary unit. Laboratory and field tests used to investigate the response of this sensor showed that the repeatability was low, the wetness threshold being activated at different *RH* levels, generally in the range $80 < RH < 95\%$. In addition, they are affected by hysteresis, i.e. they easily reach equilibrium during the wetting phase but retain water and remain damp for long time after the surface has become dry (Camuffo et al., 2018).

19.1.5 Leaf Wetness Sensor (Rain Detector)

A traditional device derived from agriculture is the 'leaf wetness sensor', also known as 'rain detector'. It is

[1] See Chapter 18.

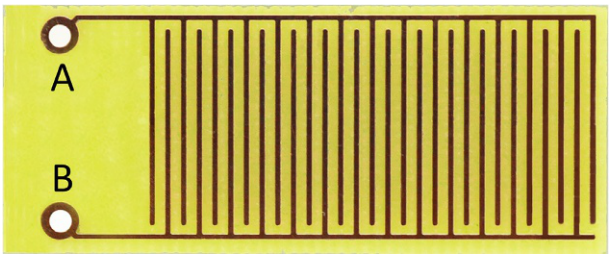

FIG. 19.1 The leaf wetness sensor (also known as raindrop detector) produced in the laboratory. It consists of a comb-like resistive sensor, composed of two electrically conductive combs A and B, with close interlacing, but separated between them. When some dewing starts forming on the sensor, the electrical resistance between A and B drops to short circuit.

a comb-like resistive sensor, composed of two electrically conductive combs with close interlacing, but separated from each other (Fig. 19.1). The electrical resistance across the gap between the two combs is extremely high. However, in proximity of the dew point, when the sensing surface starts dewing, the electrical resistance drops until short circuit is reached. The same occurs when some raindrops fall on it. The output may be 0 or 1 (i.e. dry or wet) and the sensor is often used as an on–off switch. Depending on the physical characteristics of the printed circuit board, and the distance between the two combs, the on–off threshold may change.

A popular leaf wetness sensor is the Wetcorr sensor (Haagenrud et al., 1982) developed by the Norwegian Institute for Air Research (NILU). This sensor, also known as grid sensor, is composed of an interdigitated pair of gold alloy electrodes (with a 130-μm spacing between them), on a sintered alumina backing with a sensing area of 20 × 20 mm, the electrodes connected to an astable multivibrator circuit.[2] The frequency is inversely dependent on impedance between the sensor electrodes and is measured to give wet–dry indication. Grid sensors are defined as being wet above a reading of 0.5 Hz relative to an open circuit (lowest frequency, 0.3 Hz) for the purpose of excluding the response of the sensor itself to changes in *RH* (Schindelholz et al., 2013).

Another popular leaf sensor available on the market consists of interdigitated gold alloy electrodes deposited on a fibre-reinforced circuit board, with overall sensing area 50 × 50 mm and 1 mm spacing between electrodes. Resistance is measured across the electrodes using a DC half-bridge circuit. The leaf sensor is defined as being wet below a reading of 7.3 MΩ corresponding to the resistance measured across a clean sensor at 95%*RH*. (Schindelholz et al., 2013).

In the agricultural and environmental applications, it is common practice to paint these sensors with a latex paint to increase sensitivity and create a surface more closely resembling the wetting characteristics of leaves (Sentelhas et al., 2004). In the field of cultural heritage, this practice is not common, and a different latex paint should be selected for every type of material and the physical conditions of its surface.

In laboratory tests, some leaf wetness sensor indicated 'dry' when $RH < 60\%$, 'wet' when $RH > 80\%$, in agreement with ISO 9223. However, in the range $60 < RH < 80\%$ they indicated either dry or wet, depending on the contaminants. The sensors were successfully applied in rural and remote areas, e.g. to study the formation of water films for the adsorption of NH_3 and SO_2 on the leaf surface or the attack of pathological fungi (Van Hove et al., 1989; Van Den Ende et al., 2000; Wichink Kruit et al., 2008) or to know the number of dew nights (Jacobs et al., 2006). In urban areas, however, the situation was different. A sensor was applied to measure the time of wetness of stained glass windows of the St Eustache church, Paris. It operated normally for two weeks, but later it started to drift, it increased hysteresis on the drying phase, and provided false readings. The sensor was analyzed in the laboratory and was found contaminated by dust and pollution particles from the heavy traffic of Paris, which formed a hygroscopic conductive layer. The sensor is highly vulnerable to urban environments, polluted and coastal areas, for the presence of airborne particulate matter or marine aerosols (Camuffo et al., 2018). However, even simple dust may be sufficient to change the hydrophilic properties of a surface (Thickett, 2008).

19.1.6 Safety Sensor

Safety sensors have been devised to protect electronic devices against short circuits for dewing, typically when the device enters a very humid or cold environment. The operating principle is based on a sensitive polymer layer deposited on a ceramic substrate; the polymer absorbs water molecules increasing exponentially its electrical resistance when the *RH* level increases. When the sensor approaches saturation, e.g. $RH > 95\%$, the polymer increases very much its electrical resistance and stops the power supply. It is an on/off switch, especially conceived to operate at condensation level. Laboratory and field tests demonstrated that the sensors are very reliable, with small inertia: at increasing *RH* they reach equilibrium in less than 10 s; less rapidly, i.e. 150–200 s, when *RH* is dropping. However, this small lag is irrelevant. The size of the sensor is very small, i.e. 5 mm × 5 mm × 3 mm (Fig. 19.2). The sensor has been successfully used to monitor dampness in monuments (Camuffo et al., 2014, 2018). It is very cheap and reliable.

[2] Astable multivibrators, also known as free-running multivibrators, are cross-coupled transistor switching circuits that have no stable output states as they change from one state to the other all the time producing two square wave output waveforms.

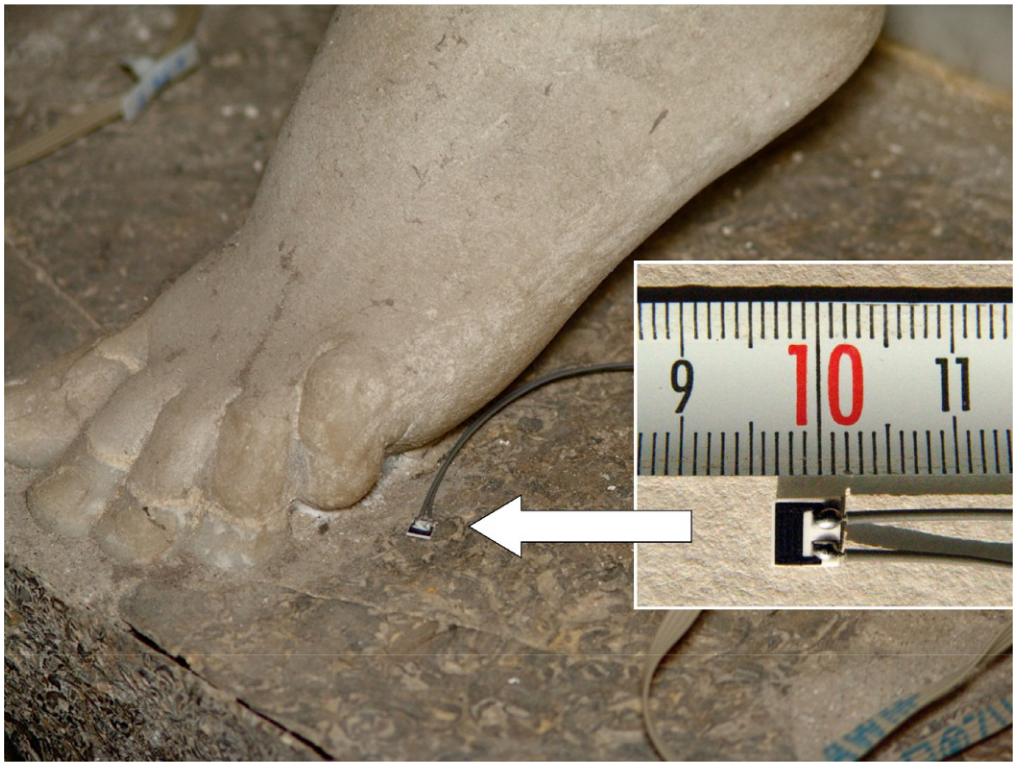

FIG. 19.2 The safety sensor used to detect surface wetness in a statue, and square with expanded view to highlight the sensor size.

19.1.7 IR Reflection Sensor (Dewing Sensor)

A dewing sensor that closely follows the behaviour of nonabsorbing materials is based on the extinction (or attenuation) of a reflected *IR* beam when dew droplets are forming on the surface of the body under examination. In fact, the *IR* radiation is absorbed and extinguished in a few micrometres of liquid water, so that when droplets begin to form and grow on the surface, the reflected beam is immediately attenuated and its intensity progressively diminishes until it is completely extinguished; this happens when the surface is completely wet. However, as metals are good *IR* reflectors, a tiny metal mirror is introduced as reference surface, which is in contact with the target body and assumes the same temperature. The mirror is part of the measuring device (Fig. 19.3), being mechanically fixed at the appropriate distance to receive the *IR* beam from a light-emitting diode (i.e. an *IR*-emitting diode) and to reflect it into the sensor (i.e. a Photo-Darlington). The mirror is at the centre of a small, blackened metal board over which a shielding sheet is placed at short distance to allow free air circulation but to stop external radiation and avoid false reflections. The emitter is activated by a pulse current in order to reduce the power supplied by the *IR* beam and the bias for heating. The output of the Photo-Darlington is amplified, transformed into a continuous level by a peak detector, and then compared with a reference voltage that can be adjusted to calibrate the threshold at a selected dimension of the microdroplets (Camuffo and Valcher, 1986).

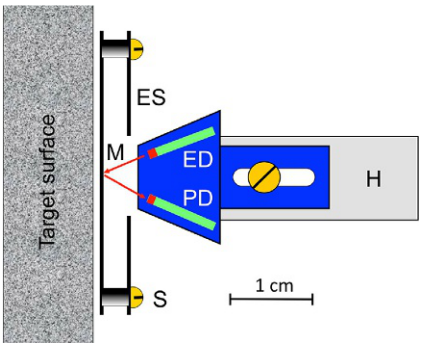

FIG. 19.3 Dewing detector. The optical transducer is composed of an *IR* emitting diode (ED), a Photo-Darlington (PD), a blackened metal board with mirror (M), an external shield (ES), and four spacers fixed with screws (S). It may be glued to the target surface or kept in position with a holder (H). *Modified from Camuffo and Valcher (1986) by kind permission of Kluwer Academic Publishers, see Credits.*

A dewing sensor may be used to monitor ToW or to activate heaters when droplets begin to form on cold windows, or dewing may affect statues or frescoes. To prevent a surface from dewing, it should be directly

heated by means of *IR* radiation or electrical wire resistors; it is not convenient to blow warm air because it is less efficient in warming and may increase particle deposition and induce efflorescence.

Simple prototypes and improved versions have operated in the cathedral of Torcello Island, Venice, the Sainte Chapelle, Paris, the St Urbain Basilica, Troyes, France (Bernardi et al., 2006), and Petrarca's tomb, Padua (Becherini et al., 2010). Like the leaf wetness sensor, a critical situation is when the mirror surface is contaminated by candle smoke, dust, pollens, marine aerosols, or other airborne particles that may affect the IR beam reflexion. When the mirror is tarnishing, a drift develops that may be misinterpreted for an apparently increasing trend of ToW.

19.1.8 Fibre-Optic Sensor

The metal pipes of organs are often affected by corrosion, especially for the synergism with acid VOCs released from wood and high *RH* levels or even condensation. A miniaturized fibre-optic sensor was developed under the EU project Sensorgan to assess the risk for condensation inside organ pipes without causing any disturbance when the organ was played (Baldini et al., 2008; Bergsten et al., 2010; Camuffo et al., 2018; Korotchenkov, 2018). The sensor (Fig. 19.4A) is composed of fibre optic, having a refraction index close to the index of water. The fibre is highly flexible and easily fixable to the internal surface of pipe, and its diameter is a fraction of mm. A LED light is supplied at one extreme of the fibre. At the other extreme, most light is emitted, but a fraction is reflected back by the molecules of water on the terminal end. The reflected light is monitored with a CCD camera and transformed into voltage. The output may change from fibre to fibre, depending on the end cut and the specific hydrophilic properties of the fibre surface, but the problem may be solved with individual tuning or normalizing the output as a percent of its plateau value at $RH = 50\%$.

The back reflection is governed by the number of molecular layers of water sticking on the terminal end of the fibre, and a sharp drop occurs when microdroplets begin to form on the fibre.

The output (Fig. 19.4B) decreases at increasing *RH* levels, i.e. when the number of molecular layers increases. When *RH* exceeds 80%, a marked bending corresponds to the quick formation of additional molecular layers of water, until the signal reaches 75% of its normalized value at $RH = 98\%$. At dewing, the output drops to 55% of its plateau value.

This sensor has been conceived to operate inside organ pipes, i.e. in the dark and in the absence of dust. If particles deposit on the distal end where the fibre is truncated, they may affect the back reflection.

19.2 MEASURING MOISTURE IN MATERIALS

19.2.1 Introduction to Moisture Content (or Water Content)

Water is responsible for many forms of deterioration, either based on physical, chemical, or biological mechanisms. Relative humidity is mainly responsible for the transfer of moisture from the air to the objects and vice versa, and the equilibrium reached. Objects deteriorate not from the moisture dispersed in air, but for the moisture actually present on materials, either on the surface (typically surface corrosion) or in their interior (typically shrinking and swelling, hydrolysis, deterioration, mineral transitions, mould development, insect activity).

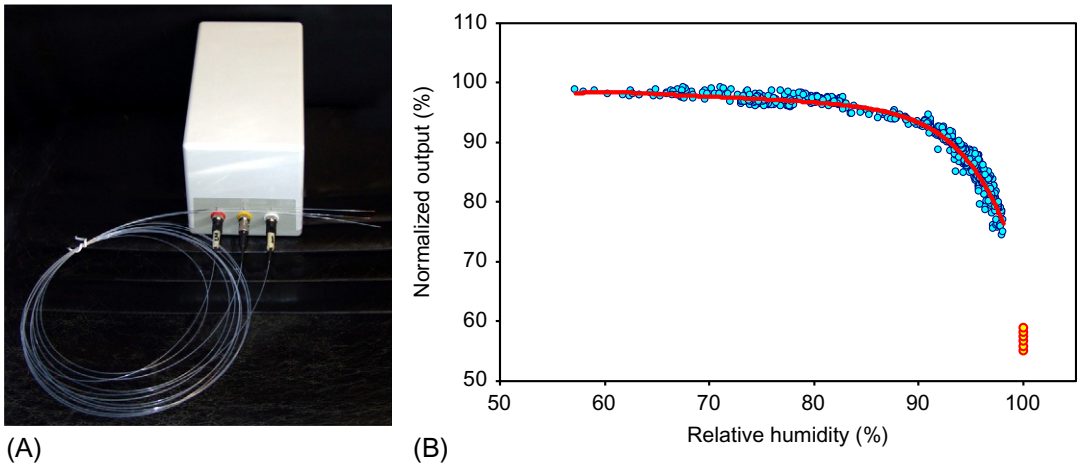

FIG. 19.4 (A) Three fibre-optic sensors connected with the electronic box to process the signal. (B) Normalized output of a fibre-optic sensor, showing a strong relationship with *RH* at high *RH* levels. *Blue dots*: instrument readings versus observed *RH* during a field exposure; *Yellow dots circled red*: readings at condensation; *red line*: 6th-order polynomial interpolation of *blue dots*.

Accurate measurements of the moisture content in materials are crucial for preventive conservation and maintenance of cultural heritage.

Several methods exist to measure moisture content in materials, and they are described in the literature (Carr-Brion, 1986; Milota, 1994; Doebelin, 1990; Dill, 2000; Healy, 2003; Lipták, 2003; Larsen, 2004; Sandrolini and Franzoni, 2006; Kumaran et al., 2006; Beall, 2007; Saïd, 2007; NWFA, 2008; Palaia et al., 2008; Capitani et al., 2009; Weritz et al., 2009; Mitchell, 2010; Mortl et al., 2011; Nilsson, 2018). Several methods are also regulated by national and international standards, e.g. EN 322 (1993), EN 772-10 (1999), EN 13183-1 (2002), EN 13183-2 (2002), EN 13183-3 (2005), EN 1428 (2012), EN-ISO 11461 (2014), EN-ISO 15512 (2014), ISO 11465 (1993), ISO 12570 (2013a), ISO 16979 (2003), ISO 760 (1978), ASTM D4442 (2007), ASTM D2216 (2010).

However, the cited literature and standards are suitable for 'normal'[3] commercial products, in good conditions, that could be called 'regular'. The definition of 'regular' may be applied to a material when the main physical properties (e.g. thermal and electric conductivity, density, specific heat and thickness), the chemical composition, and the molecular structure are known and homogeneous within the whole sample and are the same in all samples. In addition, the material has not been weathered, corroded, rusted, rotted by moulds, nor have woodworms excavated tunnels in them. This situation is fundamentally different from cultural heritage materials because these have variable density, sometimes unknown composition or transformations resulting from past treatments; may have suffered weathering, deterioration, or degradation. In addition, it is ethically forbidden taking samples and for this reason not all methodologies are convenient for cultural heritage, some of them being invasive or destructive. The difficult situation of cultural heritage has rarely been dealt with in the literature (Camuffo and Bertolin, 2012; Agliata et al., 2018; Camuffo, 2018; Franzoni, 2018), and one European Standard, i.e. EN 16682 (2017),[4] has been produced to assist cultural heritage professionals engaged with this difficult task. In the following sections, the most popular methodologies will be commented on to discuss their application in the field of cultural heritage.

19.2.2 Absolute and Relative Methods

By definition, '*absolute methods*' are characterized by the fact that readings can be expressed in terms of the International System of units (SI). Dealing with moisture content, the typical unit is the gram, because the method is based on a series of determinations, e.g. the mass of a moist specimen (m_M), the mass after it has been dried (m_O), the mass of the moisture that has been extracted (m_w), all these readings being expressed in grams. The basic formula to determine the *moisture content* (*MC*) is

$$MC = \frac{m_w}{m_O} \times 100 = \frac{m_M - m_O}{m_O} \times 100\,(\%) \tag{19.1}$$

i.e. the moisture content is the amount of water extracted from the specimen and expressed as a percentage (%) of the dry mass of the specimen, i.e. *MC* on dry basis. It is also possible to express the extracted moisture as a percentage of the moist specimen, i.e. MC_W on wet basis

$$MC_W = \frac{m_w}{m_M} \times 100 = \frac{m_M - m_O}{m_M} \times 100\,(\%) \tag{19.2}$$

The traditional use of gravimetry is to produce results on a dry basis, while in analytical chemistry it is to produce results on a wet basis. The European Standards EN 16682 recommends the dry basis for all absolute methods to make them homogeneous and to obtain easily comparable data. The following formulae are used to transform determinations from the wet to the dry basis or vice versa, i.e.

$$MC = \left(\frac{MC_W}{100 - MC_W}\right) \times 100\,(\%) \tag{19.3}$$

$$MC_W = \left(\frac{MC}{100 + MC}\right) \times 100\,(\%) \tag{19.4}$$

At the end, when the result is expressed in %, the units formally disappear, but the single determinations in grams have been essential in assessing the final value. In practical terms, a method can be defined 'absolute' when it fulfils any of the previous equations, and this definition is even better, because it avoids the academic struggle that the result is formally expressed in %, not in SI unit.

The individual mass determinations may be made with physical instruments, e.g. a precision balance, or from chemical analysis, e.g. Karl Fischer Titration (KFT), azeotropic distillation, reaction with calcium carbide. It may be useful to remember that the *MC* is the typical result of methods, like gravimetry, where not all water molecules are extracted from the specimen and the weight loss due to VOC released form the specimen may be interpreted for moisture. As opposed, the chemical method KFT, that is specific for water, is not affected by VOC, but might be affected by crystallization water. To avoid misunderstanding, the result of KFT is named '*water content*' (*WC*). The water content can be expressed on the dry and wet basis,

[3] Here and in the following, the adjective 'normal' applied to materials will be used with the traditional meaning of: conforming to the standard or the common type; usual; not abnormal; regular; natural. This adjective will be in opposition to deteriorated cultural heritage materials that have undergone transformations that have severely changed their physical characteristics.

[4] See Chapter 15.

WC and WC_W, respectively, and the formulae are the same as for MC and MC_W.

The absolute methods require sampling specimens from the monument, which is not always possible for ethical reasons. Generally, sampling is made exceptionally, when it is strictly necessary, in a part of the monument where it may be acceptable, and under the supervision of the competent authority. This makes impossible to obtain a continuous record of MC, or a trend over time at selected time intervals, because of the necessity of removing samples from the object for laboratory testing. In addition, absolute measurements need the transport and preparation of the specimens, followed by laboratory determinations that may require hours or days.

Relative methods generate readings that cannot be directly expressed in terms of the International System of units (SI). Instruments may have readings in SI units, but refer to the value of the physical quantity that is used to determine the moisture content, and is not a direct measure of the moisture content. The output of the instruments may be calibrated with absolute methods and expressed in percent like true MC readings. However, whatever is done, they substantially remain relative methods. The name indicates that the readings can never be expressed in 'absolute' terms, but may be compared between them in order to see which reading is higher and which is lower, relatively to a selected one, i.e. establishing a relative order of signal intensity among readings that substantially are in arbitrary scale units.

On the other hand, relative methods have the advantages that they do not require sampling, are not destructive, and provide an immediate response and this justifies their popular use.

19.2.3 Gravimetric Method

Historically, the gravimetric method has been the first, and the most obvious absolute method to determine the moisture content. The method is specified by several international standards, e.g. EN 322 (1993), EN 13183-1 (2002), EN 772-10 (1999), ISO 11465 (1993), ISO 12570 (2013a), ISO 12571 (2013b), ISO 16979 (2003), EN-ISO 11461 (2014), and EN 16682 (2017). The only instrument it requires is a precision balance to determine the weight of the moist specimen (m_M) after it has been sampled and after it has been dried (m_O). 'Dried' means that the specimen is kept in the drying cell until it has reached a constant value of its mass, as ascertained with repeated weighing at a convenient time distance. The mass of the moisture extracted from the specimen (m_w) is given by the difference:

$$m_w = m_M - m_O \tag{19.5}$$

In masonry, the gravimetric method is unaffected by the presence of salts; in wood, by pest attack, including insect tunnelling. However, despite its apparent simplicity, it encounters a number of difficulties that must be overcome, as follows.

Sampling. For ethical reasons, it is always a problem to take specimens from cultural heritage, and when this is done, a very restricted number of small specimens can be taken from the less aesthetically disturbing areas. This implies that samples may have a limited representation of the real conditions of the object. Care should be taken to avoid moisture loss during sampling.

Handling specimens. After sampling, specimens should be immediately protected to avoid exchanges of moisture with the environment until they are transported to the laboratory and prepared for their evaluation. This means that specimens should be immediately inserted into a plastic or glass container without empty spaces, because the specimen may evaporate or absorb moisture from the air pocket. This risk is especially high with small specimens, because the surface S_S (i.e. the exchanging area) to the volume V_S (i.e. the bulk reservoir) ratio increases very much for cylindrical specimens when either the radius R_S or the height H_S becomes very small, because it tends to disappear from the numerator and increases very much the ratio acting from the denominator, i.e.

$$\frac{S_S}{V_S} = \frac{2\pi R_S(R_S + H_S)}{\pi R_S^2 H_S} = \frac{2\,(R_S + H_S)}{R_S H_S} \tag{19.6}$$

How the surface to volume ratio changes with the height of the specimen, but keeping constant the cross section, is reported in Fig. 19.5. To reduce exchanges with the environment, small ratios are preferable, i.e. large cross-sections and long specimens.

Weighing. Specimens should be weighed with a precision balance to determine their mass both after sampling and after having being dried. During the weighing operation, it is frequent to see that the weight is drifting from the initial value (closest to original value) to a final value derived from equilibrium with the new environment, especially the RH of the air that surrounds the sample in the balance. This requires care to avoid, or to correct, for such moisture exchanges.

Drying specimens. It is possible dry specimens in various ways, as follows.

(i) Drying in a ventilated oven at ambient pressure but above boiling temperature. The traditional system recommended in a number of standards is oven drying, i.e. to keep specimens in a ventilated oven at (103 ± 2) °C until the specimen weight has become stable. This temperature has been selected because it is a bit above the boiling point and may be sufficient to remove almost all the moisture in the specimen. However, the oven dries out, but does not completely dehydrate the specimens. This is not a crucial problem because all specimens are treated

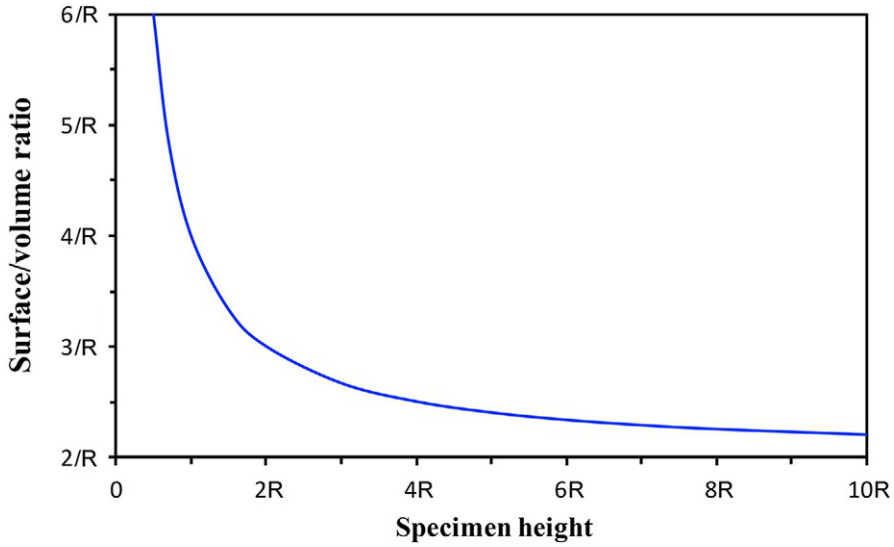

FIG. 19.5 Surface to volume ratio of a cylindrical specimen having height H = 0.5R, 1R, 2R... where R is the specimen radius.

in the same way and, even if they keep a small residual moisture, this is accepted as definition of dried specimen. A more serious problem is that some specimens may contain resins, oil, wax, or other substances that will be released as volatile organic compounds (VOCs) during oven drying, and the loss of mass will be misleadingly interpreted as evaporated moisture and included in m_w. A similar problem occurs with some unstable hydrated minerals that may dehydrate. For unstable materials, ASTM D2216 (2010) recommends lower oven temperature (e.g. 60°C) or even the use of desiccators at room temperature as in item (iv). EN 16682 (2017) offers a wider choice of drying systems, from (i) to (iv), but not alternative oven temperatures that would produce nonhomogeneous readings and therefore not comparable, with other methods and/or materials. This is the most popular drying system.

(ii) Drying at ambient temperature but below the boiling pressure. To avoid (or reduce) the VOCs problem, it may be possible to reach the boiling point of water and force evaporation at ambient temperature, by lowering the pressure. This goal may be reached with a vacuum pump. The boiling point of water is when its saturation pressure equals the ambient pressure, e.g. at 20°C the boiling pressure is 23.5 hPa, as it can be computed with the Magnus and Tetens equation.[5] As this extraction occurs at moderate vacuum, and the moisture is continually removed from the volume, this method is faster and more efficient than boiling at normal pressure and in particular it does not affect the substances that are thermolabile at higher temperatures. This is an efficient alternative way of boiling water and drying specimens.

(iii) Favouring evaporation at ambient temperature and pressure, in very dry air. Very dry air can be obtained with an air compressor, because the moisture included in the compressed air in the storage tank reaches saturation for the very short intermolecular distance, passes to the liquid state, and is removed from the system. For instance, a 10-bar compressor uptakes 10 m^3 of ambient air and reduces them to 1 m^3 in the storage tank. If before compression, the air included saturated vapour at 6 $g\,m^{-3}$ (i.e. saturation absolute humidity), after the compressed air has returned to the normal pressure, it will include moisture at 0.6 $g\,m^{-3}$ corresponding to $RH = 10\%$. This level of dryness may be sufficient for many purposes. It may be further reduced by cooling the compressed air, or applying an absorbent filter. This further drying may lower the dew point of the compressed air, e.g. from +3°C to −30°C or even −70°C.

(iv) Using a chemical desiccant. Specimens are kept inside a desiccant cell, i.e. a sealable glass enclosure typical of chemical laboratories, that contains a strong drying agent, e.g. silica gel (SiO_2), phosphorus pentoxide (P_4O_{10}), barium monoxide (BaO), magnesium perchlorate ($Mg(ClO_4)_2$), anhydrous calcium chloride ($CaCl_2$), activated alumina (Al_2O_3), aluminium silicate ($AlNa1_2SiO_5$). After the specimen has reached equilibrium with any of these dryers, it should be put in equilibrium with lithium chloride (LiCl) that reaches equilibrium at $RH = 11.30\%$, this being similar to the compressed air without drying filter. This is the cheapest (and less efficient) way to dry specimens.

In conclusion, once specimens have been dried, some moisture still remains inside. The gravimetric method is based on dried, but not fully dehydrated, specimens

[5] Magnus and Tetens equation, Chapter 3, Eq. (3.1).

and, in some cases, there is a weight loss due to VOCs. Briefly, in the real world the result of a gravimetric analysis is

$$MC = \frac{\text{total loss}}{\text{dried specimen}} \times 100 = \frac{\text{extracted moisture} + \text{VOCs}}{(\text{uncompletely})\ \text{dry specimen}} \times 100\,(\%) \quad (19.7)$$

that is (slightly) different from the initial theoretical definition aimed to establish the proportion by weight between the moisture held in a material, and the dry mass of it.

19.2.4 Thermogravimetric Method

Thermogravimetry (TGA) is a dynamic combination of the gravimetric analysis with oven drying. It records over time both the weight of the specimen and the temperature of a small oven until the specimen reaches a constant weight, i.e. from m_M to m_O. The continuous record shows anomalies in water release and the temperature at which the anomalies had occurred (e.g. release of crystallization water or condensation reactions), or the onset of degradation mechanisms with emission of gases (e.g. emission of CO_2, NH_3). The TGA apparatus can be connected with a computer for special data processing and analysis. TGA is more sophisticated than gravimetry because provides elements to interpret the final reading, is faster, and requires smaller specimens.

19.2.5 Karl Fischer Titration

Karl Fischer (1935) invented an absolute, precise analytical method to determine the water content in material samples. The method is specified in a number of international standards, e.g. ISO 760 (1978), EN-ISO 15512 (2014), and EN 16682 (2017). Of course, problems and cautions concerning sampling, handling of specimens, and weighing discussed for gravimetry apply here too. Basically, the mass of the moist specimen (m_M) is first determined with a precision balance. Then the specimen is finely crushed and dissolved (or dispersed) in a solvent and then analysed by chemical titration. *Titration* means to ascertain the amount of a constituent in a solution by measuring the volume of a known concentration of reagent required to complete a reaction with it, typically using an indicator. In this case, the titration determines the amount of water (m_w) that was included in the dissolved specimen.

The Karl Fischer titration (KFT) is a specific method for reacting with the water molecules (Wieland and Fisher, 1987; Scholz, 2012). In masonry, KFT is unaffected by the presence of salts; in wood, by pest attack, including insect tunnelling. Different from the gravimetric method, KFT it is not affected by oil, wax, or other substances that may release VOCs. Another difference is that the various forms of drying used in gravimetry may be unable to extract all water molecules from the specimen, while KFT detects all water molecules, irrespective of their role. On the other hand, KFT has a flaw if the specimen includes minerals with crystallization water that is released during the titration, because the method will interpret it as water content. Briefly, the result of KFT may differ from the result obtained using the gravimetric method, and to avoid misunderstanding, different names are used, i.e. 'moisture content' (*MC*) for the gravimetric method and 'water content' (*WC*) for KFT. Briefly, the result of a KFT is

$$WC = \frac{\text{extracted water}}{\text{dry specimen}} \times 100 = \frac{\text{extracted moisture} + \text{crystallization water}}{\text{completely dehydrated specimen}} \times 100\,(\%) \quad (19.8)$$

Both gravimetry and KFT are absolute and accurate methods, and both are considered primary methods and recommended for calibration of other methods by EN 16682 (2017). However, the result of the analyses made with the two methods may differ between them. The comparison between the *WC* and the *MC* of a moist specimen may be misleading and variable with the type of inclusion, as specified in Table 19.1. Which of the two methods is the best differs from case to case, and more specifically from the type of inclusions in the specimen.

Another practical difference with gravimetry is that KFT is quicker (e.g. 1 hour or less) because it avoids the loss of time for drying (e.g. 1 day).

Titration can be performed in one of the two basic modes: Volumetric or Coulometric mode, as follows.

TABLE 19.1 Comparison between WC and MC for the different types of inclusions in specimens that may affect readings, i.e. crystallization water and organic compounds releasing VOCs

Type of inclusion	Comparison	Explanation
None (i.e. neither VOC, nor crystallization water)	$WC > MC$	Gravimetry: incomplete drying
Organic compounds with large VOCs release	$WC < MC$	Gravimetry interprets VOCs as moisture
Organic compounds with modest VOCs release	$WC < MC$ $WC > MC$	Greater or less, depends on the balance between disturbing factors
Crystallization water (no VOCs release)	$WC \gg MC$	Crystallization water detected by KFT but not by gravimetry
Some crystallization water and VOCs release	$WC < MC$ $WC > MC$	Greater or less, depends on the balance between disturbing factors

Volumetric mode (V-KFT) based on a water volume determination. Titration is made with an iodine solution. More precisely, the iodine contained in Karl Kischer (KF) reagents reacts quantitatively and selectively with the water included in the solution where the specimen has been dissolved. The iodine of the KF reagent reacts with water following the stoichiometric reaction:

$$2H_2O + SO_2 + I_2 \rightarrow H_2SO_4 + 2HI$$

The appearance of a brown colour, typical of free iodine, means that the reaction has been completed. This mode determines the volume of water (hence the name volumetric) extracted from the reaction with the dissolved specimen, considering that the water density is close to $1\,g\,cm^{-3}$ (i.e. $0.9982\,g\,cm^{-3}$) and the mass expressed in g equals its volume in cm^3.

The mass of water (m_w) extracted from the specimen is obtained as product of the titration volume V_{Titre} (cm^3) multiplied by the titre concentration[6] T_{Conc} (grams of water per cm^{-3}). Dividing the extracted water m_w (g) by the mass of the moist specimen m_M (g) and multiplying by 100 one obtains the Water Content on wet basis, i.e. WC_W (%) as follows:

$$WC_W(\%) = \frac{V_{Titre} \times T_{Conc}}{m_M} \times 100 \qquad (19.9)$$

It is possible to calculate the Water Content on dry basis, i.e. *WC* (%) as discussed before with *MC* and MC_W i.e. Eq. (19.3).

V-KFT is a robust detection system.

Coulometric mode (C-KFT) based on an electric charge determination. The mass of the moist specimen is determined with a precision balance and its water content is measured by titration with electrolysis. More precisely, the method is based on the electrochemical production of iodine at the anode, and the iodine will react with an equivalent number of water molecules that are in the solution where the specimen has been dissolved. The amount of iodine generated that reacts with an equal number of water molecules is determined from the quantity of electrical charge employed for the electrolysis, that equals the product of the current intensity in Ampère by the operation time in seconds. The unit to measure electric charges is Coulomb ($1\,C = 1\,A \times 1\,s$); hence, the name *Coulometric mode.*

The mass of water (m_w) extracted from the specimen is obtained with the basic formula:

$$m_w(g) = \frac{M(H_2O) \times NEC}{z \times F} \times 100 \qquad (19.10)$$

where $M(H_2O) = 18.015\,g\,mol^{-1}$ is the molar mass of water, *NEC* the number of electric charges ($A \times s$), $z = 2$ is the number of electrons involved in the reaction, and F the Faraday constant that represents the magnitude of electric charge per mole of electrons ($1\ F = 96485$ coulomb mol^{-1}).

C-KFT is more sensitive than V-KFT (usually a factor of 10), and for this reason it requires smaller specimens.

Oven-vaporization KF titration (OV-KFT). In certain cases, it is impossible to perform KFT at ambient temperatures because the material releases water molecules too slowly. However, the process is speeded up at higher temperatures, with an oven to facilitate the release of water vapour from the specimen. The vaporized moisture is then analysed by C-KFT that is more sensitive, but the use of V-KFT is also possible.

Oven-vapourization KFT is similar to thermogravimetric analysis (TGA) but with a continuous record of the vapour released monitored versus oven temperature. The main advantage of OV-KFT is that it can be automated and run several specimens in a row. It is affected, however, by larger instrument drift in comparison with the normal KFT.

19.2.6 Azeotropic Distillation

The azeotropic distillation is an absolute method based on the direct determinations of the initial mass of the moist test specimen and the mass of the water collected after distillation of the specimen. The method is specified in EN 1428 (2012) and EN 16682 (2017). Of course, problems and cautions concerning sampling, handling of specimens, and weighing discussed for gravimetry apply here too. The extraction of water is made in vapour form via azeotropic distillation with a volatile solvent, immiscible with water. The water vapour is then condensed and separated in a reflux trap, recovered and measured as a volume in a graduated tube. The volume of condensed water in cm^3 numerically equals the mass in grams. The mass of the dry specimen, or the value of moisture content on the dry basis, is computed as specified for the gravimetric method. This method is specific for organic materials and can be applied when wood contains volatile oils not soluble in water. In case the sample contains high amounts of water-soluble VOCs, the result is affected by error, similar to the earlier discussion concerning the moisture content in the gravimetric method. If possible, a correction should be used to remove the contribution of VOCs (Camuffo, 2018).

19.2.7 Calcium Carbide

The calcium carbide test (also known as the CM test or calcium carbide bomb) is an absolute method that may be

[6] *Titre*: The concentration of a solution as determined by titration. The minimum volume of a solution needed to reach the end point in a titration (source: Oxford Living Dictionaries, https://en.oxforddictionaries.com/).

applied to masonry, stone, or soil and can be performed on the site with portable instruments, as specified in EN 16682 (2017). The method is based on the direct determination by weight of the initial mass of the moist sample m_M; the mass of the water m_w in the sample will be determined with a chemical reaction with calcium carbide (CaC_2) that will produce acetylene gas (C_2H_2) as follows:

$$CaC_2 + 2H_2O \rightarrow C_2H_2 + Ca(OH)_2 \quad (19.11)$$

Moist samples are crushed to a fine powder and inserted in a sealed vessel. It is important to crush the sample in a very short time to avoid the crushed grains exchanging moisture with the external environment. Then the reagent calcium carbide is also added and mixed with the crushed sample. The moisture present in the vessel will react and the gas pressure produced by this reaction is measured with a pressure gauge in Pa. The pressure is proportional to the moisture present in the sample, and with some tables it may be related to *MC*, expressed as a percentage of moist sample (Zazueta and Xin, 1994; Poděbradská et al., 2000).

Pressure readings can be transformed into percent dry mode. However, the methodology is not accurate, requires a number of large samples and is destructive. It may be recommended for measuring moisture content in soils. Measurements should be performed by qualified personnel because the method involves a potentially dangerous chemical reaction, with explosive, toxic, and flammable substances.

19.2.8 The Use of Proxies and the Equilibrium *RH*

Literally, a *proxy* is 'an authority to represent or act for another'.[7] In climatology, *proxy data* are observations based on certain physical phenomena that may represent some atmospheric variables, e.g. tree ring width may be representative of the temperature in the preinstrumental period, and a tree is used as a proxy sensor, instead of a thermometer. A *proxy sensor* is a sensor that is used to indirectly measure an unobservable quantity of interest. Although a proxy is unable to provide a direct measure of the desired quantity, it is strongly related to it and may represent, or even substitute, the desired variable.

In this section two types of proxies will be considered, as specified in EN 16682 (2017). The former is an active proxy, i.e. a capacitive or resistive sensor that will measure *RH* and from this it is possible to extract the *MC*. This is a relative determination. The latter is a passive proxy, i.e. an artificial specimen specifically built and used as it were a real sample taken from a wall. This complies with the definition 'proxy: a material or a specimen that is a substitute or a replacement for something else, under the assumption of identical behaviour of the material under investigation' (source: EN 16682, 2017). This constitutes an absolute determination, but made on a proxy.

For both of them, the rationale is based on the assumption that a closed cavity inside the material, e.g. a wall, will reach an *RH* level in equilibrium with the *MC* (Healy, 2003). The equilibrium will be determined by the sorption characteristics of the material and the interaction with the environment. The transfer function connecting *MC* with *RH*, and vice versa, is affected by a small uncertainty bar due to the moisture absorption/desorption hysteresis. However, once the selected system has been calibrated, it is possible to simply measure *RH* inside a closed cavity, or the *MC* of a proxy sample inserted into the cavity.

A particular case, but frequent in the coastal areas, is found in masonry that is impregnated with soluble salts, especially NaCl from marine water. When masonry is dry, the presence of salts is irrelevant until the *RH* threshold for salt deliquescence is reached. After this threshold is exceeded, e.g. 76 % *RH* for NaCl, the deliquescent salt starts to form a supersaturated solution and keeps the equilibrium *RH* constant. However, if the solution receives further water and the NaCl concentration falls below the saturation level, it becomes unable to buffer the *RH* in the air pocket, and the *RH* will start to rise again. The situation may be complicated when the masonry includes different soluble salts, and the individual quantities change over time. This bias is out of control, and makes uncertain the interpretation of readings.

The air pocket cavity may be obtained by drilling a hole into a wall. The hole constitutes an air pocket internal to the wall except for the opening that should be closed to avoid exchanges with the exterior. If it is not possible to drill, a cavity can be created with a small box in contact with the surface, but externally to it. The box has five insulated sides and the borders of the open side sealed to the wall surface. Even if this air pocket is external to the wall, its *RH* and temperature are governed by the wall capacity. However, the presence of the box may alter the free exchange of heat and moisture between the air and the wall, in comparison with the free wall surface, especially in the presence of thermal radiation. The external sealed chamber is less representative of the wall than a drilled hole, but constitutes a reasonable solution when drilling cannot be considered.

A *RH* record taken inside the drilled hole, or the external cavity, with a thin film sensor, either capacitive or resistive, is a virtual proxy. The *RH* sensor is enclosed

[7] Source: Oxford Advanced Learner's Dictionary of Current English, Oxford University Press (1984).

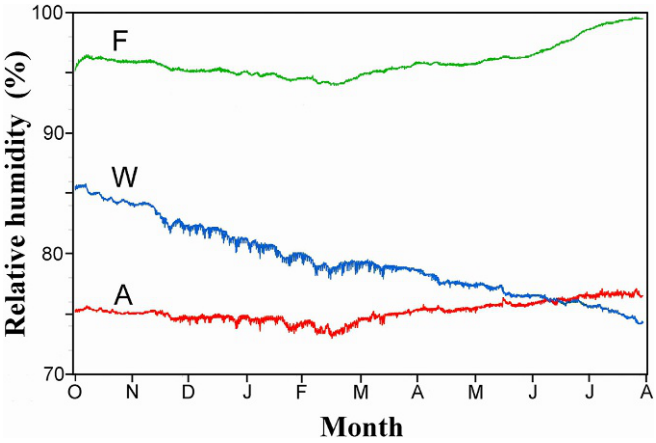

FIG. 19.6 Relative humidity measured inside drilled cavities in the facade (F), an outer wall (W) on the side of the nave, and the apse (A) of a church (i.e. St. Andrew, Chioggia, Italy) flooded with marine water. Period: October 2011 to August 2012.

in the air pocket and can continually record how *RH* changes over time from which the *MC* can be calculated. This record may be displayed in real time and is especially useful to control the effectiveness of interventions made to stop rising damp. An example is found in the case of the Church of St. Andrew, Chioggia, near Venice, Italy, that was flooded by a storm surge in the Adriatic Sea (Fig. 19.6), where three walls were selected for their different behaviour. The records show that the apse was not fully soaked of water, probably because it is an internal wall, and was partially protected by the sacristy. The plaster was removed to favour evaporation. However, being an internal wall, the ventilation and the evaporation are reduced, and the marine salt of which it was (and is) impregnated remains around the deliquescence level, i.e. 76% *RH*, keeping a saturated solution of NaCl in the pores. The outer wall on the side of the nave had also the internal and external plaster removed to favour ventilation and evaporation, and the remedy was effective, especially for the evaporation from the external side. In the record, the wall was rapidly drying and had dropped below the NaCl deliquescence threshold. In opposition, the facade that is finished with stone slabs does not favour evaporation and remains damp.

A tangible proxy is made with a passive sensor that may substitute real samples. It is constituted by a hydrophilic specimen that simulates the behaviour of a brick wall, e.g. a small cylinder of chalk or terracotta. This proxy avoids extracting specimens from the wall. In addition, it allows to repeat sampling at regular time intervals (e.g. one or a few months), and always in the same sampling point, to observe (drying) trends. The proxy specimen is inserted into the drilled hole and left inside for the selected time. As it is as hydrophilic as real bricks, it reaches the equilibrium with the cavity and assumes the same moisture content of the wall. It is necessary to drill a hole, insert the proxy specimen, and close the opening. After the selected time the cavity is opened, the proxy specimen is extracted, and its *MC* is determined, e.g. by gravimetry. Another proxy specimen can be inserted into the cavity, to repeat the analysis over time, following a monitoring programme.

Free water sensor. An active proxy requires a datalogger to keep the record. The passive proxy described in the previous section requires a subsequent laboratory analysis to determine the *MC*. A third possibility was devised, i.e. a passive sensor able to directly record the highest *RH* level reached during the exposure period in a drilled cavity, or an external box, without need of other instruments.

Inside masonry, or a porous stone, the existing moisture, or the solution that will form in the presence of soluble salts, exerts a partial vapour pressure that is a particular fraction of the maximum level determined, for each temperature, by the saturation pressure of pure water. This pressure, after it has been normalized in terms of pure water saturation pressure and is expressed in percentage, is commonly expressed in terms of '*free water*' or '*water activity*'. This is similar to the definition of *RH* but making reference to the situation in the micro-air pockets inside the pores of the material, while the saturation pressure of *RH* makes reference to a plane water surface (i.e. no meniscus, or a meniscus with an infinite curvature radius). This variable is representative of the water content exchange with the surrounding environment until the equilibrium will be reached. In a larger air pocket of an artificial cavity obtained by drilling inside a material, or in an insulated box sealed to the material surface, the free water pressure reaches equilibrium with the measurable *RH*, defining the percentage of existing free water.

An advanced passive sensor, i.e. the 'free-water sensor' (FWS), has been developed[8] under the EU-funded Climate for Culture Project. This sensor follows a dynamic equilibrium with the free water and undergoes irreversible transformations at some selected *RH* levels. The sensor is composed of a series of soluble salts that have affinity for moisture and will absorb some water from the air when their deliquescence thresholds are reached.

The sensor is shaped as a small stick, as shown in Fig. 19.7. The envelope has a transparent band on the upper side and is permeable to water vapour on the bottom in order to reach equilibrium with the free water

[8] In cooperation between CNR-ISAC (scientific leader: the Author) and Salvatore Maugeri Foundation IRCC, Padua (scientific leader: Dr Claudio Cocheo).

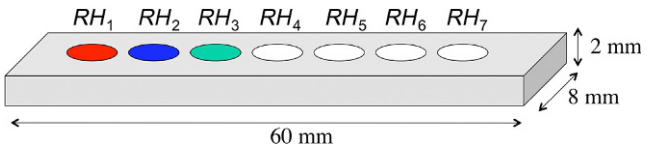

FIG. 19.7 Scheme of a free-water sensor. In this example, the top side contains seven passive sensors, and the highest *RH* level reached over the whole sampling period has exceeded the third level, but not the fourth one.

inside the masonry. It is divided into a number of specific sectors, all of them covered with a white paper disk. Each sector contains a tablet composed of dyes and salts that will become deliquescent at some selected *RH* levels (i.e. RH_1, RH_2, RH_3,…). When one of the above deliquescence thresholds has been reached, or exceeded, the absorbed moisture dissolves the salt, the solution activates a dye and the white paper disk becomes and remains permanently coloured indicating that this specific *RH* level has been reached. Each disk and each colour is related to a specific *RH* level that can be read on the front side. The selected levels can be changed on request, e.g. multipurpose with broad intervals over the whole *RH* range or specific for dampness or dryness with higher resolution in the preferred span.

The FWS is supplied in a sealed, dry bag and becomes active once it has been removed from the dry bag. The FWS is a disposable irreversible sensor that provides useful information about the highest humidity level reached over the whole sampling period, e.g. a week, a month, or a season. It is cheap in order to be single use, or utilized in arrays for multiple sampling locations. Specific advantages are that the sensors are miniaturized, can stay in unmanned areas without power supply, and are useful for preliminary field investigations to assess whether a building or an archaeological remain is at risk of moulds, has seasonal cycles in dampness, or is affected by gradients in moisture that may be an index of capillary rise, water percolation, etc. The freezing points of the selected saturated solutions are very low, e.g. from −20°C to −60°C.

Finally, the FWS is built with materials permeable to vapour but not to the liquid phase. As a consequence, it can be used inside books, placed between leaves, or can stay in contact with other vulnerable surfaces without staining.

19.2.9 Conductive/Resistive Instruments

Conductive instruments (also called *resistive*) measure the electric current passing across two contact electrodes (representative of the *MC* on the surface) or two nail pins implanted in the subsurface layer, generally from 1 mm to 10 cm. The method is specified in EN 13183-2 (2002) and EN 16682 (2017). In 'normal' materials, electrical conductivity varies with the *MC* and its gradients, but the accuracy decreases at elevated *MC* (Carll and Ten Wolde, 1996; Wilson, 1999; Dai and Ahmet, 2001; Goodhew et al., 2004; Brischke et al., 2008; Mitchell, 2010).

This is a relative method and the output is in arbitrary units. The instrument output is affected by the type, density, and temperature of the material. Instruments generally have a temperature sensor. However, only for homogeneous materials with standard physical properties can an automatic correction be made. Some producers calibrate the resistance output of their instruments in percent (%) unit by comparison with the gravimetric method. This scale should be, however, corrected for the specific material, or wooden species, and operating temperature. The main advantage is that readings are provided in real time and do not require sampling, i.e. they are nondestructive, or microdestructive when pins are inserted into the material.

Wood is highly resistive to the passage of electric currents (Fig. 19.8), and the resistivity decreases with increasing bound water content. At the fibre saturation point (*FSP*), the mechanism changes and the conductivity is favoured very much by an increasing presence of free water. Instruments are only tuned for bound water conductivity and cannot be used in the presence of free water. In addition, wood resistivity decreases at increasing water temperature. EN 16682 (2017) specifies that the method should be used for normal wood, under normal physical conditions. The method cannot be applied when wood has been attacked by pests (e.g. wood-boring insects, moulds) or has been previously treated with

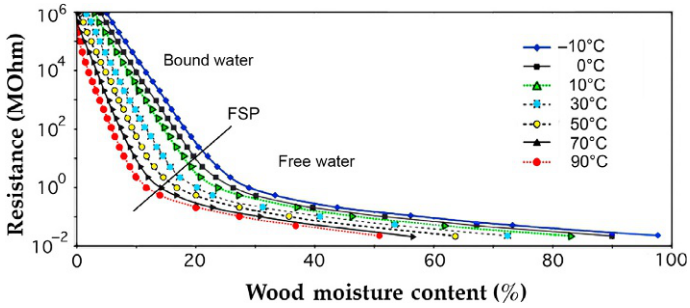

FIG. 19.8 Electric resistance of wood versus moisture content. Resistance changes regularly and decreases in the presence of bound water. After the fibre saturation point (*FSP*), the mechanism undergoes a sudden change for the increasing presence of free water. *Modified from Trotec T2000, by kind permission of Trotec Gmbh, see Credits.*

substances (e.g. oil, wax, preservatives) that alter the surface or subsurface conductivity, increasing the electrical resistance.

In stones and masonry, conductance increases with *MC* and the presence of soluble salt crystals. Readings are severely affected by efflorescence and/or subfloresce nce or the presence of soluble salts for water transport due to percolation or capillary rise. Conductivity dramatically changes above or below the threshold for deliquescence of soluble salts. The nature and concentration of hygroscopic salts changes for several reasons, responding not only to external air pollution (mainly NO_x) but also to soil pollution and underground waters. The British Standard BS 5250 (2011) counsels about the problem of soluble salts and recommends that the method is not to be used for masonry. EN 16682 (2017) specifies that electrolytes in masonry do affect readings. For a correct interpretation of data, EN 16682 (2017) recommends that the operators specify in the test report: instrument readings, air temperature; surface temperature of the material; relative humidity of the air (all at the instant of the reading and measured following EN 15758, 2010, and EN 16242, 2012). In the case of masonry, anions and cations present in the material should be determined with ion chromatography (following EN-ISO 14911, 1999 and EN-ISO 10304-1, 2009) and specified in the test report. The operator may then evaluate the reliability of the measurement, or if another method should be chosen (Camuffo and Bertolin, 2012; Camuffo, 2018).

19.2.10 Capacitive/Dielectric Instruments

Capacitive instruments (also called *dielectric*) measure the change in capacity generated by the presence of water (and other polar molecules or radicals) found at short distance (e.g. a few centimetres) from the electrodes, i.e. in the subsurface layer. The method is based on the physical principle that the dielectric response of materials increases in proportion to the moisture content. In fact, dry materials, including wood, generally have a low relative permittivity (also called dielectric constant) ε, included in the range $2 < \varepsilon < 8$. As opposed, the relative permittivity of water is much higher, i.e. $\varepsilon = 80$, and the number of water molecules that is inside the material (i.e. the moisture content) determines the bulk effect. The method is specified in EN 13183-3 (2005) and EN 16682 (2017). Readings are affected by material type, density, and temperature. Instrument calibration may be made but only for specific, normal materials (Milota, 1994; Wilson, 1999; Titta and Olkkonen, 2002; Shimamura et al., 2004; Sundara-Rajan et al., 2004; Mitchell, 2010; Larsen, 2012). For this, and the next methods, the material under investigation should not include metals or traces of past metal coatings that will cause strong interferences with the electromagnetic signal.

The instrument responds to the surface and subsurface moisture and is sensitive to the distance at which polar molecules are found, e.g. in the presence of moisture gradients. The output is not linear with *MC* and the accuracy decreases at high *MC*.

In the traditional design, both electrodes lie on the same plane to put the sensor in contact with the object. Another popular approach uses a small spherical electrode (the other electrode is virtual, at infinity) to ensure better contact with nonplanar surfaces. Often, electrodes are fed with high-frequency alternating voltage and emit a high-frequency electromagnetic field similar to microwave (see later), forming a hybrid system.

Some instruments are tuned for wood, and they can measure bound water below the *FSP*. The output depends on the wood density, e.g. wooden species, and each species requires its specific calibration or correction factor. However, calibration is possible only for commercial timber with 'normal' characteristics.

As the output is affected by local density changes, the average of several readings taken at different points is in general preferable. A knot or a resin inclusion might be interpreted as a local peak in *MC*, and may be recognized from its odd value. As opposed, mould rotting or pest attack decrease the wood density and the signal may be misinterpreted for very dry wood. Therefore, standards advise against the use of this method when wood is aged, or is affected by woodworm or mould rotting.

The output is reduced in proportion to the loss of material (% by mass) or the volume of cavities (% by volume) that fall within the electromagnetic field emitted by the sensor, with a linear relationship (Fig. 19.9). Because of this peculiarity, the method can be usefully utilized to map subsurface woodworm tunnelling (Camuffo and Bertolin, 2012). In this example of an inlaid wooden panel

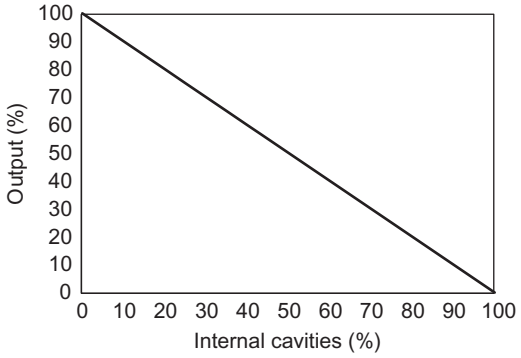

FIG. 19.9 In the presence of internal cavities, the output of capacitive sensors is reduced in proportion to the loss of material (% by mass) or the volume of cavities (% by volume) that fall within the electromagnetic field emitted by the sensor.

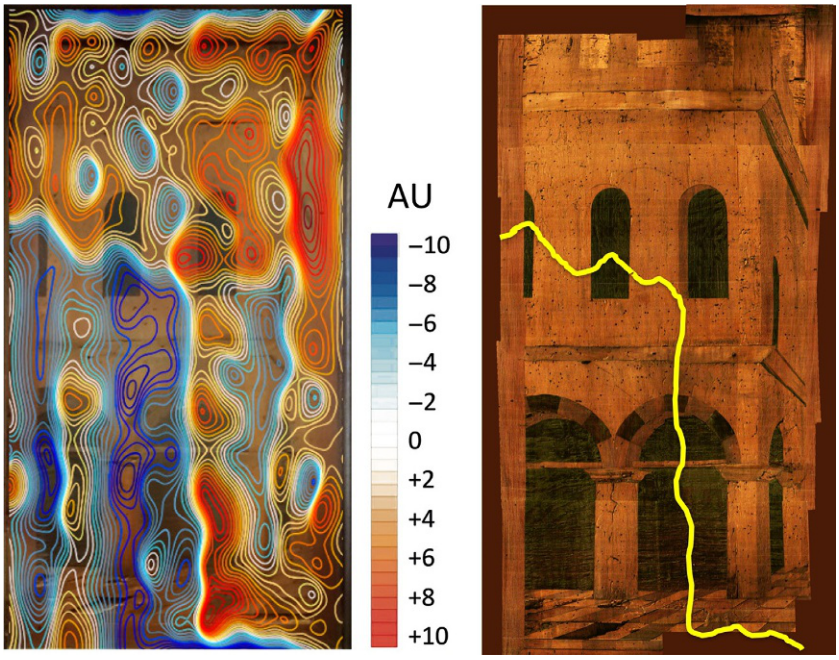

FIG. 19.10 Capacitive instrument utilized to map subsurface worm tunnelling in the inlaid wooden panel of the Old Choir of S. Giustina, Padua. Scale in arbitrary unit (AU). The zero level is the average value; *red areas* have higher density, i.e. less tunnelling, and *blue* lower density, i.e. more tunnelling. The lower left quarter *(highlighted yellow)* has been more severely attacked by woodworms. Field survey with Federica Allegretti, Aude Andreoletti, Emanuele Facchi, and Serena Mazza, SSBAP Polytechnic of Milano.

of the Old Choir (dated 1470) of S. Giustina, Padua (Fig. 19.10), readings were taken on a regular structural mesh with a capacitive sensor with spherical head, 1 cm diameter. Readings (in arbitrary unit) were plotted on a *XY* plane, establishing zero level the average value and pointing out the areas with higher signal, corresponding to higher density, i.e. less tunnelling, and blue the areas with lower density, i.e. more tunnelling. The lower left quarter has been more severely attacked by woodworms and requires a more intensive treatment against pests.

In masonry, for a wide range of frequencies, the capacitance is almost independent of the presence of soluble salts as long as they are below the deliquescence threshold. As opposed, a thin film of water formed by condensation, or adsorbed by soluble salts at deliquescence level, will behave as a mirror of the electromagnetic field and readings go out of scale. In order to ascertain the potential presence of electrolytes, the operator should perform the additional analysis of anions and cations, determined with ion chromatography, as commented for the electrical resistance method.

In masonry, the methodology is also sensitive to changes in density, presence of cavities, internal discontinuities, or metals. If a plaster, or a fresco, is detached from the wall, less H_2O molecules are encountered and the output might decrease as for a drier layer. However, if the internal surface is reflecting the signal, the output will be increased as for a damp layer. In practice, the interpretation might be difficult or even misleading, especially in the case of beam reflections for the presence of internal discontinuities.

19.2.11 Microwave Instruments

An antenna assembly radiates into the material an alternating electromagnetic field in the order of gigahertz, i.e. microwaves. When the microwave beam encounters polar molecules (e.g. H_2O and, to a lesser extent, cellulose chain or other molecules with electric charges), it interacts with them, loses energy thus decreasing in power intensity, and has a phase shift (King and Basuel, 1993; Schajer and Orhan, 2005, 2006; Camuffo and Bertolin, 2012). This method, and the next ones, have been commented in EN 16682 (2017) in the informative section. They have not been normalized for the uncertainties, or the operational difficulties, that may affect them, and their use should be limited to highly skilled researchers.

The intensity $I(x)$ of the microwave beam passing through regular matter is reduced with increasing travelling depth x, in a first approximation following an exponential law, i.e.

$$I(x) = I(0)\,\exp\left(-b_{ext}\,x\right) \tag{19.12}$$

where $I(0)$ is the incident intensity when $x = 0$ and $b_{ext} = \alpha + i\beta$ is the attenuation (or extinction) coefficient that determines how the beam intensity decreases, i.e. the fraction of energy removed from the beam per unit depth traversed. With increasing material density and *MC*, the attenuation coefficient also increases. The real part α indicates the attenuation in power at increasing depth x and the imaginary part β is related to the phase shift caused by the reduction in propagation speed through the medium. In real materials, for a number of disturbing factors, it

might happen that b_{ext} is not constant but varies from point to point, and with time too, i.e. $b_{ext} = b_{ext}(x,t)$.

In addition to absorbing or changing phase, polar molecules reflect back a fraction of energy from the incoming beam. As the interaction with the water molecules is stronger than the interaction with the other molecules of the material, the back radiation is related to the *MC* of normal materials, with a specific relationship for each material.

However, in the field of cultural heritage, objects may be complex because of the interactions between microwaves and the material itself (Camuffo and Bertolin, 2012). The penetration depth of microwaves depends on the instrument characteristics, but also on material density and moisture content. If the beam is not fully extinguished within the material, when it reaches the ending surface, it has a back reflection that alters the reading. A material thickness larger than the complete extinction of the beam may be realistic for thick walls, hardly for wooden objects.

If the material surface is not flat and glossy, the probe is not in strict contact with the target and the border of the empty space will cause back reflections and signal beatings, which depend on the distance between the sensor and the target. If the material includes an empty space, e.g. a gap, a cavity, or a fresco detached from the wall, microwaves with wavelength λ will be reflected at the borders of the cavity (Fig. 19.11), forming valleys when the gap width is an odd multiple of $\lambda/4$, and peaks when is an even multiple of $\lambda/4$. If the material is not homogeneous, but has internal discontinuities, e.g. plaster, bricks, mortar, these may reflect back part of the power, causing beating interference, i.e. the interference between the incoming and the reflecting waves. In the real world, with an instrument operating at 2.43 GHz, a gap of one or a few millimetres is hardly visible, but becomes evident when its width ranges from 1 to 5 cm.

19.2.12 Evanescent-Field Dielectrometry

Evanescent-field dielectrometry (EFD) is based on the interference of the water molecule with the electromagnetic radiation (microwave frequency). It operates at microwave frequencies (1–1.5 GHz), and this frequency range can be considered a particular case of microwave. The method focuses on distinguishing the part of the signal due to H_2O from the part due to the bulk material (mortar, plaster, and brick) that are characterized by much lower relative permittivity, i.e. $\varepsilon < 4$ (Olmi et al., 2006). EFD measures *MC* in the range 0%–20%. The signal is composed of a real and an imaginary part. The real part, measured through a resonance frequency shift, depends on *MC*, and it is nearly independent of the salt content.

The presence of soluble salts is detected and approximately quantified by looking at the resonance line width or the quality factor of the resonant probe and the result is a salinity index from 0 to 10. The material should not include metals or traces of past metal coatings, e.g. gilding. The probe is composed by a microstrip cavity loaded by the material under measurement via an open-coaxial head. Both the *MC* and the salinity index of the material in contact with the probe are elaborated in real time by means of a computer. *MC* is obtained by the shift of the resonance frequency from the real part of the signal with respect to that of the probe in air, while salinity index is related to a loaded cavity of the resonance probe (Bini et al., 2009; Riminesi et al., 2016).

19.2.13 Time-Domain Reflectometry

Time-domain reflectometry (TDR) is based on the measurement of the time between transmission and reception of a radio signal. The system consists of a radio frequency transmitter (which emits a short pulse of electromagnetic

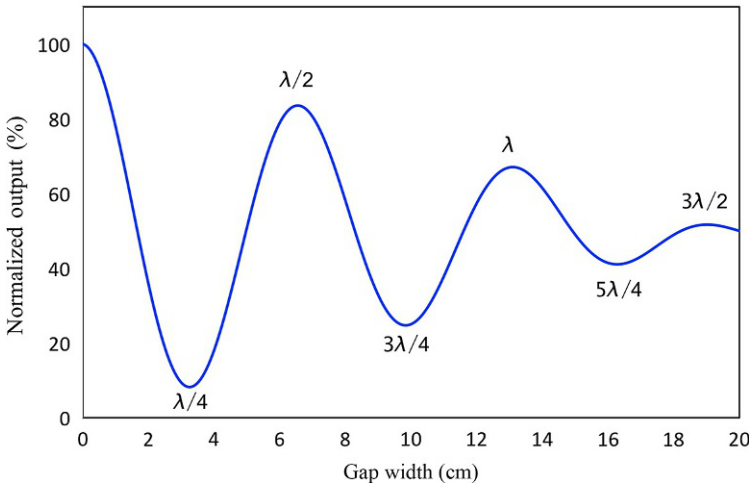

FIG. 19.11 Computer simulation of microwave beating when the material includes a gap. Microwaves will be reflected by the borders of the gap forming valleys when the gap width is an odd multiple of $\lambda/4$, and peaks when it is an even multiple of $\lambda/4$. This simulation has been made for 2.43-GHz microwaves and has been confirmed with laboratory tests (Camuffo and Bertolin, 2012).

energy), a directional antenna, and sensitive radio frequency receiver (Noborio, 2001; Cerny, 2009).

TDR determines the apparent relative permittivity of a material by measuring the travel time of a high-frequency electromagnetic wave through a wave-guide probe inserted into the material. The theory (Cai et al., 2013) is explained as follows. The velocity v of electromagnetic waves in the medium varies with the material, and can be measured as

$$v = \frac{2L}{t} \tag{19.13}$$

where L is the length of the probe and t is the travel time that can be obtained from two subsequent reflections. However, the velocity of an electromagnetic wave in a material is determined by the relative permittivity ε and the relative magnetic susceptibility μ_r of this material:

$$v = \frac{c}{\sqrt{\varepsilon \mu_r}} \tag{19.14}$$

where c is the velocity of the electromagnetic wave in free space. By equalling the two equations:

$$\varepsilon = \left(\frac{ct}{2L}\right)^2 \tag{19.15}$$

The velocity of the electromagnetic wave in the medium is detected from the travel time t and is used to determine the relative permittivity ε of the material that in turn depends on *MC*. A small change in moisture content will have a significant effect on the bulk relative permittivity.

As for the previous methods, the material under investigation should not include metals or traces of past metal coatings.

19.2.14 Nuclear Magnetic Resonance

When a magnetic field pulsed at the radio wave frequency meets hydrogen (H) atoms within a material, the H atoms are excited and subsequently relax back to their normal state, emitting a characteristic signal that is detected with Nuclear Magnetic Resonance (NMR) (Hartley et al., 1994; Capitani et al., 1999; Casieri et al., 2004; Le Feunteun et al., 2011; Proietti et al., 2018). Measurement of the relaxation signal allows the evaluation of the number of H atoms present and an absolute measure of the *MC*. To this aim, an appropriate calibration for each specific material is needed to distinguish the contribution of H from H_2O or other molecules including H (e.g. cellulose). With NMR, the H_2O molecules contained in a material are subjected to static and oscillating magnetic fields at right angles to each other. The molecular mobility of free water is appreciably higher than that of bound water and so NMR can be used to give information about the relative abundance of these two forms of internal water.

From their technological development, three types of NMR instruments can be differentiated. Traditional NMR for laboratory use, where very small samples (a few milligrams, i.e. micro-destructive) are placed in a glass tube for analysis. MRI (magnetic resonance imaging) allows the visual representation of objects or large samples. The object (or sample) size is limited by the cavity size. In the case objects are used, the method is not destructive; in the case of large samples, it is destructive. Portable NMR instruments are used to investigate large objects on-site avoiding sampling. The method can quantitatively reproduce the distribution of moisture inside the material with clear images (Fig. 19.12), and the

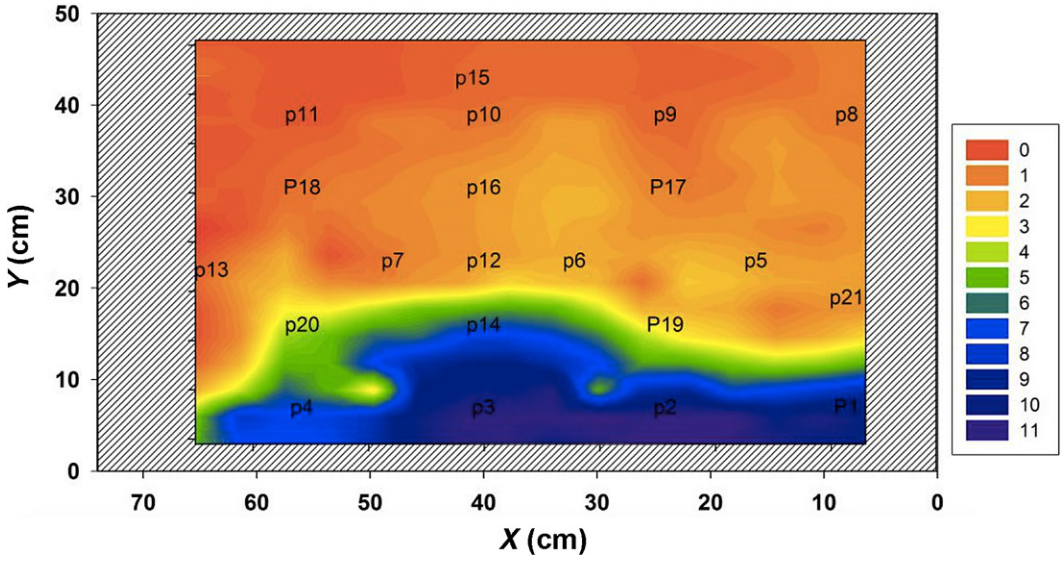

FIG. 19.12 Moisture distribution map in a tuff wall affected by capillary rise detected with nuclear magnetic resonance (NMR). The moisture level is shown as a gradient of colour: *red* corresponds to the lowest water content, while *dark blue* to the highest water content. *From Proietti et al. (2018), CC BY License 4.0.*

dynamics of moisture uptake by repeating the measurement, or by monitoring the effective volume of absorbed water, the distribution of water in porous stone specimens, and the degree of saturation (Di Tullio et al., 2017; Proietti et al., 2018). These investigations are nondestructive.

This method is accurate, can be compared to gravimetry for calibration, and may be applied in the field of cultural heritage either for organic or inorganic materials.

19.2.15 Near-Infrared Spectroscopy

Near-infrared spectroscopy (NIRS) is a fast and nondestructive technique that provides multiconstituent analysis of virtually any matrix. It covers the wavelength range adjacent to the mid-infrared and extends up to the visible region. NIR region of the electromagnetic spectrum has the wavelength range of 780–2526 nm corresponding to the wave number range 12820–3959 cm^{-1}. The most prominent absorption bands occurring in the NIR region are related to overtones and combinations of fundamental vibrations of —CH, —NH, —OH (and —SH) functional groups (Reich, 2005). NIRS application in the field of cultural heritage is appreciated for its nondestructive character, i.e. reflection, and is also used in art conservation and for diagnostic purposes, e.g. chemical identification of pigments (Mansfield et al., 1999). NIRS can also operate on finely crushed samples and this use is invasive/destructive.

NIR reflection is affected by surface roughness and other nonlinear effects caused by pores when they are filled of water, or by the incidence angle. The method can be applied to detect the water content and the water activity in a wide range of materials (Aguilar-Castro et al., 2014).

The method is fast, nondestructive, and noncontact (except when crushed samples are used) and can be employed for the real-time measurement of moisture, either in the laboratory or on site.

NIRS is repeatable, with high signal-to-noise ratio, but needs calibration, e.g. with Karl Fischer titration or gravimetry.

19.2.16 Ultrasonic Pulses

The ultrasonic method is based on the transmission or reflection of ultrasonic pulses. The method consists in measuring the propagation of ultrasonic pulses (typical frequency: 50 kHz) or even sonic pulses (typical frequency: 5 kHz) through a material to detect the time of travel (time of flight) and changes of intensity over a selected distance. The pulse velocity is a function of physical material properties, e.g. elastic modulus and density, including moisture content and temperature. The velocity increases with the moisture content, and especially when water fills pores and capillaries of materials, as in the case of stone, mortar, and cement (Mamillan, 1992; Murphy et al., 1996; Oliveira et al., 2005; Lafhaj et al., 2006; Vun et al., 2006; Calegari et al., 2011; Güneyli et al., 2017). Measurements of speed of ultrasonic pulses can be taken in the transmission, reflection, and surface modes. In the first method, the receiver is in the same straight line as the emitted beam, on the other side of the object; in the last two methods, the receiver is not aligned and is displaced in several positions at regular increasing distances. This allows controlling if the delay in receiving pulses is proportional to the increased distance. Over the pulse path, attenuations, dispersions, and reflections of the signal occur, especially in the presence of discontinuities, defects, and cracks.

19.2.17 Infrared Thermography

Thermograms are thermal images made with a camera sensitive to *IR* radiation. They only provide the temperature of a surface but, if adequately interpreted, this may be a useful tool when it is necessary to localize damp zones. The camera is not directly sensitive to the water content but to temperature changes, i.e. space gradients or time rates that might be locally affected by moisture. Infrared Thermography (IRT) may be used either in *passive mode*, i.e. taking pictures without changing the target surface temperature, or in *active mode*, i.e. with deliberate heating of the target surface to investigate anomalies when heating, or cooling (Rosina and Robison, 2002; Rosina and Spodek, 2003; Palaia et al., 2008; Grinzato et al., 2011). The method may be useful to detect invisible moisture problems, water or air leakage, but is inappropriate for quantitative assessments (Barreira et al., 2016, 2017).

As different physical processes may interact with each other, it may be misleading to consider damp the coldest areas in thermograms. Dampness increases conductivity and may form a thermal bridge. Inside, a damp area is perceived warmer when the outside of the wall is hit by solar radiation or the temperature is higher. Outside, after sunset, when temperature is dropping, damp areas appear warmer due to the higher thermal capacity. EN 16682 (2017) specifies that thermography is a useful diagnostic tool to localize damp zones but cannot be used to measure quantitative values of *MC* and the information may be misleading. If a quantitative *MC* is needed, the investigation should be continued with other methods.

Two examples are shown. The first example is a true diagnosis with rising damp on the brick wall of the Frari Basilica, Venice. The wall is based on a course of white

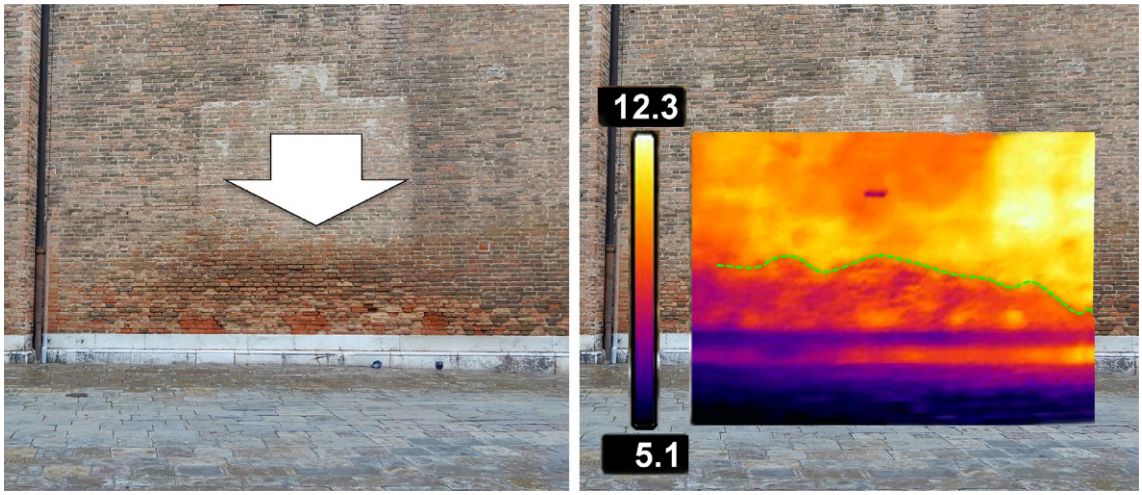

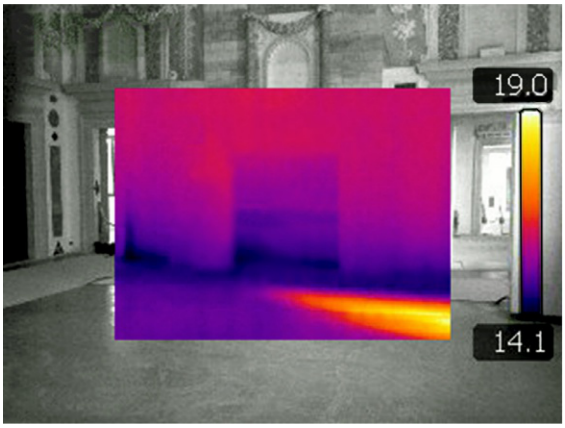

FIG. 19.13 (A) Rising damp that has deteriorated the brick wall above the white Istria stone course of the Frari Basilica, Venice. On the wall, the clear area around the *arrow* is due to a board that has recently been removed. (B) The same view in IR thermogram. Damp bricks are false colour *red*. (C) A room of Grimani Palace, Venice, heated with warm air. The edge between the floor and walls receives less heat and remains colder. This cold band might be misinterpreted for rising damp, having the same appearance.

Istria stone that is waterproof. However, the external pavement has negative slope and collects water against the wall, and the water percolates through the ground. In this position, inside the Basilica, the funeral monument of Canova is leaning against the wall,[9] and has ground inside the basement, favouring the capillary rise. This permanent damp has deteriorated the bricks, as shown in the picture (Fig. 19.13A) and in the *IR* thermogram as cold area. The second example is of false diagnosis. This room of Grimani Palace, Venice, is heated with warm air, the edge between the floor and walls receives less heat and remains colder (Fig. 19.13B). This might be mistaken for capillary rise. The room is at the third floor and is not affected by rising damp.

19.2.18 X- and Gamma Rays

When an object is irradiated with an X-ray beam, or a Gamma ray beam, the beam attenuation is due to the interaction with the material and its absorption by water. A beam of X- or Gamma rays passing through matter is reduced in intensity according to the general exponential Equation

$$I(x) = I(0)\,\exp\left(-b_{ext}\,x\right) \tag{19.16}$$

[9] See Chapter 17, Fig. 17.28.

where $I(0)$ is the incident intensity of the beam, $I(x)$ is the reduced intensity of the beam after having crossed a path length x inside the material, and b_{ext} is the extinction coefficient that depends on the physical characteristics of the material, its *MC* and the wavelength of the radiation, either X-rays or Gamma rays (Tanaka et al., 2009; Bucurescu and Bucurescu, 2011). The method is independent of temperature and is nondestructive. Measurements are made in transmission, with the object (nondestructive) or the sample (taking samples is destructive) between the emitter and the receiver. The quantitative determination of the moisture content is based on the logarithmic subtraction of a reference image (e.g. sample at dry state) from images of the wet sample. The distribution and amount of moisture can be detected and measured with a scale of grey, or with the intensity of light passing through the radiography, or by contrast variation.

Radiography is the best known and most traditional nondestructive imaging technique that uses X-rays to view the internal structure of an object. Synchrotron X-ray tomography measures images from a number of different angular positions. It is based on the detection of either the attenuation or the phase shift of the beam transmitted through the material. Synchrotron-based X-ray tomographic microscopy (SRXTM) provides high-resolution investigations and three-dimensional imaging.

Gamma rays are more energetic than X rays and may be useful to investigate very thick and massive materials, e.g. porous stone, clay brick, cement, soil (Nielsen, 1972), but also wood (Loos, 1961). Gamma radiation is emitted from a radioactive source (e.g. Caesium-137, Cobalt-60 and Americium-241) and the attenuation of the beam intensity depends on the material and its density, including moisture content. The beam attenuation is measured by counting the number of gamma photons that are back scattered by collisions with atoms of the material or with water. In the presence of water, the percentage of fractional attenuation of the gamma beam is nearly equal to the moisture content and makes possible a calibration or using conversion tables. If measurements are made at two different gamma ray energies (Gardner et al., 1972), attenuation equations may be solved simultaneously to provide both moisture content and material bulk density. By using the dual gamma method, the accuracy of water content measurements improves. In this method, it is always assumed that moisture is the only cause of variation in material density.

After calibration, the analysis of these measurements may give the amount of moisture along the path length through the material. By scanning across a surface, a measure of the moisture distribution can be assessed, and by scanning in three dimensions, by, for example, rotating the sample whilst scanning in two dimensions, it is possible to use tomography to build up a picture of the three-dimensional *MC*. High-resolution results can be obtained, but the combined effect of moisture and density distributions may add uncertainty to the data interpretation.

The analysis of the X-ray or the gamma-ray spectrum may also be useful in detecting the chemical elements of the target material. However, for the risk connected with radioactive materials, this method can be used with special precautions by authorized, well-trained personnel.

19.2.19 Neutrons

An important nondestructive method, originally devised for soil moisture measurement, is based on the principle that high-energy *neutrons* emitted from a radioactive source are slowed down to thermal energy by elastic collisions with other nuclei (Nappi and Côte, 1997; WMO, 1986, 2008; Larsen, 2004; Zawisky et al., 2010; Zhang et al., 2011; Perfect et al., 2014). The loss of energy depends on the mass of the colliding nuclei and increases with decreasing atomic number. The highest efficiency occurs with protons, i.e. hydrogen nuclei, which have the same mass as the impinging neutrons. A water molecule has two hydrogen atoms and these atoms are practically absent in traditional building materials such as brick, stone, and mortar, except for some water that may be adsorbed, in the liquid state, or in hydrated crystals. However, nonwater hydrogen is present in organic materials, and crystalline structures, clay minerals, hydroxides, and other substances also have important neutron capture properties that add uncertainty to these measurements. The number of slow neutrons is linearly related to the moisture content. After collision, neutrons are slowed down and scattered in all directions. The neutron probe has proven to be a convenient and effective means for monitoring long-term in situ soil moisture variations (Schmugge et al., 1980; Silvestri et al., 1991). However, the experimental correlation of neutron probe data (i.e. neutron counts) with moisture contents to give accurate absolute values of moisture content is a difficult task (Li et al., 2003). In general, the actual volume that is measured by the detector is never precisely known and the explored volume varies inversely with water content that is often affected by gradients.

A detector counts the number of slow neutrons per second and transforms it into moisture content. The flux density of transmitted (or diffused) slow neutrons is nearly proportional to the water content over an approximately spherical volume with a radius of 15–35 cm. Thermal neutrons are counted with either scintillation crystal detectors or gas-filled detectors and the standard error is proportional to the square root of the count. As a consequence, the error is larger at high water contents. In addition, changes in the air humidity and temperature cause drift to the equipment. The neutron interaction occurs across the whole thickness of the wall and the method cannot distinguish between surface and deep layers. Water

distribution can be recognized with cold neutron radiography (CNR) and tomography (CNT) (Matsushima et al., 2009).

This method may give further information: part of the slow neutrons is captured by heavier nuclei with a gamma ray emission having an energy that is determined by the mass of the absorbing nuclei and ranges between 3.3 and 12.6 MeV. Dealing with the risk connected with radioactive materials, this method can be only applied with special precautions by authorized, well-trained personnel.

References

Agliata, R., Greco, R., Mollo, L., 2018. Moisture measurements in heritage masonries: a review. Mater. Eval. (November), 1468–1477.

Aguilar-Castro, K.M., Flores-Prieto, J.J., Macías-Melo, E.V., 2014. Near infrared reflectance spectroscopy: moisture content measurement for ceramic plaster. J. Mech. Sci. Technol. 28 (1), 293–300.

ASTM D2216 – 10, 2010. Test Method for Laboratory Determination of Water (Moisture) Content of Soil and Rock. American Society for Testing and Materials, West Conshohocken, PA.

ASTM D4442 – 07, 2007. Standard Test Methods for Direct Moisture Content Measurement of Wood and Wood-Base Materials. American Society for Testing and Materials, West Conshohocken, PA.

Baldini, F., Falciai, R., Mencaglia, A.A., Senesi, F., Camuffo, D., della Valle, A., Bergsten, C.J., 2008. Miniaturised optical fibre sensor for dew detection inside organ pipe. J. Sens. https://doi.org/10.1155/2008/321065.

Barreira, E., Almeida, R.M.S.F., Delgado, J.M.P.Q., 2016. Infrared thermography for assessing moisture related phenomena in building components. Constr. Build. Mater. 110, 251–269.

Barreira, E., Almeida, R.M.S.F., Moreira, M., 2017. An infrared thermography passive approach to assess the effect of leakage points in buildings. Energy Build. 140, 224–235.

Beall, F.C., 2007. Industrial applications and opportunities for nondestructive evaluation of structural wood members. Maderas-Cienc. Tecnol. 9 (2), 127–134.

Becherini, F., Bernardi, A., Frassoldati, E., 2010. Microclimate inside a semi-confined environment: valuation of suitability for the conservation of heritage materials. J. Cult. Herit. 11, 471–476.

Bergsten, C.J., Odlyha, M., Jakiela, S., Slater, J., Cavicchioli, A., De Faria, D.L., Niklasson, A., Svensson, J.E., Bratasz, L., Camuffo, D., della Valle, A., Baldini, F., Falciai, R., Mencaglia, A., Senesi, F., 2010. Sensor system for detection of harmful environments for pipe organs (SENSORGAN). *e-PS* 7, 116–125.

Bernardi, A., Becherini, F., Bassato, G., Bellio, M., 2006. Condensation on ancient stained glass windows and efficiency of protective glazing systems: two French case studies, Sainte-Chapelle (Paris) and Saint-Urbain Basilica (Troyes). J. Cult. Herit. 7 (1), 71–78.

Bini, M., Ignesti, A., Olmi, R., Pieri, L., Priori, S., Riminesi, C., 2009. Microwave Sensor for Measuring the Moisture of Masonry Surfaces Comprising a Microstrip Resonator Coupled With an Open Coaxial Probe. US Patent Specification 7,560,937 B2.

Brischke, C., Rapp, A.O., Bayerbach, R., 2008. Measurement system for long-term recording of wood moisture content with internal conductively glued electrodes. Build. Environ. 43, 1566–1574.

BS 5250, 2011. Code of Practise for the Control of Condensation in Buildings. British Standard Institution (BSI), London.

Bucurescu, D., Bucurescu, I., 2011. Non-destructive measurement of moisture in building materials by Compton scattering of gamma rays. Romanian Rep. Phys. 63 (1), 61–75.

Cai, L., Chen, T.B., Gao, D., Liu, H.T., Chen, J., Zheng, G.D., 2013. Time domain reflectometry measured moisture content of sewage sludge compost across temperatures. Waste Manag. 33, 12–17.

Calegari, L., Gatto, D.A., Martins Stangerlin, D., 2011. Influence of moisture content, specific gravity and specimen geometry on the ultrasonic pulse velocity in Eucalyptus grandis hill ex Maiden wood. Braz. J. Wood Sci. 2 (2), 64–74.

Camuffo, D., 2010. The role of temperature and moisture, pp. 9-30 in: Camuffo, D., Fassina, V. and Havermans, J. (Edts), 2010. Basic Environmental Mechanisms Affecting Cultural Heritage—Understanding Deterioration Mechanisms for Conservation Purposes. COST Action D42 "Enviart", Nardini, Florence.

Camuffo, D., 2018. Standardization activity in the evaluation of moisture content. J. Cult. Herit. 31S, S10–S14.

Camuffo, D., Bertolin, C., 2012. Towards standardisation of moisture content measurement in cultural heritage materials. *e-PS* 9, 23–35.

Camuffo, D., Valcher, S., 1986. A dew point signaller for conservation of works of art. Environ. Monit. Assess. 6, 165–170.

Camuffo, D., Bertolin, C., Schenal, P., 2014. Climate change, sea level rise and impact on monuments in Venice. In: Rogerio-Candelera, M.A. (Ed.), Science. Technology and Cultural Heritage. CRC Press - Taylor & Francis Group, London, pp. 1–18.

Camuffo, D., della Valle, A., Becherini, F., 2018. A critical analysis of one standard and five methods to monitor surface wetness and time-of-wetness. Theor. Appl. Climatol. 132 (3–4), 1143–1151.

Capitani, D., Emanuele, M.C., Bella, L., Segre, A.L., Attanasio, D., Focher, B., Capretti, G., 1999. 1H NMR relaxation study of cellulose and water interaction in paper. TAPPI J. 82 (9), 117–124.

Capitani, D., Proietti, N., Gobbino, M., Soroldoni, L., Casellato, U., Valentini, M., Rosina, E., 2009. An integrated study for mapping the moisture distribution in an ancient damaged wall painting. Anal. Bioanal. Chem. 395, 2245–2253.

Carll, C., Ten Wolde, A., 1996. Accuracy of wood resistance sensors for measurement of humidity. J. Test. Eval. 24 (3), 154–160.

Carr-Brion, K., 1986. Moisture Sensors in Process Control. Elsevier Applied Science, Amsterdam.

Casieri, C., Senni, L., Romagnoli, M., Santamaria, U., De Luca, F., 2004. Determination of moisture fraction in wood by mobile NMR device. J. Magn. Reson. 171, 364–372.

Cerny, R., 2009. Time-domain reflectometry method and its application for measuring moisture content in porous materials: a review. Measurement 42, 329–336.

Corvo, F., Pérez, T., Martin, Y., Reyes, J., Dzib, L.R., González-Sánchez, J., Castañeda, A., 2008. Time of wetness in tropical climate: considerations on the estimation of ToW according to ISO 9223 standard. Corros. Sci. 50 (1), 206–219.

Dai, G., Ahmet, K., 2001. Long-term monitoring of timber moisture content below the fiber saturation point using wood resistance sensors. For. Prod. J. 51 (5), 52–58.

Di Tullio, V., Capitani, D., Proietti, N., 2017. Unilateral NMR to study water diffusion and absorption in stone-hydrogel systems. Microporous Mesoporous Mater. 269. https://doi.org/10.1016/j.micromeso.2017.07.011.

Dill, M.J., 2000. A review of testing for moisture in building elements. CIRIA Report No. CIRIA-C538, London.

Doebelin, E.O., 1990. Measurement Systems—Application and Design. McGraw-Hill, New York.

EN 13183-1, 2002. Moisture Content of a Piece of Sawn Timber—Part 1: Determination by Oven Dry Method. European Committee for Standardization (CEN), Brussels.

EN 13183-2, 2002. Moisture Content of a Piece of Sawn Timber—Part 2: Estimation by Electrical Resistance Method. European Committee for Standardization (CEN), Brussels.

EN 13183-3, 2005. Moisture Content of a Piece of Sawn Timber—Part 3: Estimation by Capacitance Method. European Committee for Standardization (CEN), Brussels.
EN 1428, 2012. Bitumen and Bituminous Binders—Determination of Water Content in Bituminous Emulsions—Azeotropic Distillation Method. European Committee for Standardization (CEN), Brussels.
EN 15758, 2010. Conservation of Cultural Property—Indoor Climate—Procedures and Instruments for Measuring Temperatures of the Air and of the Surfaces of Objects. European Committee for Standardization (CEN), Brussels.
EN 16242, 2012. Conservation of Cultural Heritage— Procedures and Instruments for Measuring Humidity in the Air and Moisture Exchanges Between Air and Cultural Property. European Committee for Standardization (CEN), Brussels.
EN 16682, 2017. Conservation of Cultural Heritage— Methods of Measurement of Moisture Content, or Water Content, in Materials Constituting Immovable Cultural Heritage. European Committee for Standardization (CEN), Brussels.
EN 322, 1993. Wood-Based Panels—Determination of Moisture Content. European Committee for Standardization (CEN TC 346), Brussels.
EN 772-10, 1999. Methods of Test for Masonry Units— Part 10: Determination of Moisture Content of Calcium Silicate and Autoclaved Aerated Concrete Units. European Committee for Standardization (CEN), Brussels.
EN-ISO 10304-1, 2009. Water Quality—Determination of Dissolved Anions by Liquid Chromatography of Ions—Part 1: Determination of Bromide, Chloride, Fluoride, Nitrate, Nitrite, Phosphate and Sulfate. European Committee for Standardization (CEN)/International Organization for Standardization (ISO), Brussels/Geneva.
EN-ISO 11461, 2014. Soil Quality—Determination of Soil Water Content as a Volume Fraction Using Coring Sleeves—Gravimetric Method. European Committee for Standardization (CEN)/International Organization for Standardization (ISO), Brussels/Geneva.
EN-ISO 14911, 1999. Water Quality—Determination of Dissolved Li^+, Na^+, NH^{4+}, K^+, Mn^{2+}, Ca^{2+}, Mg^{2+}, Sr^{2+} and Ba^{2+} Using Ion Chromatography—Method for Water and Waste Water. European Committee for Standardization (CEN)/International Organization for Standardization (ISO), Brussels/Geneva.
EN-ISO 15512, 2014. Plastics—Determination of Water Content. European Committee for Standardization (CEN)/International Organization for Standardization (ISO), Brussels Geneva.
Fischer, K., 1935. Neues Verfahren zur maßanalytischen Bestimmung des Wassergehaltes von Flüssigkeiten und festen Körpern. Angew. Chem. 48 (26), 394–396.
Franzoni, E., 2018. State-of-the-art on methods for reducing rising damp in masonry. J. Cult. Herit. 31S, S3–S9.
Gardner, W.H., Campbell, G.S., Calissendorf, C., 1972. Systematic and random errors in dual gamma energy soil bulk density and water content measurements. Soil Sci. Soc. Am. Proc. 36, 393–398.
Goodhew, S., Griffiths, R., Woolley, T., 2004. An investigation of moisture content in the walls of a straw-bale building. Build. Environ. J. 39, 1443–1451.
Grinzato, E., Ludwig, N., Cadelano, G., Bertucci, M., Garfano, M., Bison, P., 2011. Infrared thermography for moisture detection: a laboratory study and in-situ test. Mater. Eval. 65 (1), 97–110.
Güneyli, H., Karahan, S., Güneyli, A., Yapıcı, N., 2017. Water content and temperature effect on ultrasonic pulse velocity of concrete. Russ. J. Nondestruct. Test. 53, 159–166.
Haagenrud, S., Kucera, V., Gullman, J., 1982. Atmospheric corrosion testing with electrolytic cells in Norway and Sweden. In: W.H., Ailor (Ed.), International Symposium on *Atmospheric Corrosion*, Hollywood, FL, Wiley, New York, pp. 669–693.
Hartley, I.D., Kamke, F.A., Peemoeller, H., 1994. Absolute moisture content determination of Aspen wood below the fiber saturation point using pulsed NMR. Holzforschung 48, 474–479.
Healy, W.M., 2003. Moisture sensor technology—a summary of techniques for measuring moisture levels in building envelopes. ASHRAE Trans. 109 (1), 232–242.
ISO 11465, 1993. Soil Quality—Determination of Dry Matter and Water Content on a Mass Basis—Gravimetric Method. International Organization for Standardization (ISO), Geneva.
ISO 12570, 2013a. Hygrothermal Performance of Building Materials and Products—Determination of Moisture Content by Drying at Elevated Temperature. International Organization for Standardization (ISO), Geneva.
ISO 12571, 2013. Hygrothermal Performance of Building Materials and Products—Determination of Hygroscopic Sorption Properties. International Organization for Standardization (ISO), Geneva.
ISO 16979, 2003. Wood-Based Panels—Determination of Moisture Content. International Organization for Standardization (ISO), Geneva.
ISO 760, 1978. Determination of Water—Karl Fischer Method (General Method). International Organization for Standardization (ISO), Geneva.
ISO 9223, 2012. Corrosion of Metals and Alloys. Corrosivity of Atmospheres. Classification. International Organization for Standardization, Geneva.
Jacobs, A.F.G., Heusinkveld, B.G., Wichink Kruit, R.J., Berkowicz, S.M., 2006. Contribution of dew to the water budget of a grassland area in the Netherlands. Water Resour. Res. 42, W03415. https://doi.org/10.1029/2005WR004055.
King, R.J., Basuel, J.G., 1993. Measurement of basis weight and moisture content of composite boards using microwaves. For. Prod. J. 43 (9), 15–22.
Korotchenkov, G., 2018. Handbook of Humidity Measurement—Methods, Materials and Technologies. Volume 1: Spectroscopic Methods of Humidity Measurement. CRC Press, Taylor and Francis Group, Boca Raton, London, New York.
Kumaran, M.K., Mukhopadhyaya, P., Normandin, N., 2006. Determination of equilibrium moisture content of building materials: some practical difficulties. J. ASTM Int. 3 (10), 1–9.
Lafhaj, Z., Goueygou, M., Djerbi, A., Kaczmarek, M., 2006. Correlation between porosity, permeability and ultrasonic parameters of mortar with variable water/cement ratio and water content. Cem. Concr. Res. 36 (4), 625–633.
Larsen, P.K., 2004. Moisture measurement in Tirsted Church. J. Archit. Conserv. 10 (1), 22–35.
Larsen, P.K., 2012. Determination of water content in brick masonry walls using a dielectric probe. J. Archit. Conserv. 18 (1), 47–62.
Le Feunteun, S., Diat, O., Guillermo, A., Poulesquen, A., Podor, R., 2011. NMR 1D-imaging of water infiltration into mesoporous matrices. Magn. Reson. Imaging 29 (3), 443–455.
Leygraf, C., Graedel, T., 2000. Atmospheric Corrosion. Wiley-Interscience, New York.
Li, J., Smith, D.W., Fityus, S.G., Sheng, D., 2003. Numerical analysis of neutron moisture probe measurements. Int. J. Geomech. 3 (1), 11–20.
Lipták, B.G., 2003. Instrument Engineers' Handbook: Process Measurement and Analysis. The Instrumentation System and Analysis (ISA). vol. 1 CRC Press, Boca Raton, FL.
Loos, W.E., 1961. The relationship between gamma-ray absorption and wood moisture content and density. For. Prod. J. 11 (3), 145–149.
Mamillan, M., 1992. Méthodes d'évaluation des dégradations des monuments en pierre. In: Zezza, F. (Ed.), Weathering and Air Pollution. Adda, Bari, pp. 175–181.
Mansfield, J.R., Sowa, M.G., Majzels, C., Collins, C., Cloutis, E., Mantsch, H.H., 1999. Near infrared spectroscopic reflectance imaging: supervised vs. unsupervised analysis using an art conservation application. Vib. Spectrosc. 19, 33–45.
Matsushima, U., Graf, W., Zabler, S., Kardjilov, N., Herppich, W.B., 2009. Application of Cold Neutron and Synchrotron X-Ray Imaging to Investigate Rose Bent Neck Syndrome. Acta Hortic 847, 279–286.

Milota, M.R., 1994. Specific gravity as a predictor of species correction factors for a capacitance-type moisture meter. For. Prod. J. 44 (3), 63–68.
Mitchell, P., 2010. Methods of moisture content measurement in the lumber and furniture industries. Wood Product Notes, Department of Wood and Paper Science, Raleigh, NC.
Mortl, A., Muñoz-Carpena, R., Kaplan, D., Li, Y., 2011. Calibration of a combined dielectric probe for soil moisture and porewater salinity measurement in organic and mineral coastal wetland soils. Geoderma 161, 50–62.
Murphy, W., Smith, J.D., Inkpen, R.J., 1996. Errors associated with determining P and S acoustic wave velocities for stone weathering studies. In: Smith, B.J., Warke, P.A. (Eds.), Processes of Urban Stone Decay. Donhead, London, pp. 228–244.
Nappi, A., Côte, P., 1997. Non-destructive methods applicable to historic stone structures. In: Baer, N.S., Snethlage, R. (Eds.), Saving Our Architectural Heritage: the Conservation of Historic Stone Structures. Wiley, Chichester, pp. 151–166.
Nielsen, A.F., 1972. Gamma-ray-attenuation used for measuring the moisture content and homogeneity of porous concrete. Build. Sci. 7 (4), 257–263.
Nilsson, L.O., 2018. Methods of Measuring Moisture in Building Materials and Structures: State-of-the-Art Report of the RILEM Technical Committee 248-MMB. Springer, Cham.
Noborio, K., 2001. Measurement of soil moisture content and electrical conductivity by time domain reflectometry: a review. Comput. Electron. Agric. 31, 213–237.
NWFA, 2008. Appendix C—Moisture Guidelines & Moisture Testing. National Wood Flooring Association, www.nwfa.org/member/.
Oliveira, F.G.R., Candian, M., Lucchette, F.F., Salgon, J.L., Sales, A., 2005. Moisture content effect on ultrasonic velocity in Goupia glabra. Mater. Res. 8 (1), 11–14.
Olmi, M., Bini, M., Ignesti, A., Priori, S., Riminesi, C., Felici, A., 2006. Diagnostics and monitoring of frescoes using evanescent-field dielectrometry. Meas. Sci. Technol. 17 (8), 1623–1629.
Palaia, L., Sánchez, R., López, V., Gil, L., Monfort, J., Tormo, S., Navarro, P., Álvarez, M.Á., 2008. Procedure for NDT and traditional methods of ancient building diagnosis by using thermograph, digital images and other instrument data analysis. In: 17th World Conference on Nondestructive Testing, Shanghai.
Perfect, E., Cheng, C.-L., Kang, M., Bilheux, H.Z., Lamanna, J.M., Gragg, M.J., Wright, D.M., 2014. Neutron imaging of hydrogen-rich fluids in geomaterials and engineered porous media: a review. Earth Sci. Rev. 129, 120–135.
Poděbradská, J., Maděra, J., Tydlitát, V., Rovnaníková, P., Černý, R., 2000. Determination of moisture content in hydrating cement paste using the calcium carbide method. Ceramics-Silikáty 44 (1), 35–38.
Proietti, N., Capitani, D., Di Tullio, V., 2018. Review. Nuclear magnetic resonance, a powerful tool in cultural heritage. Magnetochemistry 4, 11. https://doi.org/10.3390/magnetochemistry4010011.
Reich, G., 2005. Near-infrared spectroscopy and imaging: basic principles and pharmaceutical applications. Adv. Drug Deliv. Rev. 57 (8), 1109–1143.
Riminesi, C., Marie-Victoire, E., Bouichou, M., Olmi, R., 2016. Moisture and salt monitoring in concrete by evanescent field dielectrometry. Meas. Sci. Technol. 28 (1), 080101.
Rosina, E., Robison, E.C., 2002. Applying infrared thermography to historic wood-framed buildings in North America. APT Bull. XXXIII (4), 37–44.
Rosina, E., Spodek, J., 2003. Using infrared thermography to detect moisture in historic masonry: a case study in Indiana. APT Bull. XXXIV (1), 11–16.
Saïd, M.N., 2007. Measurement methods of moisture in building envelopes—a literature review. Int. J. Archit. Herit. 1 (3), 293–310.
Sandrolini, F., Franzoni, E., 2006. An operative protocol for reliable measurements of moisture in porous materials of ancient buildings. Build. Environ. 41, 1372–1380.
Schajer, G.S., Orhan, F.B., 2005. Microwave non-destructive testing of wood and similar orthotropic materials. Sens. Imaging 6 (4), 293–313.
Schajer, G.S., Orhan, F.B., 2006. Measurement of wood grain angle, moisture content and density using microwaves. Holz Roh Werkst. 64, 483–490.
Schindelholz, E., Kelly, R.G., 2012. Wetting phenomena and time of wetness in atmospheric corrosion: a review. Corros. Rev. https://doi.org/10.1515/corrrev-2012-0015.
Schindelholz, E., Kelly, R.G., Cole, I.S., Ganther, W.D., Muster, T.H., 2013. Comparability and accuracy of time of wetness sensing methods relevant for atmospheric corrosion. Corros. Sci. 67, 233–241.
Schmugge, T.J., Jackson, T.J., McKim, H.L., 1980. Survey of methods for soil moisture determination. Water Resour. Res. 16 (16), 961–979.
Scholz, E., 2012. Karl Fischer Titration: Determination of Water. Springer Verlag, Berlin.
Sentelhas, P.C., Monteiro, J.E.B.A., Gillespie, T.J., 2004. Electronic leaf wetness duration sensor: why it should be painted. Int. J. Biometeorol. 48, 202–205.
Shimamura, Y., Urabe, T., Todoroki, A., Kobayashi, H., 2004. Electrical impedance change method for moisture absorption monitoring of CFRP. Adv. Compos. Mater. 13 (3–4), 297–310.
Silvestri, V., Sarkis, G., Bekkouche, N., Soulie, M., Tabib, C., 1991. Laboratory and field calibration of a neutron depth moisture gauge for use in high water content soils. Geotech. Test. J. 14, 64–70.
Sundara-Rajan, K., Byrd, L., Mamishev, A.V., 2004. Moisture content estimation in paper pulp using fringing field impedance spectroscopy. IEEE Sensors J. 4 (3), 378–383.
Tanaka, T., Avramidis, S., Shida, S., 2009. Evaluation of moisture content distribution in wood by soft X-ray imaging. J. Wood Sci. 55 (1), 69–73.
Thickett, D., 2008. Investigation into role of inert dusts in corrosion and corrosion mitigation in an aggressive marine environment. In: da Silva, A.C.F., Homem, P.M. (Eds.), Ligas Metálicas. University of Porto, Porto, pp. 75–90.
Titta, M., Olkkonen, H., 2002. Electrical impedance spectroscopy device for measurement of moisture gradients in wood. Rev. Sci. Instrum. 73 (8), 3093–3100.
Van Den Ende, J.E., Pennock-Vos, M.G., Bastiaansen, C., Koster, A.T.H. J., Van Der Meer, L.J., 2000. BoWaS: a weather-based warning system for the control of Botrytis blight in lily. Acta Hortic. 519, 215–220.
Van Hove, L.W.A., Adema, E.H., Vredenburg, W.J., Pieters, G.A., 1989. A study of adsorption of NH_3 and SO_2 on leaf surfaces. Atmos. Environ. 23, 1479–1486.
Veleva, L., Alpuches-Aviles, M.A., 2002. Outdoor atmospheric corrosion. In: Townsend, H.E. (Ed.), ASTM, STP 1421. American Society for Testing and Materials International, West Conshochoken, PA.
Vun, R.Y., Bhardwaj, M.C., Hoover, K., Janowiak, J., Kimmel, J., Worley, S., 2006. Development of non-contact ultrasound as a sensor for Wood Moisture Content. ECNDT 2006—Tu.4.2.3, 1–7.
Weritz, F., Kruschwitz, S., Maierhofer, C., 2009. Assessment of moisture and salt contents in brick masonry with microwave transmission, spectral-induced polarization, and laser-induced breakdown spectroscopy. Int. J. Archit. Herit. 3 (2), 126–144.
Wichink Kruit, R.J., Jacobs, A.F.G., Holtslag, A.A.M., 2008. Measurements and estimates of leaf wetness over agricultural grassland for dry deposition modelling of trace gases. Atmos. Environ. 42 (21), 5304–5316.
Wieland, G., Fisher, K., 1987. Water Determination by Karl Fischer Titration: Theory and Applications. GIT Verlag, Darmstadt.

Wilson, P.J., 1999. Accuracy of a capacitance-type and three resistance-type pin meters for measuring wood moisture content. For. Prod. J. 49 (9), 29–32.

WMO, 1986. Compendium of lecture notes on meteorological instruments for training class III and class IV. Meteorological personnel. WMO Technical Publication No. 622, World Meteorological Organisation, Geneva.

WMO, 2008. Guide to meteorological instruments and methods of observation. WMO Technical Publication No. 8, World Meteorological Organisation, Geneva.

Xia, D.H., Song, S., Jin, W., Li, J., Gao, Z., Wang, J., Hu, W., 2017. Atmospheric corrosion assessed from corrosion images using fuzzy Kolmogorov–Sinai entropy. Corros. Sci. 120, 251–256.

Zawisky, M., Hameed, F., Dyrnjaja, E., Springer, J., Rohatsch, A., 2010. Digitized neutron imaging with high spatial resolution at a low power research reactor: applications to steel and rock samples. Nucl. Inst. Methods Phys. Res. B 268 (15), 2446–2450.

Zazueta, F.S., Xin, J., 1994. Soil moisture sensors. In: Bulletin 292 Florida Cooperative Extension Service. Institute of Food and Agricultural Sciences, University of Florida.

Zhang, P., Wittmann, F.H., Zhao, T.J., Lehmann, E.H., Vontobel, P., 2011. Neutron radiography, a powerful method to determine time-dependent moisture distributions in concrete. Nucl. Eng. Des. 241 (12), 4758–4766.

CHAPTER

20

Measuring Wind and Indoor Air Motions

OUTLINE

20.1 PART 1: HISTORICAL OVERVIEW: THE DEVELOPMENT OF EARLY ANEMOMETERS AND BASIC IDEAS

20.1.1 Introduction

This section deals with the history of science and a critical analysis of early instruments and their development. Science cannot be separated from culture. Even if historical and cultural aspects may be involved, this section helps to better understand problems and solutions concerning measurements of wind direction and speed.

20.1.2 The Wind in Antiquity

Since the remote antiquity winds were considered extremely important, and were represented by a god: Eolus. There was no need of sophisticated instruments, because the wind direction was evident from flags, smoke, dust, leaves of trees, clouds, the transport of remote sounds, and personal feeling. Similarly, the wind force was easily recognizable from its consequences.

The Mediterranean civilization was based on two connecting mediums: the water of the Sea, and the wind blowing on it. The local populations recognized that the dominant wind in the Central Mediterranean is from North West. There are, however, some violent winds that enter the Mediterranean and change weather or characterize the seasonal climate (Fig. 20.1A). These winds blow as violent spells from mountain and coastal gates, and generate rough sea and surges (UK Meteorological Office, 1962; Reiter, 1975; Wallén, 1977; Bolle, 2003; WEU, 2004). In addition, there are other local regular winds, i.e. the land and sea breezes.

Winds were crucial for sailing and the early ships were small, unable to afford the rough sea. Phoenician, Greek, and Roman ships had square sails and exploited the breezes and their veering, i.e. by cabotage. The plots of the epic poems by Homer,[1] i.e. the *Odyssey*, with the journey of Odysseus, and by Virgil,[2] i.e. the *Aeneid*, with the journey of Aeneas, are grounded on a realistic scenario based on these difficulties. It was easy to sail from Greece to Troy, on Turkey, but the return trip was very difficult.

[1] Homer (late 8th or early 7th century BC).

[2] Virgil (1st century BC).

https://doi.org/10.1016/B978-0-444-64106-9.00020-1

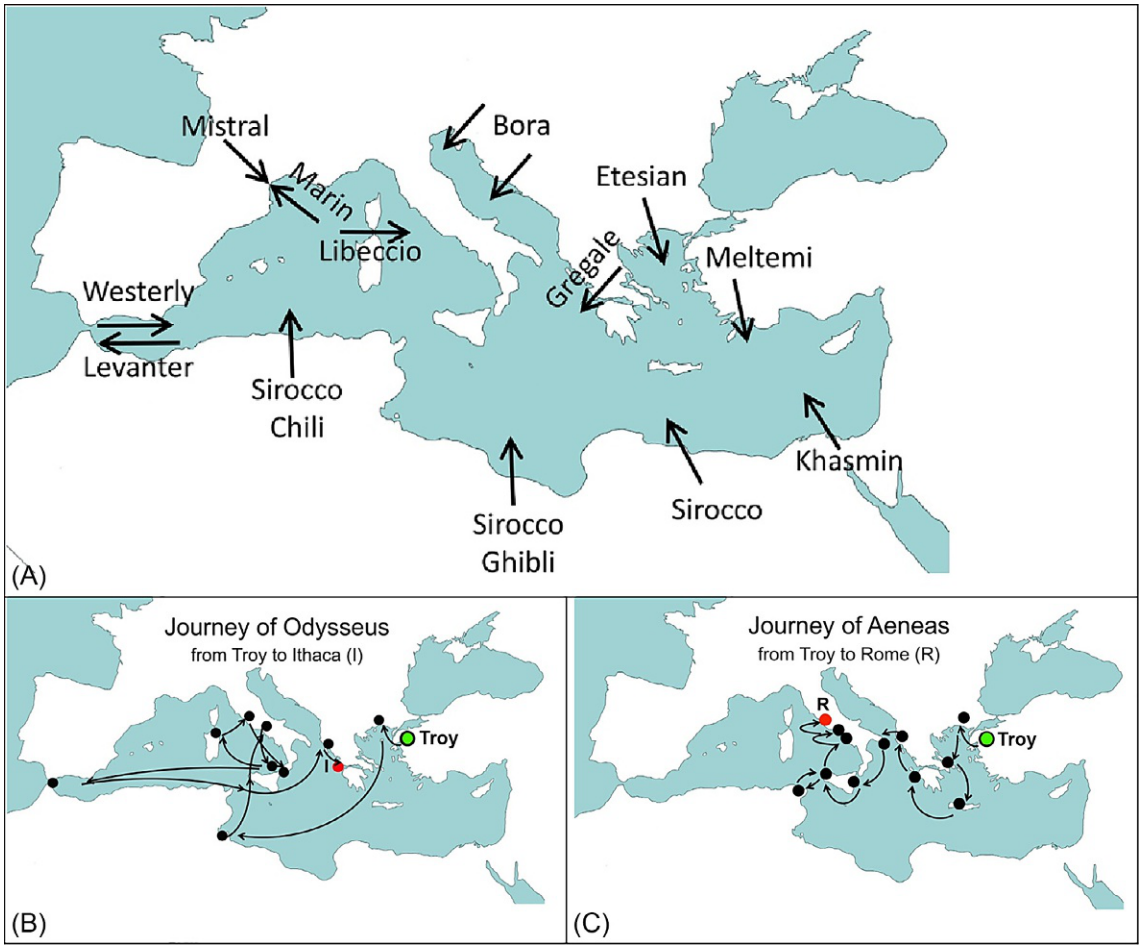

FIG. 20.1 (A) Main winds in the Mediterranean Basin. (B) Hypothetical reconstruction of the journey of Odysseus from Troy to Ithaca (I, *red dot*). (C) Hypothetical reconstruction of the journey of Aeneas from Troy to Rome (R, *red dot*).

This required to sail daytime along the coasts with breezes, and sometimes to venture high seas. The consequence was that Odysseus went up and down for years across the Mediterranean Fig. 20.1B, reaching Tunisia, the Straits of Gibraltar, Sardinia, the western coast of Italy (today from Naples to Rome), Sicily, Malta, Corfu Island on the Ionian Sea and, finally, Ithaca. Similarly, Aeneas from Troy reached Crete, made cabotage along the coast of Greece, arrived to Sicily, from Sicily to Cartago on the coast of Tunisia and back to Sicily again, and finally to the west coast of Italy where Rome will be founded later (Fig. 20.1C).

20.1.3 The Tower of Winds in Athens: The Mother of All Anemometers

The wind was considered characterized by the blowing direction that lasted for hours or days, with a related weather. Winds were classified by the name of the region from which they blew. The intensity was considered variable, less relevant, or an obvious character for some violent winds. The scientific spirit of Greeks classified 12 winds blowing in Greece and the Aegean Sea and created a wind compass divided into 12 sectors each of 30 degrees. Romans used a slightly different wind compass focused on the main winds blowing in Rome and the Central Mediterranean, with 8 main winds and the wind compass was divided into eight sectors each of 45 degrees. In order to improve resolution, the bisector of each sector was considered, i.e. 22.5 degrees.

The earliest anemometers considered the wind direction only. Around 50 BC, Andronicus of Cyrrhus built in Athens the Tower of Winds, 12 m tall and 8 m in diameter (Fig. 20.2). This was an octagonal tower[3] with a combination of sundials, a water clock, and a wind vane. Each side had a sundial and a frieze representing the wind that had the same direction, i.e. Boreas (N), Kaikias (NE), Eurus (E), Apeliotes (SE), Notus (S), Lips (SW), Zephyrus (W),

[3] The Tower of the Winds highlighted eight directions, following the Roman style. This is not surprising because Athens was under the control of Rome and the Tower was built in the Roman Agora (i.e. the Square dedicated to Romans).

(A)

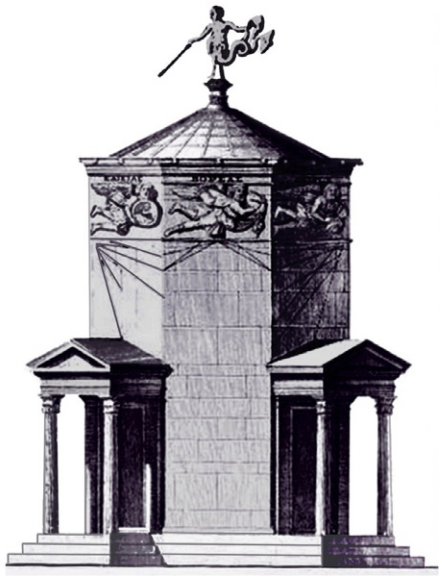

(B)

FIG. 20.2 (A) The Tower of the Winds with sundials, by Andronicus of Cyrrhus (50 BC), Athens, as it is today. (B) A reconstruction of the 20th century. Each side represented a particular wind and had a sundial. Upper frieze: bas reliefs of the eight winds. *Black lines* visible on the reconstruction: sundials. (A) From Photo Joanbanjo, CC BY-SA 3.0; https://commons.wikimedia.org/w/index.php?curid=18715396; (B) reconstruction from Vitruvius (1st century BC).

and Skiron (NW). On the top, the wind vane was a three-dimensional mobile statue of a Triton, i.e. a deity with body of man and fish tail that could turn on a pivot. When the wind blew, the Triton was pushed by the wind force, and stopped in the position of minimum drag, i.e. when it was facing the wind. He had a pointer rod in his hand, and was indicating which wind was blowing. The Tower was described by the contemporary Roman architect Vitruvius (1st century BC) in his book *De Architectura* (on Architecture).

A rich Roman writer and farmer, Varro (37 BC), described a device closely inspired by the Tower of Athens that he installed in his countryside farm-palace (Varro, 37 BC). In a room with a dome and a hole on the summit, he installed a wind vane, and inside the room he added a pointer projecting from the axis. In the walls of the room, he painted the eight winds as in Athens, and the pointer, rotating, indicated the wind which was blowing, so that it was possible to know it, staying inside.

The Greek and Roman tradition continued with smaller devices with different shapes, e.g. tritons as in Athens, flags, weather cocks,[4] comets, angels, or other symbolic forms, positioned on the top of the bell towers. The classical style survived till end of the 16th century, as illustrated with the 'weather station' shown in Fig. 20.3A, composed of a wind vane and a sundial on the top two marble columns, to be well visible even at some distance (Pini, 1598). The wind vane represents the Greek god Hermes[5] the messenger, sounding a straight trumpet with banner to announce the new wind, following the herald style. Hermes rotates under the wind push, and holds a rod to point at one of the letters engraved on the capital, with the name and face of the wind. Trumpet and banner are on the front side, while the pointing rod and the half-raised leg on the back, to compensate for the mass distribution and strengthen the wind drag. In the illustration, a Roman wind rose, i.e. 8-point star, is drawn between the two columns. The book is focused on the theory and construction of sundials, but makes a detailed explanation to build a rotating statue, moved by wind pushing on the flag and the body, and how to insert an iron bar into the leg as a pivot.

It was possible to use more sophisticated, clock-like representations of the horizontal wind direction on a vertical circle. The gear technology to transmit the rotation of an outdoor vane (i.e. the metal flag) in an indoor clock-like pointer (Fig. 20.3B) is reported in a handbook of the 16th century to build astrolabes and sundials, which includes two chapters about winds and anemometers (Danti, 1578).

[4] On the bell towers, the cock is a symbol of the rising sun; it recalls that Peter denied three times Jesus Christ before the cock crowed in the morning; it becomes symbol of repentance and redemption. For this reason, it is widespread in countries with Christian culture.

[5] In Rome, Hermes was named Mercury.

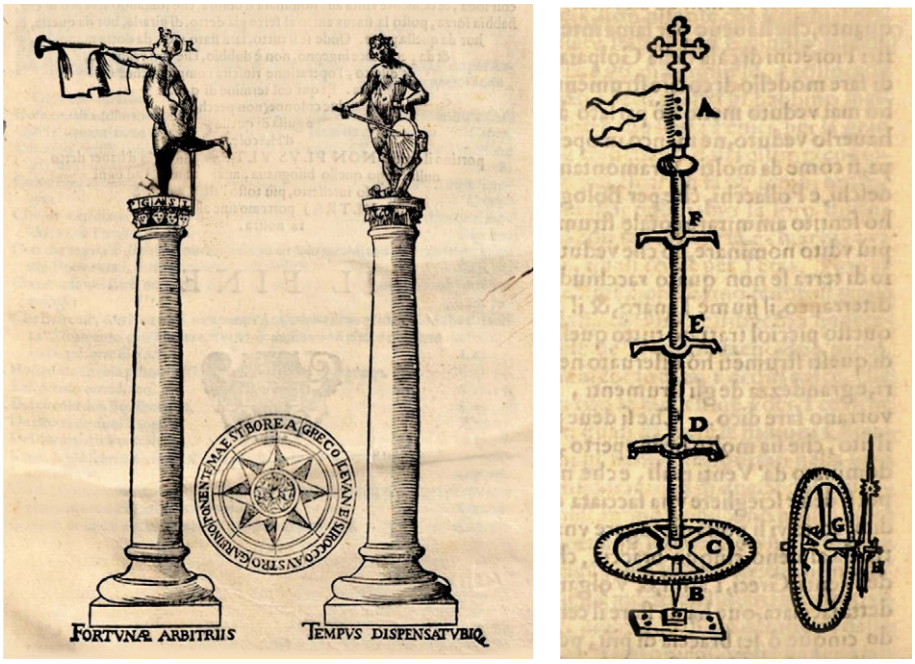

(A) (B)

FIG. 20.3 (A) A 'weather station' of the 16th century composed of a wind vane (left) and a sundial (right) on the top of two marble columns. In the wind vane, the trumpet with banner faces the wind and the rod on the back points at a letter engraved on the capital, with the name and face of the wind. Between the two columns is an 8-point Roman wind rose. The Latin motto under the column of winds is: 'To the whims of Fortune'; under the sundial: 'Time rules everywhere'. From Pini (1598). (B) Gear technology to transform the rotation of an outdoor vane in an indoor clock-like pointer. From Danti (1578).

20.1.4 Art or Instrument? The Mediaeval Giants on Towers

The earlier examples are undoubtedly ancestors of the modern wind vanes, but at that time they were conceived as a cultural curiosity and a touch of distinction. However, they inspired a series of gigantic three-dimensional wind vanes that were built since the Middle Ages on towers, or bell towers, conceived to be visible from far away. These were real Giants, tall from 3 to 6 m. They were real artworks that joined impressive scientific intuitions, surprising technical skills and beauty, and merit a short overview with some selected examples.

One of the earliest and best preserved gigantic wind vane is an Angel of gilded copper, 9 Padua feet (i.e. 3.20 m) tall (Fig. 20.4), stacked on an iron pivot that was installed on the top of the main dome of the Basilica of St Antony, Padua, Italy, when it was erected in 1231 (Corradi Bianchi, 1768). The Angel is blowing a straight trumpet pointed into the wind. This is an obvious symbol for annunciation, judgement and resurrection, but it also has a dynamic function. The front trumpet keeps the head to the wind and stabilizes the Angel. In fact, trumpet and wings provide a symmetric distribution of masses. By increasing the distance of a certain mass (i.e. trumpet and wings) from the axis of rotation, the total angular momentum[6] will increase, reducing the rotation speed and damping short-term fluctuations. In addition, the two divergent wings on the back, like two sails, govern the Angel rotation to minimize the resistance to wind push. When the wind turns a bit, the differential pressure and the vortex shears that develop at the two wings generate angular momentum and the Angel will immediately rotate until it is aligned with the blowing wind. To minimize the load and the exceedingly high friction, the Angel is empty, being made of embossed copper plates fastened together and supported by an internal iron structure. During maintenance works in 1999, after 768 years, the Angel was found in bad conditions, and was substituted with a copy made with laser-assisted technique. This model was replicated in several cities in Northern Italy and abroad, although with some changes over time.

The gigantic Archangel Gabriel (Fig. 20.5A), built in 1517, on the top of the bell tower of the San Marco Basilica, Venice, 100 m above the city floor, is clearly inspired to the Angel of Padua. The Archangel was tall (16 Venice feet, i.e. 5.60 m) and gilded, (Gallicciolli, 1795), to be visible from far away. It was made of carved wood to be

[6] In classical mechanics, the *linear momentum*, or simply *momentum*, is a *vector* representing the product of the mass by the velocity of an object, and is oriented as the velocity. The *angular momentum* is its rotational equivalent. However, it is a *pseudovector*, given by the cross product of the spatial position vector and the linear momentum vector. Its direction is normal to the plane determined by these two vectors. It is a conserved quantity, i.e. the total angular momentum of a system remains constant unless acted on by an external torque. As a consequence, if a mass is displaced from the rotation axis, the rotation speed of the system is slowed down. This helps to cut off short-term fluctuations.

FIG. 20.4 The Angel with divergent wings, used as a wind vane St Anthony Basilica, Padua, Italy. The Angel holds a trumpet and a lily, symbol of Saint Anthony. (A) The dismissed original, built AD 1231, brought down. It has lost the gold plating and the damaged lower petticoat is missing. (B, C) Front and back view of the laser-assisted copy of the original, substituted in 1999. On the top of the gilded Angel, a lightning rod.

light and reduce friction; it was covered with a thin gilded copper layer to be weatherproof and shining. Instead of the trumpet it had an arm raised, pointing to the sky, with dynamic function and distribution of masses similar to the trumpet. In the three centuries of his life, the Archangel was hit several times by lighting strokes and fire, and in 1822 it was substituted with a smaller copy (i.e. 3.68 m) by Zandomeneghi. This copy fell to ground when the bell tower collapsed in 1902. It was restored in 1911, and installed again on the tip of the bell tower where is today.

In Seville, Spain, another magnificent three-dimensional vane was built in 1568, i.e. *The triumph of the Victorious Faith* nicknamed *El Giraldillo* (Fig. 20.5B). The statue is made of bronze, is 3 m tall, and is located on the top of the Giralda bell tower of the Seville Cathedral. The statue representing Faith holds a palm branch, symbol of victory and technical asset for dynamic stabilization (like the trumpet of the Angel in Padua). The innovation is that the wind pressure is sensed with a flat shield, as in most modern wind vanes: this was an easier solution, and left the body less sensitive to fluctuations, and at the same time to light breeze. The shield, the palm branch, and the arms are kept at some distance from the axis to increase angular momentum and enhance dynamic stability.

On the top of the Punta della Dogana (i.e. Custom Point), Venice, the wind vane built in 1677 represented the Fortune goddess (Fig. 20.5C), selected to remind that it is mobile and may turn at every moment. The Fortune stands on the top of a gilded globe, supported by two bronze atlases and holds a flat rudder that acts as a sail, kept at some distance to enhance angular momentum, similar to that of *el Giraldillo*. The monument was built by Bernardo Falconi and is about 6 m tall; the Fortune is half this height.

20.1.5 Development of Wind Vanes

The triton in the Tower of Athens, and the mediaeval Giants on towers, were three dimensional. As opposed, in the early instrumental period, vanes were flat. Cotte (1774) illustrated a typical anemometer of the mid-18th century, with a flat vane and a gear mechanism to transmit the direction to a pointer on a clock like system[7](Fig. 20.6A). Apparently, to pass from a subjective estimation of the wind direction to a pointer moving on a graduated compass was a big qualitative improvement. However, the complex gear mechanism had exceedingly high friction and was soon abandoned.

The first aerodynamic improvement was made at the end of the 18th century, when Parrot[8] introduced the splayed vane (Fig. 20.6B), composed of two divergent sides, forming a V on the horizontal plane, thus obtaining on the front only one cutting edge, and on the back two spaced tails (Parrot, 1797), like the Angel in Padua or the Archangel in Venice. The two tails generated a more consistent turbulent wake behind the vane and,

[7] A reconstruction of it, or of a very similar model, is found at the *Museo Galileo—Institute and Museum of the History of Science*, Florence, Room XIV, catalogue number 848.

[8] Georg Friedrich Parrot (1767–1852).

FIG. 20.5 (A) Archangel Gabriel with divergent wings on the top of the San Marco bell tower, Venice, front and back view. Lightning rods (the *black rod* above the head and on the top of wings) are visible. (B) 'The triumph of the Victorious Faith' nicknamed *el Giraldillo*, on the top of the Giralda bell tower of the Seville Cathedral, Spain, 1568. Between the statue and the sphere four lightning rods. Photo by Carlos Teixidor Cadenas—CC BY-SA 4.0. (C) The Fortune goddess with a rudder used as wind vane, at the Punta della Dogana, Venice. Monument by Bernardo Falconi, 1677.

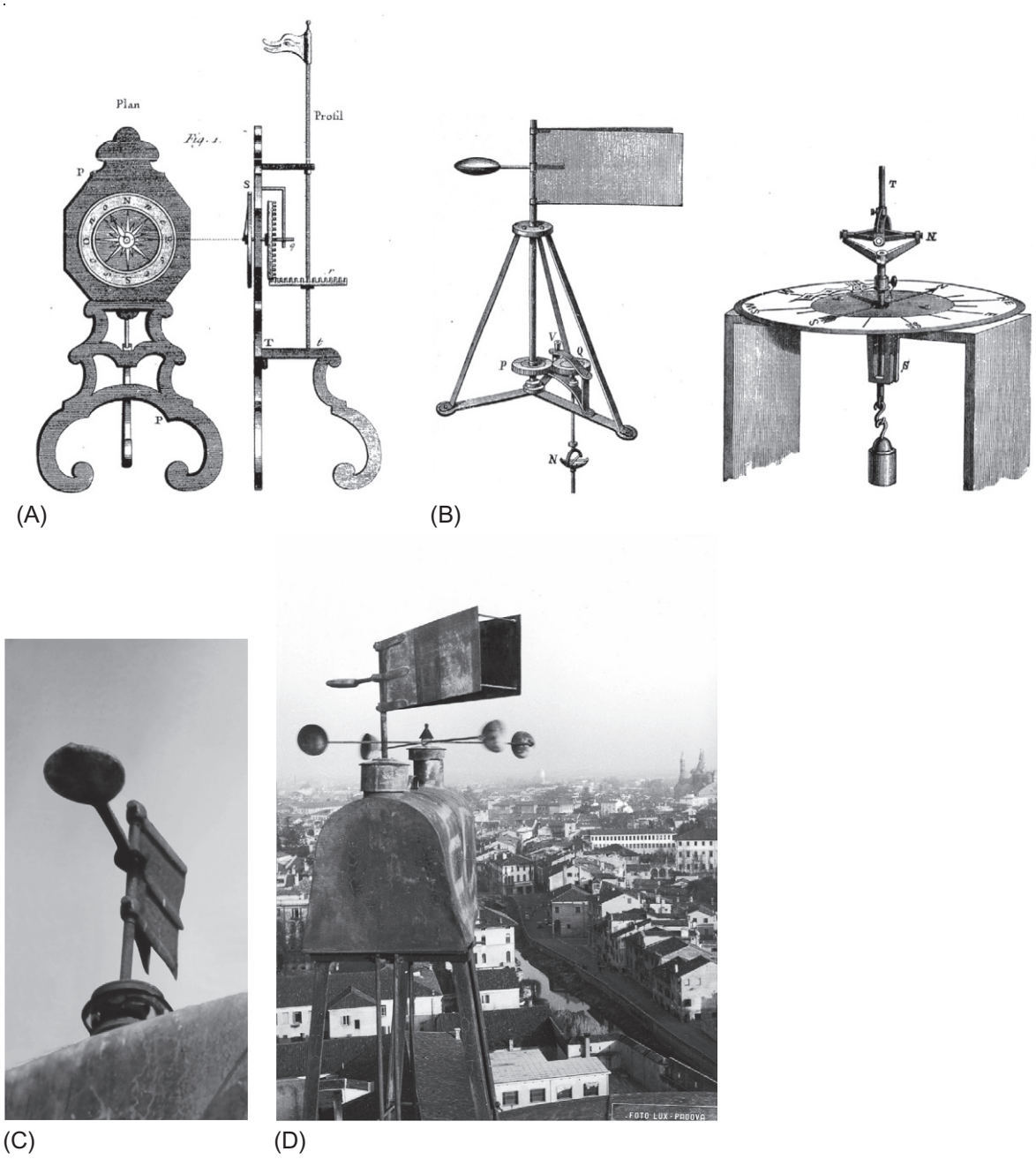

FIG. 20.6 (A) Front and side view of a wind vane (a metal flag) with transmission of the direction on a clock-like system. The gear system transformed the wind rotation into the pointer rotation, passing from the horizontal to the vertical plane. From Cotte (1774) (B) Parrot's V-shaped splayed vane and the mechanism to transmit the direction to a pointer on a compass. From Gerosa (1898). (C) Front view of the Parrot vane with the characteristic disc to balance the mass distribution. (D) A Parrot vane in combination with a Robinson cup anemometer on the tower of the Astronomical Observatory, Padua. By courtesy of Valeria Zanini, *Historical Archive of INAF-Astronomical Observatory*, Padua. Photo Archive Collection, © Used with permission.

consequently, higher sensitivity to light winds, greater turning moment, and higher dynamic stability. V-shaped vanes are still commercially available as well as flat tails with aerodynamic protrusions to generate turbulence and stabilize the vane around the mean direction. Both types are convenient for meteorological purposes. However, a large number of commercial products are oriented toward flat tails that may be preferable for pollutant dispersion studies because they are more respondent to fluctuations.

The next relevant improvements to vanes were made in the 20th century, when several forms of anemometers and wind vanes were introduced with advanced aerodynamic features to respond to different aims, e.g. to filter fluctuations and highlight the main direction for meteorological purposes or, as opposed, to be sensitive to

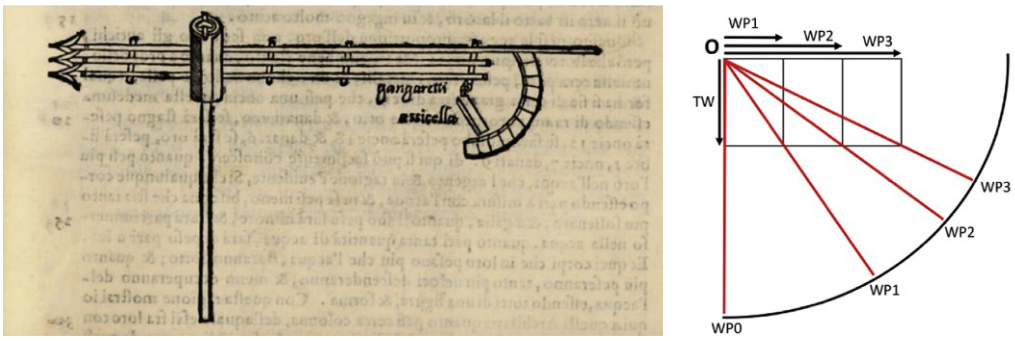

(A) (B)

FIG. 20.7 (A) The wind vane and pressure-plate anemometer proposed by Alberti in 1542. From Alberti (1452). (B) Explanation of the operating principle. The tablet *(red line)* is hinged in O and is in vertical position, but is rotated backwards by the wind force. *Arrows* indicate: TW the weight of the tablet; WP1, WP2, WP3, the wind vectors, as well as the related position of the tablet on the curved graduated scale. WP1, WP2 and WP3 should be intended as the actual force exerted on the effective cross section of the inclined tablet.

fluctuations for studies on pollutant dispersion (Slade, 1968; Jones, 1970; Monteith, 1972; Monna and Driedonks, 1979; Wyngaard, 1981; Walker and Swift, 2015).

It was possible to apply the remote transmission of wind direction with the advent of electromechanical instruments, and subsequently, with electronics devices. From the classical antiquity since the 19th century, the main reference was a bi-dimensional wind vane, located on the top of bell towers, or on towers of public buildings. Consequently, early meteorological series started observing metal flags, weather cocks, etc. on the bell towers and made a crude estimation of the wind direction and force.

20.1.6 Measuring the Wind Pressure Exerted on a Plate

The wind intensity was naturally associated to the concept of the force that wind exerted on sailing boats or on windmills, generating a strong pressure or a rotation, respectively. The concept of pressure inspired the first method to measure the wind force. Leon Battista Alberti[9] invented the first anemometer to measure both wind direction and force (Alberti, 1452, printed 1568 posthumously). The instrument (Fig. 20.7A) had a vane composed of three arrows to keep the wind direction; on the back, it had a tablet hinged on the top, but free to rotate. The angle of inclination, representative of the wind force, was read on a circular graduated scale. The principle (Fig. 20.7B) is the following: the tablet is hinged in the upper edge (O) and has a certain weight (TW) that is represented by a constant vector, directed downward, while the wind force is horizontal and exerts a certain pressure (WP) on the tablet. In the absence of wind (WP = 0), the tablet is vertical and its extreme points to WP0. If the wind intensity increases, and higher pressures are exerted, e.g. WP1, WP2, WP3, the inclination angle will increase and the tablet will point to the positions WP1, WP2, WP3 of the circular scale. It is evident that the response is not linear. In addition, the exerted force is the product of the wind pressure by the effective tablet surface, and this decreases with the cosine of the angle. Therefore, WP1, WP2 and WP3 should be intended as the actual force that wind exerts on the effective cross section of the tablet. Finally, the wind drag changes with the onset of the turbulent regime that develops behind the tablet. In addition, the turbulence causes instability and violent flapping of the tablet. Briefly, the idea was good, but readings, and their interpretation, were difficult.

Leonardo da Vinci,[10] in his famous *Codex Atlanticus* and *Hammer Codex*, drafted two devices in line with the still-unpublished Alberti's idea (Leonardo, 1487). The first device was to measure the wind force, i.e. the hinged tablet rotated by the wind force (Fig. 20.8A from the *Codex Atlanticus*). Leonardo added the note that this instrument should be used with a clock to record the wind force versus time. He also gave an explanation for the tablet sensor, i.e.: when air blown at high speed is struck by a body, it becomes compressed in proportion with its speed. This is correct, except for the additional turbulent drag that was discovered later. On the same *Codex Atlanticus*, Leonardo included a sketch showing the positions of the hinged tablet in response to the wind force (Fig. 20.8B). In the *Hammer Code*x (c 100 r), which includes flight studies, Leonardo drafted a wind vane. The tail was represented with four short strokes of a pen, probably feathers that were normally used in arrows to keep the same flying direction. It is not clear whether the tail was flat with the four feathers on the same vertical plane, or was three dimensional, like a shuttlecock. A hypothetical

[9] Leon Battista Alberti (1405–72), humanist, architect, and principal initiator of the Renaissance art theory.

[10] Leonardo da Vinci (1452–1519).

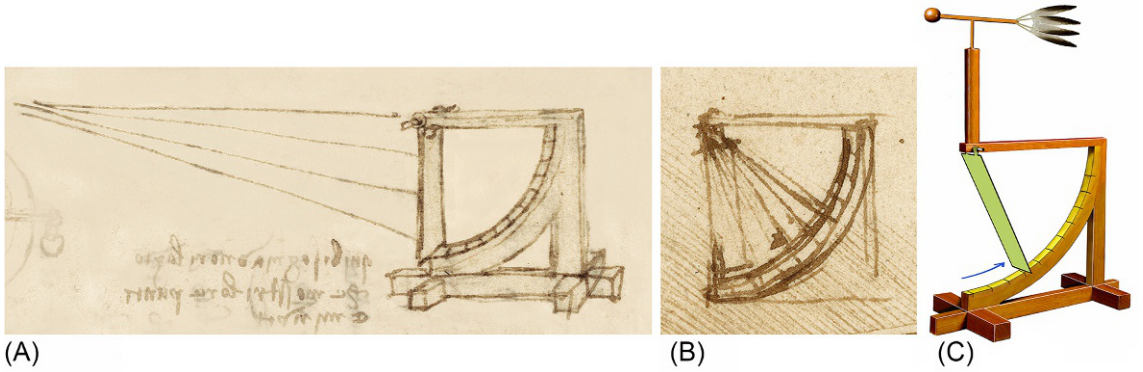

FIG. 20.8 (A) pressure anemometer with the hinged tablet in Zero position in the absence of wind. Original drawing by Leonardo da Vinci, Codex Atlanticus, sheet 675 recto. (B) Various positions reached by the hinged tablet under the push of wind at different intensities. Original drawing by Leonardo da Vinci, Codex Atlanticus, sheet 100 recto. (C) A reconstruction of Leonardo's anemometer, with the pressure plate and wind vane assembled together. The *blue arrow* indicates the rotation of the pressure plate when wind blows. Parts (A) and (B) from © Veneranda Biblioteca Ambrosiana/Metis e Mida Informatica/Mondadori Portfolio.

reconstruction of Leonardo's pressure-plate anemometer, assembled together with the feather wind vane installed on the blowing wind side, is shown in Fig. 20.8C.[11]

Two centuries later, Sanctorius[12] devised a similar method to determine the wind intensity (Fig. 20.9A), and the velocity of river streams, by measuring the force exerted on a plate, weighing it with a steelyard (Sanctorius, 1625).

Around 1670, Hooke[13] returned to the Alberti, Leonardo, and Sanctorius idea, proposing a rectangular swinging plate supported at the upper edge, and a quadrant to indicate its inclination to the vertical. The instrument became popular and was proposed with various variants in size and shape for over two centuries[14] (Middleton, 1969a,b).

In 1733, Poleni[15] won the prize of the Royal Academy of Sciences, Paris, for an anemometer to evaluate the actual wind force (Fig. 20.9B) (Poleni, 1734). Poleni was a professor of the University of Padua, after Galileo and Sanctorius and he was likely inspired by the paper by Sanctorius, published a century before. However, although the sensing element was the same, Poleni devised a scientific way to determine the wind force. He applied a rope to the plate and observed the force necessary to balance the weight of the plate at every degree of the inclination angle. He also calculated the effective surface of the plate that decreased with the cosine of the angle and produced a Table with three columns: the degrees of inclination of the plate, the apparent wind force, and the true wind force. Theoretically, it was possible to observe the inclination angle and determine the wind force with the help of his Table. However, things were more complex because it was necessary to keep the instrument in line with the wind direction, and the plate was swinging. Poleni devised this instrument for ships, but he never used it in his daily weather records, where the wind column included the direction only, determined looking at the wind vane of a bell tower in front of his house.

A further variant of the wind force sensor (Fig. 20.9C) was invented by Bouguer[16] who used a vertical pressure plate pushed back by wind until equilibrium was reached with a counteracting spiral spring (Bouger, 1746). The back position, corresponding to a certain wind velocity, was read on a graduated rod. The use of a spring may be considered an improvement. Another advantage of the Bouguer anemometer was that the push could be easily recorded with mechanical devices, while the other plate anemometers that changed inclination angle were less easily recordable. Other methods were proposed to quantify the wind push (e.g. lifting loads), but the spring was the most efficient solution.

Two centuries after Hook, and one after Bouguer, another pressure-plate anemometer was proposed by Wild,[17] i.e. *Wild's tablet anemometer* (Fig. 20.9D). It was identical to the Leonardo and Poleni anemometers.

[11] The *Museum of Science and Technology 'Leonardo da Vinci'*, Milan, has a slightly different reconstruction made in 1952–53 by A.M. Soldatini and V. Somenzi, with the vane installed downwind and a flat metal tail.

[12] Sanctorius Sanctorius (1561–1636).

[13] Robert Hooke (1635–1703).

[14] It has been reproduced by the *Museum of History and Technology of the Smithsonian Institution*, now *National Museum of American History*, Washington. Catalogue number MHT 318,489. Smithsonian Photo number 61902-B.

[15] Giovanni Poleni (1683–1761).

[16] Pierre Bouguer (1689–1758).

[17] Heinrich Wild (1877–1951).

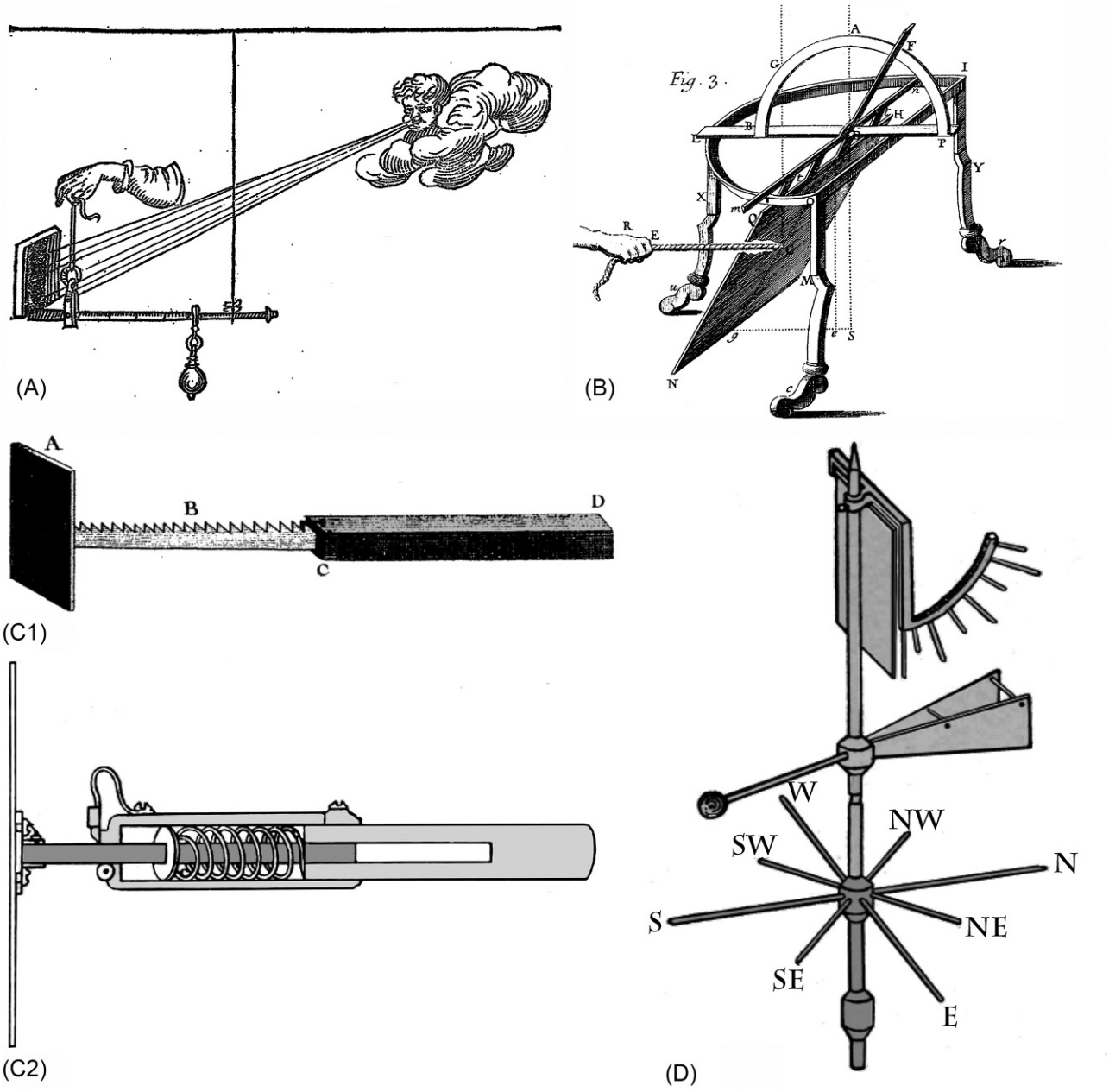

FIG. 20.9 (A) Sanctorius wind force sensor, weighing the force exerted on a plate, i.e. counteracting it with a steelyard. From Sanctorius (1625). (B) Poleni wind force sensor with graduated circular scale. A man is exerting a traction force with a rope to find the correspondence between force and angle. Poleni provided a table to transform inclination angles into wind force. From Poleni (1734). (C) Two models of Bouguer wind force sensors that measured the wind pressure exerted on a plate from its displacement counteracted by a spring (C1): external view, from Cotte (1774); (C2): cross section of a pressure anemometer, showing the spring, from Brewster (1832). (D) Wild's *tablet anemometer* in combination with a V-shaped vane. Both had visual readings. From Eredia (1929).

The Wild anemometer became very popular in Europe (Eredia, 1929, 1936), was frequently mentioned in the literature, but with scarce documentation about its performance. A synthetic description of it is the following: "The Vienna Congress[18] has recommended the introduction of Professor Wild's pressure gauge which is in use in Russia and Switzerland. This consists of a rectangular plate hung on hinges on a horizontal axis. The angle that

[18] The Vienna Congress was held in 1873 and was concerned on the foundation of *the International Meteorological Committee* aimed to coordinate, collect, harmonize, share, and publish weather records. The first president was Christoph Buys Ballot.

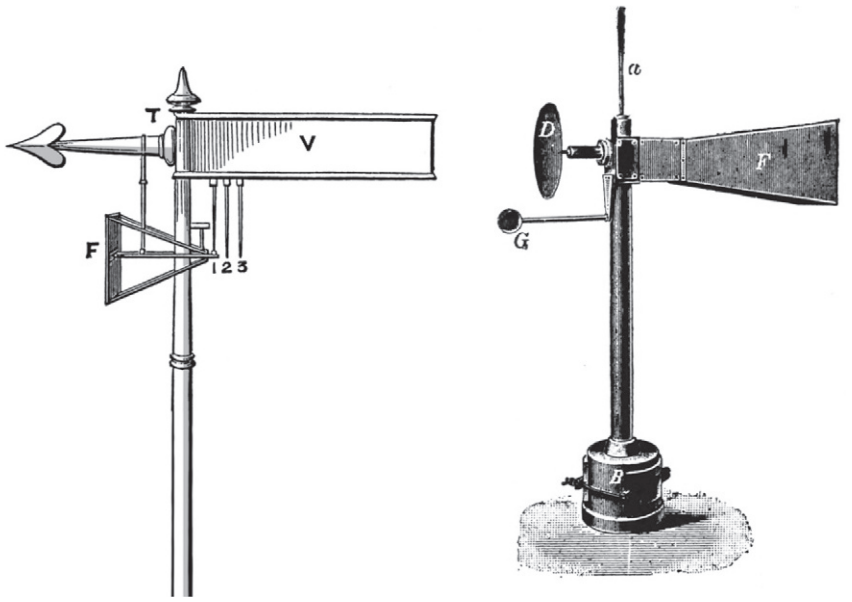

(A) (B)

FIG. 20.10 Pressure-plate anemometers recording the wind force. (A) Osler's mechanical pressure-plate wind force recorder in combination with a flat vane. From UK Meteorological Office (1875). (B) Electro-mechanical development of wind recorder, with circular plate, electrical resistance for the wind force, and electrical contacts for the compass direction. From Eredia (1936).

this makes with the vertical indicates the force of the wind. This instrument gives sufficiently accurate results for light winds, but fails in the case of strong winds. A plate which is light enough to mark the differences between forces 1 and 2 of Beaufort's scale, will be kept in a nearly horizontal position by even a moderate breeze, so that there will be no perceptible difference in the indications for forces 6 or 7 and those for forces 10 or 11" (UK Meteorological Office, 1875). As a matter of fact, Wild was active in Switzerland, became Director of the Central Physical Observatory, St Petersburg, Russia, was member of international commissions, and this favoured the dissemination of his anemometer. Especially in eastern Europe and Russia, this instrument was considered a must, and is still used as an auxiliary one.

The next effort was to pass from visual to recording anemometers. The self-recording pressure plate by Osler[19] (Fig. 20.10A) (Lloyd 1844–1847) was used in the *Magnetical and Meteorological Observatory*, Dublin. It was similar to the Bouguer wind force sensor but was more complex, and was highly appreciated: "Until recently, the most perfect pressure anemometer was Osler's in which the force of the wind is measured by the distance to which the pressure plate is driven back on the springs. This motion is communicated to a pencil, and the record preserved on paper" (UK Meteorological Office, 1875). It was further developed with circular plate in combination with electrical resistance to record the wind pressure, and electrical contacts to record the compass direction (Fig. 20.10B). This advanced instrument had the threshold around $4\,m\,s^{-1}$ (Eredia, 1936) and other limitations as discussed earlier for pressure-plate anemometers.

Except for some local traditions, the pressure-plate method was abandoned by the majority of the weather services in the first decades of the 20th century.

20.1.7 Measuring the Wind Pressure Exerted on a Tube

The physical principle of the higher pressure exerted upwind, and the lower pressure downwind stimulated another, more fruitful invention. Huet[20] considered that the wind blowing against the open end of a tube should increase the pressure at this end, and decrease at the other end (Huet, 1722 posthumously). If the tube is bent forming a U and is filled with a liquid, in the absence of wind the liquid reaches the same level in both arms of the U. If wind is blowing, the difference between the two arms increases with the wind speed. Huet considered it more convenient to use a tube with variable section, like a horn, i.e. large upwind and thin downwind (Fig. 20.11A). In order to magnify and transmit the signal on the thin section, he used a combination of two liquids: quicksilver in the U and a column of water above the quicksilver in the thin arm, where the

[19] Abraham Follett Osler (1808–1903).

[20] Pierre Daniel Huet (1630–1721).

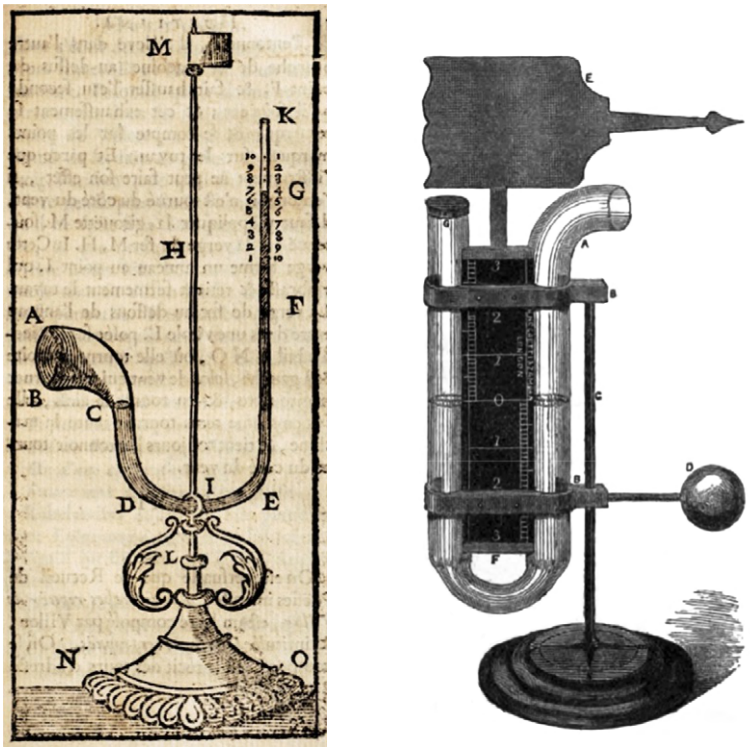

(A) (B)

FIG. 20.11 (A) Huet pressure anemometer, with the characteristic horn shape. From Huet (1722). (B) Lind pressure anemometer combined with wind vane. From Negretti and Zambra (1864).

tube was graduated. Unfortunately, Huet died before he could complete his instrument, and his publication. However, his idea had some followers.

Fifty years later, Lind[21] built a pressure anemometer very similar to Huet, but the tube had constant section except the lower part of the U-shaped glass tube that was narrowed to damp oscillations for wind gusts (Lind, 1775). He used only one liquid: quicksilver. One century later, Arthur Forbes combined Lind's anemometer with a wind vane to keep the pressure sensor aligned with the blowing wind (Forbes, 1863–1865; Negretti and Zambra, 1864) (Fig. 20.11B). Lind's anemometer was mentioned in several scientific journals and used in a number of weather stations. The mercury, however, was too heavy and this instrument had a too high threshold and its use was limited to windy regions.

Ten years after Huet, Henri Pitot[22] found a fruitful solution based on an advanced theoretical approach. He devised an instrument to detect the stream velocity in rivers or a ship speed (Pitot, 1732). The original device was composed of two open-ended glass tubes, fixed to a wooden frame, and placed vertically inside a water stream (Fig. 20.12A) (Pitot, 1732; Weisbach, 1847; Napier, 1872). The first tube was straight and was immersed vertically; it had the opening facing the stream and experienced the static pressure. The second tube was L-shaped, with the lower extremity bent to a right angle. It also was immersed vertically, but the lower opening was oriented facing the current. It experienced a higher pressure (i.e. the stagnation pressure) that caused the water to rise above the surface of the stream. The river surface had the same level as the water in the straight tube, but inside the tube, it was more easily readable, being less affected by capillary waves and other disturbances. In addition, the capillary error was equalized. The difference between the two levels was related to the stream velocity.

Pitot considered that, in a dynamic system, the *stagnation pressure*[23] p_t in front of a tube oriented with the stream is higher than the pressure tangent to it (i.e. along the side of the tube), more precisely p_t equals the sum of

[21] James Lind (1716–94).

[22] Henri Pitot (1695–1771).

[23] In fluid dynamics, the *stagnation pressure* is the static pressure reached in the point (called stagnation point) where the fluid velocity is zero and all kinetic energy is converted into pressure energy. It is also called *total pressure*, being the sum of the static and dynamic pressure. The *static pressure* (or, simply, pressure) is the pressure that a fluid exerts when it is not moving. The *dynamic pressure* is the pressure that a fluid exerts on a surface because of its motion and corresponds to the kinetic energy per unit volume of the fluid particle.

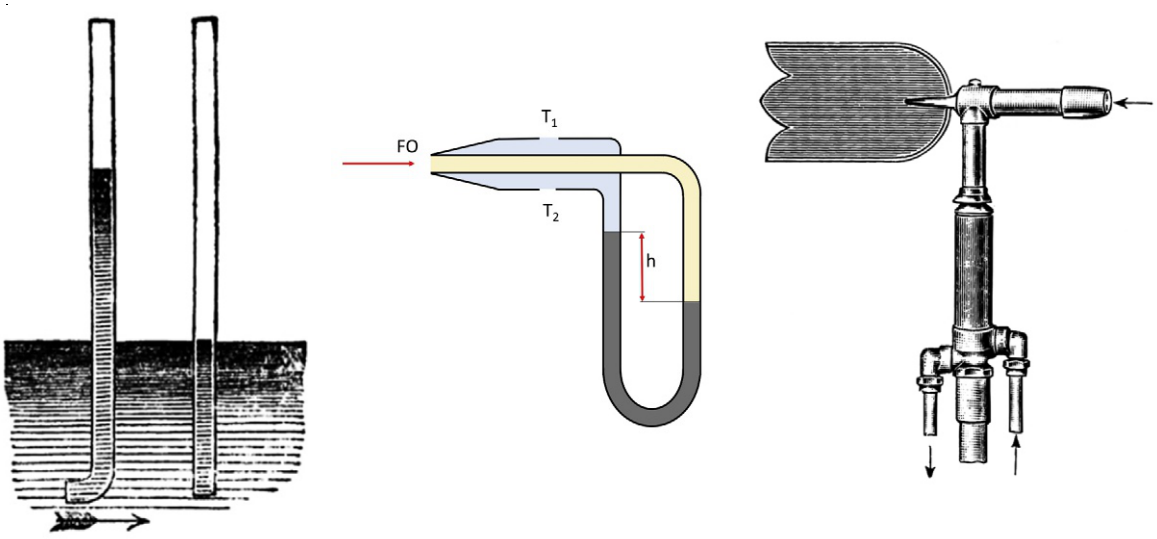

FIG. 20.12 (A) The solution devised by Pitot with two tubes to detect the stream velocity in rivers. From Napier (1872). (B) Operating principle of a Pitot-Darcy tube. The airflow undergoes stagnation at the frontal orifice (FO) and the stagnation pressure there is compared with the static pressure at two tangent orifices (T_1 and T_2). The dynamic pressure is given by the difference in level h between two arms of a U-shaped manometer and is related to the airspeed. (C) Dines anemometer composed of a Pitot-Darcy tube fixed to a wind vane. From Vercelli (1933).

the *static pressure* p_s and the *dynamic pressure* $p_d = \rho u^2/2$, where ρ is the density of the fluid (e.g. $\rho = 1.205 \times 10^{-3}$ g cm^{-3} for air; $\rho = 1.0$ g cm^{-3} for water) and u the stream velocity, i.e.

$$p_t = p_s + \left(\frac{\rho u^2}{2}\right) \tag{20.1}$$

hence the flow velocity:

$$u = \sqrt{\frac{2(p_t - p_s)}{\rho}} \tag{20.2}$$

where the pressure difference $(p_t - p_s)$ is related to the difference of level h reached in the two arms of the instrument.

The original device was based on a poor technology and was not very useful. One century later, Darcy[24] improved the idea and developed a good instrument (Darcy, 1858). A modern Pitot-Darcy tube (popularly named Pitot tube) is sketched in Fig. 20.12B, with a hole in correspondence of the stagnation point in front of the tube, and two holes perpendicular to the lateral surface, where the stream exerts the static pressure. The instrument measures the dynamic pressure, i.e. the difference between the pressure at the stagnation point, and the static pressure. This is determined by the fluid density and the square of its velocity. The densities of water and air are in the ratio of 1 to 0.0012. Therefore, the Pitot-Darcy tube is especially convenient for liquids (i.e. high density, e.g. to determine ship velocity). Gases need very high stream velocities (e.g. aircraft velocity). It is also used in the industry, but not in the field of cultural heritage where light airstreams are better measured with other methods, e.g. hot wire, film, or sonic anemometers.

In 1892, Dines[25] combined a Pitot-Darcy tube with a wind vane (Fig. 20.12C) and connected the ducts to a sensitive pressure gauge. This anemometer had a satisfactory response to medium-to-high wind speeds. In particular, for its compact size, it was very robust and efficient with gale winds reaching 180 km h^{-1} (Gold, 1936). However, it had low performance with low wind speeds for the poor response of the flat vane that was unable to keep the tube aligned with the wind. After the instrument was refined with more efficient vanes, it was the primary recording instrument used in Australia until 1990s, when it was replaced with cup anemometers (Miller et al., 2013).

[24] Henry Philibert Gaspard Darcy (1803–58).

[25] William Henry Dines (1855–1927).

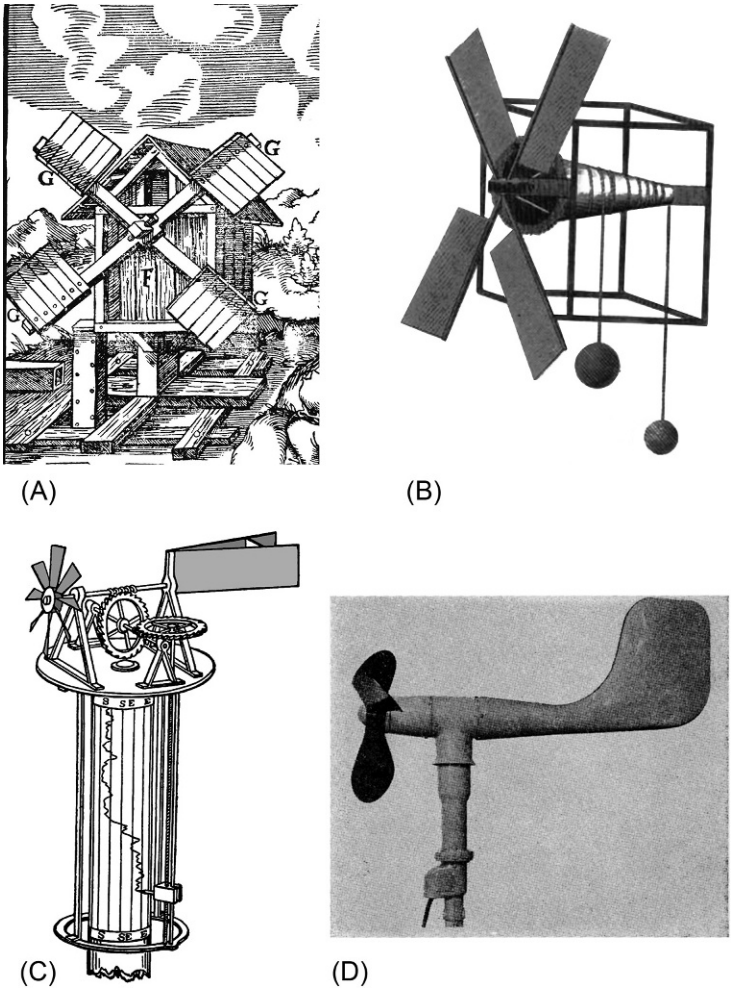

FIG. 20.13 (A) Wind mill with wooden blades, mid-16th century. From Agricola, (1556). (B) Wolfius wind mill anemometer. From Brewster (1832). (C) Whewell recording blade anemometer coupled with a V-shaped vane. From Tomlinson (1861). (D) The earliest aerovane. From Wood (1945). © American Meteorological Society. Used with permission.

20.1.8 From Windmills to Blade Anemometers

Wind pumps and windmills (Fig. 20.13A) use the wind pressure exerted on canvas sails, or wooden blades. Wind pumps were used to raise water since the 9th century in what is now Afghanistan, Iran, and Pakistan (Lucas, 2006), and are still used in United States, Argentina, China, New Zealand, and South Africa. In Europe, windmills appeared in the 12th century to grind grain or to lift weights (Agricola, 1556). Where wind had a dominant direction, mills were fixed. Otherwise, they could be rotated to follow the wind direction.

Around 1672, Robert Hooke made an estimation of the wind speed by counting the number of rotations of a windmill in a given time interval, by using a gear system (Feldman, 1998), and this was an excellent start.

In 1709, Wolff[26] (1679–1754) built an anemometer, known as the *Wolfius anemometer*, inspired by windmills (Fig. 20.13B) (Wolff, 1709). It was employed as an instrument to detect the wind speed, by evaluating the behaviour of a load and a counterpoise on conical axis that rotated with the blades. However, it was also employed as a machine to wind up weights or pump underground water (Brewster, 1832).

From 1834 to 1846, Whewell[27] invented and improved anemometers, and built an interesting recording blade anemometer (Fig. 20.13C) (Tomlinson, 1861; Todhunter, 1876) that may be considered an ancestor of modern instruments.

Blade anemometers are robust and powerful, but required a continuous alignment with the wind. For this reason, they were combined with a vane: the blades upwind and the vane downwind.

[26] Christian von Wolff (1679–1754).

[27] William Whewell (1794–1866).

As the effective surface of a blade changes with the cosine of the angle with the blowing wind, measurements were sensitive to the instrument's orientation relative to the wind direction, i.e. the *attack angle*. Relevant underestimations could derive when the wind swings around the main direction.

The aerodynamic combination of a blade and a vane is the *aerovane* (Fig. 20.13D), invented in 1945 by Wood[28] (Wood, 1945). The aerovane produced by Belfort is very similar to the Wood model; other firms developed slightly different models to fit with specific peculiarities. The aerovane has aerodynamic shape, linear response, rugged construction, and can resist to harsh environments, e.g. marine, polar, mountain sites. The rotational inertia of the blades stabilizes the anemometer cutting off the short-term fluctuations, but this introduces the (small) error of a continually variable attack angle. The instrument is excellent for meteorological or agricultural purposes, not convenient for pollution studies where the variance is relevant.[29] Today propeller anemometers are very popular for meteorological purposes, especially appreciated for the stability generated by the angular moment of rotating blades that cuts off directional fluctuations.

Outdoor wind and indoor ventilation require different instruments. In 1837, Combes[30] made a monumental work about mining technology, including ventilation, and introduced a hand-held whirling anemometer to determine ventilation and air currents in mines (Combes, 1837, 1844; Dikinson, 1876). It was defined a revolving instrument, being put into motion by the impact of the wind, upon four vanes, fixed like the sails of a windmill, at an angle with the direction of the wind, and required the application of a formula to reduce the numbers indicated by its index to the actual velocities (Atkinson and Daglish, 1861). The whirling anemometer was not combined with a vane, because in a tunnel the airflow direction is fixed, and the only variable is the airspeed. In 1842, Biram[31] patented a similar anemometer, but with eight blades (Fig. 20.14A), called the *revolving anemometer*, which was used in the coal mines of England (Biram, 1843; Byrne, 1869) and in other applications. Hand-held whirling anemometers became soon popular, had various developments (e.g. Fig. 20.14B), and are still today used to measure air speed in ducts, corridors, or from one room to another, or when air blows in a fixed direction.

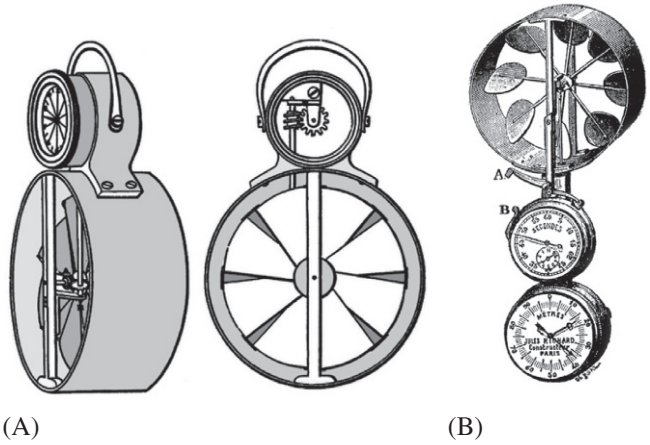

(A) (B)

FIG. 20.14 (A) Side and front view of Biram's hand-held blade anemometer. From Byrne (1869). (B) Hand-held circular blade anemometer produced by Jules Richard firm. From Eredia (1929).

20.1.9 Cup Anemometers

The cup anemometer (Fig. 20.15A) was invented in 1846 by Robinson[32] (Robinson, 1880). It was self-sufficient, i.e. it didn't need a vane to follow the alignment with wind. The real advantage of its symmetry was that it was always equally exposed to wind, without the problem of attack angles. A weather station needed two separate instruments: a cup rotor for the wind speed and a vane for the direction.

The easiest mechanical solution was the four-cup anemometer, composed of two perpendicular arms having two hemispherical cups at their extremes, mounted on a vertical shaft, to balance the centrifugal force. The Robinson cup anemometer was highly appreciated and recommended for use at international level, and produced in slightly different versions by instrument factories (Simons's, 1866). For instance, Casella, London (Casella, 1871), produced a weather station anemometer with Robinson cups, but assembled with a wind vane and a recording system and an improved mode of indicating readings (Fig. 20.15B). Negretti and Zambra, London (Negretti and Zambra, 1864), produced another slightly different assembly.

The operational principle of cup anemometers is based on the different drag coefficient of the two sides (i.e. concave and convex) of a hemispherical cup. This is a very efficient system, although the theoretical approach

[28] Louvan E. Wood (1907—unknown).

[29] Air pollution studies should be performed with more suitable instruments, e.g. three-axial sonic anemometers, three axial micro-propellers, cup anemometer combined with a flat vane.

[30] Charles Pierre Mathieu Combes (1801–72).

[31] Benjamin Biram (1804–76).

[32] Thomas Romney Robinson (1792–1882).

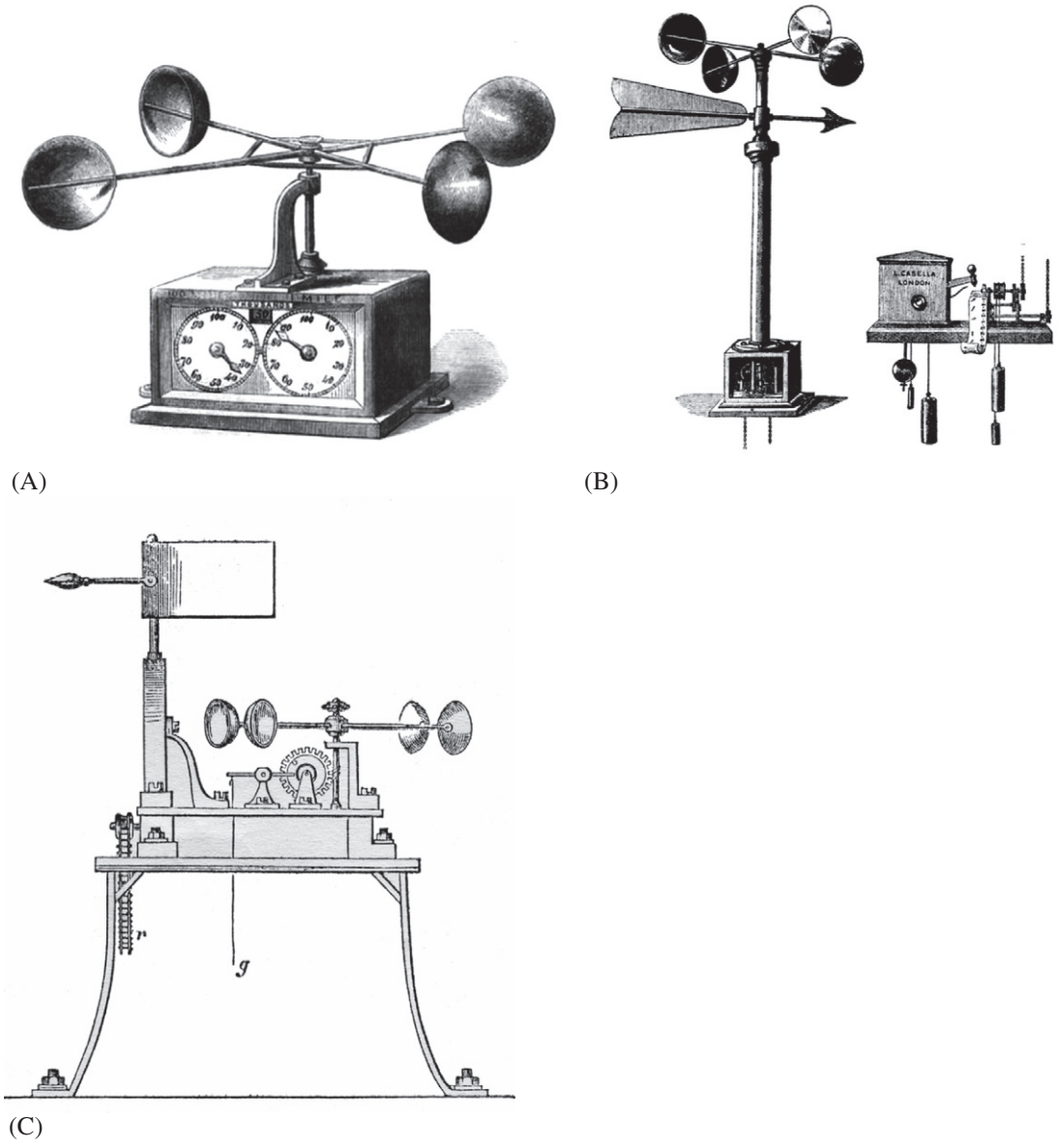

FIG. 20.15 (A) Robinson cup anemometer. From Tomlinson (1866). (B) Casella cup anemometer with flat vane and transmitter. From Simons's (1866). (C) The self-recording anemograph Parnisetti-Brusotti with Robinson cups and flat vane recommended by the Italian Ministry for Agriculture, Industry and Trade in 1872. From IMAIT (1872).

needed improvements, wind tunnel tests, and aerodynamic simulation. Historically speaking, Robinson neglected the self-induced turbulence. He believed that the wind was the same for each cup, but the pressure exerted by the wind, and the air drag, was 1/4 greater on the concave side than in the convex one (Simons's, 1866). The situation is illustrated in (Fig. 20.16). In the absence of turbulence (i.e. only in laminar regime), the wind vectors W1, W2, W3, and W4 are the same. The push of W1 was estimated to be 1/4 greater than that of W4, while the pushes of W2 and W3 are equal and opposite. However, each hemisphere creates a turbulent shear. The upwind cup W2 creates dissipation and subtracts energy to the downwind cup W3 that receives less push, i.e. $W3 < W2$. As turbulence increases not linearly with wind intensity, the response of the anemometer was not linear and needed a correction for speeds higher than 9 mph (14.48 km h^{-1}). In addition, as all anemometers, the response was affected by the impact of raindrops and their momentum.

In 1926, Patterson[33] suggested the three-cup array that has better aerodynamic performances, including lower

[33] John Patterson (1872–1956).

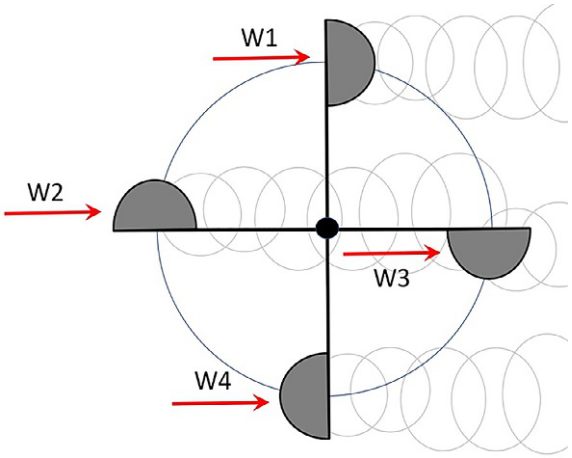

FIG. 20.16 Diagrammatic section of a Robinson cup anemometer, and the wind vectors (W1, W2; W3 and W4) on cups. Robinson supposed that the push of W1 on the concave side was 1/4 greater than W4 on the convex side, and the effects of W2 and W3 were equal and opposite. However, for the turbulence wake *(small grey circles)* generated by the cups, W3 < W2 and the system is neither symmetric nor linear.

dynamic inertia and higher linearity (Patterson, 1926). This type has practically substituted Robinson's and is the most popularly used anemometer in meteorology, agriculture, and other environmental applications.

20.2 PART 2: MODERN TECHNOLOGY TO MEASURE WIND AND AIR MOTIONS

20.2.1 Measuring Outdoor Wind Speed and Direction

Introduction

For meteorological purposes, the wind speed and direction are mostly measured with anemometers and wind vanes, respectively. The two transducers may be separated or combined in only one instrument. For air pollution studies, the transducers may be three, e.g. three orthogonal propellers for the three wind vectors. For special studies, other instruments are used, e.g. hot wire, sonic, laser, and Doppler (Lipták, 2003; WMO, 2008; Tropea et al., 2007; Burt, 2012).

Anemometers are based on one of the various physical properties of winds. Some of them have already been introduced in the historical overview; however, they will be reconsidered and discussed in this part to be comprehensible even for readers that may have skipped the overview.

Anemometers Based on Wind Kinetic Energy

Wind kinetic energy causes rotation of cup wheel or propeller anemometers. The cup arms are supported by a vertical shaft and are insensitive to the wind direction; the propeller is continually oriented by a vane. The rotation is transformed into electrical signal by means of photo choppers, magnet system output signal, contact switches, direct current generators (i.e. tachometers), or other systems. The threshold varies with the friction and the energy subtracted by the transducer. Photo choppers do not subtract energy, reed switches subtract a very small amount and tachometers subtract a considerable amount.

This anemometer type has low sensibility but is resistant to unfavourable environments and is reliable; for this reason, it is typically used by military and weather services, especially in remote stations. Some miniature types may be used in micrometeorological studies for the dispersion of air pollutants.

Cup anemometers are composed of three or four conical or hemispherical cups revolving about a vertical shaft. Originally, a four-cup mounting was used (Robinson type), but the dynamic response of three cups (Patterson type) is better and the majority of instruments follow this finding. The maximum torque produced by a single cup does not occur when the wind blows directly into the concavity of the cup but when it forms an angle of about 45 degrees. The output is essentially linear with constant wind speed up to about 30 m s^{-1} when the cup anemometer is calibrated in a wind tunnel but, in the field, with gusts and lulls, it overestimates the speed as the rotor is more sensitive to increasing than decreasing wind speed, so that it is practically accelerated during fluctuating wind speeds (Moses, 1968; Ramachandran, 1970; Hyson, 1972).

Propeller anemometers (either simple combinations of blades and tail, or combined aerodynamic structures like *aerovanes* or *windmills*) are composed of a propeller and a tail on the same axis. The propeller revolves about a pivoted horizontal shaft that is oriented along the direction from which the wind is blowing. The orientation is governed by the pressure/turbulent drag exerted by wind on the vane tail that is incorporated on the backside of the instrument. The rate of rotation of the propeller is linearly proportional to the wind speed from 1 m s^{-1} up to 45 m s^{-1}. The propeller responds in a different way as a function of the *angle of attack*, i.e. the angle between the axis of the anemometer and the wind direction, and indicates a lower wind speed when the angle of attack increases. As propellers are oriented by a vane, fluctuating wind directions lead to an underestimation of the wind speed because the inertia of the system forces the vane to smooth out and follow with delay the changes in direction and the angle of attack is generally different from 0. The inertia of the system is given not only by the friction and the distribution of the mass in the system, which dominate at low wind speed, but also by the moment of inertia of the blades under rotation, which dominates at high wind speed.

Propellers should respond, to a good approximation, with a cosine law to the angle of attack. Only in this case can they be used to measure the orthogonal components of the wind vector (Camp et al., 1970; Horst, 1973).

It should be noted that both cups and propeller blades are not symmetrical, when observed downwards, on the same vertical. This means that rainfall impresses kinetic energy on initially motionless anemometers. On the contrary, rainfall slows down the rotation at high wind speed, especially when large drops impact on cups having motion opposite to the wind field or when drops impact on uprising blades.

Cups and *propellers* are generally made of metal in order to be rugged and to resist bad weather conditions. However, very sensible sensors are built of thin aluminium or plastic to reduce inertia and thresholds. For low wind speed, polycarbonate cups or polystyrene foam propellers are used, with threshold around 0.1 m s^{-1}. Mechanical sensors cannot be employed for very low wind speed, i.e. below 0.1 m s^{-1}.

Vanes may be either flat or splayed, i.e. vanes composed of two divergent flat plates. Flat vanes offer minimum resistance to the wind, and for this reason they may swing or be unstable. In contrast, splayed vanes increase the resistance to wind and generate turbulence, and this helps to keep the vane oriented with the wind. Therefore, splayed vanes follow even small changes in wind direction better than flat plates. However, the heavy mass of these devices increases the inertia of the system, which is unable to follow high-frequency fluctuations in wind direction. When fast response is needed, e.g. for air pollution and dispersion purposes, low-inertia vanes should be used. Flat vanes are preferred for micrometeorological and air pollution studies and splayed vanes are preferred for meteorological applications where the average wind direction is needed (UK Meteorological Office, 1981).

*Aerovane*s and/or *windmills* have an aerodynamic-shaped structure like an aircraft without wings. They are very resistant but have a very high inertia due to both the distribution of mass (i.e. some 15% torque more than a flat vane with similar physical dimensions) and the moment of inertia of the rotating blades. They operate as a low-pass filter acting on the wind fluctuations and their use is recommended when average values are needed (UK Meteorological Office, 1981).

Anemometers Based on Wind Pressure

Wind pressure is the physical principle behind the pressure tube (Pitot) or pressure-plate anemometer. The *Pitot tube* is based on the Bernoulli law for moving airstreams and consists of a manometer that measures the dynamic pressure, i.e. the difference between the stagnation pressure and the static pressure sampled at orifices on the front of the tube (i.e. the stagnation point) and where the wind field is tangent to the tube. The dynamic pressure is calculated with Eq. (20.1) and is reported in Fig. 20.17.

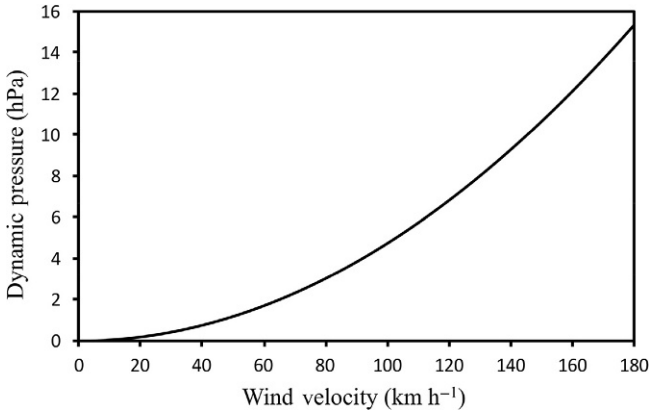

FIG. 20.17 Dynamic pressure exerted by wind.

As the Pitot tube is rugged and responds well to high and very high speeds, it is especially used to measure wind during hurricanes or the aircraft speed.

Wind turbulence, Reynolds stress, and drag coefficient have been measured using a table tennis ball as a sensor, pierced with a vertical metal axle whose tilting is measured with two orthogonal transducers (Smith, 1970).

Anemometers Based on Wind Property of Transmitting Light

The *Doppler effect* is the change in observed frequency of a wave due to relative motion of the source and observer. Laser Doppler anemometry has developed different configurations (Albrecht et al., 2003; Strunck et al., 2004). One of the most important is the differential Doppler, or *fringe* mode, which concerns the interference fringe of two laser beams; suspended particles, transported by the air movement across the dark and light fringe pattern, determine the frequency of electric signals that are then processed to compute the airspeed. The velocity of the suspended particles causes a Doppler shift in the frequency of the light that is scattered, and this is measured with a photodetector. In a relatively clean atmosphere, instruments need the introduction of tracer particles in the airstream. The main advantages are direct method of measuring velocity leaving the flow undisturbed, very small sensing volume (e.g. a cube of 0.2 mm on a side), very high-frequency (e.g. MHz) response, and use for extremely low airspeed. This system is expensive and is more suitable for scientific research than routine measurements. It is better justified for indoor studies (see later).

Installing Anemometers

There are several sources of error in wind speed and direction measurements, but the largest errors are due to the presence of the transducer, which perturbs the wind field, or generates turbulence, or the presence of eddies generated by buildings, trees, or other obstacles; also, the presence of the tower or mast to which the instrument is attached cannot be neglected.

Meteorological measurements of wind speed and direction are regulated by a normative that is extensively reported in many handbooks and that can be summarized as follows. The anemometer should be placed on a mast at 10 m above the ground, over open, level terrain with no obstructions within 300 m. Obstacles, if any, should be at a distance not less than 10 times their height if they are upwind or 5 times if they are downwind. The aim is to observe the wind 'undisturbed', except for the action of the soil friction, i.e. the wind that an aeroplane experiences when it is preparing to land or take off. The same normative has been then applied for use in pollutant transport and dispersion.

For aircraft take-off and landing, and pollution studies, the *wind shear*, i.e. the vertical change of wind speed and direction, is an important parameter. This vertical profile is obtained by installing some anemometers on a tower or tall mast, at heights increasing logarithmically from the soil. Also, vertical profiles of the wind field are obtained launching pilot balloons and measuring their position with two theodolites at regular time intervals (e.g. every 15 s). The wind field is then calculated with trigonometry.

Measuring Wind Vector Components

First of all, *an anemometer measures the total amount of air masses that in unit time is passed through the sensible part of the instrument*, supplying part of its kinetic energy to the cups or propellers that are induced to rotate. The wind gustiness and the smaller-scale turbulence oblige every air parcel to fly not in a straight line but with many vicious loops around the main direction. As a consequence, the space length computed by means of the integral $\int u(t)\mathrm{d}t$, where $u(t)$ is the instantaneous wind speed, is much greater than the real distance travelled by the air parcel from the sensor, and is represented by the average wind vector. If this vector is needed to model the transport of pollutants, three methods are appropriate, as follows.

1. To use a *two-component anemometer*, which measures the two orthogonal vectors of the wind speed. The anemometer is composed of two tachometric generator transducers, mounted at right angle on a common mast. Each propeller measures the component of the wind that is parallel to its axis of rotation. Propellers have been studied in order to have a response to the wind angle that approximates the cosine law. When wind and propeller rotation reverse, signal polarity also reverses. The same principle is adopted for the so-called *UVW* anemometer, which measures the three orthogonal wind vectors *U* and *V* on the horizontal plane and *W* along the vertical. The lateral and vertical fluctuations of the wind are important in micrometeorological investigations of the dispersion of airborne pollutants. Another possibility is to measure the wind components with a three-directional sonic anemometer.
2. To use a *wind vane with a sine–cosine transducer* supplied with a voltage proportional to $u(t)$. This method is much more convenient but needs a special anemometer (Camuffo, 1976). This is substantially composed of a generating anemometer, e.g. a dynamo connected with the propellers (or the cups) that supplies an output proportional to $u(t)$ and this output is used to feed the terminals of the sine–cosine potentiometer of the vane that measures the wind direction. This potentiometer has a continuous-rotation resistance element that varies with the sine function of the shaft rotation and two independent brushes, spaced 90 degrees between them: consequently, one monitors $\sin \alpha(t)$ and the other $\sin(\alpha(t)+90°) = \cos \alpha(t)$, where $\alpha(t)$ is the instantaneous wind direction. When the potentiometer is supplied with the tension $u(t)$, the two potentiometer outputs give $u(t) \sin \alpha(t)$, $u(t) \cos \alpha(t)$, respectively. Continuous resistance elements, e.g. cermet, biofilm, or conductive plastic, should be preferred to wire-wound ones, as the noise is reduced when the brushes oscillate following the wind fluctuations. Generating aerovanes are preferred, as they furnish only one compact and strong instrument. The same result can also be obtained with ordinary anemometers by substituting the linear potentiometer with a sine–cosine one and using the output of the airspeed transducer to supply the power to the potentiometer.
3. To carry out a very frequent sampling of $u(t)$ and $\alpha(t)$ and then *compute* for each instant the vector components $u(t) \sin \alpha(t)$, $u(t) \cos \alpha(t)$. This method is less convenient, for it requires a huge amount of data to be monitored and processed, but can be made with ordinary anemometers.

Averaging Wind Direction

Application of statistical formulae in meteorology needs particular care to avoid inappropriate calculations and misleading conclusions. For instance, during the first part of the summer nights in the plain of northern Italy, cold air flows from the mountain valleys on the southern lee of the Alps and enters the plain, which is

characterized by warmer and moister air masses. These cold tongues force the moist air of the plain to rise up generating local violent thunderstorms very similar to the thermoconvective ones that often occur in the early afternoon. By beginning at midnight, the meteorological observations of the day, some of these thunderstorms are recorded in 2 days and attributed half to the previous and half to the next day, thus misleadingly increasing the frequency of occurrence.

This example helps to understand the behaviour of two air masses when they meet, and vector algebra has to be applied in a correct way to interpret it. When two air masses meet, their dynamic state is represented by two wind vectors but, in general, the resultant is not the vector obtained as the algebraic sum of the two original vectors. If the density of the two air masses is not the same, a frontal situation is generated and the denser one continues nearly unaffected its motion, whereas the lighter one slips above.

It is useful to remember that a wind vane will always point a direction, with or without wind. When the wind drops, the vane remains oriented on the last direction. When the average wind direction is computed, all the directions recorded in the absence of wind speed must be rejected.

Another problem occurs when the mast or the vane shaft is not perfectly vertical. The distribution of the weight in a vane is not always balanced with the rotation axis passing across the centre of gravity of the vane. Out of balance, it shows a bias towards the tilting direction, especially in presence of low wind speed or during calm periods.

In climatology, the frequency distribution makes more sense than the arithmetic average represented by the *mean*. Consider, e.g. the case of a coastal site, with the sea breeze from east (90 degrees) and the land breeze from west (270 degrees). The distribution of the wind direction is bimodal with two peaks at 90 and 270 degrees; as opposed, the mean gives the dominance of a non-existing wind from south (180 degrees). However, although in the long term frequency distributions are necessarily used, in the short term of a sampling interval (e.g. 10 min), the wind is considered to oscillate around a main direction and an arithmetic average is used to compute the mean value.

A common problem, not statistical but technological, is averaging the wind direction with fluctuations in the northern sector. In fact, ordinary potentiometers present a discontinuity between 0 and 360 degrees, so that in the case the wind fluctuates symmetrically around north, averaging the data one obtains 180 degrees, i.e. exactly the opposite direction. If recording is being performed in a strip chart recorder, the trace is a line going back and forth across the whole chart width. Several solutions have been devised to overcome this drawback. Here only a few of them will be presented for their practical interest. Other original devices have been described elsewhere (Camuffo, 1979).

The first system is composed of two identical potentiometers connected with the same vane, the first having the range 0–360 degrees and the second 180–540 degrees being assembled rotated at 180 degrees, i.e. when the brush of the first one reaches the discontinuity 0–360 degrees, the brush of the second is positioned in the middle of the second potentiometer, on the opposite side of the discontinuity. When this happens, the output is switched from the first potentiometer to the second one, so that continuity is ensured for 1½ revolution. The range extension can also be performed with only one potentiometer and an electronic translator, in order to reduce friction and wind threshold. The range extension 0–540 degrees ensures continuity for most of the cases, except when the upper limit 540 degrees is reached and the output is switched to 180 degrees, and as well as the lower limit 0 degrees is reached and the output is switched to 360 degrees.

The second system (Camuffo and Denegri, 1976) can be applied to standard instruments, i.e. a vane coupled to an ordinary potentiometer and only one sliding contact. The principle is as follows. Suppose that the compass is divided into 100 parts, so that each one is represented by a two-digit number from 00 to 99. If north is set at 00, a wind blowing from north and fluctuating around 00, will generate a series of small numbers close to 0, and a series of large numbers close to 99. A solution is found adding 100 to the values close to 00, and then performing the average without the 00–99 discontinuity because it has been transformed into 100–99. By summing 1000 of these numbers, a five-digit number is obtained and the first two figures represent the mean value within this resolution. If three-digit numbers are used, and the first figure is considered as an index of periodicity, then the two figures following the first one in the sum of 1000 numbers represent the mean value related to the compass card. The index of periodicity disappears if the first figure is neglected, even if it has been used to compute the sum. In this example, an index of periodicity from 0 to 2 can be used, which is sufficient to allow complete rotations of the wind vane during the averaging period; in practice, only one extension is necessary to avoid the discontinuity around north. The method consists in adding or subtracting only one unit to the index, depending on whether the wind vane arrives to the discontinuity rotating clockwise or counter-clockwise, i.e. from west or from east. Actually, at the beginning, the index is put equal to 1 and becomes 0 or 2 during the addition. Therefore, when the wind is rotating from the direction labelled 99–00, the corresponding numbers are 199–200, without discontinuity. In our example, making 1000 samplings equally distributed around the former potentiometer discontinuity, i.e. 199–200, the total 199,500 is obtained.

Disregarding the first figure and considering the last three as decimal values, the mean direction 99.5 is obtained. The resolution may be increased by dividing the compass into 1000 parts.

This principle can be applied to ordinary potentiometric wind vanes in two ways. The first is to supply the potentiometer with a fixed voltage and convert the brush output into digital numbers. These numbers, with the proper index, can be summed to obtain the mean value as explained. The second method is obtained with the help of a tension to frequency converter and by counting the pulses during the sampling interval. In this case, before conversion, the voltage applied to the terminals of the potentiometer must be added to the signal measured at the brush if this has moved to the lower value across the discontinuity, or subtracted for the opposite rotation.

Another method is based on the principle that in climatology, frequency statistics are better than performing averages. On this ground, the instantaneous direction is monitored at regular time intervals and after the sampling time, the prevalent direction is found as the middle of the sector with the largest population, i.e. where the mode is located; sometimes, the mode is found by looking at the frequency distribution.

Measuring Wind Variance

The wind variance is a key variable in computing the dispersion of airborne pollutants, and the Brookhaven and Pasquill stability classes were focused on estimating this parameter in the absence of direct measurements. In this case, the actual measurements are concerned and how to transform anemometer readings into variance. Following the definition, the standard deviation σ_θ of the wind direction can be measured as

$$\sigma_\theta = \sqrt{\frac{\left(\Sigma\theta'^2\right)}{(n-1)}} \tag{20.3}$$

where θ' is the angular wind fluctuations determined after recording n measurements of $\theta(t)$, taken with very short sampling time, for a certain time interval. Determination of the variance, made by means of this mathematical definition of σ_θ, has a negative aspect: it needs huge amounts of data, which should be recorded on a data logger having a very large capacity and, therefore, expensive. For this reason, other methods may be preferred and one of them is here described (Camuffo, 1976). In general, fluctuations are symmetrically distributed around the mean wind direction $\langle\theta\rangle$ and the distribution function is fairly well approximated by a Gaussian. As a consequence, the third spectral moment of the fluctuations, called *skewness*, is 0.

As $\theta = \langle\theta\rangle + \theta'$ and recalling the formula for the sum of angles in trigonometric functions,

$$\langle\sin\theta\rangle = \langle\sin(\langle\theta\rangle + \theta')\rangle = \langle\sin\langle\theta\rangle\cos\theta' + \cos\langle\theta\rangle\sin\theta'\rangle$$
$$= \sin\langle\theta\rangle\langle\cos\theta'\rangle + \cos\langle\theta\rangle\langle\sin\theta'\rangle = \sin\langle\theta\rangle\langle\cos\theta'\rangle = \sin\langle\theta\rangle \tag{20.4}$$

$$\langle\cos\theta\rangle = \langle\cos(<\theta> + \theta')\rangle = \langle\cos\langle\theta\rangle\cos\theta' - \sin\langle\theta\rangle\sin\theta'\rangle$$
$$= \cos\langle\theta\rangle\langle\cos\theta'\rangle - \sin\langle\theta\rangle\langle\sin\theta'\rangle = \cos\langle\theta\rangle\langle\cos\theta'\rangle = \cos\langle\theta\rangle \tag{20.5}$$

as $\sin\langle\theta'\rangle = 0$ in that the sine is an odd function and the fluctuations are randomly distributed around 0, and $\langle\cos\theta\rangle = 1$ for the symmetrical reason. Therefore,

$$\frac{\langle\sin\theta\rangle}{\langle\cos\theta\rangle} = \tan\langle\theta\rangle \tag{20.6}$$

where the mean direction is related to the average values of the trigonometric functions sine and cosine. Also in the case of a skew distribution of the fluctuations, i.e. near an obstacle or other disturbing factors, by expanding the sine function in MacLaurin series, i.e.

$$\sin\langle\theta'\rangle = \langle\theta'\rangle - \frac{\left\langle\theta'^3\right\rangle}{3!} + \frac{\left\langle\theta'^5\right\rangle}{5!} - \frac{\left\langle\theta'^7\right\rangle}{7!} + \cdots \tag{20.7}$$

it can be recognized that the error is very small, i.e. less than 1%.

When the fluctuations are randomly distributed, then the central moments are

$$\left\langle\theta'^{2n}\right\rangle = 1\times3\times5\times\cdots\times(2n-1)\sigma_\theta^{2n} \tag{20.8}$$

Substituting this equation in the MacLaurin expansion of $\cos\theta'$ in Eq. (20.4) and Eq. (20.5),

$$\frac{\langle\sin\theta\rangle}{\sin\langle\theta'\rangle} = \frac{\langle\cos\theta\rangle}{\cos\langle\theta'\rangle} = \exp\left(-\frac{\sigma_\theta^2}{2}\right) \tag{20.9}$$

the variance of the wind fluctuations is obtained:

$$\sigma_\theta^2 = -2\ln\frac{\langle\sin\theta\rangle}{\sin\langle\theta'\rangle} = -2\ln\frac{\langle\cos\theta\rangle}{\cos\langle\theta'\rangle} \tag{20.10}$$

The dispersion coefficient is simply obtained from average values measured with a sine–cosine transducer or by computing averages of these trigonometric functions.

20.2.2 Investigating Wind Microstructure and Indoor Air Motions

Weather analysis for general purposes (e.g. meteorology, traffic, agriculture) is focused to know the main wind on the mesoscale and to measure it in the open countryside far from obstacles. Wind measurements for air pollution studies are focused to determine the wind in the real environment, with special focus on the

variance and any other characteristics useful to determine dissipation, transport, and deposition of airborne pollutants. Cultural heritage conservation requires accurate studies in close proximity to monuments, to ascertain their interaction with the atmosphere.

On an open site, wind is represented by the speed that is only a function of time, i.e. $v(t)$, and the same for its direction α on the horizontal plane, i.e. $\alpha(t)$. In proximity to monuments, wind changes both in time and space, point by point, for the aerodynamic interactions, i.e. $v(x, y, z; t)$. In addition, it departs from the horizontal plane so that the angle of attack θ too should be considered, i.e. $\alpha(\theta;t)$. Briefly, it becomes a function of five variables x, y, z, θ, t instead of only one.

This means that standards concerning the best practice to make wind measurements in meteorology may be of little help when considering architectural heritage. Field observations should be only made after a preliminary analysis of the problem, the site topography, and monument features, in order to determine *why*, *what*, *where*, *when*, and *how* to measure.

Observations of low airspeed, turbulence, thin airstream on a developing surface boundary layer, or thin airstream passing below a closed door cannot be made with ordinary mechanical anemometers (e.g. cup or propeller types), for their elevated inertia and threshold or the unbalanced effect on the opposed cups or the inhomogeneous pressure distribution on blades.

Sonic Anemometers

Ultrasonic anemometers, popularly called 'sonic' anemometers are grounded on the wind property of transmitting sounds. They provide very fast sampling at very low threshold, and are very useful in microphysical studies of the planetary boundary layer, e.g. to measure the exchanges of heat or momentum, as well as in the field of cultural heritage, because they can detect airstreams in close proximity to the monument surface as well as to assess draughts and thermal comfort in cold environments (Camuffo et al., 2010).

The velocity of a sonic wave in a medium is known and depends on the elastic properties of the medium. When a sonic wave is superimposed on an airstream, its transmission speed equals the sum of the velocity of the sound with respect to the medium plus the velocity of the medium. Sonic pulses are transmitted in opposite directions over the same path for each axis of measurement. Pulses are exchanged between two miniature piezoelectric transducers that are used to transmit and then to receive. The sonic anemometer measures the average value of the speed of propagation of these pulses. The measurement is representative of the average airflow that crosses a cylinder, i.e. the sonic beam having the cross-section determined by the transducer size and the path length L equal to the transducers spacing. The space resolution is determined by the transducer size (typically of the order of 1 cm diameter) and the value of L, which varies with the model, e.g. 15 cm, 40 cm. However, the higher the space resolution, the greater the perturbation caused by the transducers to the air motion.

Sonic anemometers may be divided into two classes. The continuous-phase sonic anemometer transmits across the path of interest a continuous beam of sonic energy; the phase of the received signal is compared with a fixed or reference phase. The pulse sonic anemometer transmits sonic energy in bursts over the path of interest. Sonic pulses are transmitted in opposite directions over the same path on each axis of measurement. Pulses travelling with the wind arrive sooner than those travelling against the wind. The main advantages of this instrument are: it is linear, has a very fast response (i.e. a few milliseconds, so that it can respond to high-frequency wind fluctuations), and has a very low threshold.

The operating principle (Beaubien and Bisberg, 1968; Tropea et al., 2007) is that the sound wave transmitted in still, or moving air, introduces a time lag that depends on the airspeed and direction. The first equation that governs the operating principle concerns the velocity C of sound in still air, i.e.

$$C = \sqrt{\frac{\gamma \Re T}{M}} \tag{20.11}$$

where γ is the ratio between the specific heats at constant pressure and volume, $\Re$ the universal gas constant, and M is the molecular mass of the gas, i.e. 28.97 g mol^{-1} for dry air. At $T = 273.15$ K, the speed in the air is 33,145 cm s^{-1}.

Therefore, a sonic anemometer is always associated with a precise thermometer whose measurements are necessary to enter the formulae and compute the sonic velocity. However, the elevated presence of moisture may also cause departures from the measurements increasing the sonic speed. As water vapour has mass ($M_W = 18.015$ g mol^{-1}) noticeably different from the other gases constituting the atmosphere, the following empirical equation holds for humid air

$$C = 2006.7\sqrt{T\left(1 + 0.3192\frac{e}{p}\right)} \ (\mathrm{cm\,s^{-1}}) \tag{20.12}$$

where e is the water vapour pressure and p the atmospheric pressure. The variable vapour pressure is a source of error and the largest errors occur in summer, e.g. at $T = 303$ K and relative humidity = 70%, $e = 30$ hPa, and this is equivalent to 0.3°C shift in air temperature. The error is smaller in the cold season.

When the airstream is moving at speed u and angle θ with reference to the transducer alignment, the sonic anemometer measures the speed component $u \cos\theta$ by means of the sonic transit time Δt, which is given by

$$\Delta t = \frac{2Lu\cos\theta}{C^2\left(1-\frac{u^2}{C^2}\right)}\ (\mathrm{s}) \qquad (20.13)$$

that is the basic equation for sonic anemometry.

The main interest for the sonic anemometer is that it has very low threshold (e.g. 1 cm s^{-1}), and is a totally passive instrument that does not interfere with the fluid motion, except for the presence of the transducers that may generate turbulence.

Flux measurements are accurate with a good cosine response of the sensors (Gash and Dolman, 2003; van der Molen et al., 2004). The experimental array can be composed of one, two, or three axes, each having a pair of aligned transducers, depending on the number of dimensions that should be taken into account (Fig. 20.18). For these mentioned reasons, the measurements are not as punctual as with a hot wire and cannot go close to a surface such as a hot wire, but these goals are much better attained with a laser Doppler anemometer.

Sonic anemometers are useful to measure either fast or slow air motions in the free air or in proximity of objects. This helps in evaluating deposition rates and soiling or other variables useful in preventive conservation.

Laser Doppler Anemometers

A number of different configurations exist, of Laser-Doppler anemometers, but the most used is the differential Doppler, also called *fringe mode*. The air is transparent to laser light but a number of reflecting particles introduced in the airflow may diffuse light, introducing a Doppler shift generated by their movement. By crossing two coherent light beams having plane wavefronts (i.e. two laser beams generated by the same source), an interference fringe is generated in the crossing area. The fringe

(A)

(B)

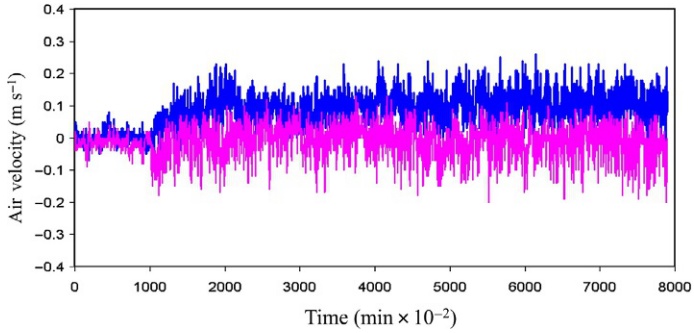

(C)

FIG. 20.18 (A) Outdoor use of a bi-dimensional sonic anemometer to measure the ventilation in proximity of a monument surface. (B) A sonic anemometer positioned above pews to monitor air draughts when pew heating is operated. (C) Record of the two orthogonal components *(blue and magenta)* of the air movements. The air is initially still, but when the heating is turned on (time = 1000) the intensity of air movements increase, with fluctuations from −20 to +20 cm s^{-1}.

spacing is proportional to the wavelength of the light λ and inversely proportional to the angle 2θ between the two beams. A particle moving in the intersection of the two beams will scatter light whose intensity will vary according to the intensity pattern of the light as determined by the brightness of the interference fringe. The frequency of the light scattered by the airborne particles is characterized by a Doppler shift generated by the velocity of the particles. A photomultiplier detects these variations and the frequency of the resulting signal is determined from the Doppler analysis (Durst et al., 1981; Albrecht et al., 2003; Strunck et al., 2004). The frequency f of the electric signal generated by a particle moving across the fringe volume with velocity component u normal to fringes is

$$f = 2\frac{u \sin\theta}{\lambda} \tag{20.14}$$

so that for a typical wavelength and $\theta = 30°$, f is of the order of 10^5 Hz (Doebelin, 1990). The method is more sensitive when the fringe pattern is perpendicular to the airflow and hence the fringe can be rotated to obtain the highest sensitivity (and find the airstream direction) or to obtain the two components of the velocity vector in the plane parallel to the surface.

This method is very accurate as the interference fringe area can be very small (i.e. with size of the order of a tenth of millimetre) and can be sited very close to the surface, or in contact with the surface, i.e. within the internal boundary layer that develops on the surface. This instrument is able to measure air motions very close to a surface and is potentially very useful for studying air–surface interactions and aerodynamic deposition. Another important advantage is that the measure is direct, the flow remaining undisturbed by measurement, without needing the introduction of solid probes or mobile items into the airstream. The response is immediate.

The negative aspects are substantially three. The first is that the airflow must be seeded with tracers, i.e. particles that may deposit on the surface, soiling and potentially damaging it. The second is that the introduction of tracers near the surface perturbs the natural dynamic equilibrium under investigation. Last but not least, the instrument is very expensive.

Hot Wire and Hot Film Anemometers

The airstream cooling power is used in hot wire or hot film anemometry. The principle is to measure the current required keeping constant the temperature of an overheated wire. Alternatively, to measure the change of temperature of a wire heated at constant current. As the wire is very thin, the probe is very small and sensible, fast response, particularly suitable for microclimatic studies and to monitor low-speed air movements as well as short-term fluctuations. The sensor is very fragile and must be used with great care and is more suitable for indoor studies.

Miniature *hot wire* (or *hot film*) anemometry is appreciated for its simple use and low cost (Fig. 20.19). The size of the sensor is of the order of one or few millimetres in length and the diameter is of the order of 5 μm. The hot wire measures airspeeds above 10 cm s^{-1} and the time constant is of the order of 0.001 s. A lower threshold, i.e. 5 cm s^{-1}, is obtained with a nickel thin film deposited by sputtering on a spherical glass sensor, with a diameter of 3 mm (Dantec, 1996). The relatively larger mass increases the time constant to 0.08 s and the overheating generates a convective motion that interferes with the air movement at low airspeeds. This interference determines the lower limit of reliable measurements, which is around 3 cm s^{-1}.

As a single wire responds to the velocity component perpendicular to it, a variety of probes exist, mounted either single or coupled orthogonally in a plane or three-dimensionally, suspended between the tips of a fork-like support, for detecting one, two or three components of the airstream. Some probes are inserted into a cylindrical shield (a tube) in order to measure the stream component along the cylinder axis. However, the edges of the tube disturb the flow field and generate departures, instability or even turbulence. It is convenient to remove this shield and insert the bare probe into the airstream, with the wire normal to the flow direction.

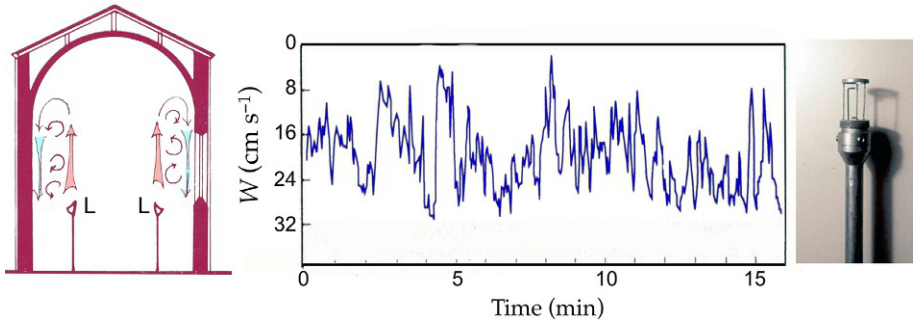

FIG. 20.19 A hot wire anemometer (to the right) was used inside the Giotto Chapel, Padua to monitor the vertical flow (W) of warm air *(red arrows)* ascending over the incandescent lamps (L) and the cold return flow *(cyan arrows)* along the frescoed walls (to the left). The observed flow along the frescoes has speed fluctuating between 0 and 32 cm s^{-1}. From Camuffo and Schenal (1982) (see credits).

The physical principle (DISA, 1976; Doebelin, 1990; Tropea et al., 2007) is the thermal loss of an overheated wire operating as resistance sensor. The heat loss not only depends on the airspeed but also on a number of parameters such as air temperature and pressure. If only the airspeed changes, or the influence of the other parameters is compensated through other sensors and suitable electronic units, the output gives the airspeed. The characteristic transfer function is in first approximation composed of an exponential and a square root function, but the signal can be linearized, so that the processed output is simply proportional to the airspeed.

Two different circuits are available for these kinds of sensors: the *constant-temperature* and the *constant-current* anemometer. The constant-temperature type consists of a Wheatstone bridge and a servo amplifier and the sensor acts as the active arm of the bridge. The current through the wire is adjusted to keep the wire temperature constant and is a measure of the flow velocity. The constant-current type has the sensor powered by a constant current supplied by a generator having high internal resistance in order to be independent of any resistance changes in the bridge. The wire reaches an equilibrium temperature that is determined by the heat exchanges with the airstream. The heat generated is the product of the electrical resistance, the square of the current intensity and the wire temperature. Briefly, the airspeed is measured in terms of the electrical resistance. In practice, constant-temperature anemometers are preferable and are effectively popular for their easy use, fast response and low cost.

A Simple Analysis of Atmospheric Turbulence

Several approaches exist to study the atmospheric turbulence, and several books have been written on this subject, e.g. Sutton (1960), Pasquill (1962, 1974), Lumley and Panofsky (1964), Tennekes and Lumley (1973), Csanady (1980), Vinnichenko et al. (1980), Newstadt and Van Dop (1984), Landahl and Mollo-Christensen (1986), and Clifford et al. (1993) and many others exist on the statistical analysis of time series. However, it may be useful to report some notes on a statistical method that was originally introduced by Rice (1944, 1945) for the telephone random noise and then adapted by some oceanographers (Cartwright and Longuett-Higgins, 1956; Longuett-Higgins, 1957, 1962; Kinsman, 1965) to the analysis of the sea waves. Simple analytical methods were necessary in times before the advent of powerful computers that can easily handle huge amounts of data and perform sophisticated mathematical analyses.

The methodology can be applied to the atmospheric turbulence, as the instrumental records of the instantaneous sea level and the wind speed are very similar between them: the average sea level is substituted by the mean wind speed and the fluctuating waves by eddies.

Although the theory is quite complex, the application is simple and needs only counting the number of times the signal crosses the mean level and the total number of fluctuations. It gives the mean airspeed, average period of eddies, modes of gusts and lulls, the spectral width parameter, and the first three even spectral moments.

The zero-crossing period is defined as the average period $\tau(0)$ for which a sensor placed at the average sea level (which is assumed as zero level) is alternatively submersed by waves and then emerges and is expressed as $\tau(0)=T_i/N(0)$ where T_i is the observing time interval and $N(0)$ represents the number of times that the waves have exceeded the calm sea level. In the same way, the crossing period $\tau(\eta)$ is defined as the number of crossings $N(\eta)$ for every arbitrary level η, i.e.:

$$\tau(\eta)=\frac{T_i}{N(\eta)}=\tau(0)\frac{N(0)}{N(\eta)} \tag{20.15}$$

and the mean zero-crossing frequency $F(0)$ and the η-level frequency $F(\eta)$ are obviously defined as the inverse of $\tau(0)$ and $\tau(\eta)$, respectively. To apply this statistical method to wind or air movements, the following obvious substitutions are required: eddy turbulence for waves, airspeed or wind direction for sea level, mode of the instantaneous air velocity or direction for the average sea level.

If m_o is the zero-order moment, i.e. the standard deviation of the wave height, the second-order moment of the spectrum is $m_2=m_o(2\pi\ f(0))^2$. The plot of the distribution $N(\eta)$ versus η (Fig. 20.20A) is bell shaped with the maximum at $N(0)$ and the standard deviation can be graphically obtained by measuring the half of the segment that intercepts the plot of $N(\eta)$ at the frequency level $\sqrt{e}N(0)=0.607\,N(0)$. Please note that the maximum at $N(0)$, i.e. the mode, is determined as a first approximation, being conditioned by the choice of the crossing levels, the resolution being the step between two levels. The distribution $N(\eta)$ lies between two limit distributions, i.e. the symmetric Gaussian one

$$N(\eta)=N(0)\exp\left(-\frac{\eta^2}{2m_o}\right) \tag{20.16}$$

for a wide-band spectrum, i.e. random components, and the asymmetric Rayleigh distribution

$$N(\eta)=N(0)\frac{\eta}{m_o}\exp\left(-\frac{\eta^2}{2m_o}\right) \tag{20.17}$$

for a narrow-band spectrum, i.e. when the spectrum is sharply peaked around a definite frequency. Cartwright and Longuett-Higgins (1956) found a general analytical expression for the distribution of any shape of spectrum,

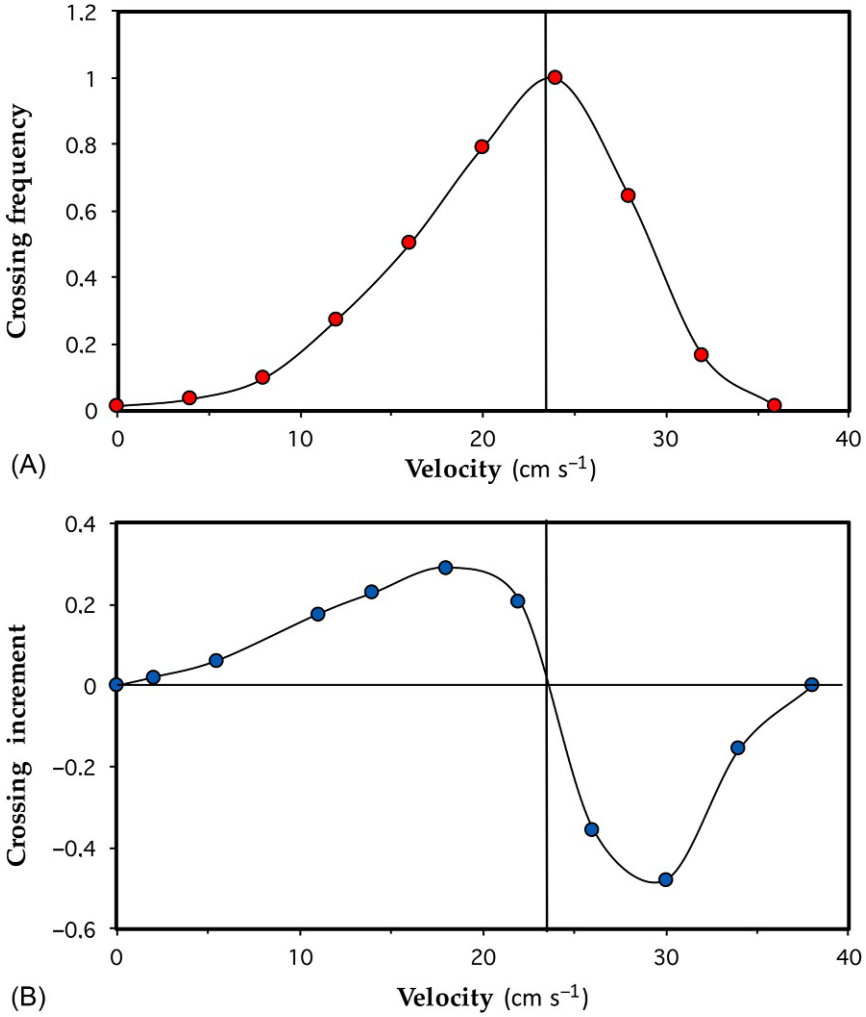

FIG. 20.20 Zero-crossing frequency analysis. (A) Normalized crossing frequency of the velocity levels 0, 2, 4, 6, … cm s^{-1} in an internal boundary layer along a wall. The distribution is skew, being slowed down by entertainment of calm air. (B) Plot of the incremental values $N(\eta_i) - N(\eta_{i-1})$, i.e. the number of times the speed has exceeded the velocity level η_{i-1} but not the level η_i, plotted versus the airspeed. The mode of the frequency in (A) corresponds to the change of sign of the increment in (B).

given by the probability distribution $Pr(\zeta)$ of the maxima between the levels η and $\eta+\delta\eta$

$$\Pr(\zeta) = \frac{1}{\sqrt{2\pi}}\left[\exp\left(-\frac{\zeta^2}{2\varepsilon^2}\right) + \zeta\sqrt{1-\varepsilon^2}\exp\left(-\frac{\zeta^2}{2}\right)\int_{-\infty}^{\omega}\exp\left(-\frac{x^2}{2}\right)dx\right] \tag{20.18}$$

where $\omega = (\zeta/3)\sqrt{1-\varepsilon^2}$. The transition from the Gaussian to the Rayleigh distribution is determined by the value of the spectral width parameter ε, which ranges from 0 to 1 and is defined by the zeroth-, second-, and fourth-order moments, i.e.

$$\varepsilon = \frac{m_o m_4 - m_2^2}{m_o m_4} \tag{20.19}$$

The Gaussian distribution is obtained with $\varepsilon = 1$ and Rayleigh with $\varepsilon = 0$. The above authors demonstrated that the value of ε can be simply determined by counting the number of the zero crossings and the number of maxima N_m that have occurred in the same interval, i.e.

$$\varepsilon = \sqrt{1 - \frac{N(0)^2}{N_m^2}} \tag{20.20}$$

and in addition, the mean frequency of the zero crossings $F(0)$ and the mean frequency of the maxima $F(max)$, are linked with the even moments as follows:

$$F(0) = \frac{1}{\sqrt{2\pi}}\sqrt{\frac{m_2}{m_o}}; \qquad F(\max) = \frac{N_m}{T_i} = \frac{1}{\sqrt{2\pi}}\sqrt{\frac{m_4}{m_2}} \tag{20.21}$$

The graphs of the incremental values $N(\eta_i) - N(\eta_{i-1})$, i.e. the number of times the fluctuations (originally: the waves) have exceeded the level η_{i-1} but not the level η_i, plotted versus η are more or less symmetrical with reference to the origin and are characterized by a peak and a valley (Fig. 20.20B). The intercept between the plot of observations and the line 0 crossings (which corresponds to the average level that is assumed as 'zero' reference level, and that is characterized by the maximum of the crossing frequency) gives a better approximation of

the mode. The peak and the valley provide useful information about the distribution of the fluctuations that recur most frequently, i.e. the mode of gusts and lulls.

The method simply requires counting the number of times some arbitrarily selected levels of speed (or some directions) have been crossed by the instantaneous wind speed (or direction) and the number of maxima of this independent variable during the observing interval. There are two operational procedures: (1) to measure continually or to sample with a high frequency the variable, and the arbitrary crossing levels can be selected after the measurement, by subdividing into equal intervals the range of variability; (2) to select the crossing levels before the measurement and simply record the number of crossings and the number of maxima. The former method requires storing a huge amount of data and the memory of the recording instrument should have an elevated capacity. The latter requires a special device, or a data acquisition system, programmed to this aim; the advantage is that a much smaller memory capacity is sufficient and the data processing is simpler.

This approach can also be used to measure the time distribution of the wind direction, based on the principle of dividing the compass into a number of equally spaced directions and counting the number of times these directions have been crossed, which avoids the problem of averaging around the discontinuity 0–360 degrees.

References

Agricola, G., 1556. De Re Metallica, Hieron, Basel.

Alberti, L.B., 1452. Opuscoli Morali. Franceschi, Venice (1568 posthumous).

Albrecht, H.E., Damaschke, N., Borys, M., Tropea, C., 2003. Laser Doppler and Phase Doppler Measurement Techniques. Springer Verlag, Berlin.

Atkinson, J.J., Daglish, J., 1861. The velocities of currents of air in mines. Trans. North Engl. Inst. Min. Eng. 10, 207–242.

Beaubien, D.J., Bisberg, A., 1968. The Sonic Anemometer. Cambridge System, Newton, MA.

Biram, B., 1843. Mr Biram's instrument for measuring the current of air in mines (see Mech. Mag. Vol. XXVII, p. 385). In: Robertson, J.C. (Ed.), The Mechanic's Magazine, Museum, Register, Journal and Gazette. In: vol. 39, p. 47.

Bolle, H.J. (Ed.), 2003. Mediterranean Climate. Springer, Berlin.

Bouger, P., 1746. Traité du Navire, de sa Construction et de Ses Mouvements. Joumbert, Paris.

Brewster, C., 1832. The Edinburgh Encyclopedia. First American Edition, vol. 2 Parker, Philadelphia.

Burt, S., 2012. The Weather Observer's Handbook. Cambridge University Press, Cambridge.

Byrne, O., 1869. Spons' Dictionary of Engineering, Civil, Mechanical, Military, and Naval. vol. 1 Spon, London.

Camp, D.W., Turner, R.E., Glichrist, L.P., 1970. Response tests of cup, vane and propeller wind sensors. J. Geophys. Res. 75, 5265–5270.

Camuffo, D., 1976. How to obtain mean value and variance of wind direction by using a sine-cosine transducer. Atmos. Environ. 10, 167–168.

Camuffo, D., 1979. Graphic recording and averaging the wind direction. Il Nuovo Cimento 2C, 607–618.

Camuffo, D., Denegri, A., 1976. A method for measurement of mean wind direction with the use of standard potentiometric transducers. Atmos. Environ. 10, 415.

Camuffo, D., Schenal, P., 1982. Microclima all'interno della Cappella degli Scrovegni: scambi termodinamici tra gli affreschi e l'ambiente, Bollettino d'Arte special issue "Giotto a Padova", pp. 107–209.

Camuffo, D., Pagan, E., Rissanen, S., Bratasz, Ł., Kozłowski, R., Camuffo, M., della Valle, A., 2010. An advanced church heating system favourable to artworks: a contribution to European standardisation. J. Cult. Herit. 11, 205–219.

Cartwright, D.E., Longuett-Higgins, M.S., 1956. The statistical distribution of the maxima of a random function. Phil. Trans. R. Soc. A 237, 212–232.

Casella, L., 1871. An Illustrated and Descriptive Catalogue of Surveying, Philosophical, Mathematical, Optical, Photographic, and Standard Meteorological Instruments. Casella, London.

Clifford, N.J., French, J.R., Hardisty, J., 1993. Turbulence. Wiley, Chichester.

Combes, C., 1837. Sur le mouvement de l'air dans les tuyaux de conduite. Annales des Mines Série 3 (12), 373–466.

Combes, C., 1844. Traité de L'exploitation Des Mines. vol. 2. Chapter 8. Ed. Carillan-Goeury and Dalmont, Printed by Fain and Thunot, Paris.

Corradi Bianchi, P.L., 1768. Guida del forestiero nella basilica di S. Antonio di Padova con la Dichiarazione di Altre Chiese più Riguardevoli Della Città. Anastasi, Padua and Venice.

Cotte, L., 1774. Traité de Météorologie: contenant 1. l'histoire des observations météorologiques, 2. un traité des météores, 3. l'histoire & la description du baromètre, du thermomètre & des autres instruments météorologiques, 4. les tables des observations météorologiques & botanicométéorologiques, 5. les résultats des tables & des observations, 6. la méthode pour faire les observations météorologiques. Imprimerie Royale, Paris.

Csanady, G.T., 1980. Turbulent Diffusion in the Environment. Reidel, Dordrecht.

Dantec, 1996. 54N50 Low Velocity Flow Analyzer Mark II. Dantec Electronics, Skovlunde, Denmark.

Danti, E., 1578. Primo volume dell'uso et fabbrica dell'Astrolabio, et del Planisferio. Giunti, Florence.

Darcy, H., 1858. Note relative à quelques modifications à introduire dans le tube de Pitot. Ann. Ponts Chaussees 15, 351–359. Series 3.

Dikinson, J., 1876. On measuring air in mines. In: The Chemical News. vol. 33. Crookes, London, pp. 25–27.

DISA, 1976. Description of the DISA Constant Temperature Anemometry System. DISA Electronics, Skovlunde, Denmark.

Doebelin, E.O., 1990. Measurement Systems—Application and Design. McGraw Hill, New York.

Durst, F., Melling, A., Whitelaw, J.H., 1981. Principles and Practice of Laser-Doppler Anemometry. Academic Press, London.

Eredia, F., 1929. La Meteorologia. Cremonese, Rome.

Eredia, F., 1936. Gli strumenti di meteorologia ed aerologia. Bardi, Rome.

Feldman T.S.,1998. Anemometer. Entry in R. Bud and D.J. Warner (Eds), Instruments of Science - An Historical Encyclopedia. The Science Museum, London, with The National Museum of American History, Smithsonian Institution, Washington D.C and Garland Publishing Inc., London.

Forbes, A., 1863–1865. On Lind's anemometer. In: Proceedings of the British Meteorological Society. vol. 2, pp. 275–277.

Gallicciolli, G.B., 1795. Memorie Veneziane antiche profane ed ecc1esiastiche. Book 1, Chapter 8, §280, Fracasso, Venice.

Gash, J.H.C., Dolman, A.J., 2003. Sonic anemometer (co)sine response and flux measurement I. The potential for (co)sine error to affect

sonic anemometer-based flux measurements. Agric. For. Meteorol. 119 (3–4), 195–207.
Gerosa, G., 1898. Meteorologia. UTET, Torino.
Gold, E., 1936. Wind in Britain: the Dines anemometer and some notable records during the last 40 years. Q. J. Roy. Meteorol. Soc. 62 (246), 167–206.
Horst, T.W., 1973. Corrections for response errors in a three-component propeller anemometer. J. Appl. Meteorol. 12, 676–725.
Huet, P.D., 1722. Huetiana, ou pensées diverses de M. Huet, évêque d'Avranches. Estienne, Paris (posthumous).
Hyson, P., 1972. Cup anemometer response to fluctuating wind speeds. J. Appl. Meteorol. 11, 843–848.
IMAIT, 1872. Norme per le osservazioni meteoriche. Supplemento alla Meteorologia Italiana. Italian Ministry for Agriculture, Industry and Trade, Rome, pp. 28–33.
Jones, J.I.P., 1970. A new recording wind vane. J. Phys. E: Sci. Instrum. 3, 9–14.
Kinsman, B., 1965. Wind Waves. Prentice Hall, Englewood Cliffs, NJ.
Landahl, M.T., Mollo-Christensen, E., 1986. Turbulence and Random Processes in Fluid Mechanics. Cambridge University Press, Cambridge.
Leonardo da Vinci, Leichester Hammer Codex, Wind vane: Manuscript folio 100 recto. Bill Gate Private Collection, New York.
Leonardo da Vinci, 1487. Codex Atlanticus. Biblioteca Ambrosiana, Milano. Anemometer: Manuscript folio 675 recto (former 249), Drawings also published in the book: "Il Codice Atlantico di Leonardo da Vinci nella biblioteca Ambrosiana di Milano". Hoepli, Milan, pp. 1894–1904.
Lind, J., 1775. On a portable wind-gauge. Phil. Trans. 65, 353–365.
Lipták, B.G., 2003. Instrument Engineers' Handbook: Process Measurement and Analysis. The Instrumentation System and Analysis (ISA). vol. 1 CRC Press, Boca Raton, FL.
Lloyd, H., 1844–1847. On the Anemometer of Osler. Proc. Royal Irish Acad. (1836–1869) 3, 270–272.
Longuett-Higgins, M.S., 1957. The statistical analysis of a random, moving surface. Philos. Trans. R. Soc. Lond. A 249, 321–387.
Longuett-Higgins, M.S., 1962. The distribution of intervals between zeros of a stationary random function. Philos. Trans. R. Soc. Lond. A 254, 557–599.
Lucas, A., 2006. Wind, Water, Work: Ancient and Medieval Milling Technology. Brill, Leiden, Boston.
Lumley, J.L., Panofsky, H.A., 1964. The Structure of Atmospheric Turbulence. Interscience, New York.
Middleton, W.E.K., 1969a. Catalog of Meteorological Instruments in the Museum of History and Technology. Smithsonian Institution Press, Washington, DC.
Middleton, W.E.K., 1969b. Invention of the Meteorological Instruments. John Hopkins Press, Baltimore.
Miller, C., Holmes, J., Henderson, D., Ginger, J., Morrison, M., 2013. The response of the Dines Anemometer to gusts and comparison with cup anemometers. J. Atmos. Oceanic Tech. 30, 1320–1336.
Monna, W.A.A., Driedonks, A.G.M., 1979. Experimental data on the dynamic properties of several propeller vanes. J. Appl. Meteor. 18, 699–702.
Monteith, J.L., 1972. Survey of Instruments for Micrometeorology. Blackwell Scientific Publications, Oxford.
Moses, H., 1968. Meteorological instruments for use in atomic energy industry. In: Slade, D.H. (Ed.), Meteorology and Atomic Energy 1968. U.S. Atomic Energy Commission, Div. Tech. Info, pp. 257–300.
Napier, J.R., 1872. On pressure logs for measuring the speed of ships. Proc. Phil. Soc. Glasg. 8 (1), 146–160.
Negretti, E., Zambra, J.W., 1864. Meteorological Instruments: Explanatory of Their Scientific Principles, Method of Construction, and Practical Utility. Williams and Straham, London.
Newstadt, F.T.M., Van Dop, N., 1984. Atmospheric Turbulence and Air Pollution Modelling. Reidel, Dordrecht.
Parrot, G.F., 1797. Anwendung eines zweckmässigen Anemometers; in Voigts Magaz. für den neuesten Zustand der Natürgesch. Herausgeber, Riga, p. 144. Part 1, Section 2.
Pasquill, F., 1962. Atmospheric Diffusion, first ed. Van Nostrand, London.
Pasquill, F., 1974. Atmospheric Diffusion, second ed. Wiley, New York.
Patterson, J., 1926. Cup anemometers. Trans. R. Soc. Can. 20, 1–54, third series.
Pini, V., 1598. Fabrica de gl'horologi solari. Guarisco, Venice.
Pitot, H., 1732. Description d'une machine pour mesurer la vitesse des eaux courantes et le sillage des vaisseaux. Histoire de l'Académie Royale des Sciences. Année 1732 avec les mémoires de mathématique et de physique pour la même année, tirés des registres de cette Académie. 1735 Imprimerie Royale, Paris, pp. 363–376.
Poleni, G., 1734. De la meilleure manière de mesurer sur mer le chemin d'un vaisseau, indépendamment des observations astronomiques. Imprimerie Royale, Paris.
Ramachandran, S., 1970. A theoretical study of cup and vane anemometers. Q. J. Roy. Meteorol. Soc. 96, 115–123.
Reiter, E.R., 1975. Weather Phenomena of the Mediterranean Basin. EPRFNPS, Monterey, CA.
Rice, S.O., 1944. Mathematical analysis of random noise. Bell Syst. Tech. J. 23, 282–332.
Rice, S.O., 1945. Mathematical analysis of random noise. Bell Syst. Tech. J. 24, 46–156.
Robinson, T.R., 1880. On the determination of the constants of the cup anemometer by experiments with a whirling machine—Part II. Phil. Trans. R. Soc. London 171, 1055–1070.
Sanctorius, S., 1625. Commentaria in primam fen primi libri Canonis Avicennae. Iacobus Sarcina, Venice.
Simons's, S., 1866. Monthly Meteorological Magazine. vol. 1 London, Stanford.
Slade, D.H., 1968. Meteorology and Atomic Energy 1968. USAEC TID 24190, Springfield, CA.
Smith, S., 1970. Thrust-anemometer measurements of wind turbulence, Reynold stress, and drag coefficient over the sea. J. Geophys. Res. 71, 6758–6770.
Strunck, V., Sodomann, T., Muller, H., Dopheide, D., 2004. How to get spatial resolution inside probe volumes of commercial 3D LDA systems. Exp. Fluids 36, 141–145.
Sutton, O.G., 1960. Atmospheric Turbulence. Methuen, London.
Tennekes, H., Lumley, J.L., 1973. A First Course in Turbulence. MIT Press, Cambridge, MA.
Todhunter, I., 1876. William Whewell D.D., An Account of His Writings. MacMillan and Co, London.
Tomlinson, C., 1861. The Tempest: An Account of the Origin and Phenomena of Wind, in Various Parts of the World. Society for Promoting Christian Knowledge, London.
Tomlinson, C., 1866. Cyclopaedia of Useful Arts: Mechanical and Chemical, Manufactures, Mining and Engineering. vol. III Virtute and Co, London.
Tropea, C., Yarin, A.L., Foss, J.F., 2007. Springer Handbook of Experimental Fluid Mechanics. Springer Handbooks, vol. 1. Berlin.
UK Meteorological Office, 1875. Instructions for Meteorological Telegraphy. Her Majesty's Stationary Office, London.
UK Meteorological Office, 1962. Weather in the Mediterranean. Her Majesty's Stationery Office, London.
UK Meteorological Office, 1981. Handbook of Meteorological Instruments. Measurement of Surface Wind, vol. 4. Her Majesty's Stationary Office, London.
van der Molen, M.K., Gash, J.H.C., Elbers, J.A., 2004. Sonic anemometer (co)sine response and flux measurement—II. The effect of

introducing an angle of attack dependent calibration. Agric. For. Meteorol. 122 (1–2), 95–109.
Varro, M.T., 37 BC. De Re Rustica (on Agriculture). Book 3, Chapter 5. Also, English translation by H.B. Ash, 1967. Loeb Classical Library, Cambridge.
Vercelli, F., 1933. L'aria, nella natura e nella vita. UTET, Torino.
Vinnichenko, N.K., Pinus, N.Z., Shmeter, S.M., Shur, G.N., 1980. Turbulence in the Free Atmosphere. Consultants Bureau, New York.
Vitruvius, M.P., 1st century BC. De Architectura (on Architecture). Book 1, Chapter 6, In: Marini, L. (Ed.), L'Architettura di Vitruvio. Marini, Rome (1936). Also, English translation by F. Granger, 1955. Loeb Classical Library, Cambridge.
Walker, R.P., Swift, A., 2015. Wind Energy Essentials: Societal, Economic, and Environmental Impacts. Wiley, Hoboken, NJ.
Wallén, C.C. (Ed.), 1977. Climates of Central and Southern Europe. Elsevier, Amsterdam.
Weisbach, J.L., 1847. Principles of the Mechanics of Machinery and Engineering. Theoretical Mechanics, vol. 1 Bailliere, London.
WEU, 2004. Wind and Wave Atlas of the Mediterranean Sea. Western European Union. Western European Armaments Organisation Research Cell.http://users.ntua.gr/mathan/pdf/Pages_from%20_WIND_WAVE_ATLAS_MEDITERRANEAN_SEA_2004.pdf.
WMO, 2008. Guide to Meteorological Instruments and Methods of Observation. WMO Technical Publication No. 8, World Meteorological Organization, Geneva.
Wolff, C., Wolfius, v.A., 1709. Aerometria Elementa in quibus aliquot aeris vires ac proprietates iuxta methodum Geometrarum demonstrantur. Strauss & Cramer, Leipzig.
Wood, L.E., 1945. The development of a new wind-measuring system. Bull. Am. Meteorol. Soc. 26, 361–370.
Wyngaard, J.C., 1981. Cup, propeller, vane, and sonic anemometers in turbulence research. Annu. Rev. Fluid Mech. 13, 399–423.

Further Reading

Airy, G.B., 1874. Astronomical and Magnetical and Meteorological Observations Made at the Greenwich Observatory, Greenwich, in the Year 1872. Eyre and Spottiswoode, London.
Brooks, L., 2000. Wind Dials and Their Makers. 2000. Portico Library, Manchester.
Flammarion, C., 1872. L'Atmosphère. Description des grands phénomènes de la Nature. Hachette, Paris.